EFMC6 KTH

Electronic version

Abstracts

Volume 2

KTH
VETENSKAP
OCH KONST

EFMC6 KTH - EUROMECH Fluid Mechanics Conference 6
Royal Institute of Technology STOCKHOLM, JUNE 26-30 2006

Preface

The EUROMECH Fluid Mechanics Conference 6 (EFMC 6) is held at KTH in Stockholm during June 26-30, 2006. These two volumes of abstracts comprise all presentations of the conference, including nine plenary lectures, and more than 400 contributed papers, which are presented either in oral sessions or during five different mini-symposia. The page numbers given here corresponds to the presentation number found in the conference programme booklet. At the end of each volume you will find a list of all authors and the page number(s) where their abstract appear. The **bold** page numbers correspond to presenting authors.

We like to thank the EFMC committee for their work with the evaluation and selection process. We also like to thank Veronica Eliasson and Bengt Fallenius for help with preparing the printed version of these volumes.

Henrik Alfredsson, chairman EFMC6
Jens Fransson, scientific secretary EFMC6

Session 7

Linear-stability of Blasius boundary layer on concave wall to quasi-steady and unsteady Görtler vortices: experiment and theory.

A. V. Boiko[a], A. V. Ivanov[a], Y. S. Kachanov[a] and D. A. Mischenko[a]

The Görtler instability occurring in boundary layers on concave walls is responsible for amplification of streamwise counter-rotating vortices, whose growth is able to lead to the laminar-turbulent transition. The majority of previous experiments were devoted to the *steady* Görtler vortices, despite the *unsteady* ones are also observed in real transitional flows very often. Moreover, even for the steady Görtler vortices no good quantitative agreement between the experimental and theoretical linear-stability characteristics was obtained, especially for disturbance growth rates. The experimental difficulties were connected with a rather poor accuracy of measurements at zero disturbance frequency, a possible influence of nonlinearity, and an admixture of non-modal (transient) growth mechanism (the near-field of disturbance sources). The present paper has aim to overcome all these difficulties by means of: (i) tuning-off from the exact zero frequency of Görtler vortices by means of working with quasi-steady perturbations of a very low frequency, (ii) performing measurements at low disturbance amplitudes (hundredths of a percent), and (iii) minimization and careful estimation of the disturbance-source near-filed by means of utilizing a new kind of disturbance source and performing special numerical computations. Simultaneously, we wanted to measure all linear-stability characteristics with respect to essentially unsteady Görtler vortices, to carry out calculations (based on locally-parallel and non-local non-parallel linear stability theories), and to perform a detailed direct comparison of the theoretical and experimental data. All these goals have been achieved.

The hot-wire measurements were conducted in the low-turbulence wind tunnel T-324 of ITAM SB RAS at free-stream velocity of 9.18 m/s in a boundary layer developing over a concave wall with a radius of curvature of 8.37 m. The linear-stability characteristics were measured and calculated for Görtler vortices with spanwise wavelengths of 8, 12 and 24 mm in a frequency range between 0.5 and 20 Hz. It is found that outside the disturbance source near-field, the excited perturbation represents either quasi-steady (at low frequencies) or unsteady (at high frequencies) first Görtler mode, which has the largest amplification rate. A very good quantitative agreement between all theoretical and experimental stability characteristics is obtained for all studied frequencies and spanwise wavenumbers, including the disturbance increments, the phase velocities, and the eigenfunctions. The non-local non-parallel theory is found to provide a somewhat better agreement than the parallel one. When the frequency increases, the instability region shrinks and divides into several localized regions. A paradoxical result is obtained that in a certain range of spanwise wavenumbers (close to the most amplified modes) the growth of the Görtler number is able to stabilize the flow with respect to unsteady first Görtler modes.

Supported by Russian Foundation for Basic Research (grant No 06-01-00519).

---

[a] Institute of Theoretical and Applied Mechanics of SB RAS, 630090, Novosibirsk, Russia.

Görtler vorticies in an asymptotic suction boundary layer on a concave wall

M. Matsui[*], N. Aota[†], J. Shiomi[‡] and M. Matsubara[*]

The omnipresence of flow on curved walls has given rise to vast research on flows in related geometries. This includes Görtler vorticies where the studies on the stability characteristics have revealed the essential features of the primary instability giving rise to the well-known mushroom-like shaped isovelocity contours with distinct non-dimensional spanwise wavenumber, which eventually triggers the secondary instability. In the current work, we investigate the Görtler vorticies in a concaved asymptotic boundary layer by means of experiments and direct numerical simulations. As the constant boundary layer thickness simplifies the streamwise variance of the vortex scales, the current system is convenient for stability analyses. The concaved asymptotic boundary layer also allows us to clarify the influence of boundary layer thickness on the growth of the Görtler vorticies.

In experiments, the concaved wall is made of porous material through which suction at nearly constant and homogeneous suction velocity can be applied to realize the concaved asymptotic boundary layer. Initial perturbation was applied by projections placed equidistantly in spanwise direction on a straight wall followed by the concave wall. The direct numerical simulation was formulated in a spectral method.

In both experiments and numerical simulations, three-dimensional velocity mappings (figure 1) clearly exhibit the formation of Görtler vorticies in the concaved asymptotic boundary layer which exhibits the nontrivial difference from the ones in the concaved boundary layers without suction, especially in the low speed part of the vorticies. By computing the energy evolution along the streamwise direction, it was observed that the growth rate strongly depends on the spanwise length scale of the initial perturbation and the most destabilizing wavelength was found to be about two times larger than the counterpart case without suction.

Overall results will be discussed in connection with the influence of the boundary thickness and the hydrodynamics imposed by the suction.

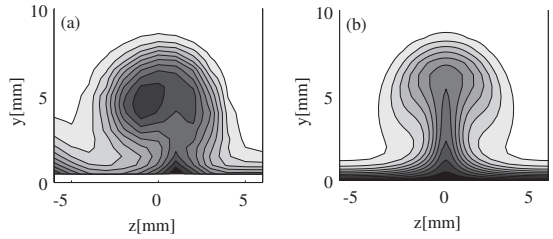

Figure 1: Contour maps of the mean streamwise velocity . (a) Experiment (b) Numerical simulation.

[*]Shinshu University, 4-17-1 Wakasato, Nagano 380-8553, Japan
[†]Atman Software Inc., 1-1-11 Yanagibashi, Taito-ku, Tokyo 111-0052, Japan
[‡]The University of Tokyo, 7-3-1 Hongo, Bunkyo-ku, Tokyo, 113-8656, Japan

Streak growth and breakdown in a boundary layer with steady uniform suction

E. N. Davidsson*

Turbulent flow processes play an important role in many flow systems. To optimize and control energy losses of such systems, knowledge of the mechanisms leading to and maintaining turbulence is required. Steady, uniform suction through porous materials is one control method known to stabilize the flat plate boundary layer flow. As wall suction is applied, the growth of Tollmien-Schlichting waves are decreased and a critical Reynolds number of 54000 is reported[1]. Wind tunnel experiments show that also disturbances arising due to free stream turbulence are dampened by wall suction[2] [3]. A common observation for parallel shear flows, and boundary layers in particular, is that streamwise streaks pre-date transition to turbulence[4]. Thus a numerical study of streak instabilities and breakdown is a natural step in elucidating the stabilizing effects of wall suction.

In this work, several scenarios of breakdown to turbulence of a flat plate boundary layer with wall suction is studied. Calculations have been performed by means of direct simulations of the Navier-Stokes equations in the temporal domain. This approach allow for the study of the evolution of periodic disturbances such as streaks and oblique waves found in figure 1. The studied disturbances are found to trigger transition to turbulence by similar mechanisms as other flows. Energy thresholds for transition to turbulence is calculated and transition at the lowest energy is provided by the oblique wave scenario for all investigated Reynolds numbers. The next step of the investigation is to study the flow further into the turbulent state, which requires the simulation code to be run in a spatial setup.

*Luleå University of Technology, SE-971 87 Luleå, Sweden.

[1]Hocking, *Q. J. Mech. Appl. Math.* **28**, 341 (1975).
[2]Fransson and Alfredsson, *J. Fluid Mech.* **482**, 51 (2003).
[3]Yoshioka et al., *Phys. Fluids* **16**, 3530 (2004).
[4]Matsubara and Alfredsson, *J. Fluid Mech.* **430**, 149 (2001)

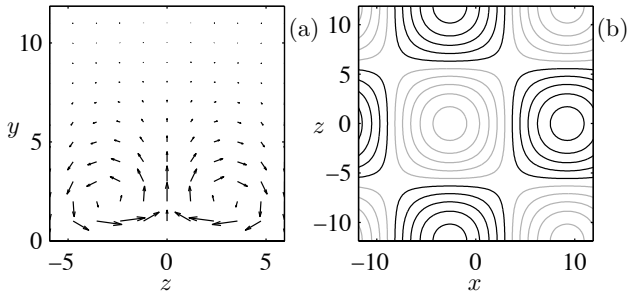

Figure 1: Initial optimal disturbances. (a) Cross-flow plane of the optimal streamwise vortices. (b) Contours of normal disturbance velocity of the oblique waves in a horizontal plane.

Optimal disturbances in suction boundary layers

M. G. Byström*, O. Levin* and D. S. Henningson*

An adjoint-based optimization procedure[1] is used to calculate the optimal disturbance in a boundary layer where constant suction is applied at the wall. A region at the leading edge is however free from suction, allowing a Blasius boundary layer to develop up to the point where the suction starts. Downstream of this point the flow evolves into the asymptotic suction boundary layer. This boundary layer, herein denoted the semi suction boundary layer, emulates a recent wind-tunnel experiment in which streaks induced by free-stream turbulence was studied[2]. The optimal disturbance, which consists of streamwise vortices that develop into streamwise streaks, experience the greatest energy growth over the suction-free region at the leading edge. The optimal spanwise scale in the semi suction boundary layer is thus the same as in the Blasius boundary layer. This corresponds well to experimental findings[2,3], which indicates that the spanwise scale of the streaks is set in the leading edge region.

Furthermore, the optimal disturbance in the asymptotic suction boundary layer is calculated and compared to a previous temporal study[4]. It is shown that the spatial framework gives a 16% higher energy growth. The wall-normal distribution of the optimal disturbances differ between the semi suction boundary layer and the asymptotic suction boundary layer, while the downstream responses collapse as shown in figure 1.

*KTH Mechanics OB 18, SE-100 44 Stockholm, Sweden.

[1]Levin and Henningson,*Flow, Turb. Combust.* **70**, 183 (2003).
[2]Fransson and Alfredsson, *J. Fluid Mech.* **482**, 51 (2003).
[3]Yoshioka et al.,*Phys. Fluids* **16**, 3530 (2004).
[4]Fransson and Corbett, *Eur. J. Mech. B/Fluids* **22**, 259 (2003).

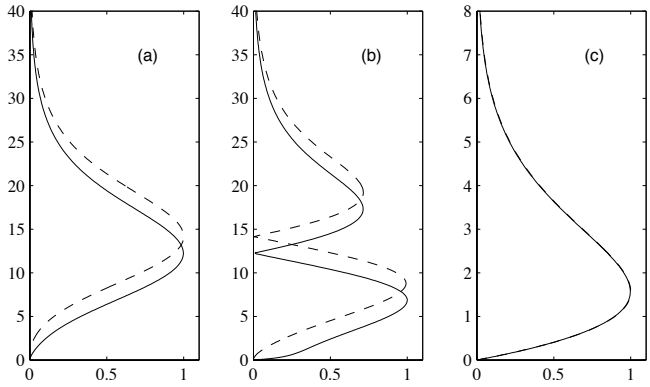

Figure 1: The wall-normal (a) and spanwise (b) components of the optimal disturbances and the downstream response (c) in the semi suction boundary layer (solid line) and the asymptotic suction boundary layer (dashed line).

Development of subharmonic disturbances in low-speed streaks

Y. Konishi[a] and M. Asai[b]

Development of streak instability and the resulting transition to turbulence are examined experimentally through artificially generating spanwise-periodic low-speed streaks in a flat-plate laminar boundary layer by using small screens set normal to the boundary-layer plate.[1] Spanwise-periodic streaks are unstable to fundamental and/or subharmonic disturbances whose dominant spanwise wavelengths are the same as the streak spacing and twice the streak spacing respectively. In the present study, we focus on the subharmonic sinuous mode, which has the largest growth rate in our low-speed streaks.

Up to the nonlinear saturation stage of the streak instability, the disturbance development along each low-speed streak is similar to that observed in a singe low-speed streak[2], that is, interactions of disturbances developing along the neighbouring streaks are not so strong in the early stage of the transition. Beyond the saturation stage, quasi-streamwise vortices developing along each low-speed streak interact with each other, causing an arch-like vortex structure to develop away from the wall, as shown in Fig. 1. This is not the case for the development of fundamental sinuous mode[3]. After the breakdown of the primary low-speed streaks, near-wall streaks newly develop downstream. Importantly, the newly-developed low-speed streaks have lateral spacing of 100 wall units, the same as the value in developed wall turbulence. The time-mean velocity profile (averaged over the spanwise wavelength) exhibits the log-law at that stage.

---

[a] Tokyo Metropolitan Institute of Technology, Hino, Tokyo 191-0065, Japan.
[b] Tokyo Metropolitan University, Hino, Tokyo 191-0065, Japan.

[1] Konishi and Asai, *Fluid Dyn. Res.* **34**, 299 (2004).
[2] Asai et al., *J. Fluid Mech.* **455**, 289 (2002).
[3] Brandt and Henningson, *J. Fluid Mech.* **472**, 229 (2002).

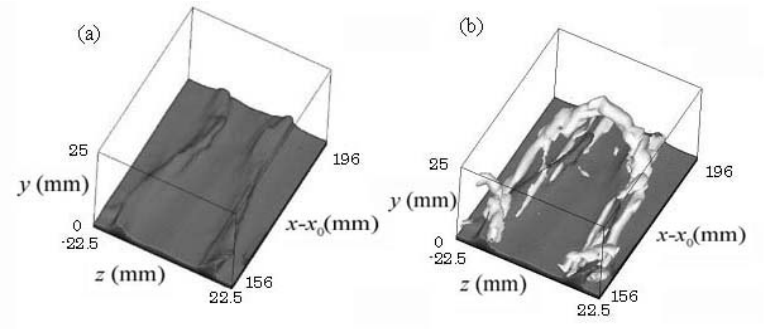

Figure 1: Vortices generated by the subharmonic streak instability. (a) Iso-velocity surface (50% of U_∞). (b) Vortex structure identified by λ_2-method.

Receptivity of an infinitely thin flat plate to free-stream vorticity

G. El Khoury* and L. Brandt*

In boundary layers subject to free-stream turbulence intensities of 1% or more, transition occurs rapidly, bypassing the classical scenario due to the amplification of the Tollmien-Schlichting waves. The former scenario is characterised by the growth inside the boundary layer of low-frequency streamwise-elongated streaky structures of alternating high and low streamwise velocity. The growth of these structures can be explained by non-modal growth theory[1]. As the streaks grow downstream, they undergo secondary instabilities which precede the breakdown into turbulent spots[2]. By compiling data from different studies, it is observed that different experiments with apparently similar conditions can disagree on the onset and extent of transition. Therefore, several different parameters affect the receptivity of the boundary layer; not only the free-stream turbulence intensity, but also its spatial scales, energy spectrum and degree of homogeneity and isotropy play an important role.

In the present study, we analyse in detail the effect on the boundary layer flow of streamwise vortical disturbances in the free stream upstream of an infinitely thin flat plate. Perturbations consisting only of streamwise vorticity are considered since previous works[1] show that this is the component responsible for the growth of the streaks. The incoming vorticity is assumed to be periodic in the wall-normal and spanwise directions, as well as in time. The aim of the study is to identify the most dangerous length and time scales of the external perturbation and to assess whether it is possible, with a linear approach, to reproduce the whole receptivity process by comparing with experimental findings. To compute the flow response, the parabolic time-dependent linearised boundary layer equations are used, following Ref.[3].

The effect of the wall-normal scale of the incoming vorticity is first considered. The results show that perturbations of smaller scale induce higher amplitude streaks closer to the leading edge, whereas large-scale vorticity is responsible for the largest amplitudes, which occur farther downstream. When fixing the wall-normal wavelength and the temporal frequency, it is observed that smaller spanwise wave-numbers are dominant further downstream. However, by scaling the spanwise spacing by the local displacement thickness the value of the most amplified wavelength becomes almost independent on the streamwise location considered. Finally, the smallest time frequencies are the most effective whereas the larger-frequency streaks start to decay further upstream.

To be able to predict which amplitudes and perturbation scales are most likely to be observed, knowledge of the spectrum of the free-stream perturbation is needed. We will initially assume homogeneous isotropic turbulence and correlate the receptivity results with the analytical expression of the spectrum suggested by von Karman. Some examples of the effect of the turbulence intensity and length scale will be shown.

*KTH Mechanics, SE-100 44 Stockholm, Sweden.

[1]Andersson et al., *Phys. Fluids* **11**, 134 (1999); Luchini, *J. Fluid Mech.* **404**, 289 (2000).
[2]Brandt et al., *J. Fluid Mech.* **517**, 167 (2004).
[3]Levin and Henningson, *Flow, Turbulence and Combustion* **70**, 183 (2003).

On the stability and decay of turbulent Couette flow

Paul Manneville and Maher Lagha*

In the transitional regime, the plane Couette flow (pCf) can be in one of two states, laminar or turbulent, that do not play symmetrical roles. When studying the decay from *turbulent* towards *laminar* flow upon sudden decrease of the Reynolds number (quench experiment), difficulties arise because the initial state cannot be represented without introducing statistical features. This matter can however be studied using semi-realistic models simplifying the Navier–Stokes equations.[1]

We present results obtained from quench experiments using a model extending our previous stress-free system to the case of no-slip boundary conditions at the plates.[2] Numerical simulations were performed in a "wide" domain ($32 \times 32 \times 2$) for which turbulence behaved extensively. An interesting feature, observed for the first time in partial differential models, is the behavior of the escape times from the turbulent state that is consistent with a divergence in $1/(R - R_g)^2$ close to the global stability threshold R_g (Fig. 1). Curiously, this is similar to what Chaté obtains from his abstract model expressed as a coupled map lattice designed to display spatio-temporal intermittency, whereas Bottin's experiments seemingly suggest a $1/(R - R_g)$ type of divergence.[3]

Implications of these results and a more thorough analysis of the very concept of stability applied to the turbulent pCf in the "thermodynamic" sense of Pomeau[4] are currently under study.

*LadHyX, École Polytechnique, F-91128 Palaiseau, France

[1] P. Manneville, in *IUTAM Symposium on Laminar-Turbulent Transition and Finite Amplitude Solutions*, T. Mullin & R. Kerswell eds. (Springer, 2005).

[2] M. Lagha & P. Manneville, in preparation for *Eur. Phys. J. B*.

[3] S. Bottin *et al.*, *Europhys. Lett.* **43** 171–176 (1998); S. Bottin & H. Chaté, *Eur. Phys. J. B* **6** 143–155 (1998).

[4] Y. Pomeau, *Physica D* **23** 3–11 (1986).

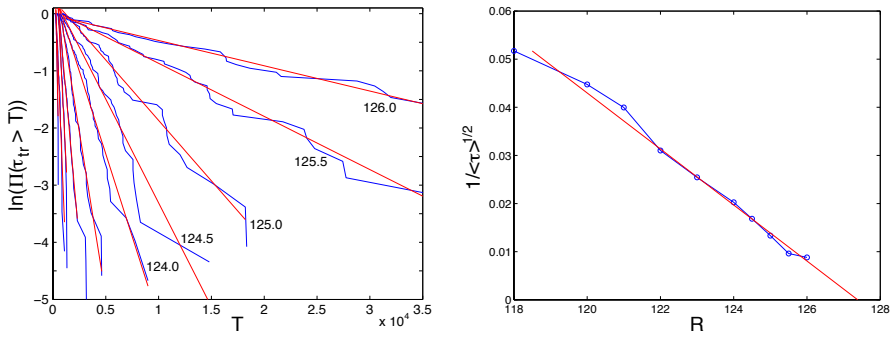

Figure 1: Left: distribution of transient durations for increasing R. Right: The inverse square-root of average transient duration $\langle\tau\rangle$ extrapolates to zero for $R = R_g \approx 127.4$.

Features of hydrodynamic fluctuations of stochastically forced 3D plane Couette flow

G. Khujadze*, M. Oberlack*, G.Chagelishvili†

The background of three dimensional hydrodynamic/vortical fluctuations in a stochastically forced, laminar, incompressible, 3D plane Couette flow is simulated numerically. The simulations were performed on the IBM supercomputer (Regatta-H) at Technische Universität Darmstadt. For the direct numerical simulations we used the code developed at KTH, Stockholm[1], using a spectral method. We modified the original code implementing stochastic forcing satisfying the condition of fluctuation-dissipation theory.

The performed simulations revealed evident features of statistically stationary fluctuating field of a laminar plane Couette flow. Especially, they show:
(i) The non-normal (non-exponential) growth of the hydrodynamic perturbations – the finite statistically stationary level is defined by the non-normality of the non-equilibrium flow system[2]);
(ii) Predominance of the streamwise *non-constant* fluctuations with the characteristic scale of the order of the channel width in the fluctuating spectrum. This fact should be important for correlations (especially, for asymmetric time correlations[3]);
(iii) Existence of structural regularities in the fluctuating background that may be considered as seeds of the found recently nonlinear stationary/coherent structures[4];
(iv) Stochastic forcing destroys the spanwise reflection symmetry inherent to the linear and full Navier-stokes equations in a case of the Couette flow – it inputs an asymmetry in the equations (see figure 1) and, consequently, on dynamical processes. This asymmetry should become apparent in the nonlinear/turbulent regime.

*Technische Universität Darmstadt, Petersenstr. 13, Darmstadt, Germany.
†Center for Plasma Astrophisics, Abastumani Astrophysical Observatory, Kazbegi Ave. 2A, Tbilisi, Georgia

[1]Skote, *Doctoral thesis* KTH, Stockholm, Sweden, (2002).
[2]Chagelishvili and Khujadze, *JETP* **85**, 907 (1997).
[3]Eckhardt and Pandit, *European Phys. J. B* **33**, 373 (2003).
[4]Fitzgerald, *Physics Today*, February, (2004).

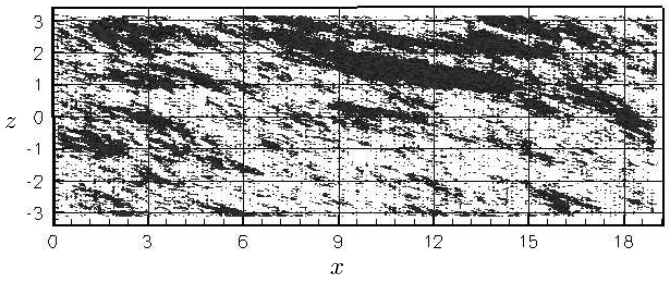

Figure 1: The fluctuation energy on a plane xz at $y = 0$. Black (white) areas relate to the values of the energy more (less) than the value 2.7 10^{-7}.

Modulated plane Couette flow subject to the system rotation

K. Kitagawa*and M. Nagata*

We consider an incompressible fluid motion with the kinematic viscosity ν between two parallel plates separated by the distance $2d$ subject to a constant angular velocity Ω about the spanwise direction[1]. One of the plates moves along in its own plane with a velocity U_0, whereas the other moves in the opposite direction with $U_0(1-\epsilon\cos\omega t)$. The motion is controlled by three non-dimensional parameters: the Reynolds number R, the Coriolis parameter τ and the oscillation number γ, defined by

$$R = U_0 d/\nu, \qquad \tau = 2\Omega d^2/\nu, \qquad \gamma = \sqrt{\omega d^2/2\nu}, \tag{1}$$

respectively, in addition to the modulation amplitude ϵ.

Our linear stability analysis based on the Floquet theory indicates that the modulation has a stabilizing effect when τ is small, whereas it destabilizes the flow at large τ as indicated in figure 1. It is found that the frequency of the unstable mode for the small τ region is the same as that of the basic state whereas it is halved for large τ.

The time development of the flow in the supercritical region obtained by DNS for two different β's is shown in figure. 2. It is seen that the period of the secondary flow with $\beta = 1.5$ is the same as that of the basic flow, whereas it is doubled in the case with $\beta = 3.5$. We plan to discuss physical flow properties for both cases in detail.

*Dept. of Aeronautics and Astronautics, Kyoto University. Kyoto 606-8501, Japan.

[1]Nagata, *J. Fluid Mech.* **358**, 357 (1998).

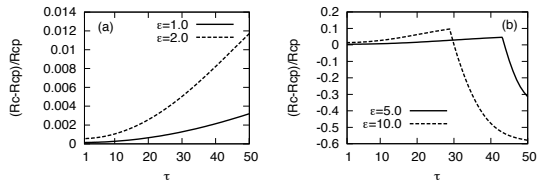

Figure 1: $(R_c - R_{cp})/R_{cp}$ against τ with $\gamma = 5.0$. R_c and R_{cp} are the critical Reynolds numbers with $\gamma \neq 0$ and $\gamma = 0$, respectively. Unstable mode is streamwise independent and its spanwise wavenumber β at the criticality varies along each curve. (a): $\epsilon = 1.0, 2.0$. (b): $\epsilon = 5.0, 10.0$.

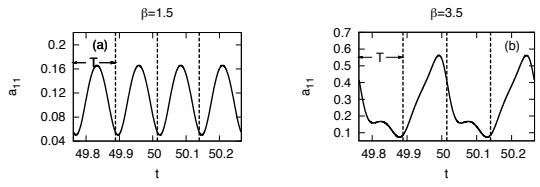

Figure 2: The development of the flow calculated by DNS at $\gamma = 5.0$, $R = 37.0$, and $\tau = 29.0$. T is the period of the basic oscillatory state. (a): β=1.5, (b): β=3.5

Experimental observations in rotating plane Couette flow

K. Hiwatashi[*], N. Tillmark[†], P. H. Alfredsson[†] and M. Nagata[*]

Placing the apparatus used for the investigation on plane Couette flow[1] on a rotating table, we observe the breakdown of the laminar state and successive streamwise roll cell flow structures experimentally by changing the Reynolds number R (based on the wall speed and the half fluid depth) and the Coriolis parameter Ω (based on the viscous diffusion time). The aim of the present work is to present an experimental evidence for, in particular, stable tertiary flows predicted by Nagata(1998)[2] theoretically. He showed that the tertiary flows are stable for $4.75 < \Omega < 6.63$ at $R = 50$, and for $1.63 < \Omega < 1.85$ and $8.0 < \Omega < 10.5$ at $R = 100$.

Experiments are carried out for three cases, $(\Omega, R) = (5.61, 48.4)$, (9.31, 100) and (1.73, 101), each of which corresponds roughly to the theoretically predicted region described above for the existence of stable tertiary flows.

For the cases with $\Omega = 5.61, R = 48.4$ and $\Omega = 9.31, R = 100$ visualization of the tertiary flow as shown in figure 1. indicates that the flow structures, such as observed wave length, match the theoretical findings by Nagata (1998) very well.

For the case with $\Omega = 1.73, R = 101$, however, steady stable tertiary state cannot establish itself. In stead, transition from streamwise roll cells to tertiary flows is observed only occasionally, where the tertiary flow is unable to keep its structure for a long time and the flow pattern returns to the roll cells cyclically, roughly once in a few minutes.

Figure 1: The tertiary flow observed experimentally. $R = 100, \Omega = 9.31$.

[*]Dept. of Aeronautics and Astronautics, Kyoto University. Kyoto 606-8501, Japan.
[†]Department of Mechanics, Royal Institute of Technology, SE-100 44 Stockholm, Sweden.

[1]Tillmark, N. and Alfredsson, P. H., *J. Fluid Mech.* **235**, 89 (1992).
[2]Nagata, M., *J. Fluid Mech.* **358**, 357 (1998).

Double Hopf bifurcation in spiral Poiseuille flow

M. Avila*, A. Meseguer *, F.Marques *

The spiral Poiseuille problem deals with the behaviour of an incompressible viscous fluid confined between two coaxial cylinders independently rotating around their common axis. In addition, the fluid is enforced to flow downstream by an imposed pressure gradient in the axial direction. The resulting steady flow, termed *spiral Poiseuille flow* (SPF), has an helicoidal profile, being the superposition of the azimuthal Couette flow and the axial Poiseuille flow. This classical fluid problem was experimentally studied by Nagib in the seventies, and has been recently numerically studied [1]. New experiments have been undertook in this problem by Prof. Pfister and his group in Kiel.

A recent linear stability analysis of this flow was carried out in [2], focusing on the co-rotating regime and for medium gap geometry. In particular, a bicritical curve of stability where modes associated to azimuthal wavenumbers of opposite sign $\pm n$ coexist was found. The unstable eigenfunctions correspond to spiral patterns featuring unexpected changes in their angle and propagation speed.

However, linear stability results do not help in predicting the dominance and stability of the secondary flows arisen when the basic SPF becomes unstable. For this reason, the full three-dimensional nonlinear Navier–Stokes have been solved by means of accurated spectral computations. A double Hopf bifurcation point for the $n = \pm 1$ case, which gives rise to spiral vortices of opposite helical orientation, has been studied. These spiral regimes are termed Left Spirals, corresponding to $n > 0$ case, and Right Spirals for the $n < 0$ case. Both regimes are time-periodic and co-rotate with the cylinders, although the Left Spirals are associated to the inner cylinder and propagte downstream, whereas the Right Spirals are associated to the outer cylinder and proapgate upstream. A mixed mode of interpenetrating spirals, exhibiting the features of the aforementioned regimes has also been found. Figure 1 shows an isosurface of the azimuthal vorticity for this regime. The spatiotemporal properties of these solutions will be explained and discussed in terms of equivariant bifurcation and normal form theories.

*Applied Physics Department, Universitat Politècnica de Catalunya, Barcelona, SPAIN.

[1] Hoffman et al., *Phys. Rev. E* **69**, 056309 (2004).
[2] Meseguer and Marques, *Phys. Fluids* **17**, 094104 (2005).

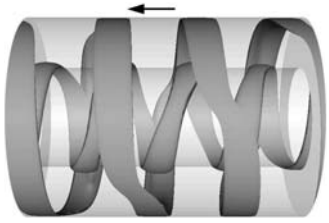

Figure 1: Azimuthal vorticity isosurface for the interpenetrating spirals.

Global Doppler frequency shift detection with near-resonant interferometry

A. Landolt*, and T. Rösgen*

We propose to measure global Doppler frequency shifts by using a dispersive element in an interferometric setup. In any interferometer with uneven optical path lengths, changes in frequency will result in a phase shift and hence in a local distortion of the interference fringe pattern By adding a dispersive element to one leg, optical path length difference becomes strongly frequency dependent.

Using Iodine vapor near a resonant transition as a dispersive medium, the system sensitivity is predicted. Near resonance, the refractive index can be obtained from absorption data trough use of the Kramers-Kronig relationships [1]. In the present study, Forkey's [2] absorption model has been used to predict the Iodine absorption. The theoretical data is compared with good agreement to measurements of both transmission and system sensitivity in a test setup.

Rotating disc experiments with a pulsed laser light source show the applicability of the proposed method in planar Doppler velocimetry (Figure 1). As in other global Doppler techniques, laser frequency stabilization and system calibration need to be considered with care. The interferometric setup, susceptible to changes of the optical path length difference due to vibrations or density variations, poses its own challanges.

The proposed method simplifies the measurement compared to the standard Doppler Global Velocimetry setup. It is inherently a single camera, single image technique without image alignment and camera calibration issues. The measurement range, in contrast to the limitations with transmission based techniques, is virtually unlimited. The choice between numerous dispersive media such as molecular and atomic gas cells or Stark and Faraday effect filters, and the many ways to influence their dispersive properties, creates a highly adaptable technique.

*Institute of Fluid Dynamics, ETH Zurich, 8092 Zurich, Switzerland.

[1] Peiponen and Vartiainen, *Phys. Rev., B Condens. Matter* **44**, 8301 (1991).

[2] Forkey et al., *Appl. Opt.* **36**, 6729 (1997).

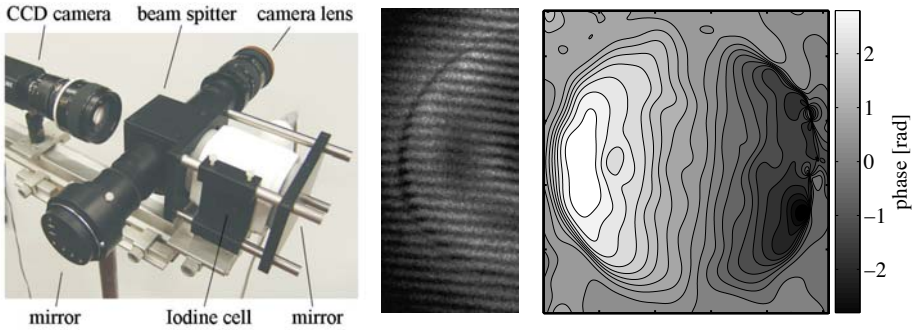

Figure 1: a) current experimental setup, b) the unprocessed interference fringe pattern from a rotating disc experiment and c) the computed phase shift.

Hydrodynamics of oscillating microcantilevers

O. E. Jensen*, R. J. Clarke†, J. Billingham*, P.M. Williams‡

The atomic force microscope (AFM) employs a V-shaped or rectangular cantilever, the latter having typical dimensions $0.5 \times 20 \times 200$ m. Deflections of the cantilever are measured using reflected laser light. The AFM can be used to image biological samples in their native liquid environment, making it important to understand how hydrodynamic forces affect the cantilever's motion. Cantilevers oscillate at high frequencies either under external forcing (in so-called 'tapping' mode) or under thermal fluctuations. In fitting a theoretical model to the thermal spectrum in order to determine the cantilever's mechanical properties, previous studies[1] have relied on two assumptions: (1) the hydrodynamic loading may be described using Stokes' expression for the drag per unit length on a circular cylinder oscillating at small amplitude and high frequency in unbounded fluid; and (2) the thermal noise is δ-correlated (i.e. the Brownian forcing has no memory), allowing equipartition of energy among *in vacuo* cantilever modes. Here we revisit both assumptions, (1) by determining the drag on a finite-length cantilever near a plane substrate, accounting both for the presence of the wall and the finite length of the cantilever, and (2) by using the fluctuation–dissipation theorem,[2] tested against new experiments, to examine how memory effects (associated with unsteady fluid inertia) influence thermal spectra.

Predictions of drag on a cantilever oscillating at small amplitude and high frequency are determined using the unsteady Stokes equations. The cantilever's slender geometry allows its motion to be described with a new formulation of slender body theory,[3] extended to account for unsteady inertia and the presence of a nearby wall. Two effects are shown to screen the cantilever from three-dimensional flows: high frequencies and proximity to the wall. This justifies the use of a simpler two-dimensional theory[4] that uses a boundary integral method to capture explicitly the shape of the cantilever's cross-section.

The fluctuation–dissipation theorem[2] allows the power spectrum of the cantilever tip's angle of deflection to be predicted directly from a deterministic simulation in which the cantilever is subject to a torque at its tip and then released. Analysis for a cantilever far from a wall reveals both discrete and continuous contributions to the spectrum (corresponding respectively to disturbances that decay exponentially and algebraically in time, the latter associated with unsteady fluid inertia). When compared to experiment, the fluctuation–dissipation approach is more accurate than previous methods,[1] particularly at frequencies below the first harmonic. Using our new drag predictions, validated against experiment, we also show how a nearby wall, and cantilever tilt, can both have a significant effect on the thermal spectrum.

*School of Mathematical Sciences, University of Nottingham, Nottingham NG7 2RD, UK
†DAMTP, CMS, University of Cambridge, Cambridge CB3 OWA, UK
‡School of Pharmacy, University of Nottingham, Nottingham NG7 2RD, UK

[1] Sader, J. E. *J. Appl. Phys.* **84**, 64 (1998).
[2] Paul, M. R. & Cross, M. C. *Phys. Rev. Lett.* **92**, 235501 (2004).
[3] Clarke, R. J. et al. *Proc. Roy. Soc. London* A (to appear) (2006).
[4] Clarke, R. J. et al. *J. Fluid Mech.* **545**, 397 (2005).

Stall Induced Vibration & Flutter In A Symmetric Airfoil

Sunetra Sarkar*, Hester Bijl†

This paper investigates the aeroelastic stability of a wind turbine rotor in the dynamic stall regime. Increased flexibility of modern turbine blades make them more susceptible to aeroelastic instabilities. Further, complex oscillation modes like flap/lead-lag are of particular concern, which give way to potential structural damage Chaviaropoulos (1999), Chaviaropoulos *et al.* (2003). We study the stall induced oscillations in pitching direction and in combined flapwise, lead-lag wise directions. The aerodynamic loads acting on the rotor body in the stall regime are nonlinear. We consider a wide ranging parametric variation and underline their effect on the aeroelastic instability and overall nonlinear dynamical behavior of the system. An engineering dynamic stall model (Onera) Tran and Petot (1981), Dunn and Dugundji (1992) has been used to calculate the aerodynamic loads. They represent the aerodynamic loads well in the dynamic stall regime and captures the bifurcation behavior and the chaotic routes of the aeroelastic system under study. The aerodynamic loads are given in terms of differential equations which are combined with the governing equations of the aeroelastic system; the resulting system of equations are solved by a $4/5^{\text{th}}$ order variable step Runge-Kutta method. Parameters considered for the pitching oscillation case are nondimensional airspeed (U), mean angle of attack (α_m), initial condition (α_{init}), structural nonlinearity (K_{nl}) and reduced frequency (k) and amplitude ($\bar{F}_0$) of external forcing. Both the self excited and forced system reveal existence of routes to chaos. For different α_m, period doubling routes to chaos have been obtained with different initial conditions. A cubic structural nonlinearity has been seen to alter the bifurcation pattern of the above system. Varying k as a bifurcation parameter in the forced system shows presence of period-3 orbits near chaos. The second case of flap/edgewise oscillation in the stall regime identifies nondimensional rotational speed of the rotor along with structural stiffnesses and nonlinearity as most important parameters of the self excited system. However, no chaotic response has been obtained. External forcing shows presence of higher harmonics and quasi-harmonics in the response. Once again, no chaotic attractor has been found.

Flap/lead-lag aeroelastic stability of wind turbine blade section. [1].

Viscous and aeroelastic effects on wind turbine blades. [2].

Nonlinear stall flutter and divergence analysis of cantilevered graphite/epoxy wing. [3]

Semi-empirical model for the dynamic stall of airfoils in view of the application to the calculation of responses of a helicopter blade in forward flight. [4]

*Aerospace Engineering Department, Technical University of Delft
†Aerospace Engineering Department, Technical University of Delft

[1] Chaviaropoulos, P., *Wind Energy* **2**, 99–112 (1999).
[2] Chaviaropoulos, P., *Wind Energy* **6**, 387-403 (2003).
[3] Dunn and Dugundji, *AIAA Journal* **30**, 153-162 (1992).
[4] Tran and Petot, *Vertica* **5**, 35-53 (1981).

A nonlinear model of the dynamics of a large elastic plate with heavy fluid loading

N. Peake [*], S.V. Sorokin[†]

We describe the derivation of a new model for the weakly nonlinear dynamics of a thin elastic plate of large extent under conditions of heavy fluid loading. This is a situation of considerable practical interest in marine engineering, in which the dynamic response of, for instance, a ship hull to unsteady excitation by vibrating machinery is crucially affected by the unsteady motion of the surrounding water, which is fully coupled to the motion of the hull itself. Much previous work has been done on models of finite elastic baffles, but we aim here to study the situation in which the baffle length is much longer than typical wavelengths, which allows us to consider an infinite plate and develop a model which is very amenable to analysis.

Two situations are considered. First, we consider the case in which transverse motion of the plate generates a weaker in-plane motion, which is in turn coupled back to the evolution of the transverse motion. This results in the familiar nonlinear Schrodinger equation for the amplitude of a transverse plane wave, and we show that solitary-wave solutions are possible over the range of (nondimensional) frequencies $\omega > \omega_c$, which depends on the material properties. Dimensional values of ω_c are physically realisable for a typical composite material underwater. Second, we consider the case in which the amplitudes of the transverse and in-plane motion are of the same order of magnitude, possible at a single resonant frequency, which leads to an evolution equation of rather novel type. We find a range of travelling-wave solutions, including cases in which incident in-plane waves can generate localised regions of transverse displacement.

Although formulated initially for a simple plate, our nonlinear theory will also be extended to the case of materials of sandwich construction. The issue here is that the in-plane and transverse motions of the sandwich panel are coupled even at linear order, leading to an unexpected relationship between the in-plane panel motion and the fluid loading. Furthermore, the inclusion of a mean fluid flow above the plate is known to have a significant effect in the linear regime, leading for instance to possible divergence instability. The effect of the inclusion of nonlinearity, and in particular the way this instability saturates, will also be considered.

[*]Department of Applied Mathematics & Theoretical Physics, Centre for Mathematical Sciences, Wilberforce Rd., Cambridge CB3 0WA. UK

[†]Centre for Machine Acoustics, Institute of Mechanical Engineering, Aalborg University, Pontoppidanstraede 101, DK9220, Aalborg, Denmark.

Vortex-induced vibration of a splitter plate: Effect of plate material

Tero Pärssinen, Hannu Eloranta and Pentti Saarenrinne

Flow separation from the trailing edge of a flat plate in a convergent channel involves a fluid-structure interaction (FSI) modifying the fundamental instability related to vortex shedding. Under certain conditions, the FSI introduces cellular vortex shedding from the trailing edge due to a standing wave mode of the flat plate, leading to strong spanwise variation of flow properties. This paper provides measurements of the effect of the plate material on the nature of the FSI. Experimental techniques including High –Speed Digital Imaging (HSDI), used to measure the response of the plate, and Particle Image Velocimetry (PIV), used to measure flow fields in the near wake (streamwise – spanwise plane), are utilised. Combining data from these techniques, the development of the plate vibration frequency and the material effect thereafter can be addressed together with the imprint of the vibration (and FSI) in the flow.

The results show that over the measured Re number range, the vibrational response is modified due to material properties. Fig. 1 presents the response of the flat plates with three different materials measured with HSDI. Both the vibration frequency of the plate (*f*) and the corresponding St number, based on free-stream velocity (U_E), trailing-edge thickness (D) and vibration frequency of the plate (f) are presented. The frequencies in the plot correspond to the dominating peak in the spectrum at given Re number. As the Re number is increased, the frequency of the dominant vibration mode does not increase linearly. The vibration locks to a rather constant frequency over a range of Re numbers. After certain Re number threshold is exceeded the frequency jumps to a new lock-in region. This behaviour is explained by the natural frequencies of the combined fluid-structure –system. At the discontinuity the FSI system drifts out of equilibrium and finds the next state sustained by the instability. With increased mass ratio and stiffness the vibration frequencies are higher, the amplitudes lower and the FSI system is less susceptible to excitation. The average St number increases and drifts away from the theoretical value of a fixed body.

Tampere University of Technology, Energy and Process Engineering,, P.O.Box 589, FIN-33101
tero.parssinen@tut.fi

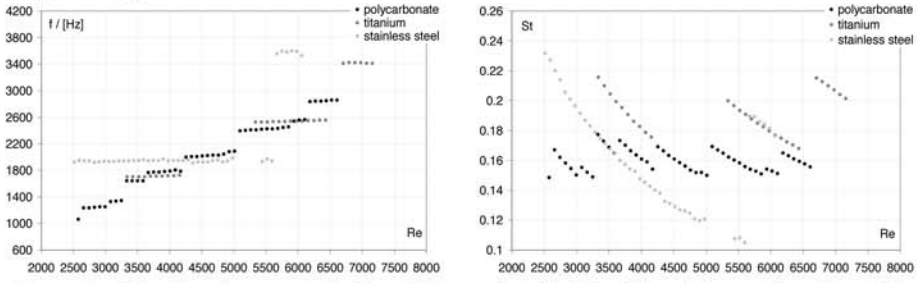

Figure 1: Vibration frequency (left) and St number (right) of the plate as a function of Re.

Experimental investigation of wind turbine wake meandering

D. Medici*† and P. Henrik Alfredsson*

It is well known that vortex shedding may occur behind bluff bodies, the most well known example is the two-dimensional Karman vortex street behind a circular cylinder. Also three-dimensional bodies, such as a circular disc, can give rise to vortex shedding, which is seen as a low frequency meandering of the wake. It has also been observed from measurements behind full-scale wind turbines that low frequency variations occur in the wake, suggesting that large scale vortex shedding occurs also behind wind turbines. The only wind tunnel data that has been provided on wake meandering behind wind turbines is from KTH Mechanics[1]. Wake meandering in a wind farm can be important with respect to the interaction between wakes and a downstream turbine. Previous numerical studies[2] have shown the dependency of the wake stability on the axial interference factor (normalised velocity defect at the rotor), the tip-speed ratio (tip speed/wind speed) and the blade circulation. The wind tunnel measurements found a strong meandering of the wake with a low frequency (f). The Strouhal number, i.e. the frequency f normalised with the freestream velocity and the turbine diameter, was found to be independent of the freestream velocity or turbulence level. However the meandering was only observed when the tip-speed ratio (or equivalently the drag coefficient) was high. The dependency of the Strouhal number with the blade passage frequency (bpf) is shown in figure 1 for a wind turbine model with two and three blades ($N = 2, N = 3$). The data group together accordingly to the value of the blade pitch angle (the angle between the blade chord and the rotor plane) and show a dependence with the drag coefficient which increases with the *bpf*. The one bladed turbine did not give rise to any meandering motion, but its blade passage frequency was low compared to the other turbine models.

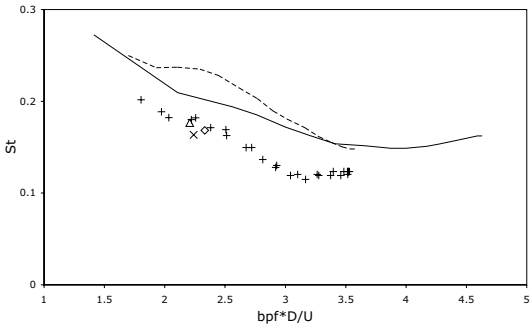

Figure 1: Strouhal number versus the normalised blade passage frequency. Blade pitch angle 8°, $N = 2$: single points. Blade pitch angle 11°: dashed line: $N = 2$, solid line: $N = 3$.

*KTH Mechanics, SE-100 44 Stockholm, Sweden.
†present address: Garrad Hassan & Partners Ltd., Bristol, BS2 0QD, UK

[1]D. Medici, *Doctoral thesis, TRITA-MEK Tech. Rep. 2005:19* (2005).
[2]V. L. Okulov and J. N. Sørensen, *In Proc. XX ICTAM, Warsaw, Poland* (2004).

Feedback control in spatially growing boundary layers

M. P. Chevalier*, J. Hœpffner†, E. Åkervik† and D. S. Henningson†

Linear feedback control has been applied to transitional boundary layer flows. Information from wall-mounted sensors is used to estimate the flow state. The estimated state is then used to compute the optimal feedback control which is applied as blowing and suction with zero net mass-flux through the wall.

The performance of the combined controller and estimator[1], also known as a compensator, is tested in direct numerical simulations of parallel and spatially growing boundary layers for some typical transition scenarios. The extension to spatial boundary layer flows is an important step toward real applications. In figure 1(a) the wall-normal disturbance velocity is shown in a Falkner–Skan–Cooke boundary layer where traveling cross-flow vortices[2] are triggered upstream in the flow. In figure 1(b) the flow is controlled by means of a compensator where the measurement region is located at $x_m = [40, 150]$ and the control region is located at $x_c = [175, 325]$. For this particular flow exponential disturbance growth is turned into exponential decay over the control area. Downstream of the control area the disturbance starts to grow again due to the inherent instability in the flow.

By applying control to such flows with strong inherent instabilities, through sensors and devices acting only on small parts of the flow, one may achieve dramatic effects by only minute amounts of control energy expenditure. Such control devices can be used in a wide variety of applications, for example, maintaining laminar flow on aircraft wings, relaminarizing/decreasing drag in turbulent flows and enhancing mixing in turbulent flows.

*Department of Computational Physics, The Swedish Defence Research Institute (FOI), Stockholm, Sweden

†Department of Mechanics, Royal Institute of Technology (KTH), Stockholm, Sweden

[1] Hœpffner et al. *J. Fluid Mech.* **534**, 263 (2005).

[2] Högberg and Henningson *J. Fluid Mech.* **470**, 151 (2002).

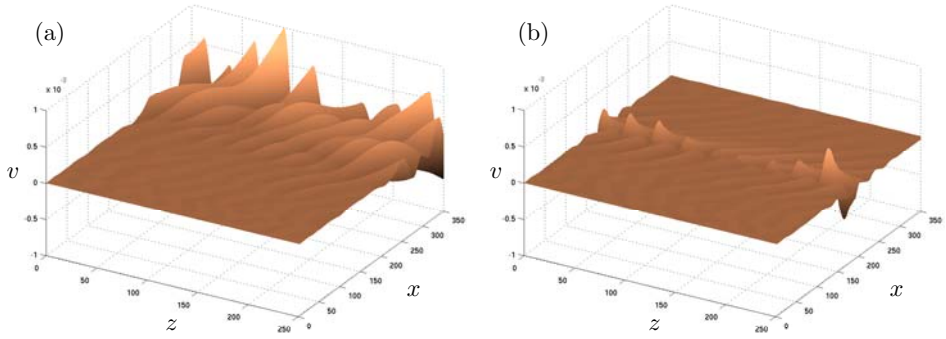

Figure 1: The wall-normal disturbance velocity at $y = 0.5$ for the (a) uncontrolled case and (b) controlled case.

Wiener filters in active-feedback drag reduction of turbulent channel flow

P. Luchini*, M. Quadrio†, T. Bewley‡

Feedback control of developed turbulence was first demonstrated[1] in the form of an instantaneous and pointwise opposition control with an empirically adjusted coefficient. Högberg & Bewley[2] then applied modern optimal control to the linearized Navier-Stokes equations in order to develop a spatially localized convolution kernel and tested the controller so obtained on a turbulent DNS with encouraging results. Quadrio & Luchini[3] suggested that a larger amount of physical information could be embodied in the controller if the linearized problem was replaced by a linear response of the full turbulent flow to external disturbances, and presented preliminary results for the computation of such linear response from a DNS.

Luchini et al.[4] presented an optimal controller based on the linear response of the turbulent flow, and announced the first successful test of such a controller on the DNS of a fully developed turbulent flow. There it was emphasized that the standard optimal-control approach based on Kalman filters and matrix Riccati equations does not apply to this problem because the state equations of the system are not available, and because the noise to be damped is composed of the actual turbulent fluctuations rather than a white noise.

The impasse was overcome by replacing the Kalman filter with a Wiener filter (known to be theoretically equivalent, but based on the input-output response rather than on state equations). For this purpose an original technique was developed in order to transform the control problem into a filtering problem, in a similar way as the so-called "separation principle" does in Kalman's approach.

In this conference the Wiener-based optimization technique will be illustrated, and its drag-reduction potential explored. Following the initial test, the technique has been applied to several possible feedback configurations involving one or all velocity components at the wall as actuators and one or all stress components as sensors. Attention has also been paid to comparing the energy gain offered by the drag reduction with the energy spent to operate the actuators themselves. A key ingredient has been the adoption of the dissipation rather than the kinetic energy as optimization objective.

A numerical version of the Wiener-Hopf method allowed us to quickly compute the controller convolution kernel corresponding to any given set of physical quantities chosen as actuators and sensors.

*DIMEC, Università di Salerno, 84084 Fisciano, Italy.
†DIA, Politecnico di Milano, 20158 Milano, Italy.
‡Dept. MAE, University of California San Diego, U.S.A.

[1] Choi et al. *J. Fluid Mech.* **262**, 75 (1994).
[2] Högberg & Bewley, Automatica (2001).
[3] 9th Eur. Turbulence Conference, Southampton 2-5 July 2002.
[4] 58th APS-DFD meeting, Chicago 20-22 Nov. 2005.

A Deterministic Model of Sub-layer Streaks for flow control

P.W. Carpenter[a], R. Ali[a], K. Kudar[a] and C. Davies[b]

Sub-layer streaks are well-known features of the near-wall region of turbulent wall layers. They are widely considered to play a crucial role in creating and maintaining the high wall shear stress and turbulence levels that characterize such turbulent flows. In particular, high levels of wall shear stress are generated when the streaks 'burst'. In applications of boundary-layer control there is frequently interest in reducing the levels of skin-friction drag but, also, sometimes the aim is to raise turbulence levels in order to delay flow separation. In the first example this implies suppressing the growth of sub-layer streaks, whereas in the latter case we would seek to enhance their growth. A simple deterministic model of the sub-layer streaks would be very useful for assessing the impact of flow-control techniques.

Our simple deterministic model is based on an analogy with Klebanoff modes and was originally introduced to study the control of sub-layer streaks by means of pulsed microjets[1]. The streaks are created in a numerical simulation based on a linearized version of our velocity-vorticity formulation of the Navier-Stokes equations[2]. They are generated by forcing the undisturbed turbulent boundary layer at a selected location above the wall by a spanwise varying body force (equivalent to a source of streamwise vorticity) for a short fixed duration. The body force/vorticity source generates an array of streamwise vortices that alternate in sign in the spanwise direction. These act as an approximate model for the streamwise ('hairpin') vortices in the near-wall region that in turn generate the streaks. The simulated streaks continue to grow after the vorticity source is switched off before finally reaching a maximum and subsequently decaying. The strongest streaks are found by optimizing the spanwise wave-length of the forcing and its wall-normal location. These strongest streaks are assumed to correspond to the most commonly found streaks in the turbulent wall layer; their optimal spanwise wave-length agrees well with the experimentally determined statistically averaged mean spanwise spacing of the sub-layer streaks. The use of a linear model for the streaks in flow-control applications finds support in the recent work of Lee and Kim[3]. We shall present examples of the application of the model to flow control by means of compliant walls and polymer additives.

[a] School of Engineering, University of Warwick, Coventry, England, CV4 7AL, U.K.
[b] School of Mathematics, Cardiff University, Senghennyd Road, Cardiff, Wales, CF24 4AG, U.K.

[1] Lockerby *et al. AIAA Journal* **43** (9), 1878 (2005).
[2] Davies and Carpenter *J. Comp. Phys.* **172**, 119 (2001).
[3] Lee and Kim *Phys. Fluids* **14**, 2523 (2002).

Heat transfer in turbulent channel flows with roughness on one wall.

S. Leonardi*, P. Orlandi & R.A. Antonia†

In laminar flows, the convective heat transfer can be augmented or reduced only by changing the transporting fluid. In turbulent flows a reduction or an increase of the heat transfer can be achieved by changing the vortical structures near the walls. Passive or active means can be used to modify the turbulence close to the wall. In the present study the effect of passive means such us roughness elements is considered. Direct numerical simulations of a turbulent channel flow with roughness on the bottom wall are carried out using square, circular and triangular roughness elements. A variety of w/k values has been investigated, (w is the cavity width, and $k = 0.1h$ the roughness height). To avoid very fine grids at high Pr, and resolve temperature scales smaller than the velocity scales, Pr has been taken equal to 1. The Navier-Stokes equations have been discretized in an orthogonal coordinate system using a staggered second-order finite-difference approximation. To deal with different types of wall geometries, an accurate method consists in maintaining the equations in orthogonal coordinates and approximate the complex wall geometry by the immersed boundary method. The roughness elements on the bottom wall induce a recirculating flow within each cavity. The strength of the recirculation depends on the shape of the elements, the most intense occurring with triangular elements, the weakest with square elements. The normal velocity induced by the elements at the plane of the crests is proportional to the strength of the recirculation and hence depends on the shape of the elements and this is the driving factor contributing to the changes of the vertical structures of the overlying flow. It is larger for triangular elements and smaller for square elements.

Figure 1: Instantaneous visualizations of passive scalar fluctuations, $\theta = 0.8$ superimposed on contours of wall–normal velocity fluctuations.

Due to the larger normal velocity at the roughness crest plane, the passive scalar is transported further away from the wall with the triangular elements. For square elements, the iso-surface has weak undulations similar to those observed near a smooth wall, thus underlying the weak communication between the cavities and the overlying flow.

*Dip. Mecc. Aer. Università di Roma "La Sapienza" Rome, Italy
†Discipline of Mechanical Engineering, University of Newcastle, NSW 2308 Australia

Effects of drag reducing polymers in turbulent rotating channel flows

C. Tesauro*, M.A. Hulsen† and B.J. Boersma*

This work builds on previous work carried out in our group[1], where drag reduction has been analyzed in turbulent channel flow. Polymers are modeled using elastic dumbbell theory, which helps to derive an evolution equation to be used for the polymer stress. The constitute equation is solved simultaneously with the Navier-Stokes equations in a rotating frame of reference. Results of Newtonian rotating flow are in good agreement with the literature[2]. Results of the DNS show that polymers are able to decrease the frictional drag also in rotating channel flow, the profile of the mean velocity are shifted up-wards parallel to the Newtonian profile and the drag reduction decreases increasing rotation (fig. 1). At lower rotation, polymers are preferred oriented in the stream-wise direction: this component of the polymer conformation tensor is very high, and the values reached by other components are much lower. However, these values increase increasing rotation, as effect of secondary motions of the flow (fig. 2).

*TU Delft, 2628CA Delft, The Netherlands.
†Eindhoven University of Technology, 5600 MB Eindhoven, The Netherlands.
[1]Ptasinski et al., *J. Fluid Mech.* **490**, 251 (2003).
[2]Kristoffersen and Anderson, *J. Fluid Mech.* **256**, 163 (1993).

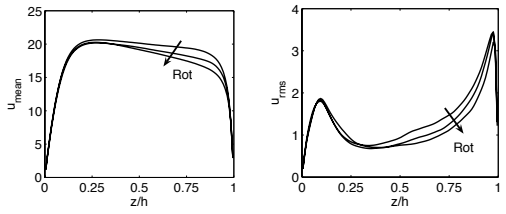

Figure 1: Profiles of the mean (a) and root mean square (b) velocity as function of the distance from the wall.

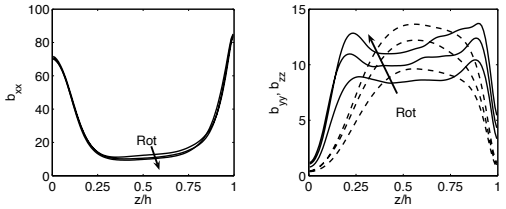

Figure 2: Profiles of stream-wise (a), span-wise (b, solid line) and wall-normal (b, dashed line) polymer conformation tensor component as function of the distance from the wall.

Control over the splitting of a liquid jet using two-frequency excitation

J. F. Olsen[a]

This work documents the effects of two-frequency, axial excitation applied to a liquid jet operating in the Rayleigh regime. From previous work[1], we know that excitation applied at a single frequency f_e within the range $f/2 < f_e < 3f/2$ (where f is the natural instability frequency of the jet), improves the organisation of both the size and spacing of drops that breakaway from the end of the intact jet column. Also within this range, the passage frequency of drops f_p equals f_e. At lower excitation frequencies, viz. $f/3 < f_e < f/2$, $f_p = 2f_e$ and we occassionally observe that the spacing between drops is uneven. Flow visualisations show that this uneven spacing can give rise, possibly through aerodynamic effects, to collisions between drops which can cause the flow to split into two separate streams at some location downstream of the breakaway location.

To gain control over the initial spacing between drops, excitation is applied at two frequencies simultaneously, i.e. at $f_e = f + (f/2 + \phi)$ (where ϕ is the phase difference between the two excitation frequencies). Figure 1 shows signals which represent the passage of drops measured just downstream of the drop breakaway location. When the excitation phase difference is in the range $40^O < \phi < 80^O$, we observe reasonably stable jet splitting. The signals indicate that the initial spacings between alternate drops are periodic but uneven (i.e. alternately close and far apart). Outside this range, the jet does not split and so the drops fall along the axis of the jet. The signals in this range show an increase in the spacing between alternate drops, though in many cases, it is difficult to clearly distinguish the drops pairs. Work is still continuing on further stabilising the jet splitting. At this stage, we believe that the presence of a helical instability also has some influence.

[a] School of Mechanical and Manufacturing Engineering, UNSW, Sydney NSW 2052, Australia.

[1] Olsen, PSFVIP-5-242, (2005).

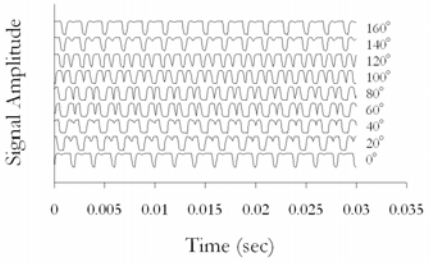

Figure 1. The effect of ϕ on drop spacing

Constraints for the Pressure-Strain Correlation Tensor Derived from Spectral Representation

S.R.Bogdanov[a], T.J.Jongen[b]

The Reynolds stress closure problem is strongly related to the problem of modelling of the pressure-strain correlations. Although derived from physical considerations, these correlations are essentially semiempirical, heuristic and approximate. As a result, one cannot guarantee that the equations will always lead to physically correct solutions. For example, the so-called realizability criteria (Reynolds stress tensor $<u_\alpha u_\beta>$ is positive definite) are often violated, and the area of validity is difficult to predict.

On the other hand, simple constraints on the components of the mean flow-induced part $\mathbf{\Phi}$ of the pressure-strain correlation tensor can be derived from the spectral representation of this tensor, giving the opportunity to check the models a priori before any complicated analytical or numerical solution step. The constraints are based on the fact that the spectral tensor $\mathbf{F}$ of the two-point velocity correlations is positive definite: $F_{ij}\,\xi_i\,\xi^*_j > 0$, where ξ_i denotes an arbitrary complex vector, and the star (*) denotes the complex conjugate.

When the vector ξ does not depend on the wave vector $\mathbf{k}$, the integration of the inequality on all $\mathbf{k}$ leads to the mentioned realizability conditions. When choosing $\xi_i = U_{ij}\,\theta_j$, with $\theta_j = k_j/k$, a similar procedure leads to the new constraints on the product $\{\mathbf{\Phi U}\}$ and the double inequality, connecting Reynolds stress tensor components and the set $\{C_i\}$of the model constants. As a result maps of "allowed areas" can be derived for any model. Examles are presented by fig. 1 for the well-known models SSG[1] and LRR[2]. On the other hand, the mentioned constraints give also simple restrictions for the set of the constants, in particular $4 - C_3 > C_2 > 2\,C_3/3$.

---

[a] Karelian State Pedagogical University, Petrozavodsk, 185680, Russia.

[b] Unilever Research, P.O. Box 114, 3133 AT Vlaardingen, The Netherlands.

[1] Speziale et al. *J. Fluid Mech.* **227**, 245 (1991).

[2] Launder et al., *J.Fluid Mech.* **68**, 537 (1975).

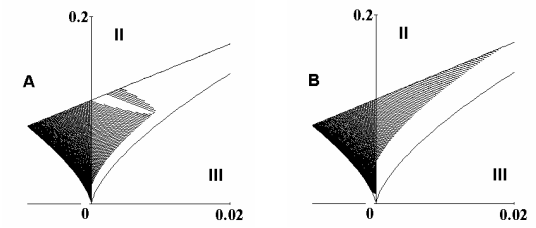

Figure 1: Examples of the "allowed areas" for SSG (A) and LRR (B) models.

A two-point closure based on a Lagrangian timescale

W.J.T. Bos and J.-P. Bertoglio*

Analytical theories of turbulence are known to provide a substantial contribution to the understanding of turbulence and in particular to its interactions with mean velocity gradients or external effects such as rotation or buoyancy. For example, the Lagrangian History Direct Interaction Approximation[1] is a self consistent theory, free of any ad-hoc constant, that leads to predictions of the kinetic energy spectrum, compatible with a $K^{-5/3}$ inertial range. The equations of this closure are very complex and depend on the entire Lagrangian history of the flow. In contrast, single-time two-point closures, like the Eddy Damped Quasi-Normal Markovian theory (EDQNM), are less complicated. Single-time closures can be obtained from two-time theories by assuming an exponential decay of both the response function and the two-time correlations. The EDQNM closure contains an unknown function, the eddy damping. This damping corresponds to the inverse of the correlation time of the turbulent velocity field. In the framework of a Lagrangian formulation of the theories, this correlation time can be defined along fluid particle trajectories. A definition, corresponding to LHDIA for isotropic turbulence, is (Kraichnan[1]):

$$\tau(K,t) = \int_0^t \frac{E(K,t|s)}{E(K,t)} ds \tag{1}$$

with $E(K,t)$ the energy spectrum and $E(K,t|s)$ the Lagrangian two-time spectrum. Generally, in single-time closures, this time scale is determined by dimensional analysis or crude physical assumptions, introducing one or more constants.

In the present communication, we propose to use equation (1) to build a single-time closure free of these ad-hoc assumptions. To express $E(K,t|s)$, we work with the one-time two-point fluid particle displacement-velocity correlation $< a_i(\mathbf{x},t)u_j(\mathbf{x}+\mathbf{r},t) >$. An analogy between the displacement of a fluid particle and a non-diffusive scalar in the presence of a uniform scalar gradient, allows to use existing closure equations[2] to calculate the turbulent timescale (1). The resulting closure yields, as shown in the figures, inertial range spectra in agreement with classical Kolmogorov theory.

*Laboratoire de Mécanique des Fluides et d'Acoustique, UMR CNRS 5509 - Ecole Centrale de Lyon, France

[1]R.H. Kraichnan, *Phys. Fluids* **8**, 575 (1965).

[2]W.J.T. Bos, H. Touil, and J.-P. Bertoglio, *Phys. Fluids* **17**, 12 (2005).

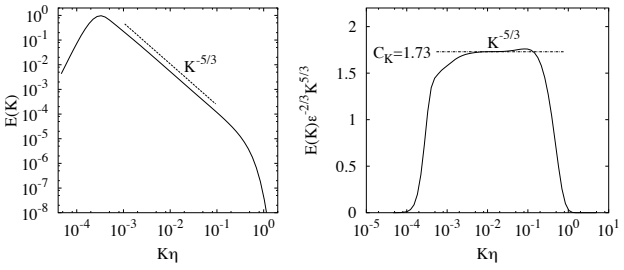

Anisotropic velocity fluctuations in a homogeneous shear flow

P. Gualtieri*, B. Jacob †, C. M. Casciola *, R. Piva*

In turbulence it is often assumed that large scale anisotropic effects are progressively lost during the process of energy cascade towards the smaller scales where isotropy is eventually recovered. Based on these ideas the Kolmogorov theory provides the framework of many closure models for RANS and LES. However, close to solid walls, the range of scale where energy transfer prevails is limited by the distance from the wall and a substantial anisotropic range exists. As a consequnce also small scales quantities such as the energy dissipation tensor $\epsilon_{\alpha,\beta} = 2\nu < \partial u_\alpha/\partial x_\gamma \partial u_\beta/\partial x_\gamma >$ are found to be affected by strong anisotropic effects.

Purpose of this contribution is to provide a systematic analysis of the anisotropic velocity fluctuations via the SO(3) decomposition of longitudinal structure functions measured in a homogeneous shear flow[1] [2] ,see figure 1 (left). Actually, a strong shear is able to modify scaling laws of the isotropic component, see figure 1 (right). We show here that the anisotropic sectors are affected by the shear leading to a different hierarchy for the scaling exponents which controls the process of isotropy recovery at small scales. This implies that significant anisotropic effects appear in the correlarion $< \delta u_\alpha \delta u_\beta > /r_\gamma r_\gamma$ which, in the limit $r \simeq \eta$, determine the nature of the energy dissipation tensor $\epsilon_{\alpha,\beta}$.

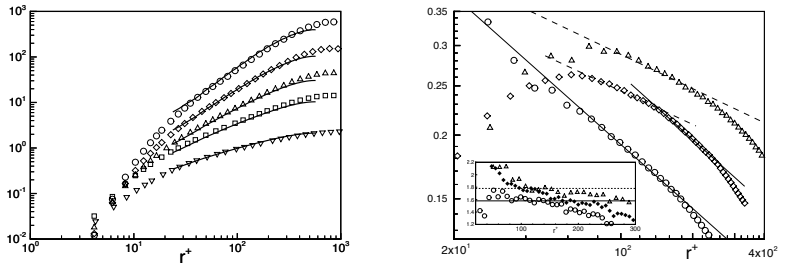

Figure 1: Left: different moments of longitudinal structure functions for the experimental data (symbols) and corresponding LES data (lines). In the experiment $S^* \simeq 8$ and $Re_\lambda \simeq 220$. In the LES $S^* = 7$ and $Re_\lambda = 150$. Right: isotropic projection for the sixth order longitudinal structure function $S_{00}^{(6)}/r^2$. High shear (circles), Low shear $S^* = 2.2$ (triangles) and intermediate shear $S^* = 5$ (diamonds). The slope of the solid line is -0.42 corresponding to $\zeta(6) = 1.58 \pm 0.08$. The slope of the dashed line is -0.22, i.e. $\zeta(6) = 1.78 \pm 0.08$. In the inset local slopes

*Dipartimento di Meccanica e Aeronautica, Università di Roma *La Sapienza*, Via Eudossiana 18, 00184 Roma, Italy

†INSEAN, Via di Vallerano 128, Roma Italy

[1] Casciola, C.M., Gualtieri, P., Jacob, B., Piva, R., *Phys. Rev. Lett.* **95**,(2005).

[2] Jacob B., Biferale, L., Iuso, G., Casciola, C.M. *Phys. Fluids* **16**, (2004).

Measurement of velocity-pressure correlation in a free shear flow

Y. Naka*, S. Obi* and S. Masuda*

Simultaneous measurement of fluctuating velocity and pressure has been one of challenging issue of experimental fluid dynamics. Recently, several successful attempts by using the technique which was developed by Toyoda et al.[1] were reported.

In our previous study[2], the technique was extended to estimate pressure-diffusion terms of transport equation of Reynolds stress in a plane turbulent mixing layer, where a miniature static pressure probe was combined with an X-wires hot-wire anemometry. The balance of the representative terms for $\overline{uv}$ component are demonstrated in Fig. 1(a), where the measured values coincide well with the DNS result[3].

In order to confirm the applicability of this technique, the spatial resolution is further investigated in the present study. Fig. 1(b) indicates the profile of correlation coefficient between two streamwise velocity components as a function of the spanwise distance between the probes Δz at three different streamwise locations; integral length scale $\mathcal{L}$ was also evaluated. At x=100mm, $\mathcal{L}$ = 1.93mm and this was equal to the probe distance. As it moves upstream, $\mathcal{L}$ decreases to 1.31mm at x=50mm and further down to 1.15mm at x=25mm.

In the presentation, further achievement will be included. The effect of distance between the pressure- and velocity-probes is estimated in terms of integral length scales as well as spectral characteristics. The probes are carefully arranged to achieve high spatial resolution while avoiding mutual interference by them. Based on these considerations, criteria for the probe distance will be provided.

*Department of Mechanical Engineering, Keio University, Yokohama, 223-8522, Japan.

[1]Shirahama and Toyoda, *Trans. JSME, Series B* **59-567**, 3381 (1993), in Japanese.
[2]Naka et al., *Proc. 4th Int. Symp. on Turbulence and Shear Flow Phenomena*, 1125 (2005).
[3]Rogers and Moser, *Phys. Fluids* **6**(2), 903 (1994).

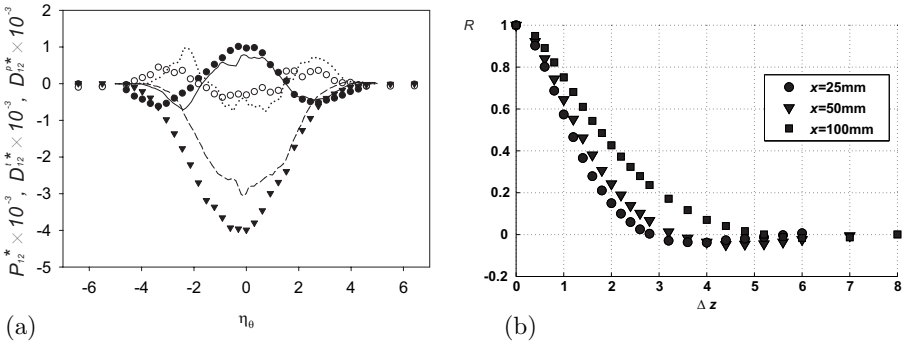

Figure 1: (a) Estimated turbulent-diffusion D_{12}^t and pressure-diffusion D_{12}^p; Symbols • : D_{12}^t, ○ : D_{12}^p, ▼ : P_{12}, —— : D_{12}^t (DNS), · · · · · : D_{12}^p (DNS), - - - - - : P_{12} (DNS). (b) Correlation coefficient in the developing region of a turbulent mixing layer.

Turbulent channel flow analysis by a statistical method

A. Pozzi*, R. Tognaccini*

The state of the art of the available methods for the simulation of turbulent flows is well described in[1]. Methods which do not depend on empirical correlation are not expected to be operative for practical calculations in the near future.

Statistical methods are a possible alternative. However accurate methods not relying on empirical results and sufficiently fast are still missing. A stochastic formulation not requiring empirical information was performed in the last century by Hopf and improved by others; this theory can be found in many books, for instance[2]. Stanisic writes: "Remains much more to learn in functional calculus in connection with computer technology; and we hope that in the near future such technical difficulties in computer technology will overcome. If this occurs, then probably among all the others only Hopf's formulation of turbulence will be retained, since this is the only exact formulation in the entire field of turbulence".

In the present paper we propose a method for the analysis of turbulent flows based on the probability equation derived by Hopf. This equation provides the probability, at a given time, of a velocity field among the infinite possible fields. The analysis of the motion of an incompressible fluid in a spatial domain R is articulated in two fundamental steps. At first, the phase space S is introduced; the elements of S (phases) are all the possible instantaneous velocity fields which are solenoidal and satisfy the boundary conditions on the boundary of R. A *complete* definition of S is obtained by a suitable series expansion of orthogonal functions satisfying the required properties. The coefficients of this expansion are unknowns, they are random variables.

The second part of the analysis concerns with the technique to adopt for solving the probability equation. Hopf proposed, as unknown, the characteristic functional F determining the probability distribution of each phase. Hopf (and others) looked for the possibility to derive a series expression for F, but, unlikely, the equation for the *n-th* approximation depended on the approximation $n+1$ (the typical closure problem in the analysis of turbulent flows). Therefore, until now, no solution has been found for the Hopf's equation.

In our work we assume, as unknown, the probability function. All the infinite weight coefficients of each phase are considered random variables with a probability distribution characterised by two unknowns: average value and standard deviation. In this way the probability equation leads to a homogeneous complex algebraic system of equations. The number of the unknowns depends on the specified order of approximation.

As example of application of the method we consider the flow in a 2D channel by assuming 2D turbulence. By using suitable expansions we reduce the problem to a system of algebraic second degree equations whose coefficients and the pertinent solution can be analytically obtained.

*Università di Napoli Federico II, 80125 Naples, Italy.

[1]Spalart, *Int. J. Heat Mass Transfer* **21**, 252 (2000).

[2]Stanisic, *The Mathematical Theory of Turbulence* (1985).

Acceleration Statistics in Turbulence

Yoshiyuki Tsuji*and Takashi Ishihara†

Pressure is a fundamental quantity contained in the dynamical equation of fluid motion. In a usual notation, pressure relates to the acceleration vector: $\mathbf{a} = D\mathbf{u}/Dt = -\nabla(p/\rho) + \nu\nabla^2\mathbf{u}$. This means that acceleration is decomposed into the contributions from the pressure gradient and viscous force while the fluid density (ρ) is constant. Although the acceleration may be important and basic representation of fluid motion, and Lagrangian acceleration is the core of the kinematic theory of turbulent dispersion, its direct measurement was very difficult and has only recently been achieved in laboratory flow[1]. In this paper, we evaluate the acceleration by means of pressure fluctuation because, at large Reynolds numbers, the viscous contribution to the acceleration can be ignored. Accordingly, the acceleration is evaluated as the pressure gradient. Measured data are compared with direct numerical simulation[2].

The measurement of pressure fluctuation is accomplished with a small piezoresistive transducer, and a standard 1/8-inch condenser microphone. The probe is a standard Pitot-static tube measuring 0.5 mm in outside diameter and 0.05 mm in thickness. Four static-pressure holes (0.15 mm in diameter) are spaced 90° apart and located at a distance of 22 tube diameters from the tip of the probe to minimize sensitivity to cross-flow error [3]. The data were measured on the centerline in a free jet. The Reynolds numbers are in the range of $200 \leq R_\lambda \leq 1200$.

Figure 1(a) shows the spectra of pressure and acceleration measured by experiment for $R_\lambda \simeq 700$. In the inertial range, pressure spectrum indicates the $-7/3$ power-law behavior predicted by Kolmogorov. Fig. 1(b) is the probability density function of acceleration. Experimental result matches sufficiently with previous result[1]. These results encourage us to investigate more detailed statistics of acceleration, such as conditioned acceleration, Reynolds number dependence of acceleration variance, and the relation with velocity structure functions, which will be presented at the conference.

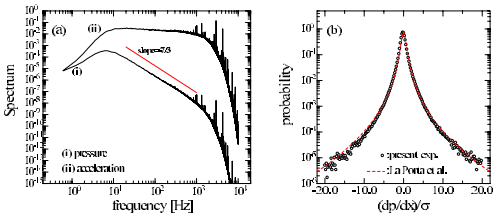

Figure 1: (a) Spectra of pressure and acceleration. (b) Probability density function of acceleration compared with [1].

*Department of Energy Engineering and Science, Nagoya University, Nagoya, Japan.
†Department of Computational Science and Engineering, Nagoya University, Nagoya, Japan.

[1] A. La Porta et al., *Nature* **409**, 1017 (2001)
[2] Y. Tsuji and T. Ishihara, *Phys. Rev. E* **68**, 026309 (2003).
[3] Y. Tsuji, J. Fransson, H. Alfredsson, A. Johansson, Proceedings of TSFP4, 27,(2005)

Focusing of strong shocks in an annular shock tube

V. Eliasson*, N. Apazidis* and N. Tillmark*

Two methods to produce converging shocks of different shapes are investigated experimentally and numerically. The experiments where performed in a horizontal annular shock tube at KTH Mechanics. First, a plane shock wave is created and is then transformed into an annular shock wave which is focused in a thin test section mounted at the end of the shock tube.

The first method to shape the shock wave is to change the outer boundary of the test section. So far, four different shapes of outer boundaries have been used; a circle, a smooth pentagon, a heptagon and an octagon. The second method is to place disturbance elements in the flow. The disturbance elements consist of cylindrical rods with different diameters. The cylindrical rods create disturbances in the flow and make it possible to shape the shock wave in a desired manner. In figure 1 (a) and (b) the octagonal outer boundary and a schlieren photograph of a shock wave obtained with this boundary are shown. In figure 1 (c) and (d) the template used for obstacle positioning and an example of a schlieren photograph from a case with eight obstacles placed in an octagonal pattern can be seen.

Results confirm that regular polygonal converging shock waves keep reconfiguring at successive intervals. An octagonal shock wave transforms into a double-octagonal form and then back to an octagonal form again. It is the nonlinear coupling between the shape of the shock wave and the velocity of the shock propagation that causes this behavior. Concave parts of the shock wave travel faster than the plane parts of the shock which leads to the reconfiguring and reorientation process. It is also shown that a cylindrical shock wave is unstable and is easy to perturb. The results are in agreement with earlier experimental[1] and analytical results[2].

*KTH Mechanics OB 18, SE-100 44 Stockholm, Sweden.

[1]Takayama et al., *Exp. Fluids* **5**, 315-322 (1987).

[2]Schwendeman and Whitham, *Proc. R. Soc. Lond. A* **413**, 297-311(1987).

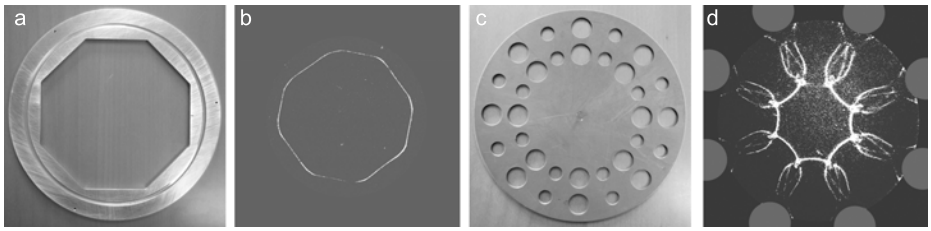

Figure 1: (a) Octagonal outer boundary. (b) Schlieren photograph with boundary in (a). (c) Template for obstacle positioning (d) Schlieren photograph from the case with 8 cylindrical obstacles placed in an octagonal pattern, the gray circles represent the obstacles.

Study of shock associated noise generated at jet engine exhausts

O. Rask[a], E. Gutmark[a], R. Szasz[b], L. Fuchs[b], S. Martens[c]

One way to reduce the noise generated by the exhaust jets is to use chevron nozzles which increase the exchange of momentum from the core stream to the fan stream, and from the fan stream to the free stream. This increased mixing leads to low frequency jet noise reduction. However, as a consequence of the more aggressive mixing, excess turbulence is created immediately downstream of the chevron nozzle. This results in a significant high frequency penalty. Over the past several years, chevrons have been studied extensively in subsonic flows. As an airplane climbs to higher altitude, the atmospheric pressure drops while the operating pressures in the engine remain constant. At a certain altitude, the exhaust jet will becomes under-expanded and will produce a series of quasi periodic shock cells. With respect to chevrons, this creates an entirely new set of conditions that has not yet been addressed in the literature. Broadband shock associated noise is created when turbulent structures pass through the quasi periodic shock cells of an imperfectly expanded jet. This type of noise radiates predominately at 90° and upstream relative to the direction of flow, or with respect to an airplane, straight at the cabin. As the jet noise associated with turbulent mixing is reduced, shock associated noise emerges as the predominant problem. Thus, it would be ideal if chevrons could be used to reduce both the jet noise associated with turbulent mixing and broadband shock associated with the under-expanded condition.

In this paper we use experimental and numerical tools to study the influence of the chevron nozzles on the noise generated by the exhaust jets at cruise conditions. In order to simulate cruise conditions, a free stream Mach number of approximately 0.80 was required. Since the test facility does not have the capability to create a third flow, the core stream is used to simulate the combined core *and* fan discharge of an aircraft engine, while the fan stream is used to simulate the free stream, or flight condition. To extend the experimental results to real flight conditions computational (LES based) tools are used. These are validated against the simplified experimental rig data mentioned above. The experimental results have shown that the jet noise will decrease with increasing flight speed when an aircraft engine is operated at constant power. This occurs because, as flight speed increases, the gradient of the fan/free shear layer is reduced, which in turn reduces the level of turbulence in that shear layer and thereby the jet noise it creates. The enclosed figure depicts the narrow-band spectrum at 150° for baseline nozzles at the four different cycle conditions. The results from the numerical computations are compared with the measured data. Two cases are considered, one with fan NRP (Nozzle Pressure Ratio) equals unity (i.e. no driving pressure for the fan) and the case with fan NRP=1.6, that yields a M=0.8 fan flow.

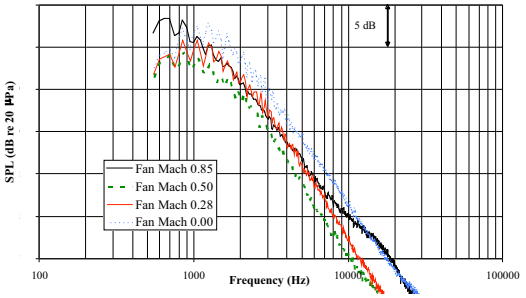

Figure 1: Baseline Configuration, 150°, Core Mach number = 1.18 (fully expanded)

[a] Div. Fluid Mech., LTH, SE-22100 Lund, Sweden.
[b] Dept. Aerospace Eng. and Eng. Mech., U. Cincinnati, Cincinnati, USA
[c] General Electric Aircraft Engines, Evendale, USA

Numerical simulation of supersonic jet noise

J. Schulze*, Ch. Schaupp* and J. Sesterhenn*

Shock-induced noise is generated by supersonic jets which are not perfectly expanded. This means that their nozzle exit pressure is above or below the ambient pressure. The flow adapts to the ambient pressure by a series of oblique shocks, compression and expansion waves. These interact with the shear layers, producing *shock-induced* or *shock-associated* noise. The issue of shock-induced noise is found to be of particular interest for civil and military aircraft propelled by jet engines at high subsonic or supersonic speeds. It adds a significant contribution to cabin noise in civil aircraft, especially in the forward sections of the cabin, and may lead to structural damage due to high dynamic loads.

To investigate this phenomenon a direct numerical simulation of a full supersonic, overexpanded jet, its acoustic field and its sound generation mechanisms is performed. Modelling the noise generated by such jets requires detailed knowledge about the sound generation mechanisms involved. The main challenge was to simultaneously resolve the small-scale nonlinear turbulent structures and, at the same time, the large-scale, small amplitude acoustic waves they produce. Hence the computational domain is limited and acoustic analogies like the one of Lighthill or Ffowcs Williams and Hawkings are used to enlarge the acoustic far field. In the present study a DNS of a three-dimensional supersonic mixing layer ($M = 1.44$) with an impinging shock (see fig. 1(a)) was computed on a grid with $768 \times 384 \times 72$ (approx. 21 million) points and a Reynolds number, based on the vorticity thickness at the inlet, of $Re_{\delta_\omega} = 2000$. In addition to this, the more realistic case of a plane three-dimensional overexpanded supersonic jet is calculated. The far field sound of both cases is compared to the DNS using the acoustic analogy based on both Lighthill's and Ffowcs Williams and Hawkings equation (see fig. 1(b)). This allows a detailed investigation of the noise generation mechanism at the shock tip.

*Fachgebiet Strömungsmechanik, Technische Universität München, 85748 Garching, Germany

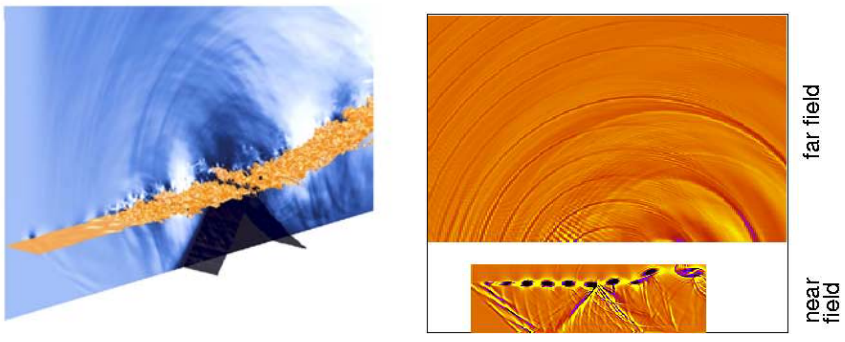

Figure 1: Interaction of a mixing layer with an oblique compression wave. *Left:(a)* DNS (isosurface $M = 1$ 3d and pressure 2d). *Right:(b)* Lighthill's solution (pressure).

Application of TVD and ENO schemes for solving the equations of compressible inviscid flow

M. Hajžman*, J. Vimmr*

This contribution is concerned about the comparison of the finite volume formulation of the explicit two-step MacCormack scheme with different types of artificial viscosity terms and of the finite difference ENO scheme. The explicit two-step MacCormack scheme with Jameson's artificial viscosity term and with TVD-type artificial viscosity term proposed by Causon[1] is defined on a structured quadrilateral non-rectangular grid. The finite difference ENO scheme is suitable only for calculations on regular Cartesian meshes, therefore the system of the Euler equations is remapped from the physical space to the rectangular computational space.

All above mentioned numerical schemes are applied for the solution of the high speed inviscid fluid flow through the upper half of a plane symmetric converging-diverging channel. At the inlet, the total pressure, the total density and the inlet angle were specified. At the outlet, all quantities were extrapolated.

The isolines of the Mach number obtained using the explicit two-step MacCormack scheme with Jameson's artificial viscosity are shown in figure 1(a). In figure 1(b), the pressure distribution along the channel wall computed using the MacCormack scheme with Jameson's artificial disipation (ploted with solid line) and using the TVD MacCormack scheme proposed by Causon (ploted with dashed line) are compared. Our numerical results computed using the finite volume formulation of the MacCormack scheme and the finite difference ENO scheme are compared with the results obtained by other authors[2].

*University of West Bohemia in Pilsen, Univerzitn´ 22, CZ-306 14 Pilsen, Czech Republic.
[1]Causon, *Notes on Numerical Fluid Mechanics* **24**, 63 (1989).
[2]Lilek, *Thesis* (1995).

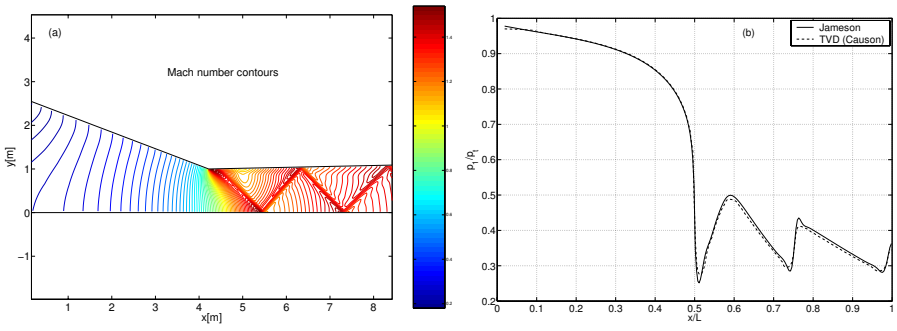

Figure 1: (a) Mach number contours in the upper half of a 2D symmetric converging-diverging channel. (b) Comparison of the pressure distribution along the channel wall.

Statistical features of the natural disturbances in supersonic boundary layer at the transition

A.D.Kosinov[a], A.I.Semisynov[a]

The natural disturbance experiments are executed in the flat plate boundary layer at Mach 2. Modified diagram technique is applied for pulsation decomposition in compressible flow. The method is more suitable for measurement by constant temperature anemometer and increases accuracy of estimations. Mass flow and temperature fluctuations and their relation are obtained in transition region of the supersonic boundary layer. Statistical diagram of pulsations from laminar to turbulent stage is obtained.

The investigations of laminar-turbulent transition in supersonic boundary layer are usually carried out in conditions of controlled and natural fluctuations. The experimental researches of stability of shear flows with the help of controlled disturbances allow to compare the obtained data to calculations and to develop theoretical models. To study late stages of laminar-turbulent transition it is necessary to use the joint approach, in parallel conducting researches of development of natural and controlled disturbances. In this case for detection of character of nonlinear interaction of natural disturbances use a high-order spectrum analysis[1], and simulate mechanism of this nonlinear interaction in controlled experiments[2]. Motivation of usage of this method at research of late stages of laminar-turbulent transition in a supersonic boundary layer is the absence of theoretical models of nonlinear interaction of waves and necessity of the substantiation of experiments with controlled disturbances. In the paper the experiments on natural disturbance development in flat plate boundary layer are executed at Mach 2. A modified diagram technique (Kovasznay's method[3]) in relation to constant temperature anemometer is proposed and applied for pulsation decomposition in compressible flow.

The study of the statistical characteristics of natural pulsations in supersonic boundary layer is carried out. Linear and nonlinear regime of transition is determined. The data indicates on the weak disturbance interaction in some regions of the turbulent boundary layer. Total temperature pulsations to mass flow pulsations ratio is not changed significantly during transition at $\rho U \approx const$.

[a] ITAM SB RAS, 630090, Novosibirsk, Russia

[1] Kendall and Kimmel. *AIAA paper*-91-0320. (1991)
[2] Kosinov et al.. *Nonlinear Instability of Nonparallel Flows*. Springer-Verlag, (1994).
[3] Kovasznay. *J. Aero Sciences*. **17**. (1950)

Axisymmetric stagnation flow obliquely impinging on a rotating circular cylinder with uniform transpiration

Asghar B. Rahimi[a] Vahid M. Nik[b]

The problem of finding exact solutions of the Navier-Stokes equations is a very difficult task. This is simply due to the fact that these equations are non-linear. However, it is possible to find exact solutions of Navier-Stokes equations only in certain particular cases. An exact solution of these equations governing the problem of two-dimensional stagnation flow against a flat plate has been given by Hiemenz[1]. Gorla[2] in a series of papers, studied the steady and unsteady flows over a circular cylinder in the vicinity of the stagnation-point for the cases of constant axial movement, and special case of harmonic of a non-rotating cylinder. Saleh and Rahimi[3] have considered the stagnation flow problem on a circular cylinder moving with time-dependent axial velocity when the free stream fluid is impinging on the cylinder normally.

In this paper the unsteady viscous flow in the vicinity of an axisymmetric yet obliquely stagnation point of an infinitely long rotating circular cylinder is investigated when the angular velocity varies arbitrarily with time. The outer stream with a constant strain rate of k is composed of a rotational axial flow superposed onto irrotational radial stagnation flow normal to the cylinder. The relative importance of these two flows is measured by a parameter γ. An exact solution of the Navier-Stokes equations is derived in this problem. The general self-similar solution is obtained when the angular velocity of the cylinder varies as certain functions. The cylinder may perform different types of motion: it may rotate with constant speed, with exponentially increasing/decreasing angular velocity, with harmonically varying rotation speed, or with accelerating/decelerating oscillatory angular speed. For completeness, some sample semi-similar solutions of the unsteady Navier-Stokes equations have been obtained numerically using a finite-difference scheme. These solutions are presented for special cases when the time-dependent is step-function, linear, and non-linear with respect to time. All the solutions above are presented for Reynolds numbers, $\mathrm{Re} = ka^2 / 2\nu$, ranging from 0.1 to 1000 where a is the cylinder radius and ν is kinematic viscosity of the fluid. Shear stresses corresponding to all the cases increase with the Reynolds number. An inner-outer analysis is also used for the cases of high Reynolds numbers. The maximum value of the shear-stress increases with increase of oscillation frequency and amplitude. An interesting result is obtained in which a cylinder spun up from rest with certain angular velocity function and at a particular value of Reynolds number is azimuthally stress-free.

---

[a] Professor, Engr. Faculty, Ferdowsi Univ. of Mashhad, P.O. Box 91775-1111, Mashhad, Iran
[b] Graduate student

[1] Hiemenz, *Dinglers Polytechnic J.* **326**, 321 (1911).
[2] Gorla, *Int. J. Engr. Science*, **17**, 87 (1979).
[3] Saleh and Rahimi, *J. of Fluids Engr.*, **Nov.**, 997 (2004).

Session 8

Two-layer film flow : a temporal and spatio-temporal stability analysis inluding viscosity and density stratification effects.

J.Hu[a], V. Botton[a], S. Millet[a], D. Henry[a] and H. BenHadid[a]

The temporal, spatial and spatio-temporal linear stability analysis of two-layer film flow down an incline is revisited, with the aim of investigating the combined effects of viscosity and density stratification. We study here the interface mode only.

Historically, the first studies were made through an infinite wavelength approximation. However, Lowenhertz and Lawrence[1] showed that, at least in the inertialess case, the primary interfacial instability is more likely to be observed at finite wavelength than at infinite wavelength. Later studies thus usually account for finite wavelengths. Lowenhertz and Lawrence[1] however assumed equal density in the two layers.

Here, a first approach relies on a zero Reynolds number approximation to the Orr-Sommerfeld equations, following Lowenhertz and Lawrence[1], but accounting for density stratification. It is shown that increasing the density ratio (upper fluid over lower one) is always destabilizing; decreasing it below 1 surprisingly slightly increases the range of viscosity ratios where the instability is triggered and also selects the long wave instability to the detriment of the finite wavelength instability. A maximum in peak-growth-rates is also observed for moderate values of viscosity ratio, around 2, whatever the value of the density ratio. The spatio-temporal analysis shows that the instability is convective in all the investigated parameters range. The spatial amplification of externally excited waves is also studied, leading to the same trends as in the temporal study.

The influence of inertia is then taken into account, relying on a spectral approach (based on *Tchebichev* polynomials) to the linear stability problem. When the thicker layer is the lower one, a similar influence of density is found as in the zero Reynolds number case. The evolution of temporal and spatial growth-rates with inertia si discussed for moderate values of Reynolds numbers.

At last, an experimental facility dedicated to the investigation of this problem is also presented.

---

[a]LMFA (UMR-CNRS 5509), Ecole Centrale de Lyon, 36 avenue G. de Collongue,69134 Ecully, FRANCE.

[1] Loewenherz, D. S., and Lawrence, C. J., *Phys. Fluids* 1, 1686-1693 (1989).

Instability of superposed fluids subjected to tangential oscillation

Harunori N. Yoshikawa[a] & José-Eduardo Wesfreid[b]

We present a study on a pattern formation on an inmiscible interface of superposed fluids with very large viscosity contrast. The fluids are subjected to horizontal oscillatory motion at a moderate frequency. Beyond instability threshold, static waves are formed and grow up until saturation, forming fingers of more viscous fluid as reported by Shyh[1]. We carried out theoretical calculations and also laboratory experiments for comparison. Both theory and experiment showed that the critical wavelength is controlled by the oscillation amplitude. A detailed theoretical analysis reveals that the origin of the instability is pressure distribution in the less viscous phase like ordinary Kelvin-Helmholtz instability. This distribution is, however, mainly related to averaged flow (steady streaming) in the less viscous fluid and, consequently, selected wavelength differs from that of inviscid Kelvin-Helmholtz instability.

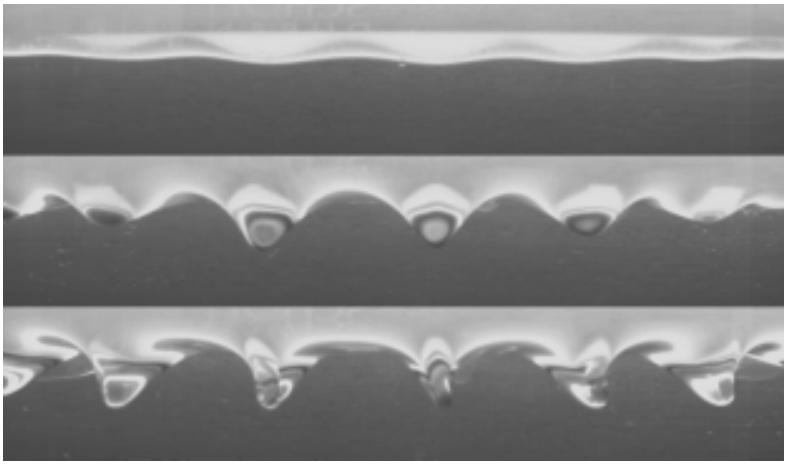

Figure 1: Finger formation of highly viscous silicone oil (upper phase). The lower phase is water. The oscillation amplitude A and frequency f are given as $A = 13\,\mathrm{mm}$ and $f = 1.1\,\mathrm{Hz}$.

[a] PMMH-ESPCI (UMR7636 CNRS), 10, rue Vauquelin 75005 Paris, France, harunori@pmmh.espci.fr

[b] PMMH-ESPCI (UMR7636 CNRS), 10, rue Vauquelin 75005 Paris, France, wesfreid@pmmh.espci.fr

[1] Shyh et al., *J. Fluids Engin.* **108**, 89 (1986)

Stability of a free edge on a liquid curtain.

J.-S. Roche*, L. Lebon* and L. Limat*

Thin liquid sheets have been studied since years for their practical applications, such as coating or atomization. In this talk, we present experiments on vertical liquid curtains falling between two vertical wires, under a horizontal cylinder. The flow is driven by gravity, so that the Weber number (ratio between inertia and surface tension) increases downstream. We examine the behavior of a free edge created behind an obstacle, such as a needle (figure 1 (a)). The shape of the free edge is determined from a balance between surface tension, inertia, and the weight of the rim. We demonstrate that this last force stabilizes the free edge even if the Weber number on the needle is smaller than one, which contradicts the well-known Brown stability criterion of the curtain. Furthermore, we present a model based on those three forces that accurately describes the experimental shapes. Finally, it is observed that when Weber number near the needle decreases, the rim has a complex dynamics, during which it detaches forming drops or filaments.

*Laboratoire de Physique et Mécanique des Milieux Hétérogènes, UMR 7636 CNRS, 10, rue Vauquelin 75005 Paris (France)

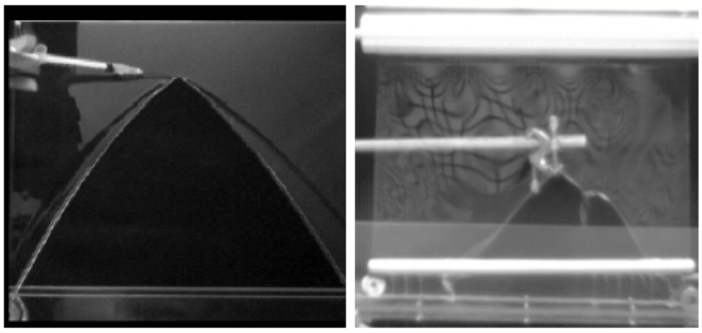

Figure 1: (a) Static free edge behind a needle. (b) Oscillations of the rim near We=$\rho h U^2/2\gamma$=1. (h is the thickness of the curtain, U is the speed of the liquid.) The grid is observed after reflection on the curtain

Two-dimensional disturbance growth of a plane liquid sheet

A. Sasaki[a], M. Tosaki[a] and M. Matsubara[a]

Instability of a thin liquid sheet, which is related to industrial applications such as atomization or curtain coatings, has been studied experimentally. This instability is due to aerodynamic interaction of liquid sheet with its surrounding gas medium[1], while the principal sources of liquid column instability are the capillary forces for Rayleigh instability. Linear stability analysis including the effect of surface tension and viscosity shows that liquid sheet instability was dominated by Reynolds number, Weber number, density and viscosity ratio of gas and liquid and that antisymmetrical mode is the only absolutely unstable mode on the plane liquid sheet with uniform velocity profile[2]. In spite of exist of the sophisticated theory, few detail experiments with comparison with theories on the liquid sheet instability to author's knowledge

The present study focuses on acquisition of quantitative data for measuring the wave number dependence on disturbance growth. A plane liquid sheet plunged from two-dimensional nozzle into stationary gas. In a natural case, the sheet starts flattering downstream with a certain streamwise wavelength and breaks down. In order to control the disturbance frequency an initial disturbance introduced by loudspeaker connected to the nozzle. As shown in figure 1, the instability was well-controlled indicating two-dimensional regular surface oscillation. Oscillation amplitude exponentially increases downstream regardless of the streamwise wave number and liquid velocity. For estimation of the growth rate of the disturbance, amplitude variation in the streamwise direction was measured by touching the needles to water surface. To obtain frequency components, surface gradient was also measured by detecting the laser reflection on the water surface. The experimental results revealed that the growth rate reaches to maximum at the wave number corresponds to the unexcited flow.

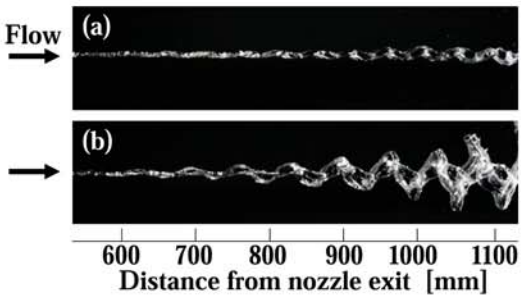

Figure 1: Surface oscillation with streamwise wave number. Liquid sheet thickness is 1mm, and velocity at the nozzle exit is 7m/s. Wave number of disturbance is (a) 135 m^{-1}, (b) 99 m^{-1}.

---

[a] Shinshu University Mechanical systems engineering Wakasato4-17-1, 380-8553 Nagano, Japan.

[1] Li & Tankin, *J. Fluid. Mech.* **226**, 425 (1991).

[2] Söderberg, *J. Fluid. Mech.* **493**, 89 (2003).

Spatiotemporal evolution of Interfacial Waves between a Gas Boundary Layer and a Thin Liquid Film

M. G. Vlachomitrou[a] and N. A. Pelekasis[a]

The stability of interfacial waves is examined. They appear when a thin liquid film that covers a solid surface is driven to motion by a boundary layer of air, which flows above this surface. Such a flow arrangement arises above wing sections under conditions of rainfall, in the context of steam condensation etc. The simulation of the boundary layer is based on the triple deck theory, whereas the model for the liquid film is simplified by neglecting inertia terms. As interfacial waves appear at larger times compared to Tollmien-Schlichting waves the lower deck of the boundary layer can be treated as quasi-stationary and therefore any changes in the gas phase occur only as a result of the changes in the liquid phase. The overall problem is solved using the finite element methodology with the 2D B-cubic splines as basis functions in conjunction with the 4th order Runge Kutta time integrator in the liquid film.

Linear stability analysis[1] predicts that interfacial waves can be either convectively or absolutely unstable. In order to obtain the results predicted by linear theory we consider the basic flow as nearly parallel and we use open-ended or periodic boundary conditions for all variables. As a result the convective or absolute nature of interfacial waves is recovered and their characteristics (e.g. wave length, period and group velocity) are calculated. The spatiotemporal evolution of nonlinear disturbances is also followed and interesting phenomena such as sideband instabilities are captured.

Based on the frequency selection criterion[2] it can be shown that the above flow configuration may exhibit a global instability in the proper range of We and Fr numbers. This aspect of the problem is currently under numerical investigation by allowing the base flow to vary in the streamwise direction and employing open-ended boundary conditions.

---

[a] Dept. of Mechanical and Industrial Engineering, University of Thessaly, Volos 38334, Greece.

[1] Pelekasis & Tsamopoulos, *J. Fluid Mech.* **436**, 321 (2001).

[2] Huerre & Monkewitz, *Annu. Rev. Fluid Mech.* **22,** 473-537 (1990).

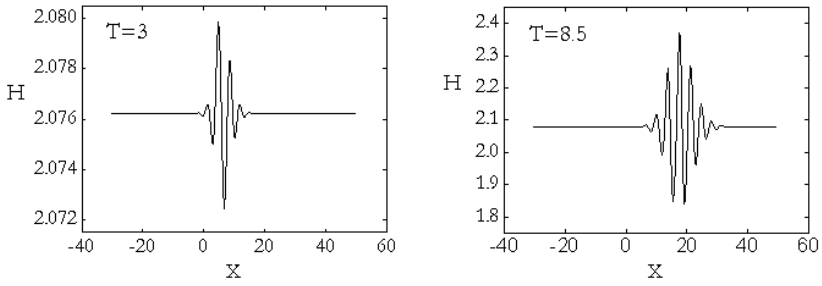

Figure 1: Spatiotemporal evolution of a pulse disturbance originally applied at the Gas-Liquid interface at X=0; $X=x'/(LRe^{-3/8})$, $T=t'/(Re^{-2/8}L/U_\infty)$, $H=h'/(LRe^{-5/8})$.

Convective structures in a thin layer of evaporating liquid in the presence of wind-induced shear flow

V. P. Reutov[a], A. B. Ezersky[a], G. V. Rybushkina[a] and V. V. Chernov[a]

The convective structures arising in a thin liquid layer blown up by an air current are studied experimentally and theoretically. The experiments were made with ethanol filling up a cavity placed in the operating part of the wind tunnel. The attention is focused on the evolution of patterns with increasing current velocity. The main result is that the hexagon structure, which has unclear contours in the absence of blowing, is bifurcated into the convective rolls presented in Fig. 1,a. Cooling of the liquid surface due to evaporation (Fig. 1,b) gives rise to the degeneration of the convective rolls.

A numerical simulation is performed for the two-dimensional periodic roll flow when there are only two counterrotating rolls on the period specified from the experiment. Axes of the rolls are oriented along the flow direction. Such a roll system is autonomous and does not depend on the shear flow inside the liquid layer. The closed boundary conditions on the liquid surface are derived using the self-similar solutions for the diffusion of heat and vapour within the turbulent boundary layer of the air current. Formation of a thin temperature boundary layer is obtained and the dynamical mechanism of its maintaining is elucidated. The time of the liquid cooling (Fig. 1,b) corresponds to the experiment very well. The results of the simulation are used to describe the defects in the quasiperiodic roll system. The proposed model is based on usage of the Ginsburg-Landau equation and involves the stability analysis for the oblique convective perturbations subjected to the shear flow. Note that the considered phenomena pertain to the so-called cold film which is frequently observed near the sea surface[1]. The paper can be regarded also in the context of the general problem of convection in the presence of a shear flow[2].

The work was performed with financial support from the Russian Foundation for Basic Research (project No. 04-05-64627).

---

[a] Institute of Applied Physics RAS, 46 Ulyanov Str., Nizhny Novgorod 603950, Russia.

[1] Panin. *The heat-mass transfer between the basin and atmosphere under natural conditions*. Nauka-press, Moskow, 1985 (in Russian).

[2] Tveitereid and Müller. *Physical Review E* **50,** 1219 (1994).

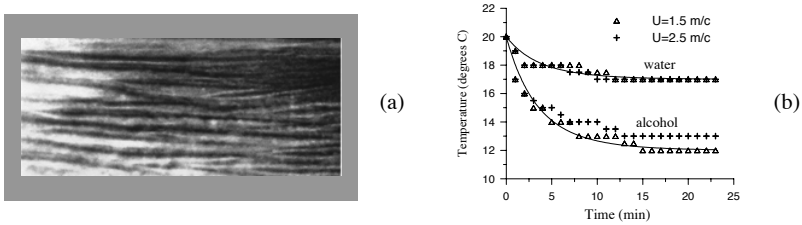

Figure 1: (a) Strip-like patterns on the liquid surface which are visualization of the convective rolls. (b) Run of the surface temperature in time after start of blowing.

Interfacial capillary wave stability in the presence of electric fields

S. Grandison*, D. Papageorgiou† and J.-M. Vanden-Broeck

Liquid films arise in many diverse physical phenomena including problems in combustion and biological systems. In many of these applications questions regarding the nonlinear states of such systems and methods by which the stability properties can be enhanced is of fundamental interest.

In this talk we will consider the dynamics of periodic travelling waves propagating on the surface of a two-dimensional liquid film of density ρ_1 bounded by a second incompressible fluid of density $\rho_2 < \rho_1$ in the presence of an electric field. The electric field acts in the plane of the sheet driven by a constant potential difference and the two fluids have differing dielectric responses. The system modelled is non-linear and, by analogy with the nonlinear Kelvin-Helmholtz instability, the initial boundary value problem is not guaranteed to have global existence when the surface tension is zero. The addition of the electric field complicates the problem mathematically and it is of interest to consider its effects on solution properties and features.

In order to obtain an understanding of the well-posedness of the initial value problem we begin with a linear stability theory. This allows the identification of parameter ranges where the presence of the electric field competes and indeed completely cancels the Kelvin-Helmholtz instability, even when surface tension is absent.

We will also present time-dependent long-wave asymptotic models showing the evolution of the system with time and fully non-linear results calculated using boundary integral equation techniques which allow us to compute stable non-linear waves of arbitrary amplitude by reducing the problem to one with unknowns only on the interface.

*School of Mathematics, University of East Anglia, Norwich NR4 7TJ, England
†Department of Mathematical Sciences, New Jersey Institute of Technology, University Heights, Newark, USA

Interfacial instabilities in horizontally vibrated liquids

A. Juel*, E. Talib* and S. Jalikop*

Horizontally vibrated interfaces exhibit a rich variety of interesting dynamics which have been surprisingly neglected to date. Oscillatory shear-driven instabilities of liquid-liquid interfaces are characterised by the formation of a steady wave pattern, which depends significantly on the viscosity ratio between the two liquid layers. Surprisingly, in the limit of very large viscosity ratios (approx. 10e4), when the very viscous liquid oscillates with the bounding cylinder nearly as a rigid body, regularly-spaced viscous fingers can nevertheless be observed to grow into the water on time scales of the order of seconds. We investigate the mechanism behind this instability using the powerful combination of theory and experiments. In so doing, we compare our experimental results with a general two-dimensional linear stability analysis of vibrated two-liquid layers, as well as previously published analytical models in order to assess their validity.

*MCND, University of Manchester, UK

Experimental investigation of pattern instabilities in the Rayleigh–Bénard–Poiseuille system

E. Grandjean*, N. Borhani* and P. A. Monkewitz*

A systematic investigation into the pattern forming hydrodynamic instabilities found in the Rayleigh–Bénard–Poiseuille (RBP) system is undertaken. These systems comprise the flow of a fluid through a horizontal rectangular channel, whose top surface is colder than the bottom. RBP instabilities manifest themselves as thermo-convective rolls whose spatio-temporal symmetries depend on the system parameters.

Depending on three non-dimensional numbers[1], the Rayleigh numbers (Ra), the Prandtl number (Pr) and the Reynolds number (Re), several modes can be observed. At a given Re, an increase of Ra from zero will lead either to the formation of transverse rolls with axes perpendicular to the Poiseuille flow direction, or to the formation of longitudinal rolls with axes parallel to the flow direction. A mixture of these two modes is also possible[2].

Recent theoretical studies have applied the concepts of absolute-convective[3] and local-global instabilities[4] to the RBP system. A third study[5] has shown that the longitudinal rolls are never absolutely unstable for $\mathrm{Re} > 0$. This implies that only transverse rolls are absolutely unstable in RBP. However, for $\mathrm{Re} > 0$ the critical $\mathrm{Ra}_{\mathrm{crit},\perp}$ for transverse rolls is larger than $\mathrm{Ra}_{\mathrm{crit},\parallel}$ for longitudinal rolls. Hence, to observe the absolutely unstable transverse rolls, the forcing of the convectively unstable longitudinal rolls by upstream perturbations has to be extremely low.

A low background noise $4 \times 170\,\mathrm{mm}$ cross-section channel has been designed. Two closed temperature controlled water circuits are used to heat and cool the bottom and top surfaces respectively. Shadowgraph and Schlieren techniques were used to quantify the spatio-temporal dynamics of the system.

We experimentally confirm the above theoretical results through a systematic mapping of the (Re,Ra) parameter space in a uniformly heated and cooled system. Cases of non-uniform heating will also be discussed.

*LMF–STI–EPFL, 1015 Lausanne, Switzerland.

[1]Nicolas, *Int. J. Therm. Sci.* **341**, 961 (2002).
[2]Lir, Chang and Lin, *Int. J. Heat Mass Transfer* **44**, 705 (2001).
[3]Huerre and Monkewitz, *J. Fluid Mech.* **159**, 151 (1985).
[4]Huerre and Monkewitz, *Annu. Rev. Fluid Mech.* **22**, 473 (1990).
[5]Carrière and Monkewitz, *J. Fluid Mech.* **384**, 243 (1999).

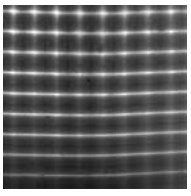

Figure 1: Shadowgraph of a mixed transverse/longitudinal state. The flow direction is upwards.

Magnetic stabilization of buoyant convection in a horizontal channel of rectangular cross-section with a longitudinal temperature gradient

A. Perminov*, D. Lyubimov*, T. Lyubimova*,
H. Ben Hadid†, D. Henry†, V. Botton†, W. Dridi†

Flows in cavities heated from the side are typical of horizontal Bridgman crystal growth situations. These flows and specifically their transitions to oscillatory behaviours are known to be responsible for defects in the grown crystals. Different ways have been found to control these flows, among which micro-gravity and magnetic field. Here, we focus on the efficiency of the stabilization by a magnetic field when the cavity is an infinite channel with rectangular cross-section.

Previous studies by Kaddeche et al.[1] have shown how the magnetic field (characterized by the Hartmann number, Ha) can stabilize the flow induced by a horizontal temperature gradient in a layer between two infinite horizontal walls: the vertical magnetic field was found to be the most efficient field with Ha^2 stabilization law for the three-dimensional oscillatory instabilities and even Ha exponential laws for the two-dimensional stationary instabilities, whereas the horizontal fields generate asymptotic Ha stabilization law at high Ha. The present study will deal with the influence of a lateral confinement (rectangular cross-section), and analyse the stabilization by a magnetic field for two orientations of the field (vertical and transverse) and different transverse dimensions l of the cross-section.

The results have still shown a very good stabilization for a vertical magnetic field with Ha exponential stabilization laws for any values of l between 0.7 and 1.5. For a transverse magnetic field, the results are more surprising: for $l = 1.5$ the stability thresholds increase slowly but regularly with Ha, but for stronger confinement ($l \leq 1$) the first effect of the transverse magnetic field is to strongly destabilize the flow with a strong decrease of the threshold when Ha is increased. An increase of the threshold is only obtained for values of Ha larger than 15 for the studied cases. Such initial decrease of the thresholds is in fact obtained for the limit case of the Prandtl number Pr equal to zero. No such decrease, but a regular increase is obtained for Pr values between 0.01 and 0.1.

An energy analysis at the thresholds has been performed in order to analyse these results. The main destabilizing factor is the fluctuating energy due to the vertical shear connected to the horizontal velocity. It has been found that it is the variation of this shear energy which is mainly responsible for the variation of the thresholds with Ha. This shear energy has then been decomposed into a shear term connected to the mean flow and a term corresponding to a product a velocity fluctuations. It has been shown that it is the particular variation of the fluctuations term which is responsible for the decrease of the thresholds at small Ha under transverse magnetic field, and more precisely the increase of the vertical velocity fluctuations.

*Perm State University, 15 Bukirev Street, 614990 Perm, Russia.
†Lab. de Mécanique des Fluides et d'Acoustique, UMR 5509, Ecole Centrale de Lyon/Université Claude Bernard-Lyon 1/INSA de Lyon, ECL, 36 Ave Guy de Collongue, 69134 Ecully Cedex, France.

[1] S. Kaddeche, D. Henry and H. BenHadid, *J. Fluid Mech.* **480**, 185 (2003).

Acoustic streaming control of natural convection instabilities.

W.Dridi[a], V. Botton[a], H. BenHadid[a], D. Henry[a] and S.Kaddeche[b]

Acoustic streaming denotes the ability of an acoustic wave to produce steady flows. It is relevant to many industrial applications such as the pumping of fluids in microflow systems or high efficiency mixing of liquids in closed containers. Acoustic streaming is also well known for its transport properties: the fluid flows without any external mechanical contact and can enhance rate-limited processes such as diffusion of heat or mass. These flows can be induced in free space by attenuation of the sound wave; in this case it is often referred to as *Eckart Streaming*.

We focus here on the possibility of using an *Eckart Streaming flow* to stabilise primary flows in differentially heated cavities. We consider the case of an horizontal liquid layer, which can be either heated from below or by the side. The acoustic beam is here horizontal, of height H1, in the middle region of the cavity; it is also characterised by the acoustic intensity number A. We consider this configuration in the frame of the linear stability theory.

For the isothermal flow, an oscillatory instability occurs when A reaches some critical value which is found to be a function of the beam width H1. In the case of heated layers, the critical Rayleigh number Ra_c was found to be sensitive to H1 and A. In particular, at fixed H1, ther exists a range of acoustic intensity, A, where a stabilizing effect is observed (*i.e.* where Ra_c is significantly higher than the threshold without acoustic streaming). This is illustrated in figure 1, for the case of a fluid layer heated from below. The physical origin of this behaviour is explained by the help of an energy stability analysis. First results of an experimental approach are also provided.

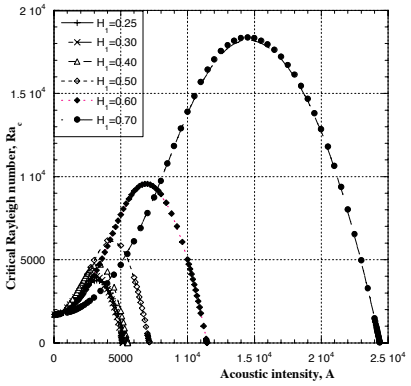

Figure 1: Neutral curves for a layer heated from below, in presence of a horizontal sound beam of height H1 and intensity A.

[a] LMFA (UMR-CNRS 5509), Ecole Centrale de Lyon, 36 avenue G. de Collongue,69134 Ecully, FRANCE.

Bifurcation diagrams, stability analysis and dynamic simulations of free convection in a differentially heated cavity in the presence of a magnetic field

N. A. Pelekasis[a]

The static equilibrium and stability of two dimensional free convection flow in a square cavity is examined, in the presence of a uniform internal heat source and a uniform magnetic field that is perpendicular to gravity and parallel to an imposed temperature gradient. The finite element method is used for calculating the equilibrium and dynamic state of the system in the parameter space defined by the dimensionless numbers, Gr, Ha, Pr and S. The trapezoidal rule is used for time integration. Linear stability analysis is performed by solving a generalized eigenvalue problem. The Arnoldi method is used for the calculation of eigenvalues. The base solution normally exhibits two recirculation regions when the heat production term is large enough. Stability analysis predicts a Hopf bifurcation to a periodic branch. A neutral stability diagram is constructed for a range of values of Ha, Gr and S for liquid lithium, Pr=0.0321. Internal heat generation, i.e. increasing S, enhances instability by decreasing the critical value of Grashof, Gr_{cr}, determining the onset of the Hopf branch, whereas intensifying the magnetic field, i.e. increasing Ha, stabilizes the flow by increasing Gr_{cr}. Dynamic simulations identify the oscillatory solution branch as a supercritical Hopf bifurcation and recover the time constants predicted by stability analysis. As Gr increases or as Ha decreases symmetric arrangement of the two rolls is eliminated and the steady flow configuration loses stability when $Gr>Gr_{cr}$. Subsequently, time periodicity sets in leading to more or less efficient heat removal in terms of lowering or increasing the average cavity temperature, in comparison with the steady flow configuration for the same Gr, depending on whether Ha lies below or above a critical value, respectively, for fixed S and Pr.

[a] Dept. of Mechanical and Industrial Engineering, University of Thessaly, Volos 38334, Greece.

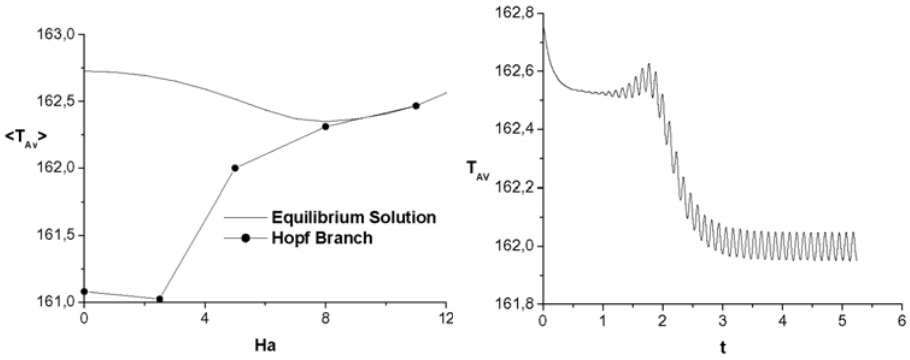

Figure 1: (a) Bifurcation diagram and (b) dynamic simulation (Ha=5); $Gr=10^4$, $S=10^5$.

Convective instability in fluid mixtures heated from above

V. Shevtsova, [1]D. Melnikov, J.C. Legros

Evolution of a convection in a cubic cell filled with a binary mixture of water (90%) and isopropanol (10%) is studied. The system is heated from above while the Soret coefficient (S_T) is negative, i.e. thermally stable Rayleigh-Benard configuration. The negative sign of S_T implies that the denser component migrates towards hot wall (opposite to buoyancy force). The considered system has very different time scales according to the physical properties of the liquid: the viscous time $\tau_\nu = L^2/\nu \approx 70$s, thermal time $\tau_{vh} = L^2/\alpha \approx 770$s and diffusion time $\tau_D = L^2/D \approx 1.15 \cdot 10^5$s. Here ν, α, D are the viscosity, thermal diffusivity and molecular diffusion measured in [m^2/s]. The size of cubic cell is L=0.01m. The 3D time dependent Navier-Stokes, energy and mass equations are computed for small but relevant Lewis number $Le=D/\alpha=6.7 \cdot 10^{-3}$, while $Pr=10.85$ and separation ratio $\psi=-0.4$.

The concentration and temperature fields are strongly coupled by Soret effect that causes concentration gradients in response to the applied temperature difference. As diffusion time is very large the concentration gradient sets in so slowly, that the Soret convection starts before this gradient reach stationary value. Due to Soret effect the heavier liquid is accumulated on the top of lighter one and buoyant convection due to a hydrodynamic Rayleigh-Taylor instability can be initiated. The latency time, during which the system remains motionless, is significantly smaller than diffusion time (by 20 times). At some moment the velocity rises up from zero to sharp peak. The heavier liquid is washed away from the hot wall. The first splash is followed by a few more pulses of convection, but not so powerful. The concentration of the heavier component near the hot wall will never achieve the same level later in time. The transient dynamic of convective flow is similar to those, experimentally observed in colloidal suspensions.

The transitions of the convective flow with increase of applied temperature difference are related to the stable steady structure of flow pattern in single fluid in cubic cell.

[1] MRC, CP-165/62, University of Brussels, 50, av. F.D. Roosevelt, B-1050 Brussels, Belgium

Nonlinear instability of a compressible mixing layer

C. A. Sparks* and X.Wu*

We consider a mixing layer between two streams of different velocities and temperatures. A small instability with an $O(\epsilon)$ amplitude is introduced. As it amplifies, nonlinearity first comes into play near the neutral position. The nonlinear development can be studied by assuming the Reynolds number R to be large. In the incompressible limit the critical layer dynamics is strongly nonlinear, whilst it is weakly nonlinear for the the case of Mach number $M = O(1)$. The present study considers the distinguished weakly compressible regime corresponding to $M \sim \epsilon^{1/4}$ in order to unify the two theories. To include the viscous effect at leading order, we take $R^{-1} \sim \epsilon^{3/2}$. Thus we write $M = \mathcal{M}\epsilon^{1/4}$, $R^{-1} = \Lambda\epsilon^{3/2}$, where the rescaled parameters $\mathcal{M}$ and Λ characterise compressibility and viscosity respectively. Asymptotic analysis leads to a nonlinear system, which after a suitable re-normalisation can be written as

$$\mathcal{L}\,T = (\mathrm{i}A\mathrm{e}^{\mathrm{i}\zeta} + \mathrm{c.c.})(\tfrac{1}{2}T_Y + \mathcal{M}^2), \tag{1}$$

$$\mathcal{L}\,Q = \tfrac{1}{2}(\mathrm{i}A\mathrm{e}^{\mathrm{i}\zeta} + \mathrm{c.c.})(Q_Y - T_Y) + \Lambda_c T_{YY} + \tfrac{1}{2}\alpha c[(A_{\mathcal{T}} + A_{\mathcal{X}})\mathrm{e}^{\mathrm{i}\zeta} + \mathrm{c.c.}], \tag{2}$$

$$\fint_{-\infty}^{\infty}\int_{0}^{2\pi} Q\,\mathrm{e}^{-\mathrm{i}\zeta}\mathrm{d}\zeta\mathrm{d}Y = J_1 A_{\mathcal{X}} + J_2 A_{\mathcal{T}}, \tag{3}$$

for a mode with wavenumber α and phase speed c, where $\mathcal{L} = Y\partial_\zeta + \partial_{\mathcal{T}} + \partial_{\mathcal{X}} - \Lambda\partial^2_{YY}$. The quantities above are as follows: $\mathcal{X}$ and $\mathcal{T}$ are slow streamwise and time variables respectively, ζ a "fast" moving streamwise coordinate, Y the critical-layer transverse coordinate, T the leading-order temperature perturbation, Q essentially the unsteady vorticity within the critical layer, and A the amplitude function. All other quantities are constants determined from the relevant mean-flow and eigenvalue calculations.

A weakly nonlinear amplitude equation can be derived from equations (1)-(3) by considering the limit $\mathcal{M} \gg 1$. The equation is of the same form as Leib(1991)[1]. Thus the strongly nonlinear system (1)-(3) is actually valid for $M = O(1)$. The advantage of (1)-(3) is that it can describe vortex roll-up, which is crucial for mixing. A typical result is shown in the figure, where we plot the vorticity (left) and temperature (right) contours at a chosen streamwise location (in the nonlinear regime). Both vorticity and temperature roll-up with large gradients at the edge of the rollers.

*Department of Mathematics, Imperial College, London SW7 2BZ

[1]Leib, *J. Fluid Mech.* **224**, 551 (1991).

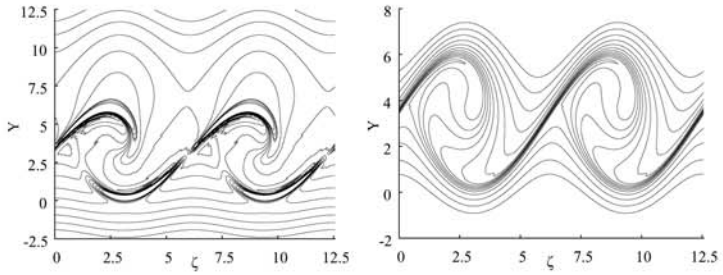

Convective flows in a two-layer system with a temperature gradient along the interface

A. A. Nepomnyashchy*, I. B. Simanovskii*

Stability of convective flows in systems with an interface has been a subject of an extensive investigation. Several classes of instabilities have been found by means of the linear stability theory for purely thermocapillary flows, and for buoyant-thermocapillary flows. The most of the investigations have been fulfilled for a sole liquid layer with a free surface, i.e., in the framework of the one-layer approach. Recently, Madruga et al. [1] studied the linear stability of two superposed horizontal liquid layers bounded by two solid planes and subjected to a horizontal temperature gradient. The analysis has revealed a variety of instability modes. Specifically, for the system 5cS silicone oil - HT70, the analysis predicts a change in the direction of the wave propagation with the growth of the ratio of the layers thicknesses.

In the present work, the nonlinear stability of two superposed horizontal liquid layers bounded by two solid planes and subjected to a horizontal temperature gradient, is investigated. The boundary value problem is solved by the finite-difference method. Two types of boundary conditions - periodic boundary conditions and heat - insulated lateral walls, are considered. The nonlinear simulations of the wavy convective regimes for the system 5cS silicone oil - HT70, are performed. It is found that the direction of the wave propagation depends on two factors, the ratio of the layers thicknesses (as it was predicted by the linear theory), and the Marangoni number. For sufficiently large values of the Grashof number values, the wave velocity is changed in a non-monotonic way. The general diagram of regimes is constructed. In long computational regions all types of traveling waves keep their perfect periodicity. Pulsating traveling waves changing their form and intensity, are observed.

*Department of Mathematics, Technion – Israel Institute of Technology, 32000 Haifa, Israel.

[1] Madruga et al., *Phys. Rev. E* **68**, 041607 (2003).

Experimental study of a vibrated bubble in microgravity

P. Kurowski*, H. Caps†, F. Zoueshtiagh‡, P. Petitjeans*

The response of an air bubble enclosed within a cylindrical cell submitted to vertical vibrations is experimentally investigated. The particular system consists of a fluid filled circular cell of 8 cm diameter which contains a small (≈ 4 ml) air bubble. The cell is put under vertical vibrations and the response of the bubble is observed from above with a high speed camera (figure 1).

The study shows that the bubble undergoes deformations which are amplified as the frequency and/or the amplitude of the oscillations is increased. If these deformations are large enough, the bubble is observed to become toroidal, then develop regularly spaced deformations along its centerline (top line of the pictures of figure 2) and finally splits into several smaller parts (bottom line of the pictures of figure 2).

It is found that the bubble dynamics is closely associated with the acceleration of the oscillations. Furthermore it appears that the onset for the division of the bubble occurs when the acceleration of the oscillations exceeds ≈ 9 m/s^2, i.e. when the bubble is nearly and temporarily in a state of reduced gravity.

In order to evaluate the influence of gravity on the bubble dynamics, we have carried out experiments in microgavity[1] and compared our result to those found on the ground. The comparison shows that the onset for bubble division is decreased by up to 20% for experiments carried out in microgravity. A dimensional analysis is proposed which appears to scale both results. The difference and similarities between the results of experiments on the ground and in microgravity will be presented.

*Laboratoire de Physique et Mćanique des Milieux Hétèrogènes CNRS 7636, ESPCI, 10 rue Vauquelin, 75231 Paris, France

†GRASP, Institut de Physique, B5, Université de Liège B-4000 Liège, Belgium

‡Laboratoire de Mécanique de Lille CNRS 8107, Bd P. Langevin, 59655 Villeneuve d'Ascq, France.

[1]The experiments were carried out in the Airbus A300 Zero-G of french aerospace agency "Centre National d'Etudes Spatiales" (CNES).

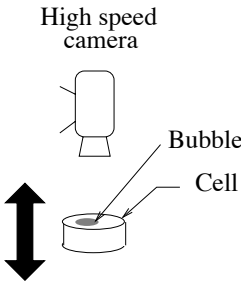

Figure 1: Experimental setup.

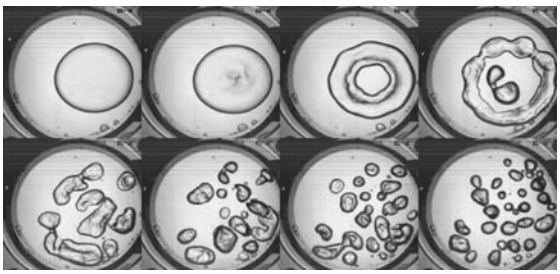

Figure 2: Successive pictures of a bubble response to vertical vibrations.

What governs the meandering instability of a rivulet?

N. Le Grand-Piteira [a,b], A. Daerr [a,b], L. Limat [a,b]

When a rivulet flows down a plate, a meandering instability can develop above a critical flow rate. This phenomenon is often observed in daily life (e.g.: rain on windshields) but surprisingly, very few studies have been made on this subject[1-2], probably due to the difficulties in achieving well controlled experiments.

We have performed experiments with water jets sliding down an inclined plastic plate (Mylar sheet), providing partially wetting conditions, and reproducible experiments. For increasing flow rates, several different regimes of the flow were identified: drops[3], straight streams, stationary meanders and non-stationary flows (see figure 1). A very strong hysteresis is observed: decreasing flow rate back to smaller values, the straight flows are never recovered in the experiments.

(a) 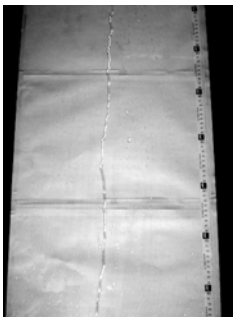 (b) 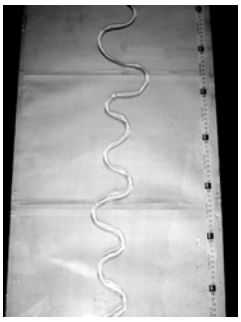 (c) 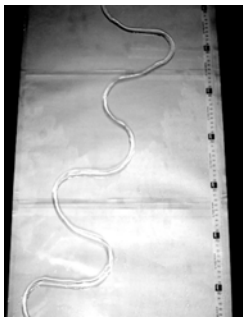

Figure 1: (a) Straight rivulet for a flow rate Q=0.64 mL/s (b) Stationary meander for Q=3.04 mL/s (c) Stationary meander for a higher flow rate Q=4.42 mL/s. Water flows from top to bottom. Plate inclination: 6° with respect to the horizontal.

The onset and shape (radius of curvature, amplitude and wavelength) of steady meanders were systematically obtained, for various plate inclinations[4]. By means of simple model equations for the force balance, including the force resulting from hysteresis of wetting, the results for the onset of meandering and the radius of curvature of the meanders are explained.

Finally, these partially-wetting meanders –and the conditions requested to obtain them– will be compared to travelling meanders achieved in totally wetting conditions, by injecting silicone oil at the top of a Hele-Shaw cell made of glass plates (totally wetting conditions).

---

[a] Laboratoire PMMH, UMR 7636 of CNRS, ESPCI, 10 rue Vauquelin, 75231 Paris Cedex 05
[b] Laboratoire MSC, UMR 7057 of CNRS, 2 place Jussieu, 75005 Paris

[1] Nakagawa and Scott, *J. Fluid Mech.*, **149**, 89-99 (1984)
[2] Schmuki and Laso, *J. Fluid Mech.*, **215**, 125-143 (1990)
[3] Le Grand et al., *J. Fluid Mech.*, **541**, 293-315 (2005)
[4] Le Grand-Piteira et al., *submitted to Phys. Rev. Lett.*

Instabilities in a salt-stratifed sedimentation boundary layer

O. S. Kerr*

When a sediment-laden fluid is in contact with the underside of an inclined wall a boundary layer of clear fluid can form if the sediment is denser than the ambient fluid. The buoyant ambient fluid can then rise up the wall, enhancing the rate of settling out of sediment from the bulk of the fluid. This is known as "the Boycott effect" and has been much studied[1].

A more recent variation of this problem[2] has a salinity stratification in addition to the sediment in the bulk of the fluid. This stratification has the effect of inhibiting the rise of the clear fluid up the underside of the boundary.

In this study we look at the evolution and stability of the buoyant boundary layer when there is a linear vertical salinity gradient present. This analysis involves several assumptions to reduce the number of parameters (and make the analysis more tractable) such as the assumption that the difference between the average density of sediment laden fluid and the density of the fluid itself is not great. We will show how the linear instabilities evolve, and that they tend towards a state where they are localized near the interface between the clear and sediment laden fluid.

*Centre for Mathematical Science, City University, Northampton Square, London EC1V 0HB, U.K.

[1]Davis and Acrivos, *Ann. Rev. Fluid Mech.* **17**, 91–118 (1985)

[2]Peacock et al., *J. Fluid Mech.* **529**, 33–49 (2005)

Spatial versus temporal instabilities in a parametrically forced stratified mixing layer

A. Yu. Gelfgat and E. Kit

The present study compares the temporal and spatial instabilities of parametrically excited stratified mixing layer flows. For this purpose a relatively simple iteration procedure yielding solutions of both temporal and spatial problems is proposed. This procedure can be easily extended to other plane-parallel shear flows with the parametric excitation of instability. Using this procedure the parametric analysis of the temporal and spatial Kelvin-Helmholtz and Holmboe instabilities is performed and characteristic features of the instabilities are compared. Both inviscid and viscous models are considered. The parametric dependences on the mixing layer thickness and on the Richardson and Reynolds numbers are studied. It is shown that in the framework of this study the Gaster transformation is valid for the Kelvin-Helmholtz instability, but cannot be applied to the Holmboe one. The neutral stability curves are calculated for the viscous flow case. It is found that the transition between Kelvin-Helmholtz and Holmboe instabilities is continuous in the spatial case and in the temporal case occurs via the codimension two Takens-Bogdanov bifurcation at which a complex pair of the leading eigenvalues merges into a multiple real eigenvalue (Fig.1). It is found also that for the same governing parameters the spatial upstream and downstream Holmboe waves have different amplification rates and different absolute phase velocities, with larger difference observed at larger Richardson numbers. It is also found that at large Richardson and small Reynolds numbers the primary temporal and spatial instabilities set in as a three-dimensional oblique Holmboe wave.

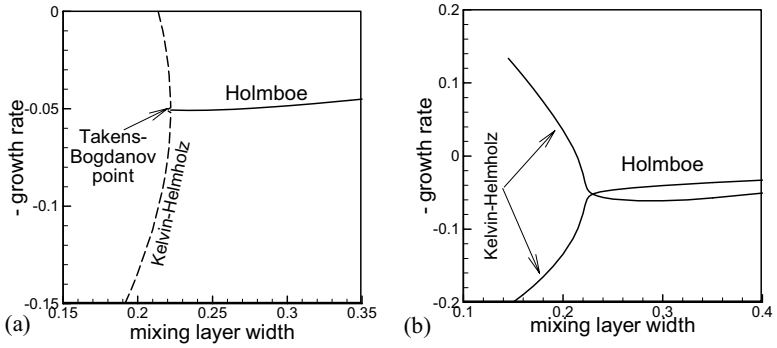

Fig.1. Transition between Kelvin-Helmholz and Holmboe modes for temporal (a) and spatial (b) instabilities.

School of Mechanical Engineering, Faculty of Engineering, Tel-Aviv University, Ramat Aviv, 69978, Israel

Particle motion and ripple growth under oscillating viscous flow

E. Larrieu*, O. Eiff* and F. Charru*

Ripple and dune formation on granular beds sheared by a liquid flow is observed in both the natural environment and engineering processes, and may strongly affect sediment transport and the fluid flow itself. The commonly accepted mechanism for the growth of such features is an hydrodynamic instability arising from fluid inertia which shifts the maximum of the bed shear stress upstream the crests of the bed disturbances. This mechanism, together with the stabilising effect of gravity for short waves and the use of an algebraic semi-empirical formula for the bedload transport, leads to predictions in agreement with experiments for sand bed under water[1]. However, several points are still unclear: are the semi-empirical bedload transport formulas still valid on ripples and dunes, especially under oscillationg flows? does the predicted gowth rate correspond to the observed ones? On which characteristic length do the observed wavelengths scale?

The answers to the above questions require a better knowledge of the motion of individual particles, which will allow better modelling of the motion of the mobile particle layer. For steady unidirectional flow, measurements of the surface density and velocity of the particles[2] allowed a new erosion-deposition model for the motion of the particle layer to be proposed recently[3]. This model explains the observed feature that ripples disappear as the fluid viscosity is increased, whereas they still grow in oscillating flow.

We will present new experimental results on ripple growth and the motion of individual particles under oscillating viscous flow. It appears that the microstructure of the bed has a strong effect. Before the ripple growth, the compacity of the bed increases and the surface density of moving particles decreases, indicating a reorganisation of the bed; after this first stage which lasts for about a thousand of oscillations, ripples grow. The growth rates are in good agreement with the erosion-deposition model of Charru and Hinch, without adjustable parameters. The motion of individual particles has been studied on two time scales: the short time scale of the period of oscillation, and the large time scale of the reorganisation of the microstructure of the bed. This study shows that, on the long time scale, the dependence of the density with the shear rate is linear as for steady flows, whereas on the short time scale a new dependence on the compacity is observed for the velocity and surface density. Besides, a mean drift of the particles to the crests is hard to detect, because particles oscillate on a few periods only before stopping in a small crevice. We will discuss the implications of these observations on the modelling of erosion and deposition.

*IMFT, allée C. Soula, 31400 Toulouse, France.

[1]Blondeaux, *J. Fluid Mech.* **218**, 1 (1990).
[2]Charru, Mouilleron-Arnould and Eiff, *J. Fluid Mech.* **519**, 55 (2004).
[3]Charru and Hinch, *J. Fluid Mech.*, in press.

About some dynamical properties of sand ripples under oscillatory flow

J. Kruithof [*], J.-E. Wesfreid[*], H. Yoshikawa[*], C. Josserand[†], and A. Stegner[‡]

We study the dynamical behavior of underwater sand ripples produced by oscillatory flow in the laboratory both in 2D and 3D geometry. Thanks to a high spatial resolution, we have been able to study the coalescence of rolling grain ripples. Then, we have compared this data with a phenomenological model equation, based on the derivation of the Cahn-Hilliard equation for the long-time dynamics of aerolian ripples[1], the logarithmic coalescence regime of the rolling-grain ripples and symmetry considerations. In figure 1 we observe a topical spatio-temporal evolution of the system from rolling grain ripples to vortex ripples. Furthermore, we have highlighted the front propagation between the rolling-grain ripples instability and the vortex ripples instability. In addition, we present results about the threshold of the instability and the threshold of grain motion, thanks to the 3D cylindrical geometry of our setup observed in Fig. 2. In figure 2 we show the effect of oscillation frequency on the separation of the two thresholds in 3D cylindrical geometry.

[*]PMMH, ESPCI, 10 rue Vauquelin, 75005 Paris, France
[†]LMM, tour 55, UPMC, 75005 Paris
[‡]LMD - UMR 8539 ENS

[1]Z. Csahok, C. Misbah et al.*Eur. Phys. J. E* **3**, pp. 71-86, (2000).

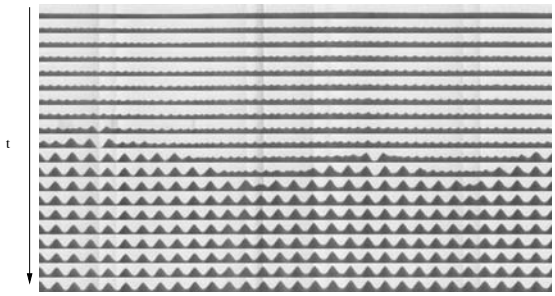

Figure 1: Spatio-temporal diagram of the 2D experimental system.

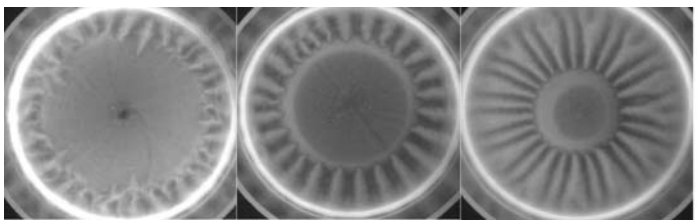

Figure 2: Experiments at constant amplitude and raising (from left to right) frequency in 3D-geometry

Rayleigh-Bénard Poiseuille of a yield stress fluid: linear and weakly nonlinear analysis

C. Metivier *, C. Nouar and J.-P. Brancher

We study the stability of the Rayleigh-Bénard Poiseuille (RBP) flow of a yield stress fluid. It is assumed that the rheological behavior is described by the Bingham model. The Bingham Poiseuille flow is characterized by a central plug zone in which τ, the second invariant of the deviatoric stress tensor, is less or equal to the Bingham number Bn, a dimensionless yield stress. The Bingham model assumes that inside this zone the material moves as a rigid solid and that, outside this zone where $\tau > Bn$, it behaves as a viscous fluid with an effective viscosity μ which depends on $\dot{\gamma}$, the second invariant of the strain rate tensor, as: $\mu = 1 + \dfrac{Bn}{\dot{\gamma}}$. The objective of our study is to examine the effect of the Bingham number on the stability conditions.

The linear stability analysis of this flow leads to propagating convective patterns, on the both sides of the plug zone, in the form of travelling waves. This analysis shows that the critical conditions, *i.e.*, critical Rayleigh and wave numbers, increase with Bn. Thus, increasing the Bingham number stabilizes the flow. This stabilization is a consequence of two effects of Bn: (i) the increase of the width y_0 of the plug zone, in which the velocity perturbation vanishes, (ii) the increase of the viscous dissipation. Indeed, the energy equation can be written as:

$$\frac{1}{Pr}\frac{dE_c}{dt} = Re\, I_{inertia} - I_{viscous} - Bn\, I_{Bingham} + Ra\, I_{buoyancy}, \qquad (1)$$

where $I_{Bingham}$ is positive and represents the viscous dissipation due to the Bingham term. Re, Ra and Pr are respectively the Reynolds, Rayleigh, and Prandtl numbers.

In the framework of linear stability analysis, the plug zone remains implicitly intact for finite Bn. When $Bn \to 0$, this condition is satisfied if $A > O(Bn^3)$, where A is the amplitude of the perturbation. Under these conditions, a discontinuous behavior is observed [1] with the Newtonian case [2]. Actually, cancelling the Bingham terms in the equations of perturbation, we recover a Couette Rayleigh-Bénard Poiseuille stability problem.

We have also performed a weakly nonlinear analysis. To our knowledge, this analysis has never been performed for yield stress fluids. New results concerning the evolution of the amplitude and of the plug zone are obtained. It is shown that, at low values of Reynolds number, the bifurcation is supercritical, similarly to the Newtonian case[3]. Beyond the critical Rayleigh number, the saturated amplitude of the perturbation A_0 decreases weakly with increasing Bn. We have checked that A_0 is not large enough to break the plug zone.

*LEMTA - 2, avenue de la forêt de Haye BP 160 - 54504 Vandœuvre cedex - France

[1] Metivier *et al.* *Phys. Fluids*, **17** (10) (2005).
[2] Nicolas *et al.* *Int. J. Heat Mass Transfer*, **43**, 589 (2000).
[3] Muller *et al.* *Europhys. Lett.* **10**, 451 (1989)

Evaluation of turbulence models through predictions of a separated flow over a hump with AFC

D. Madugundi[a], H. Nagib[a] and J. Kiedaisch[a],

Although a number of popular turbulence models are now commonly used to predict complex 3D separated flows, in particular for industrial applications, very limited full evaluation of their performance has been carried out using thoroughly documented experiments. Activities in this area have been recently intensified in view of the growing interest in Active Flow Control (AFC) of separation, as can be seen from the papers by Greenblatt et al.[1] and Rumsey et al. [2]. Unlike the hump model used in these recent publications, where the point of separation is highly localized by the surface geometry, many applications develop separation over surfaces with more gradual changes in local surface curvature. A hump model generating such a separated flow has been used as a test bed for comparing results from various models including k-ε, Spalart-Alamaras, k-ω, Menter's SST, and RSM. Our goal is a better understanding of the strengths and limitations of the various models by comparing them to each other and to experimental data recently documented[3] on this model. The results include cases without and with AFC, applied by suction, blowing or Zero-Mass Flux (ZMF) unsteady forcing from a nearly tangential narrow slot in the vicinity of the start of separation. While very high suction and blowing rates lead to near elimination of the separation zone, the surface pressure contours reveal interesting behavior that can be used to arrive at optimum AFC parameter selection.

[a] Illinois Institute of Technology, Chicago, USA.

[1] Greenblatt, D., et al. (AIAA-2005-0485)

[2] Rumsey, C., et al. (AIAA-2004-2217).

[3] Reynolds, T., Flow control using ZMF with superposition of steady suction, M.S. thesis, IIT, 2005.

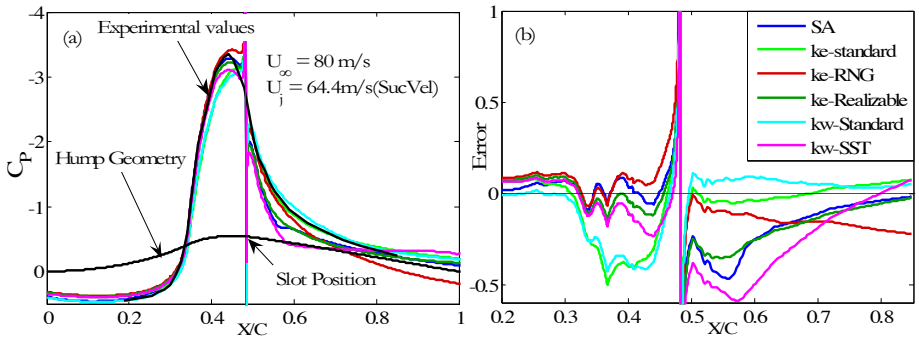

Figure 1: (a) Cp distribution over hump with AFC, Solid black curve corresponds to experimental values. (b) Deviation of computed results from experimental values.

Transient Separation Control by Pulsed Actuation

D Brzozowski and A. Glezer [a]

Time-periodic manipulation of separated flows over stalled lifting surfaces with the objective of inducing complete or partial attachment has been the focus of numerous investigations since the early eighties. As shown by Amitay & Glezer[1], flow attachment is associated with strong, transitory fluctuations of the circulation that are accompanied by the generation and shedding of large-scale vortices before nominally time-invariant lift is attained. The present work focuses on the exploitation of the receptivity of the flow over a stalled, 2-D airfoil to pulse-modulated actuation to control separation by regulated, transitory accumulation and shedding of vorticity in a manner that is similar to dynamic stall. The transient actuation couples to the wake instability and leads to remarkable global changes of the entire airfoil flow field.

Actuation is effected by momentary [O(1 msec)] pulsed jets that are generated by an array of combustion based actuators integrated into the centre section (16 cm) of an NACA 4415 airfoil (c = 46 cm, t/c = 0.16, s = 91.5 cm). The flow field is computed from PIV images in the x-y plane above the airfoil and the data in Figures 1 are presented in terms of the convective timescale, $\tau = c/U_\infty$.

The baseline flow at $t/\tau = 0$ (Re_c = 580,000, $\alpha = 19^o$) is massively separated near x/c = 0.4 and the flow is characterized by a large recirculation region over the upper surface of the airfoil. The effects of the pulsed actuation are shown for t/τ = 0.8, 1.2, and 1.7. It is remarkable that the brief actuation pulse leads to a very large transitory change in the circulation about the entire airfoil that is manifested by the shedding of a large-scale clockwise vortex that is associated with the separated shear layer. The vorticity layer that follows behind this detached vortex has a distinct sharp streamwise edge that grows in time and streamwise distance as it moves along the surface to form a CW vortex. As this leading vortex grows, it moves away from the surface and the flow begins to separate again. The full paper will include additional phase locked PIV measurements that will track the evolution cycle of the vorticity that forms during the transient attachment and separation of the flow. In addition, vorticity flux through the wake will be computed from the PIV data and will be used to determine the unsteady circulation about the airfoil.

---

[a] Woodruff School of Mech Eng, Georgia Institute of Technology, Atlanta GA 30332, USA.

[1] Amitay, M. and Glezer, A., *Int. J. Heat Transfer and Fluid Flow*, **23**, 690-699. (2002)

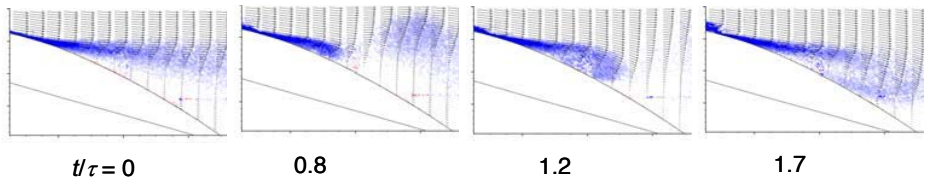

Figure 1: Phase-averaged vorticity concentrations and velocity vectors at the onset of and following pulsed actuation. The convective timescale, τ = 20 msec.

Progress in Plasma Actuator Applications for Active Flow Control

B. Goeksel [a], D. Greenblatt[b]

A plasma actuator consists of two thin metal electrodes separated by a dielectric layer which is part of the airfoil surface[1]. Sufficiently high voltages supplied to the actuator causes the air to weakly ionize at the edges of the upper electrodes. In asymmetric configuration the plasma induces a 2-D wall jet in the flow direction along the surface of the airfoil and thus adds momentum to the boundary layer. Pulsating electric fields are used to excite flow instabilities and delay leading edge flow separation. Unsteady operating acoustic actuators for efficient flow separation control are known for over 10 years[2]. Since 2004, there is increasing interest in unsteady operating plasma actuators[3].

The plasma was operated with a signal of short intermittent bursts of 5 kHz with a modulation frequency in the range of 10 to 100 Hz and a varying duty cycle from 1 to 100% at fixed voltages 8, 10 and 12 kV p-p. The flow separation on the wing could be delayed to angles of attack equal and greater than 25°. Lift and drag were improved substantially resulting in lift to drag ratio benefits of 74-165%. The maximum lift could be increased by up to 135%. The plasma actuators were operated over a range of free-stream speeds from 1.7 to 11.6 m/s giving chord Reynolds numbers from 20K to 140K. At all free-stream speeds, the maximum lift coefficient could be reached and the stall regime relaxed using unsteady operation of plasma actuators. It was even observed that excitations with duty cycles down to 1% were still capable to reattach the fully separated flow. The power to achieve this was approximately 0.6 watt per meter. Results of laser light sheet smoke visualizations and LDV measurements will be presented (see figure 1).

---

[a] Project Manager Electrofluid Systems, FESTO AG & Co. KG, D-73770 Denkendorf, Germany.

[b] Institute of Fluidmechanics, TU Berlin, D-10623 Berlin, Germany.

[1] Enloe et al., *AIAA Journal* **42**, 589 (2004).

[2] Greenblatt and Wygnanski., *Progress in Aerospace Sciences* **36**, 487 (2000).

[3] Goeksel and Rechenberg., *CEAS/KATnet Conference on Key Aerodynamic Technologies to Meet the Challenges of the European Vision 2020* (2005).

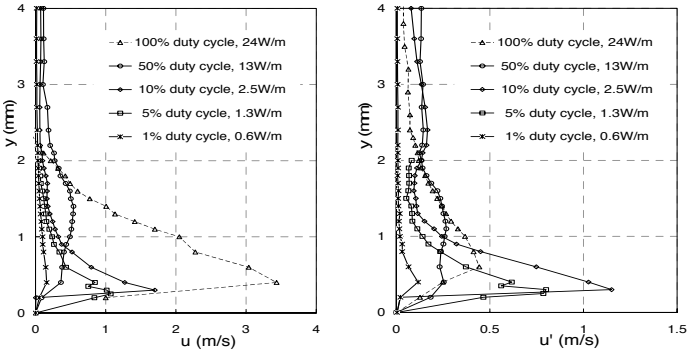

Figure 1: (a) Mean velocity. (b) Fluctuating velocity at $U_\infty = 0$.

Active control of an aerodynamic noise generating flow

S. Izawa*, K. Kobayashi*, A.K.. Xiong*, and Y. Fukunishi*

An active flow control to reduce the aerodynamic noise generated by a flow over a cavity is attempted, using a device which consists of a loudspeaker and a resonator. The experiment is conducted in a closed circuit, low-turbulence wind tunnel of the Institute of Fluid Science (IFS), Tohoku University. The test piece with a cavity is 800mm long and 230mm wide, and is mounted in an open-type test section. The upstream edge of a cavity is 450mm away from the leading edge Four controlling devices are installed side-by-side in the spanwise direction beneath the cavity, as shown in figure 1. The position of each loudspeaker x can easily be shifted along the streamwise direction. The air will be forced in and out from the thin slots by operating the loudspeakers. The basic idea for the noise suppression is to generate wavy structures in the separated shear layer over the cavity, which have 180 degrees phase differences along the spanwise direction. And because of the phase differences, the acoustic waves coming out from the cavity should cancel each other in the far field. A resonator is attached horizontally beneath the flat surface behind the cavity so as to form a deep cavity that emits a large tone noise. A condenser microphone is set 800mm above the cavity to measure the cavity noise. The freestream velocity U is 30.0m/s and the velocity fluctuation within the freestream is 1.4%. By comparing to the cases with and without the cavity, the dominant frequency of the cavity noise is found to be approximately 450Hz and the Sound Pressure Level (SPL) to be 93dB. It should be noted that the noise increases by 2dB when the all devices set at x=20mm are operated at the same phase at 450Hz.

The experimental results when the devices are operated out-of-phase are shown in figure 2. It can be found that the control effect depends on the loudspeaker position, and in some cases, the noise can be very well suppressed even when the operating frequencies f are different from the target frequency. The maximum effect reaches over 20dB at x = 20mm with f=600Hz, and x=60mm with f=500Hz. An experiment to control the flow at the downstream edge of the cavity using the same device is also conducted. The boundary layer upstream of the cavity is laminar. In this case, the same-phase mode is found to be more effective compared to the out-of-phase mode, even though the sound directly generated by the loudspeaker is larger. The maximum of 13dB noise suppression is achieved. It is shown that the optimum frequency, which can reduce the total of the cavity noise and the loudspeaker sound, exists.

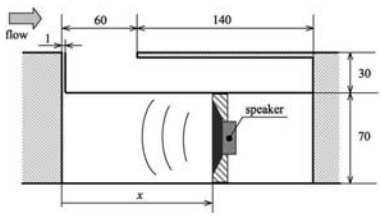

Figure 1: Control device.

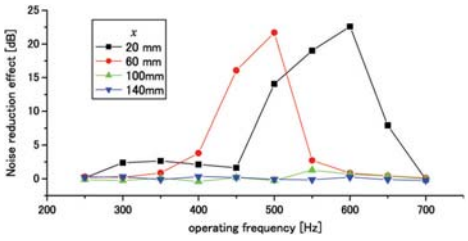

Figure 2: Control effect at various operating frequencies and loudspeaker locations.

*Department of Mechanical Systems and Design, Tohoku University, Sendai 980-8579, Japan.

Experimental and Numerical study of fluidic injection for noise reduction

E. Gutmark[a], W. B. Callender[a], R. Szasz[b], L. Fuchs[b], S. Martens[c]

Chevron nozzles have been extensively studied as means for aircraft engine exhaust noise attenuation. These studies reveal that the increased mixing generated by the chevrons leads to the attenuation of the low frequency components of the noise. However, the increased turbulence generation might cause a penalty in the high frequency domain. Fluidic injection is an alternative method for noise reduction and consists in the injection of small diameter jets in the shear layers (see Figure 1). Recent experimental work carried out at the University of Cincinnati, USA, showed that fluidic injection is a feasible approach for noise reduction in the whole frequency domain. In the experiments 16 jets have been injected in the shear layer of the core jet and the free stream (no fan jet has been considered). Several geometrical and flow parameters have been varied to identify the ones most suitable for noise control. Figure 2 shows the SPL spectrum at 90° for several injection pressures. It is observed that the noise reduction increases with increasing injection pressure. The experimental study identified the injected jet/core jet momentum ratio and the pitch angle of the injected jets as the most important factors which influence the noise attenuation.

For such optimization studies numerical methods have the advantage of higher flexibility, compared to experimental studies. These numerical methods are validated first against experimental data. We use a compressible solver to compute the flow and near-field acoustics for the base case studied in the experiments. Far-field acoutics can be computed, by using a decomposition technique. Cases with and without fluidic injection are considered. The flow field is compared to the PIV measurements. The results in term of frequency spectrum of the sound pressure level are to be presented.

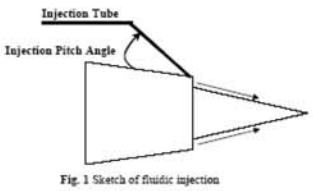

Fig. 1 Sketch of fluidic injection

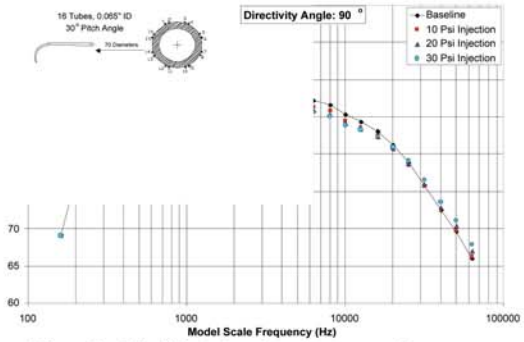

Fig. 2: Fluidic Injection Spectra, 90 .
Mean Flow NPR: 1.79, To: 70 F.

[a] Div. Fluid Mech., LTH, SE-22100 Lund, Sweden.
[b] Dept. Aerospace Eng. and Eng. Mech., U. Cincinnati, Cincinnati, USA
[c] General Electric Aircraft Engines, Evendale, USA

Critical properties of forced wakes

G. Bouchet[a], B. Thiria[b] and J.E. Wesfreid[c]

We present direct numerical simulations of a flow behind an oscillating cylinder around its axis, at moderate Reynolds number, and we compare them to experimental results.

This flow geometry represents the very typical situations observed in flow control studies.

We worked on lock-in and non lock-in regimes and, in this latter case, we analyzed the critical behavior of the global mode as a function of the forcing amplitude, as well as the forcing frequency.

We observe a modification of the Strouhal number of the wake oscillations, this Strouhal number being all the more weak as the amplitude of forcing is large.

We confirmed the results of previous experimental works dealing with the scaling properties of theses global modes, scaling with the growth rate of perturbations, themselves depending on forcing parameters. Owing to the scaling, we have been able to renormalize the global modes.

[a] IMFS, Strasbourg, France.
[b] ENSTA, Palaiseau, France.
[c] PMMH-ESPCI, Paris, France.

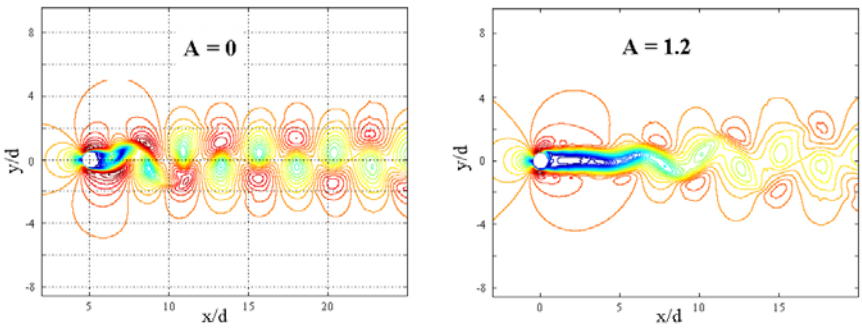

Figure 1: Velocity field around the cylinder without (left) and with (right) forcing (Re = 150 as the experiments, forcing frequency = 4.2 times the natural frequency).

Feedback Control of Laminar Wake Flows Based on Point–Vortex Models

B. Protas*

In this investigation we are interested in the control of vortex shedding in 2D laminar wake flows past a circular cylinder where the cylinder rotation is used as the flow actuation. Our objective is to reduce the flow instationarity downstream of the obstacle measured by the level of velocity fluctuations. In an earlier study[1] we used methods of the Linear Control Theory to develop a feedback stabilization strategy for a model of the flow based on the Föppl system[2]. While showing the potential of this approach, our computational experiments also revealed certain limitations of the Föppl system as a reduced–order model for flow control, most importantly the presence of uncontrollable neutrally–stable oscillatory modes. The objectives of the present investigation are essentially twofold: first we want to provide a better mathematical characterization of the Föppl model in the controlled regime, so as to understand the source of its limitations, and, secondly, we want to develop a systematic methodology that can be used to improve this model.

As regards the first question, we use methods of Nonlinear Dynamical Systems to extend our analysis of the controlled Föppl system to the nonlinear regime. In particular, by employing the Center Manifold Theory we prove that, while the linear controller was able to stabilize the linearized system, the original nonlinear Föppl system remained weakly nonlinearly unstable despite the action of the controller. We also identify the uncontrollable neutrally–stable mode as responsible for this instability.

In the second part, we show that this situation can be remedied by constructing a family of higher–order Föppl systems that can be employed as reduced–order models for flow stabilization. These higher–order Föppl systems are derived as corrections to the classical Föppl system which approximate solutions to the Euler equations with finite–area vortices with constant vorticity[3], rather than point–vortices as in the case of the original Föppl system. The higher–order Föppl systems contain an infinite number of adjustable parameters which can be tuned in order to obtain reduced–order models with desired characteristics, a degree of flexibility not present in the original Föppl system. Various properties of the higher–order Föppl system relevant from the control–theoretic point of view will be reviewed and compared to those of the original Föppl system. We will also report results of computational and experimental investigations of the wake flow stabilization using control techniques based of these higher–order Föppl systems as reduced–order models.

*Department of Mathematics & Statistics, McMaster University, Hamilton, Ontario, Canada

[1]Protas, *Phys. Fluids*, **16**, 4473–4488, 2004.
[2]Föppl, *S*itzb. d. k. Bayer. Akad. d. Wiss. **1**, 1-17, (1913).
[3]Elcrat et al., *J. Fluid Mech.* **409**, 13–27 (2000).

Passive drag control of a sharped edge cylinder using a secondary cylinder

B. Thiria*, L. -M. Malbec*, J. -F. Beaudoin† and O. Cadot*.

The turbulent drag of a bluff body whose separation points are fixed by sharped edges is investigated at large Reynolds number (Re = 30 000). The drag is controlled by means of a smaller cylinder located behind the bluff body as was studied by Sreenivasan & Strykowski for a circular cylinder at low Reynolds number[1]. Measurements of global drag versus the controlled cylinder location are first performed. Whatever its location, the effect of the controlled cylinder is to decrease the drag. In the most effective regions, the drag is reduced down to 20 % . A particular study is then investigated for the case where the location of the secondary cylinder involves the most substantial drag reduction. Statistical analysis of PIV measurements show that the eddy viscosity of the wake is largely decreased leading to a less diffused wake compared to the case of no control. The study focusses on the large coherent structure whose global mode envelop, measured with a hot wire anemometer, is found to be strongly inhibited by the presence of the controlled cylinder. The mechanism responsible for drag reduction can be explained as a stabilization due to the presence of the controlled cylinder. It is important to note that this mechanism involves neither any displacement of the separation points, which are fixed by the experiment, nor any change in the global enstrophy in the wake, but is a consequence of a reorganization of the spatial vorticity distribution in comparison to the free case. An experiment of phase averaging illustrates this effect on the large coherent structures distribution.

*Unité de Mécanique, Ecole Nationale Supérieure de Techniques Avancées, Chemin de la Hunière, 91761 Palaiseau Cedex, France.

†Department of Research and Innovation, PSA Peugeot-Citroën, 2 route de Gisy, 78943 Vélizy-Villacoublay, France.

[1]K. R. Sreenivasan and P.J. Strykowski, *J. Fluid. Mech.* **218**, 71-108 (1990).

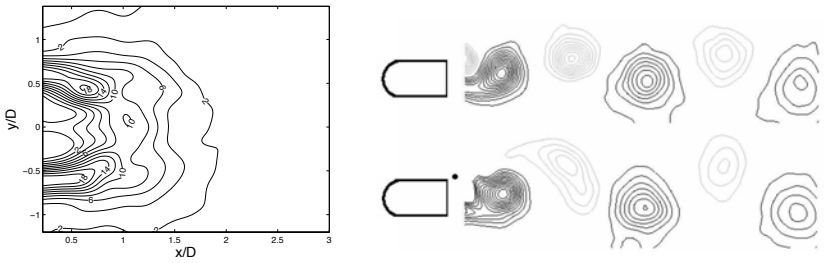

Figure 1: left: Contour plot of the drag reduction ($\Delta F(x, y)$, in %) on the primary cylinder between controlled and uncontrolled case for different location of the control cylinder. right: Phase averaged fields without (top) and with (bottom) the control cylinder.

Viscoelastic bells

L. Lebon*, L. Limat* and A. Belmonte†

We performed experiments on liquid bells resulting from the impact of a viscoelastic fluid on a circular obstacle larger than the jet diameter, in the way of water bells by Savart[1]. We used polymer solutions or giant-micelle solutions as viscoelastic fluid.

In the regime of closed bell, we observed a particular shape of bells, very different from the shape of water bells as observed and predicted by Clanet[2]. The bells shape is essentially controled here by the viscoelastic rheology. It appears also very sensitive to the pressure gap through the liquid film.

For higher flow rate, the bells do not close anymore and form liquid sheets. Their desintegration is very different from the one observed for Newtonian liquid : filaments structure extends the sheet without any drops formation. An original behaviour of growth of circular holes with a thick rim is also observed.

*Laboratoire de Physique et Mécanique des Milieux Hétérogènes, UMR 7636 CNRS, 10, rue Vauquelin 75005 Paris (France)

†Department of Mathematics, Penn State University, University Park, PA 16802 USA

[1]F. Savart, *Ann. Chim.* **54** (1833)

[2]C. Clanet, *J. Fluid Mech.* **430** (2001)

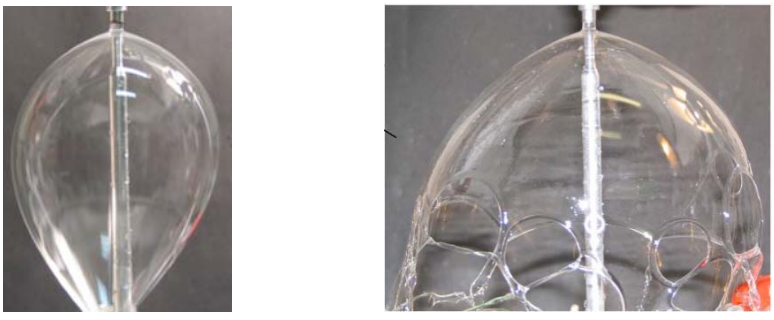

Figure 1: (a) Closed viscoelastic bell (b) Open viscoelastic bell

VISCOELASTIC SIMULATIONS OF THE EXTRUDATE SWELL PROBLEM USING THE PTT MODEL

George Karapetsas[a], John Tsamopoulos[a]

We examine the steady axisymmetric extrudate swell problem for a viscoelastic fluid. For the simulation of this process the mixed finite element method is combined with a quasi-elliptic mesh generation scheme in order to capture the deformation of the free surface of the fluid. The Phan-Thien/Tanner (PTT) constitutive equation is employed in order to model the fluid's viscoelastic behaviour. The elastic viscous stress splitting technique (EVSS-G) is used to separate the elastic and viscous contributions to the stress tensor together with a streamline upwind Petrov-Galerkin (SUPG) discretization of the constitutive equation. Our methodology allows us to compute at larger values of fluid elasticity, measured by the Weissenberg number, than earlier reported in the literature and compares favourably with them at lower We. A complete parametric analysis is performed in order to examine the effects of elastic, capillary and inertia forces as well as of the Newtonian viscosity on the process. The figure shows the dependence of the swelling ratio on the Weissenberg number.

It is widely known that extrusion of viscoelastic materials may lead to various instabilities which are of major importance in applications. In order to address this significant problem and to find under which operational parameters these instabilities arise we present a linear stability analysis of the basic axisymmetric flow with respect to both axisymmetric and non-axisymmetric perturbations.

[a] Laboratory of Computational Fluid Dynamics, Department of Chemical Engineering, University of Patras, Patras 26500, Greece

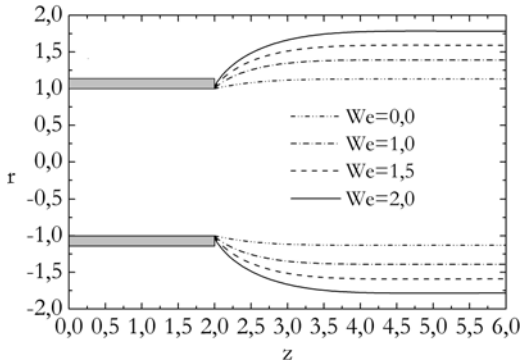

Figure 1: Swelling ratios for various Weissenberg numbers

Leaping shampoo and the stable Kaye effect

M. Versluis[a], C. Blom[a], D. van der Meer[a], K. van der Weele[a], D. Lohse[a]

Shear-thinning fluids exhibit surprisingly rich behaviour. One example is the Kaye effect[1] which occurs when a thin stream of a solution of polyisobutylene in Decalin is poured into a dish of the fluid. As pouring proceeds a small stream of liquid occasionally leaps upward from the heap. This surprising effect, which lasts only a second or so, is named after its first observer A. Kaye, who could offer no explanation for this behaviour. Later, it was suggested from 250 frames per second cine recordings[2] that the fluid must be highly shear thinning as well as elastic and 'pituitous' . In addition, it was concluded that a rigid surface is required to back the reflected liquid stream.

While the words bouncing and reflection are associated with non-continuous and elastic effects, we will show here that the Kaye effect is in fact a continuous flow phenomenon. We show that the Kaye effect works for many common fluids, including shampoos and liquid soaps. We reveal its physical mechanism (formation, stability and disruption) through high-speed imaging. The measurements are interpreted with a simple theoretical model including only the shear thinning behaviour of the liquid; elastic properties of the liquid play no role. We show that the Kaye effect can be stable and that it can be directed. We even demonstrate a stable Kaye effect on a thin soap film excluding the necessity of a rigid backing surface.

[a] Physics of Fluids, University of Twente, P.O. Box 217, 7500 AE Enschede, The Netherlands.

[1] Kaye, Nature **197**, 1001 (1963)

[2] Collyer and Fischer, Nature **261**, 682 (1976)

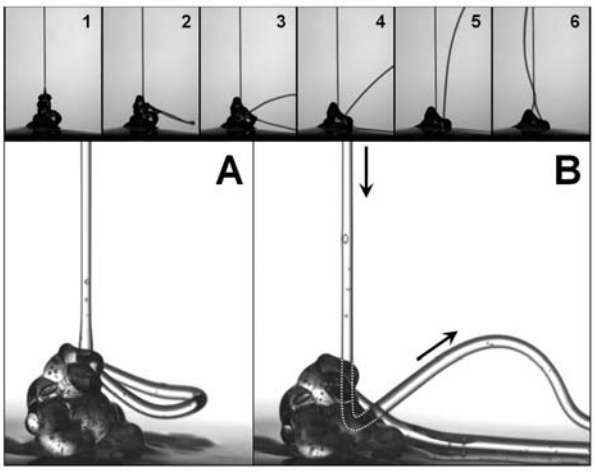

Figure 1: High-speed visualization of the Kaye effect

Initial stage of transition for plane Poiseuille flow of Bingham fluid.

C. Nouar*and A. Bottaro†

Plane channel flow of a Bingham fluid is characterized essentially by the presence of an unyielded zone, bounded by two shear regions where nonlinear variation of the effective viscosity is encountered. The width of the unyielded zone depends only on the Bingham number, B, which describes the ratio of yield and viscous stresses. The fluid within this zone is constrained to move as a rigid body: the rate of strain tensor is identically zero and the stress tensor is undetermined. The linear stability analysis based on a modal approach shows that the plane Poiseuille flow of a Bingham fluid is stable with respect to two- and three-dimensional perturbation. Nevertheless, in experiments, transition to turbulence is observed and a transitional Reynolds number, Re_t, was determined for different yield stress fluids [1]. The experimental results indicate in particular that Re_t increase with B. As the flow is linearly stable at Re_t, the transition to turbulence is therefore subcritical. The linear operators involved in the perturbation equations are non-normal. This non-normality means that there is potential for strong initial amplification of disturbances, also denoted transient growth. An other important consequence of the non-normality of the linearized operator is the high sensitivity of some eigenvalues to perturbations, such as, distorsions in the base flow [2] [3]. The objective of the present work is to investigate the influence of B on the characteristics of two possible initial paths of transition (i) transient growth scenario and (ii) exponential amplification of one (or more) mode(s) in nominally subcritical conditions when the mean flow is mildly distorted compared to its idealized counterpart. After an appropriate scaling of the variables and parameters of the problem in the linearized perturbation equations it is shown that the influence of B reduces only to the change in viscous dissipation. However, the viscous dissipation due to the Bingham terms is anisotropic. Indeed, the expressions of the shear stresses perturbation indicate that τ'_{xy} is independent of B. Here, x and y are the streamwise and the normal to wall directions respectively. As a consequence, the optimal perturbation (which provides the most energy) is oblique. The variations of the optimal streamwise and spanwise wave numbers as function of B were determined. When $B \to 0$, the optimal perturbation is characterized by a streamwise vortices as for Newtonian shear flows. Concerning the second path of transition, the sensitivity of the eigenvalues to the perturbation in the linearized operators, arising from base flow modifications was determined. The numerical results show, for instance, for streamwise perturbation that the sensitivity function is maximum for the eigenvalues at the intersection of the A, P and S Branches of the spectrum, and the maximum is practically independent of B (after scaling). The base flow distorsion that maximizes the growth rate of a mode is under investigation.

*INPL-ENSEM-LEMTA, 2, avenue de de la forêt de Haye BP 160, 54504 Vandoeuvre, France.
†DIAM, University di Genova, Via Montallegro 1, 16145 Genova, Italy.

[1] Hanks and Pratt,*Society of Petroleum Engineering Journal*, 342 (1967)
[2] Bottaro et al., *J. Fluid Mech.* **476**, 293 (2003).
[3] Gavarini et al., *J. Fluid Mech.* **517**, 131 (2004).

Stabilizing the Burnett Equations as Equations in the Fluid Dynamic Variables

Lars H. Söderholm*

For a gas, the Navier-Stokes equations are to first order in the mean free path and the Burnett equations[1] to second order. They have an unphysical instability.[2] We modify the Burnett equations to remove the unphysical instability.

In the one-dimensional case the Burnett momentum equation is when linearized (the unit of length is of the order of the mean free path and that of speed the thermal speed)

$$v_t = -p_x + \frac{4}{3}v_{xx} + \frac{2}{3}\omega_2\rho_{xxx} - \frac{2}{3}(\omega_3 - \omega_2)T_{xxx},$$

and our corresponding hybrid Burnett equation linearized

$$v_t - \omega_2 v_{xxt} = -p_x + \frac{4}{3}v_{xx} + \frac{2}{3}\omega_3\rho_{xxx}.$$

For modes $\exp(ikx + \Lambda t)$ the curves traced out by the complex growth factor Λ is plotted. In Fig. 1 we see that for the Burnett equations some modes are unstable but not for the hybrid Burnett equations.

*KTH Mechanics, SE-100 44 Stockholm, Sweden.

[1] Burnett, *Proc. London Math. Soc.* **40**, 382 (1935).

[2] Bobylev, *Soviet Physics Doklady* **27**, 29 (1982).

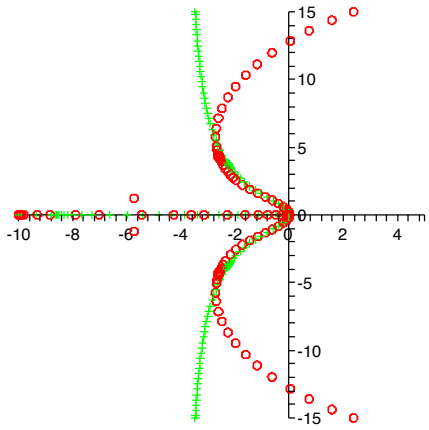

Figure 1: Complex growth factor for Burnett (circles) and for hybrid Burnett (crosses)

Bouncing Leidenfrost drops: effect of polymer additives

V. Bertola[a]

When a liquid drop impacts on a wall kept at a temperature much higher than the boiling point of the liquid, it floats on the thin vapour film that creates at the liquid-solid interface. Although it has been known for a long time, the so-called Leidenfrost phenomenon is still poorly understood, and several open questions have been addressed only recently[1]. After impact, the combined effects of surface tension and of the vapour layer may propel the drop off the wall[2], generating a "bouncing Leidenfrost drop".

This work presents an experimental study about the dynamics of bouncing Leidenfrost drops; in particular, the amplitude of rebounds and the oscillations of the drop size were measured by digital image processing of high-speed movies. Drop shape oscillations driven by surface tension are known to be spherical harmonics (eventually damped by viscosity)[3]; however, this is no longer true if convection occurs inside the droplet, because additional modes must be taken into account.

Recently, it has been shown that very small amounts (of the order of 100 p.p.m.) of flexible polymers (such as polyethylene oxide) may have a tremendous effect on the dynamics of drop impact, without changing significantly the fluid viscosity and surface tension[4,5]. Therefore, the effect of these additives on the amplitude of rebounds and drop oscillations was further investigated. The results show that additives increase the number of consecutive rebounds, as well as the maximum height reached by the drop. At the same time, they reduce mechanical energy losses due to convection within the drop.

---

[a] The University of Edinburgh, School of Engineering and Electronics, Edinburgh EH9 3JL, UK.

[1] Biance et al., *Phys. Fluids* **15**, 1632 (2003)
[2] Watchers and Westerling, *Chem. Eng. Sci.* **21**, 1047 (1966)
[3] Prosperetti, *J. Méc.* **19**, 149 (1980)
[4] Bergeron et al., *Nature* **405**, 772 (2000)
[5] Bertola and Sefiane, *Phys Fluids* **17**, 108104 (2005)

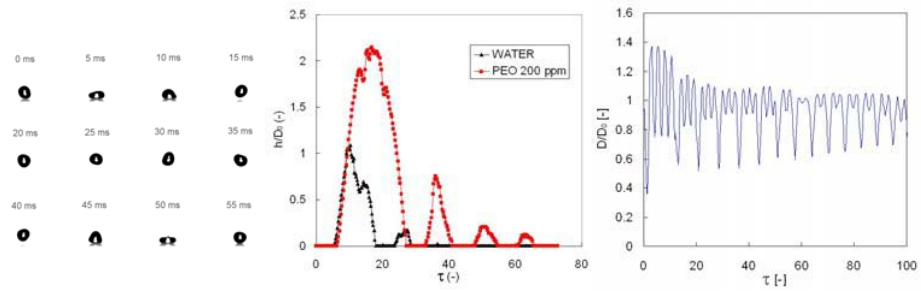

Figure 1: (a) Images of a bouncing drop. (b) Dimensionless gap between the drop and the surface. (c) Diameter fluctuations during rebound (water + 200 ppm PEO).

Molecular dynamics of polymers in a mesoscale solvent: The effect of shear

M. Chinappi[*], E. De Angelis[*], S. Melchionna[†], S. Succi[‡], C.M. Casciola[*], R. Piva[*].

The transport of long flexible polymers by hydrodynamic flows is relevant in many biotechnological applications. In this kind of problems involving a huge number of particles one is priory interested in the dynamics of a relatively small number of degrees of freedom while detailed information on the remaining ones is often not required. Typical example is the spreading of a polymer under the action of a solvent in motion, e.g. in the context of fast analysis of DNA sequences, where a polymer chain is convected in a strongly sheared environment. Here the interest is focused on the DNA configuration while the detailed dynamics of solvent molecules is of no relevance.

The basic idea to tackle this problem is to use molecular dynamics for the polymer and a macroscopic model for the solvent motion. The open issue is how to handle the coupling between polymer and solvent. Several attempts have been proposed to couple classical macroscopic flow models (Navier-Stokes equations, Lattice-Boltzmann method) with molecular dynamics. In this framework, one of the problems to deal with is how incorporating in a proper way the local fluctuations occurring in the solvent.

Here we use the so-called Stochastic Rotation Particles method introduced by Malevanets and Kapral[1], which is known to yield the appropriate Navier-Stokes hydrodynamics with correct equilibrium fluctuations (e.g. the velocity distribution is Maxwellian). Interestingly, the Navier-Stokes dynamics is reproduced to the extent that even interactions with solid boundaries are easily incorporated. This allows to reproduce with good accuracy the flow conditions encountered by the polymers in many biotechnological devices. Being a particle method, the coupling of the solvent with the detailed degrees of freedom of the polymeric chains described through molecular dynamics is easily introduced.

Our aim is to extend recent results concernig long chain molecules having one end tethered to a fixed object[2,3] to the case of a freely convected polymer. In particular, we will address the role of the imposed shear rate on extension and morphology of the chain taking into account the appropriate hydrodynamic interactions.

[1] Malevanets A., Kapral R. *J. Chem. Phys.* **110**, 8605 (1999).
[2] Zimm B.H., *Macromolecules* **31**, 6089-6098 (1998).
[3] Webster M. A., Yeomans M. *J. Chem. Phys.* **122**, (2005).

[*]Dip. di Meccanica e Aereonautica, "La Sapienza", via Eudossiana 18, 00184, Roma, Italy
[†]sdfsa
[‡]

Transport Coefficients and Orientational Distributions of Spheroidal Particles with Magnetic Moment normal to the Particle Axis (Analysis for A Magnetic Field applied normal to the Shear Plane)

Akira Satoh[a] and Masataka Ozaki [b]

We have investigated the influence of the magnetic field strength, shear rate, and rotational Brownian motion on transport coefficients such as viscosity and diffusion coefficient, and also on the orientational distributions of rodlike particles of a dilute colloidal dispersion. The rodlike particle is modeled as a magnetic spheroidal particle which has a magnetic moment normal to the particle axis; such a particle may typically be a hematite particle. In the present study, an external magnetic field is applied in the direction normal to the shear plane of a simple shear flow. The basic equation of the orientational distribution function has been derived from the balance of torques and solved numerically. The results obtained here are summarized as follows. Although the orientational distribution function shows a sharp peak in the shear flow direction for a very strong magnetic field, such a peak is not restricted to the field direction alone, but continues in every direction of the shear plane. This is due to the characteristic particle motion that the particle can rotate around the axis of the magnetic moment in the shear plane, although the magnetic moment nearly points to the magnetic field direction. This particle motion in the shear plane causes negative values of the viscosity due to the magnetic field. The viscosity decreases, attains a minimum value, and then converges to zero as the field strength increases. Additionally, the diffusion coefficient is significantly influenced by such characteristic particle motion in the shear plane for a strong magnetic field.

[a] Akita Prefectural University, 84-4, Ebinokuchi, Tsuchiya-aza, Yuri-Honjo 015-0055, Japan.
[b] Yokohama City University, 22-2, Seto, Kanazawa-ku, Yokohama 236-0027, Japan.

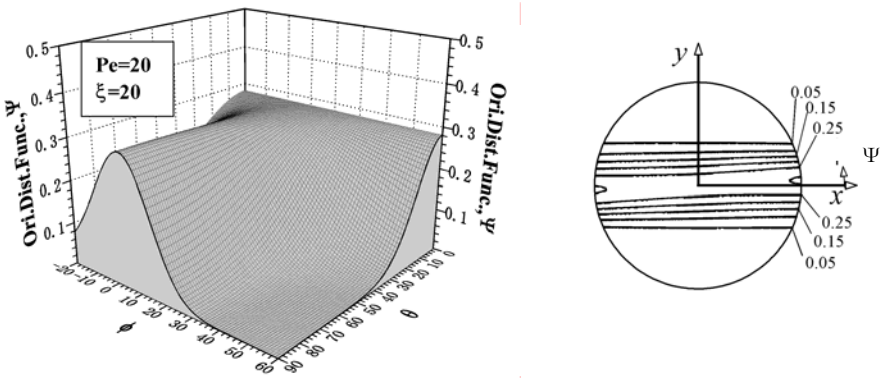

Figure 1: Particle orientational distribution function for the Peclet number *Pe*=20 and the strong magnetic field ξ =20. The figure on the right-hand side is contour lines viewed along the z-axis (θ=0°)from infinity. The shear flow and the magnetic field are applied along the *x*-axis direction (θ=90°,φ=0°) and the *y*-axis direction (θ=90°, φ=90°), respectively.

Slip flow over a lubricated rotating disk

H.I. Andersson[a] and M. Rousselet[a]

The von Kármán flow of a viscous fluid which arises due to the rotation of a disk in an otherwise stagnant fluid constitutes a prototype of three-dimensional (3D) boundary layer problems. Sparrow et al.[1] and Miklavcic & Wang[2] considered the flow of a Newtonian fluid due to the rotation of a porous-surfaced disk and for that purpose replaced the conventional no-slip boundary conditions at the disk surface with a set of linear slip-flow conditions.

The objective of the present study is to examine the laminar flow of a Newtonian bulk fluid arising from a solid rotating disk lubricated by a non-Newtonian liquid film obeying the inelastic power-law model. First, a set of non-linear slip-flow boundary conditions for the flow due to a lubricated rotating disk is derived. Similarity solutions of the resulting 3D boundary layer problem are generally prohibited by the replacement of the conventional no-slip conditions by the new slip-flow conditions, except in the particular case when the power-law index n of the non-Newtonian lubricant equals 1/3. Numerical solutions are presented for this case in Figure 1, showing that the 3D flow field is dramatically affected by accentuated velocity slip. The amount of velocity slip is controlled by a single dimensionless slip coefficient λ ($\lambda \to \infty$ in the no-slip limit). The spin-up by viscous action of the bulk fluid next to the rotating disk is reduced with increasing slip. The radially directed centrifugal force is correspondingly reduced. The radial slip turns out to be insufficient to outweigh the reduced centrifugal force. The radial slip velocity f(0) therefore reaches a maximum value slightly above 0.12 when λ is close to unity, i.e. when the lubrication length and the viscous length scale nearly equals. In particular, the axial flow towards the disk, i.e. the pumping efficiency, and the torque required to maintain steady rotation of the disk, decrease monotonically with increasing slip.

[a] NTNU Energy and Process Engineering, 7491 Trondheim, Norway.

[1] Sparrow et al., *Int. J. Heat Mass Transfer* **14**, 993 (1971).

[2] Miklavcic and Wang, *ZAMP* **55**, 235 (2004).

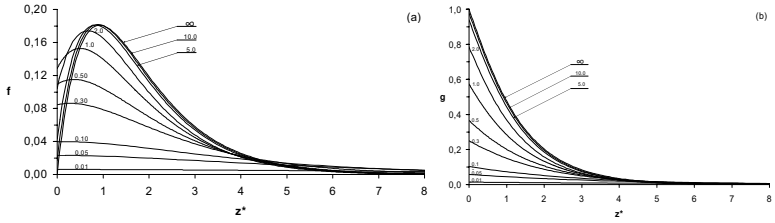

Figure 1: Similarity solutions for n = 1/3 for different values of the slip coefficient λ. (a) Radial velocity f(η). (b) Circumferential velocity g(η).

Steady Stokes flow in a two-dimensional sector

V. V. Lyakh*, V. V. Meleshko*

This paper deals with the two-dimensional creeping flow of a viscous incompressible fluid contained in a sector cavity $0 \le r \le a$, $-\theta_0 \le \theta \le \theta_0$ (r, θ – polar coordinates) of arbitrary angle θ_0. The flow is induced by a prescribed tangential velocity at the circular boundary while the radial walls of the cavity remain unmoveable. This problem amounts to solving homogeneous biharmonic equation for a scalar function when this function and its normal derivative are given at the boundary[1].

Among various mathematical and engineering approaches, the method of superposition is effective. It consists in constructing the solution of the biharmonic equation in the form of the sum of ordinary Fourier series and Fourier integral with sufficient functional arbitrariness for fulfilling the boundary conditions on the curved $r=a$ and the straight sides $\theta = \pm\,\theta_0$, respectively. The satisfaction of prescribed boundary conditions leads to an to infinite linear system of integro-algebraic for their density and coefficients. The knowledge of the leading terms in behaviour of density and coefficients allows to apply improved reduction algorithm to solving the system as well as to provide high accuracy in determination of velocity field in the cavity including its boundary. This approach is similar to that developed for other types of two-dimensional cavities with sharp corners[2], and it allows to treat analytically the flow in the finite sector with the same completeness as in the infinite wedge due to Moffatt[3].

Connection with another analytical approach, the method of homogeneous solutions, is established; some results seem to be surprising. All coefficients of expansion by homogeneous solutions are obtained. However, any truncated part or this series is worse in rescpect of satisfying the boundary conditions than that with coefficients calculated by any numerical technique, e.g. by method of less squares[4].

The streamline patterns, the tables and the graphs of other physical distributions, e.g. torque and pressure, are shown for several values of θ_0 provided a uniform velocity at the curved wall. The case when $\theta_0 > \pi/2$ is of great interst and considered too. For the semicircular cavity a simple closed-form solution is obtained. The pattern obtained for $2\theta_0 = 28.5^\circ$ completely coincides with visualization by Taneda[5]. Among other quantities the inclination angle at the points of separation of the zero streamline is of great interest. The exact formula determining the inclination angle for any θ_0 is established. Finally, it is shown that in order to find any physical distribution near the exciting curved boundary, corner points in particular, the method of superposition is indispensable while when moving to the sector center the eigenfunction expansion is sufficient, moreover only few first terms of it.

*Kyiv National Taras Shevchenko University, 01033 Kyiv, Ukraine.

[1]Meleshko, *Appl. Mech. Reviews.* **56**, 33 (2003).
[2]Krasnopolskaya et al., *Quart. J. Mech. Appl. Math.* **49**, 593 (1996).
[3]Moffatt, *J. Fluid Mech.* **18**, 1 (1964).
[4]Shankar, *Current Sci.* **30**, 107 (2003).
[5]Taneda, *J. Phys. Soc. Japan* **45**, 1932 (1979).

Long wave propagation through porous media and suspensions

William J. Parnell* and I. David Abrahams*

The study of wave propagation through inhomogenous media is a subject with very wide and important application. Examples include the calculation of wave forces on ocean oil-rig legs; the effective wavespeed of sonar waves in bubbly or fish-laden waters; ultrasound inspection of tumours through complicated biological tissues such as the lung. Of particular interest is the long wave limit, where we wish to obtain an effective or homogenized equation to describe properties of the waves (e.g. wavespeed, dispersion, anisotropy or damping). The present work should also have applications to particle laden flows, complex polymeric fluids and porous media.

The thory of homogenization has a rich history – a number of methods have been proposed to find the effective properties of multiphase fluids or fluid/solid mixtures when the wavelength of the propagating wave is much longer than the charactersitic lengthscale of the inclusions or their average spacing. For periodic arrangements of inhomogeneities the leading order solution may be found by direct asymptotic methods[1]. For random media a variety of different approaches has been employed, such as the self-consistent and T-matrix[2] methods; the latter is a useful technique but is not at all easy to employ for anisotropic phases. The case of complicated shaped micro-inclusion, with large contrast between host and inclusion phase, is therefore best approached using an integral equation method.

The paper will introduce a new integral equation formulation, based on Green's theorem, for a wave propagating through a fluid containing small inclusions (with arbitrary volume fraction). A hierachy of equations is derived by differentiating the pressure or velocity fields, and then expanding the Green's function about all the fibre locations except the one at the observation point. Integrating these equations over the domain of one of the fibres yields a system of equations for the averaged fields.

The significant advantage of the new approach is that four terms *separately* account for the physical details of the inclusion, such as the inclusion shape and orientation, its material contrast with the host fluid, and the distribution of the inclusions. It will be shown that the normalized density and sound speed of the effective medium (in the three principal directions ($j = 1, 2, 3$) of anisotropy) have the form

$$\rho^* = (1 - \phi) + d\phi + O(\epsilon), \qquad c_j^* = 1 + \mathcal{F}_j(m, S, \mathcal{A}_j)\phi + O(\phi^3) + O(\epsilon),$$

where ϵ is the ratio of inclusion size to the wavelength of waves in the host, ϕ is the volume fraction of the inclusions, d and m are the ratio of host to inclusion density and sound speed respectively, S is a simple lattice sum accounting for the inclusion geometry and $\mathcal{A}_j$ is the (first) shape factor of the inclusion. Since each of the three terms m, S and $\mathcal{A}_j$ can be separately accounted for in the solution scheme there is very little extra work if there are changes to the inclusion shape, size or geometry. The $O(\phi^3)$ terms are easily calculated but in practice the leading order terms provide excellent agreement with existing methods up to high volume fractions.

*Mathematics, University of Manchester, Manchester M13 9PL, UK.

[1]Parnell and Abrahams, *Wave Motion* submitted (2005).

[2]Varadan, Varadan and Pao, *J. Acoust. Soc. Am.* **63**, 1310 (1978)

On the formation of hydraulic jumps in two layer fluids

A. Kluwick*, R. Szeywerth*, N. Viertl*

Two layer fluids represent the simplest model of stratified flows with free surface and, therefore, have received considerable interest in the past. Studies carried out within the framework of hydraulic theory [1] have shown that nearly resonant internal waves may exhibit socalled mixed nonlinearity leading in turn to the possible formation of both positive and negative jump discontinuities. Also it was found that the admissibility of such hydraulic jumps can no longer be decided on the basis of the Oleinik criterion as in cases of strictly positive or negative nonlinearity but requires the investigation of their internal dissipative, dispersive structure. To this end Kluwick et al. [2] adopted a structure equation of the form of a modified BKdV equation which represents an ad hoc model as far as dissipation is concerned. In the present study, in contrast, we consider cases where hydraulic jump solutions of the full Navier Stokes equations can be constructed using rigorous asymptotics. Specifically, it is assumed that a suitably defined Reynolds number is large so that viscous effects in the unperturbed state are essentially confined to thin shear layers adjacent to the wall and near the interface between the two layer fluid layers where the flow is taken to be laminar, figure 1. Also, we require that the Froude number differs only slightly from it critical value for which the speed of upstream propagating internal layer waves vanishes which in turn allows for a weakly nonlinear analysis. It is then found that the flow is dominated by the dynamics inside a thin sublayer of the oncoming wall shear layer where the classical Prandtl equations hold in leading order. In contrast to classical boundary layer theory, however, the driving pressure disturbances are no longer imposed but arise form the viscous inviscid interaction between the flows inside and outside the sublayer. Representative solutions of the interaction problem will be discussed. Furthermore, it will be shown that, as in the case of the mBKdV equation, the novel structure problem admits socalled nonclassical hydraulic jumps, i.e. jumps which transmit rather than absorbe wave fronts and thus violate the Oleinik criterion. This raises the question how such jumps can form from smooth initial conditions which will be addressed in detail.

*Vienna University of Technology, Institute of Fluid Dynamics and Heat Transfer, A - 1040 Vienna, Resselgasse 3

[1] e.g. Baines P.G., Topographic Effects in Stratified Flows, Cambridge University Press (1995)

[2] Kluwick A., Scheichl S., Cox E.A., *J. Fluid Mech.*, submitted (2005)

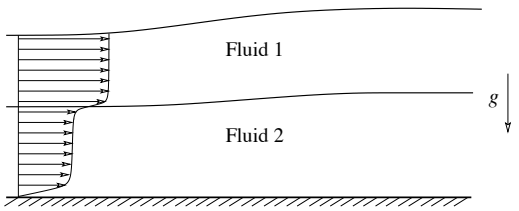

Figure 1: Schematic of weak hydraulic jump in a two layer fluid flow.

Compressible effects in water wave impacts

D.H.Peregrine[a], H.Bredmose[a, b], G.N.Bullock[c], C.Obhrai[c, d], G.Wolters[e] , and G.Müller[e, f]

When water waves are breaking on coastal or marine structures violent impacts occur. Usually in such circumstances there is a significant amount of air entrained into the water as small bubbles, and the wave impact may also trap 'pockets' of air. Pressures at impact can easily exceed one atmosphere so that compressible effects are important. This work has been developed in the context of a programme on violent wave impacts on walls that also included field measurements, and laboratory experiments at large and small scales. The main aim has been to understand details of the most violent pressure records obtained. They extend to pressures over 3 MPa.

The numerical modelling is in two stages. For the waves approaching the wall our well establishing boundary-integral method for inviscid irrotational flows was used[1, 2]. It can describe wave overturning, including examples with high pressures and uprush velocities. In this context it is used to provide initial conditions, and continuing boundary conditions for the second method used in a region close to the wall.

For this violent part of the motion a simple two-phase model is used. The air fraction is included in Euler's equations as an extra variable ranging from 0.01 up to 1.0. Air is taken to be an ideal gas and water as incompressible. A number of interesting features become apparent in the resulting computations, and some initially puzzling features of the experimental measurements can be explained.

The figures show a sequence of computed wave shapes at impact. The compression and subsequent expansion of the trapped air pocket can be seen. The irregular surface in the last profile is due to Rayleigh-Taylor instability.

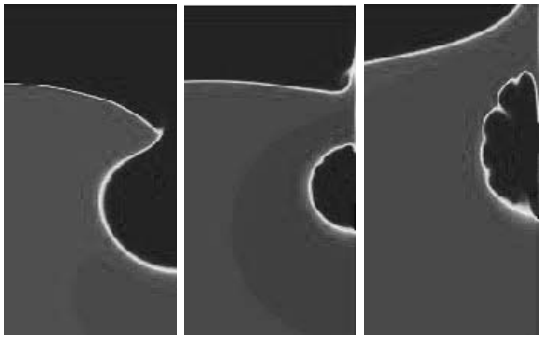

[a] School of Mathematics, Bristol University, Bristol BS8 1TW, England.

[b] now at DHI Water & Environment, DK-2970 Hørsholm, Denmark

[c] School of Engineering, University of Plymouth, Plymouth PL4 8AA, UK

[d] now at HR Wallingford, OX10 8BA, England

[e] Department of Civil Engineering, The Queen's University, Belfast BT7 1NN, U.K.

[f] now at University of Southampton, SO17 1BJ, England

[1] Cooker, M.J., Peregrine, D.H., *Coastal Engineering.* **18**, 205-229 (1992).

[2] Dold, J.W. *J. Comp. Phys.* 103, 90-115 (1992).

The interaction of the wake with the potential flow in mixed convection flow past a horizontal plate

H. Steinrück*and Lj. Savić*

The effect of weak buoyancy on the laminar flow of a fluid with kinematic viscosity ν, isobaric expansion coefficient β past a isothermally heated horizontal plate of length L and temperature $T_\infty + \Delta T$ is aligned under a small angle of attack ϕ to the oncoming free stream (velocity U_∞, temperature T_∞) will be investigated in the distinguished limit of large Reynolds numbers Re with the "reduced" buoyancy parameter $\kappa = \mathrm{GrRe}^{-9/4} = \mathrm{O}(1)$ and the inclination parameter $\lambda = \phi\kappa\mathrm{Re}^{1/4}$ being of order one and where the Grashof number $\mathrm{Gr} = \mathrm{g}\beta\delta\mathrm{TL}^3/\nu^2$ is defined in the usual way.

Considering a large Reynolds number Re temperature and density perturbations are limited to a thin boundary layer and wake, respectively. An essential assumption to determine the perturbation of the outer flow field is the validity of the Kutta condition. Thus a vortex distribution on the wake and the plate can been introduced to compensate the hydrostatic pressure differences at the trailing edge and across the wake. Due to the inclination of the wake, which is determined by the outer potential flow, the flow in the wake is accelerated or decelerated by the tangential (to the wake) component of the hydrostatic pressure gradient. Thus the wake and the potential flow interact and have to be determined simultaneously.

By considering the limiting behavior of the wake for large distances from the plate it can be observed that solutions exists (in case of a heated plate) only for positive angles of attack, such that the fluid in the wake is accelerated. Keeping the inclination parameter λ constant and increasing the buoyancy parameter κ we observe that the wake a few plate lengths after the trailing edge bends downward (see figure 1) and the flow in the wake decelerates there[1]). A numerical investigation delivers solutions only up to a critical number of the buoyancy parameter κ depending on the angle of attack. Solutions will be presented and discussed. Finally it can be shown that the lift coefficient is markedly reduced by buoyancy.

*TU-Vienna, Inst. Fluid Mechanics and Heat Transfer, 1040 Vienna, AUSTRIA

[1]Lj. Savić and H. Steinrück, TAM 32, 1-19,2005.

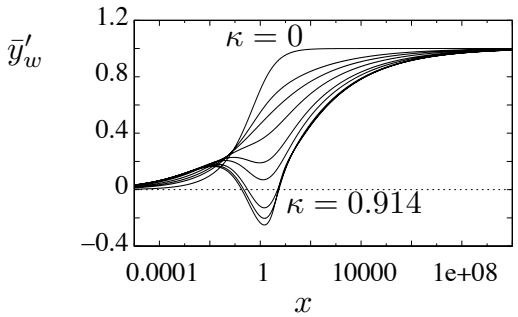

Figure 1: Scaled inclination of wake for different buoyancy parameters κ and $\lambda = 1$.

Study of Double Diffusive Finger Convection in Hele-Shaw Cell

S. Sarkar[a], J. Srinivasan[b] and K. R. Sreenivas[a]

Double-diffusive convection relies on the presence of two diffusing components having different molecular diffusivities in a fluid system. When the faster diffusing component is stabilizing and slower diffusing component is destabilizing, elongated convection cells will develop and are called *salt fingers* (Fig. 1). In this paper we present the development of finger convection in a Hele-Shaw set up. Double diffusive system used in the present study is aqueous solution having salt and sugar as faster and slower diffusing components respectively.

In this set of experiments, we monitor the variation of the length (Fig. 2) and width of the finger with time, their dependence on the governing parameters like Rayleigh numbers and density stability ratio ($R\rho$), and on the gap between the two plates in Hele-Shaw cell set up. Figure 2 indicates the transitions in the growth rate of the finger (marked as T1 and T2 in Fig. 2). We explain how these transitions will help in understanding the observed scatter in the flux ratio (R_f) reported in the literature [1] (Fig. 3). We also relate the observed variations in finger-width and rate of development of the finger front by scaling arguments. Results from experiments indicate that the growth rate of finger is inversely related to the gap width between the two plates in the Hele-Shaw cell set up.

[a] EMU, Jawaharlal Nehru Centre for Advanced Scientific Research, Bangalore- 560 064, INDIA.

[b] CAOS, Indian Institute of Science, Bangalore-560 012, INDIA.

[1] Singh et. al. *J. Fluid Mechanics*, (Under review).

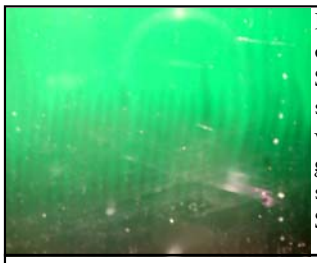

Figure 1: Observed finger convection cells in Hele-Shaw set up. Fluorescence-sodium is used for visualization. Sugar (1.05 g/l) and salt (1.01g/l) system in 5mm gap Hele-Shaw set up.

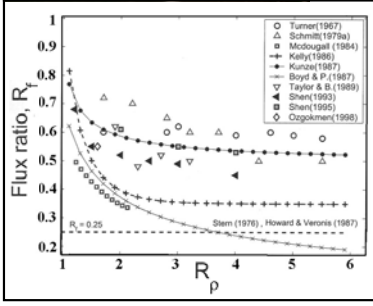

Figure 3: Various correlations reported in the literature[1], indicating the scatter in the data (detailed reference of each correlation is given in reference 1).

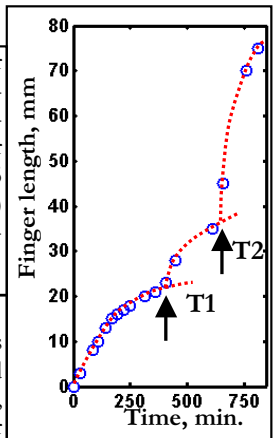

Figure 2: Development of finger length as a function of time. T1 and T2 are observed transitions in the growth rate of finger.

A reduced model for 3D heat and mass transport in PEFCs

P. A. Yakubenko*, G. A. Shugai* and M. Vynnycky*

Mathematical modelling of the operation of a polymer electrolyte fuel cell (PEFC) is rendered difficult by the vast array of physical phenomena that have to be considered[1]: flows are often highly three-dimensional, non-isothermal, multiphase, multicomponent and time-dependent, and occur over several media: flow channels, porous electrode, catalytic layer and electrolyte (see Figure 1). Contrary to the most recent trends in PEFC modelling, which typically involve extensive 3D computational fluid dynamics (CFD), here we use scaling arguments, nondimensionalization and asymptotic techniques to identify the main governing parameters in a model and, subsequently, to derive a reduced model which is considerably cheaper to compute, but which does not sacrifice any significant physical features[2].

In this paper, such a reduced model is derived for a PEFC operating under co-flow, one-phase and non-isothermal conditions; it is then implemented in the finite-element software Comsol Multiphysics. The model includes mass, momentum, species, heat and charge transfer in a cell consisting of bipolar plates, flow channels, gas diffusion layers and catalytic layers at the anode and cathode, and a membrane. The analysis indicates that the temperature variation can contribute significantly only as regards the exchange current density and Tafel law expression associated with the oxygen reduction reaction at the cathodic catalytic layer. Other possible temperature-induced variations, such as gas mixture properties, and Soret and Dufort effects are found to be negligible by comparison. These findings permit an effective decoupling of the energy equation from the rest of the problem.

The main benefit of the present approach is that it will be applicable in modelling fuel cell stacks, for which previously published models would lead to unacceptably high computational costs.

*KTH Mechanics OB 18, SE-100 44 Stockholm, Sweden.

[1]Weber and Newman, *Phys. Fluids* **104**, 4679 (2004).

[2]Vynnycky and Birgersson, in *Transport Phenomena in Fuel Cells (ed. B. Sunden and M. Faghri)*, 247 (2005).

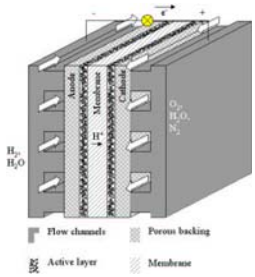

Figure 1: Heart of a PEFC.

Session 9

Rayleigh instabilities in incompressible and supersonic boundary layers

K. W. Cassel*, A. V. Obabko† and D. Bockenfeld*

Two situations are considered in which a Rayleigh instability may arise within an unsteady boundary layer. The first is an incompressible boundary layer owing to flow induced by a thick-core vortex above a plane surface. Numerical solutions of the unsteady, two-dimensional Navier-Stokes equations become unstable in the form of high-frequency oscillations in vorticity and streamwise pressure gradient along the wall, and the best fit line to the dominant wavenumber of the instability (see figure 1 (left)) is $k = 0.342Re^{0.503}$, where the exponent is very close to the one half expected for a Rayleigh instability, i.e. $k = KRe^{1/2}$. The existence of a Rayleigh instability is further confirmed through evaluation of the Rayleigh equation for velocity profiles obtained from a boundary-layer calculation, and the dominant wavenumber of the instability in the Navier-Stokes solutions (dashed line) agrees very closely with that predicted by the Rayleigh solutions (solid lines) as shown in figure 1 (right).

The second case is the supersonic flow past a compression ramp with ramp angle of $O(Re^{-1/4})$, which is governed by the supersonic triple-deck formulation. For scaled ramp angles $\alpha \geq 3.9$, Cassel, Ruban & Walker (1995)[1] have found that the triple-deck flow is unstable to long-wave Rayleigh (LWR) modes, which have wavelengths shorter than the $O(Re^{-3/8})$ streamwise length scale of the triple-deck region, but larger than the $O(Re^{-5/8})$ vertical extent of the lower deck. Rayleigh modes, which are of the same order as the $O(Re^{-5/8})$ viscous lower deck, have a faster growth rate than the LWR instability and would be expected to dominate in solutions of the full Navier-Stokes equations for the compression ramp flow. The stability problem consists of solving the triple-deck formulation for the base flow and the Rayleigh equation for the perturbations to this base flow. Results for ramp angles up to $\alpha = 5.5$ show that for all cases that are unstable to LWR modes, i.e. that contain inflectional velocity profiles, the flow is also unstable to Rayleigh modes.

*Illinois Institute of Technology, Chicago, Illinois, U.S.A.
†University of Chicago, Chicago, Illinois, U.S.A.
[1]Cassel, Ruban & Walker, *J. Fluid Mech.* **300**, 265–286 (1995).

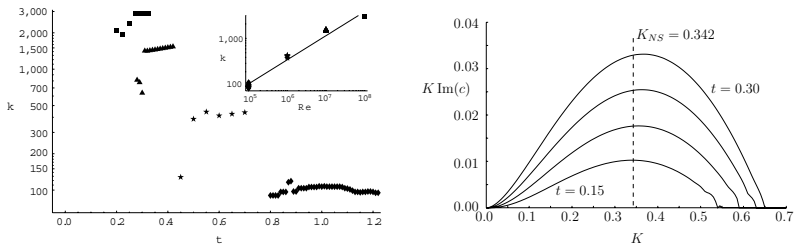

Figure 1: (Left) Dominant wavenumber as a function of time for various Reynolds numbers. (Right) Variation of the growth rate with wavenumber.

The instability of the moving wall boundary layer

A. Merlen,M. Marquillie*

There are still unstudied generic situations in the field of boundary layer stability. One of these comes from the very interesting but difficult problem of the rolling wheel. The upstream flow around a wide wheel admits a stagnation point but not on the surface of the wheel, where the velocity is constant but slightly detached up stream. From that point, one part of the flow turns around the wheel by the top. The corresponding boundary layer, initiated at the stagnation point, is then in contact with a wall that moves up stream relatively to the local external velocity. In the case of an infinite cylinder rolling on a plane the shear effect is much more intensive since three-dimensionnal deviations cannot take place. Numerical resolutions of these flows exhibited difficulties, particularly when classical algebraic turbulence models were used. Some unusual patterns were detected. Clarification came from the study of a flat moving wall which is the generic problem where the curvature and pressure gradient effects are neglected. This basic problem reduces to a modified Blasius equation with one new control parameter: the ratio $\frac{U_W}{U_E}$ between the wall velocity and the external velocity. The paper shows that this problem admits two velocity profiles for each U_W in the range $0 < U_W < 0.355U_E$. For higher values of U_W the theory shows that no self-similar solution exists. Numerical simulation confirms that point and shows that the boundary layer becomes unsteady. Therefore, here the unsteady behavior does not comes from the instability of a steady solution but from the fact that no steady solution exists. A linear stability analysis of the self-similar profiles showed that both were convectively unstable, one much more than the other. The later was never obtained until now, in numerical simulations.

*Laboratoire de Mécanique de Lille UMR CNRS 8107, Cité Scientifique, Bât M3, 59655 Villeneuve d'Ascq, Cedex

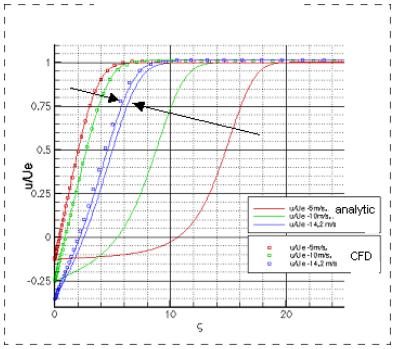

Figure 1: Self similar profile for different values of U_W

Linear and non-linear development of inviscid perturbations on an infinite shear flow

L. Håkan Gustavsson[a], E. Niklas Davidsson[a]

In studies of transition processes in parallel shear flows, the stability of streamwise streaks has been a central issue in recent years. The streaks are generated by a (3D) lift-up process and optimal (linear) growth is associated with longitudinal vortices. The initial growth is algebraic and is basically inviscid in character. The non-linear aspects of the process have been studied as a secondary instability, which is necessary when optimal disturbances are considered, since it can be shown that longitudinal structures have no non-linear feedback on the normal velocity component (v). However, algebraic growth is present also for oblique perturbations (to the mean flow) but the intrinsic non-linear character of the mechanism seems not to have been investigated in full. Therefore, in order to follow the algebraic growth into the non-linear regime, we consider the development of inviscid 3D perturbations on an infinite flow with constant shear.

First, the characteristics of the linear growth are studied and the limit amplitudes of the process are derived. Of particular interest is the long-time residue (the 'permanent scar'[1]) of the initial perturbation. The velocities and energy of the scar are presented. Then, the non-linear development is studied by calculating the non-linear terms in the v-equation. It is shown that only perturbations oblique to the mean flow exhibit non-linear self-interaction. The interaction is calculated as convolution integrals in wave number space and the non-linear terms most activated are identified. Comparisons are made with recent simulations[2].

[a]Division of Fluid Mechanics, Luleå University of Technology, Luleå, Sweden.

[1] Landahl, *SIAM J. Appl Math* **28**, 735 (1975).
[2] Suponitsky, Cohen, Bar-Yoseph, *J Fluid Mech.* **535**, 65 (2005).

Generation of highly-oblique Tollmien-Schlichting waves in a laminar boundary layer by free-stream turbulence

Pierre Ricco* and Xuesong Wu*

We compute the fluctuations induced by free-stream turbulence in a compressible laminar boundary layer using the linearized unsteady boundary region equations[1]. The boundary layer response is controlled by the parameter $\kappa = (2\pi/\Lambda)\sqrt{\nu/\omega^*}$, where Λ and ω^* are the spanwise length scale and the frequency of the free-stream gust, and ν is the kinematic viscosity of the fluid. Numerical results reveal that for $\kappa < \kappa_c \ll \mathcal{O}(1)$ the fluctuation ultimately evolves into a growing disturbance downstream, which is due to a new receptivity mechanism that operates as follows. The free-stream disturbance excites a decaying quasi-three-dimensional Lam-Rott eigensolution[2], which undergoes wavelength shortening to induce a spanwise pressure gradient. The pressure gradient then becomes comparable with the inertia in a viscous sublayer when $x^*/\Lambda \sim 1/\kappa$. At that point the Lam-Rott solution evolves into an exponentially growing mode, which is recognized to be a highly-oblique Tollmien-Schlichting wave. The growth rate and wavenumber can be predicted by the triple-deck theory. This mechanism is akin to the well known leading-edge adjustment process[3], but the difference is that it is through the spanwise rather than the streamwise pressure gradient that instability is induced. We further remark that this relatively low-frequency three-dimensional disturbance may be associated with the spanwise meandering motion of the Klebanoff modes. Figure 1(left) shows a growing disturbance for a M-3 boundary layer with $\kappa = 0.02$, which is generated closer to the leading edge than the incompressible disturbance. Figure 1(right) compares the growth rate $\mathrm{Im}(du/dx)/u$ computed by the triple-deck theory (TD) with that by the boundary region equations (BR) for $M = 0$ and $\kappa = 0.0005$. The good agreement indicates that the growing disturbance is indeed a highly-oblique T-S mode.

*Department of Mathematics, Imperial College, London, 180 Queens Gate, SW7 2BZ, UK.

[1]Leib, Wundrow and Goldstein *J. Fluid Mech.* **380**, 169 (1999).
[2]Lam and Rott, *Cornell Univ. Grad. Sch. of Aero. Eng. Dept. - AFOSR TN-60-1100* (1960).
[3]Goldstein, *J. Fluid Mech.* **127**, 59 (1983).

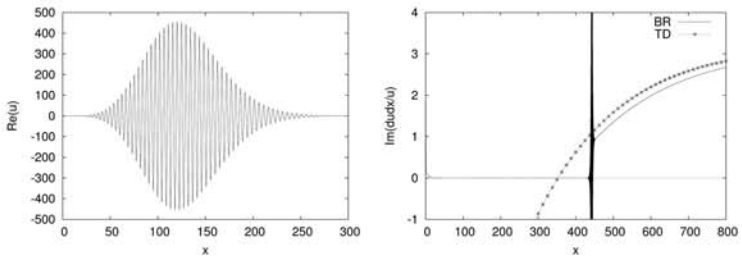

Figure 1:

Non-linear interaction of streaks and Tollmien-Schlichting waves in boundary-layer flows

S. Bagheri* and A. Hanifi*

Recent experimental results show that spanwise modulations of the mean flow caused by streaks have a stabilizing effect on TS waves in a boundary layer[1]. It has been found that the damping of TS-waves increases with the streak amplitude and that the presence of streaks can delay transition to turbulence[2]. The stabilizing effect of streaks originating from one single optimal disturbance on TS waves of low amplitudes has been numerically calculated[3]. However, the maximum streak amplitude appears to be limited by the occurrence of secondary instabilities on the streak. Therefore, it is important to investigate other streak parameters in order to achieve stabilization for a wider range of TS waves and larger Reynolds numbers. In the present work we use non-linear PSE to perform parametric studies of the interaction of streaks generated by optimal disturbances and TS waves in flat plate boundary layers. It is found that streaks with the same maximum amplitude, but larger spanwise wavenumbers have a stronger stabilizing effect and that there exists an *optimal* spanwise wavenumber β, which gives the optimal stabilizing effect on a TS wave of a frequency F (figure 1). The results also indicate that the main mechanism behind stabilization is associated with the modification of the spanwise shear of the distorted mean flow. This is in agreement with previous linear temporal stability analysis[4]. Furthermore, the stabilization is observed for TS waves with amplitudes of order 1%. We are currently investigating the delay of subharmonic and fundamental type of transition by means of streaks and the impact of pressure gradient on the stabilizing effect of streaks.

*Swedish Defence Research Agency (FOI), SE-164 90 Stockholm, Sweden.

[1]Fransson et al., *Phys. Fluids* **17**, 04110 (2005).
[2]Fransson et al., *submitted* (2005)
[3]Brandt and Cossu, *Phys. Fluids* **14**, L57 (2002).
[4]Brandt and Cossu., *Eur. J. Mech. B/Fluids* **23**, 815 (2004).

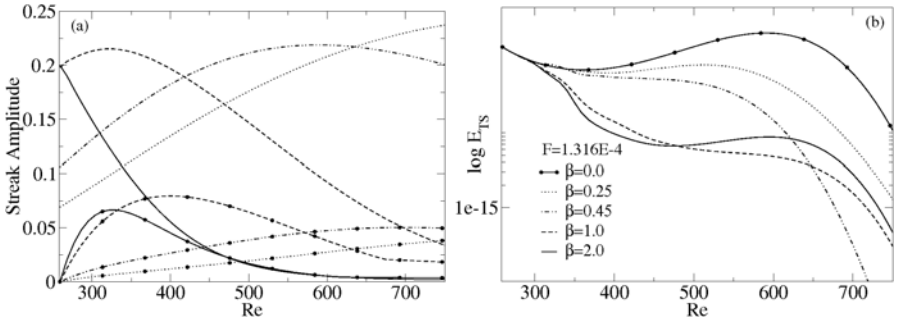

Figure 1: (a) Nonlinear downstream development of streaks with different spanwise wavelengths and the corresponding mean flow distortions (filled dots). (b) Linear downstream development of a TS wave in Blasius boundary layer.

Numerical simulation of laminar-turbulent transition in the Stokes layer subjected to outer-flow turbulence

M. V. Ustinov*

Laminar-turbulent transition in the boundary layer subjected to free-stream turbulence has become of great interest during the last decades. Dominated boundary layer disturbances at these conditions are low-frequency pulsations which grow as $\sqrt{x}$. Flow visualization[1] showed that these fluctuations are associated with longitudinal streaky structures. Processing of velocity pulsations spectra and visualization data of[1] revealed that the length of streaks l grows downstream proportionally to $\sqrt{x}$ whereas its spanwise scale d remains constant. Linear response of boundary layer to free-stream turbulence with prescribed spectrum was found in[2]. This theory gives correct amplification law but provides another scaling for sizes of streaks $l \sim x$, $d \sim \sqrt{x}$.

In present work laminar-turbulent transition triggered by free-stream turbulence is studied using temporally growing Stokes layer produced by an impulsively started plate as a model of the flat-plate boundary layer. The study is based on numerical solution of Navier-Stokes equations in rectangular box. Results of numerical modeling of homogeneous turbulence are used as an initial conditions. Such approach permits to take properly into account all factors significant for transition; namely amplitude and phase spectra of free-stream turbulence, non-uniformity of boundary layer, non-linearity. It was found that turbulence driven transition in Stokes layer involves two distinct steps. The first one consists in linear growth of streaks proportionally to $\sqrt{t}$. Profiles of pulsations at this step remains universal in self-similar vertical coordinate $\eta = z/\sqrt{t}$ and are well approximated by Crow-type solution $a \sim \eta \partial U/\partial \eta$. Streamwise wavenumber spectra of pulsations during the linear step fall into one curve if the wavenumber is scaled with Stokes layer thickness and fluctuation energy related to t. Spanwise wavenumber spectra become universal if simply normalized by t without any scaling of wavenumber. These results are in full agreement with experimental data[1].

The second non-linear step begins when amplitude of pulsations reaches $\sim 0.04 u_\infty$ and consists in origination and spreading of turbulent spots. Sharp maximum near the wall appears in pulsations profile and the growth of fluctuations accelerates at this step. Probability density functions in the Stokes layer in these conditions strongly deviate from normal law. Near the wall large positive deviations from the middle value are more frequent than negative ones. At the upper edge of the layer the situation is opposite. Computations of transition for two initial conditions with the same turbulence level but different length scales were made. Large scale turbulence was found initiate the earlier transition. This result agrees with data of experiment[3] but contradicts to findings of linear theories.

The research was supported by RFBR (Grants No. 04-01-00632, 05-01-08042).

*Central Aero-Hydrodynamics Institute, Zhukovsky, Moscow region, 140180, Russia

[1] Matsubara and Alfredsson, *J. Fluid Mech.* **430**, 149 (2001).
[2] Leib, Wundrow and Goldstein, *J. Fluid Mech.* **426**, 229 (2001).
[3] Jonas, Mazur and Uriba, *Eur. J. Mech. B* **19**, 707 (2000).

Resolvent bounds for pipe Poiseuille flow

G. Kreiss*and P.-O. Åsén*

In this talk, we consider the resolvent of linearized pipe Poiseuille flow. Despite the long history of pipe flow, linear stability has only been proved for axi-symmetric perturbations[1]. A bound of the norm of the resolvent in the entire unstable half-plane, $\mathrm{Re}(s) \geq 0$, implies linear stability. Moreover, a resolvent bound can be used to prove non-linear stability for perturbations with amplitudes smaller than some threshold value which depends on the Reynolds number[2].

We present an analytical bound of the L^2-norm of the resolvent in large parts of the unstable half-plane. This bound is derived by considering the linearized Navier-Stokes equations in Cartesian coordinates and using energy techniques. Unfortunately, the region in the unstable half-plane where the bound is not valid grows with the Reynolds number, R, and does not include the critical point $s = 0$.

In order to derive a bound in the remaining part of the unstable half-plane, we consider the Fourier transformed, in axial and azimuthal directions, linearized equations. For certain combinations of the wave numbers and the Reynolds number, we derive an analytical bound of the resolvent, valid in the entire unstable half-plane, for the Fourier transformed problem. Especially, this bound is valid for the perturbation with axial wave number $\alpha = 0$ and azimuthal wave number $n = 1$. Computations have indicated that this is the perturbation that gives the largest transient growth. Our analytical bound has the same dependence on the Reynolds number as the computations indicate.

Previous bounds of the resolvent have been based on computations in parts of an infinite parameter domain, consisting of the wave numbers, the Reynolds number and s. Our analytical bounds cover a large part of this parameter domain. However, the remaining part is still infinite. In a bounded parameter domain, rigorous numerical computations, using interval arithmetics, can be used to derive a resolvent bound. We discuss what further analytical results are needed in order to reduce the remaining parameter domain to a bounded domain. This would lead to a rigorous bound of the resolvent in the entire unstable half-plane which would finally prove the believed linear stability of pipe Poiseuille flow.

*KTH NADA, SE-100 44 Stockholm, Sweden.

[1]Herron, *Stud. Appl. Math.* **85**, 269 (1991).

[2]Kreiss, Lundbladh and Henningson, *J. Fluid Mech.* **270**, 175 (1994).

Transient Nature of Turbulence in Pipe Flow

B. Hof*, W. Tax†, J. Westerweel†

In practice pipe flows typically become turbulent once the Reynolds number exceeds 2000[1]. Stability analysis on the other hand suggests that Hagen Poiseuille flow is stable to infinitesimal perturbations for all Reynolds numbers[2]. Therefore perturbations of finite amplitude are required to initiate transition. The conventional line of thought is that once transition has occured, the flow will remain turbulent for all times. In recent numerical[3] and experimental[4] studies it has been found that for $1500 < Re < 2000$ turbulence can be of transient nature and decay after a finite time. Since the turbulent flow is advected in the downstream direction very long pipe facilities are required for an investigation of such transient phenomena. We here report results of an experimental study of turbulence in a pipe facility with a nondimensional length of 5000 pipe diameters, which is an order of magnitude larger than typical pipe facilities used in transition studies. Our investigations reveal the surprising result that even at larger Reynolds numbers turbulence decays after a finite time. The observed scaling of the lifetime with Reynolds number suggests that although the lifetime increases at an exponential rate, it only asymptotically approaches infinity as the Reynolds number is increased. Although for practical purposes tubulence will appear to be sustained once the Reynolds number exceeds 2300, on a more fundamental level our observation suggests that the turbulent state does not form an attracting region in phase space and that the laminar state is asymptotically stable even to perturbations of finite amplitude.

*Manchester Centre for Nonlinear Dynamics, Schuster Lab., University of Manchester, Manchester, M13 9PL, UK.

†Laboratory for Aero and Hydrodynamics, Delft University of Technology, Leeghwaterstraat 21, 2628 CA Delft, The Netherlands.

[1]Reynolds, *Philos. Trans. R. Soc. London* **174**, 935 (1883).

[2]Drazin and Reid, Hydrodynamic Stability *Cambridge University Press* (1981).

[3]Fraisst and Eckhardt, *J. Fluid Mech.* **504**, 343 (2004).

[4]B.Hof, in "IUTAM Symposium on Laminar-Turbulent Transition and Finite Amplitude Solutions." (Editors T. Mullin R.R. Kerswell), *Springer*, (2005)

Impulsive perturbations in pipe flow: from numerics to experiments and theory

F. Mellibovsky*, A. Meseguer*

It has long been known that the pressure-driven flow along a pipe can undergo transition to turbulence despite the linear stability of its laminar basic state (Hagen-Poiseuille flow) for all Reynolds numbers. However, the underlying mechanisms that govern this subcritical transition are far from being completely understood.

Recent numerical studies concentrating on the original problem of determining minimal initial global perturbations capable of triggering transition seem to indicate that the critical amplitude threshold asymptotically decreases as a power law of the Reynolds number ($A_{cr} \sim Re^{\gamma}$) with an exponent $\gamma = -3/2$[1].

This result is in clear contrast with experiments, which claim the exponent is $\gamma = -1$ or thereabouts[2]. Several differences regarding the approach to the problem may account for the discrepancies between numerical and experimental results. A first important difference lies on the definition of the perturbation amplitude, which is based on the injection mass-flow rate for the experimental rig while the numerical study takes into account energy considerations. Also the nature of the perturbation introduced to the basic flow is very different. While experiments perturb the flow via an injection (local, extended in time perturbation not respecting the boundary conditions at the wall), the computations use an initial condition (global, instantaneous, solenoidal perturbation respecting the boundary conditions at the wall). Finally, the problem nature also differs in that a pressure-driven pipe flow is being solved numerically while experiments have been carried out in a constant mass-flow rig.

Numerics are better suited than experiments in the quest for understanding the transition to turbulence. They allow for a much tighter control on parameters such as perturbation specification, noise, etc, higher flexibility, and a deeper insight into results insofar as full flow-fields can be retrieved anytime. Nonetheless, it is crucial that numerical results be validated/calibrated against experiments in order to be able to draw sound conclusions.

This work tries to bring together computational and experimental results by adapting an existing code devised to deal with transitional-pipe to solve a problem closer to the one posed by the experimental conditions. This is achieved by simulating the injection with a suitable volume forcing. Thus, the locality, time-extension and symmetries of the perturbation are addressed. Despite no special attention is paid to the problem of boundary conditions at the wall during the injection or to the constance of mass-flow, the agreement with experiments is reasonably good, thus endorsing future numerical work solving the transitional-pipe-flow problem as much as supporting previous studies based on the same code.

*Applied Physics Dept, Universitat Politecnica de Catalunya, Barcelona, Spain.

[1] Mellibovsky & Meseguer, *J.Phys.Conf.Ser.* **14**, 192 (2005).

[2] Hof et al., *Phys.Rev.Lett.* **91(24)**, 244502 (2003).

Developing instabilities in decaying pipe flow

James P. Denier* and N. Jewell*

The behaviour of the flow within a suddenly blocked pipe has important applications across a wide range of disciplines. Two such examples are the so-called water-hammer effect which occurs when a valve is suddenly closed in a pipe and the rhythmic opening and closing of the *aortic valve* and the *pulmonic valve* in the heart during ventricular ejection. In both applications an unsteady flow develops which typically exhibits a transient turbulent state.

A classical linear stability analysis of blocked *channel flow*, based upon an Orr-Sommerfeld equation approach that exploits a quasi-steady approximation in which the streamwise velocity field is "frozen" in time, was conducted by Hall & Parker[1] who predicted a critical Reynolds number of 148 occurring at a non-dimensional time 0.023. Our results for the blocked pipe flow predict a critical Reynolds number of a 440, at a non-dimensional time 0.02. However, our results also indicate that for Reynolds number in the vicinity of the critical Reynolds number the growth rates, although positive, are too small to allow for sufficient disturbance growth to render the flow turbulent on the time-scale over which the flow ultimately decays to We will describe the results of this work and describe an extension to consider the possibility that within the decaying flow there can be sufficient transient growth of a disturbance (in the region away from the blockage) to promote a transition. On the basis of this analysis we predict a critical Reynolds number for the flow of ≈ 1100.

This talk will also describe our study of the flow within the vicinity of the blockage. Results of numerical simulations indicate that this near blockage region is dominated by the growth of boundary layers at both the blockage and one the pipe wall and that these result in the formation of a sequence of axisymmetric vortices; a typical result is presented below. The possible role of these vortices on the transition process in the flow will be discussed.

*School of Mathematical Sciences, The University of Adelaide, South Australia 5005, Australia.

[1]Hall and Parker, *J. Fluid Mech.* **75**, 305 (1976).

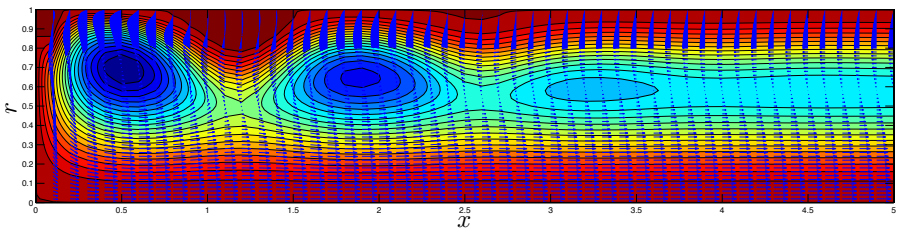

The velocity field within the end region, superimposed upon streamline contours, of the blocked pipe for a Reynolds number of 3000 at time $\tau = 0.02$.

Secondary instability in pipe flow: optimal axisymmetric and helical deviations

Guy Ben-Dov* and Jacob Cohen*

In the initial stage of transition to turbulence small initial disturbances grow into finite amplitude perturbations, for which nonlinear mechanisms become important. Such finite amplitude perturbations may trigger a secondary instability, thus introducing to the flow growing modes which may be fed back to increase the energy of the finite amplitude structures, and produce a self-sustained process.

We explore the temporal growth of disturbances developing in pipe Poiseuille flow, which has been modified by a primary axially-independent axisymmetric and helical finite amplitude disturbances. The axisymmetric distortions analysis has been explored recently by Gavarini *et. al.*[1] for the spatial case. Our aim is to explore the instability triggered by helical deviations, since such finite disturbances may occur as a result of transient growth amplifications. These helical structures may be identified as streaks which become unstable and feed energy to the self-sustained cycle. Axisymmetric deviations are analyzed for the sake of comparison. The optimal modification is defined as the primary base-flow deviation, with a specific amplitude norm, that yields the maximum growth rate for the secondary disturbances. Optimal modifications are computed by a variational technique.

Unstable modes are found to exist for small values of the primary disturbances amplitudes, in both the helical and the axisymmetric cases. The deviations energy in both cases is similar. However, helical deviations may gain energy by transient growth amplifications due to the non-normal Navier-Stokes operator. Figures 1(a) and (b) show the smallest optimal deviation which yields growing modes, for the axisymmetric and the helical deviations, respectively (for Reynolds number 2000). The optimal deviations are localized in a narrow radial range around the pipe axis. As the Reynolds number is increased the deviations become more localized.

*Faculty of Aerospace Engineering, Technion, Haifa, Israel.

[1] M. I. Gavarini, A. Bottaro and F. T. M. Nieustadt, *J. Fluid Mech.* **517**, 131 (2004).

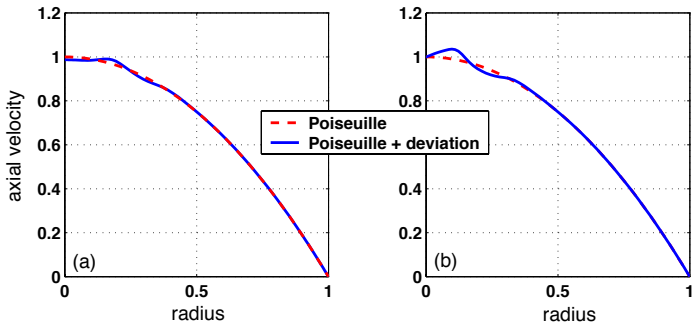

Figure 1: (a) axisymmetric deviation (b) helical deviation (for $\theta = 0$)

Direct numerical simulation of turbulent pipe Poiseuille flow

P.-O. Åsén*

Despite the believed linear stability of pipe Poiseuille flow, turbulence can appear for Reynolds numbers, R, larger than approximately 2000. However, in highly controlled experiments, laminar flow has been observed at $R \approx 10^5$. There is a threshold for the amplitude of the perturbation, below which all perturbations eventually decay. This threshold is typically assumed to behave as $R^{-\beta}$, with $\beta > 0$, as $R \to \infty$. Determining the correct value of β has proven to be a great challenge. Earlier experiments and computations have indicated values in the range $1 \leq \beta \leq 3/2$. In this talk, we present new results from direct numerical simulations, DNS, which give further insight in this question.

The fact that turbulence does not appear for Reynolds numbers below $R \approx 2000$ is a problem when doing DNS of turbulent pipe Poiseuille flow. In order to obtain an accurate estimate of the value of β, DNS must be done for large Reynolds numbers. Such simulations require state of the art codes as well as massive computer resources. We have used a code[1] based on compact finite differences of at least eighth order of accuracy in the axial direction, and Chebyshev and Fourier expansions in the radial and azimuthal directions, respectively. In order to do DNS for large Reynolds numbers, the code has been parallelized for distributed memory computers.

We have considered wall imposed disturbances in the form of suction and blowing. Our results include highly resolved simulations of turbulent pipe flow with Reynolds numbers in the range $R = 2000$ to $R = 10000$.

*KTH NADA, SE-100 44 Stockholm, Sweden.

[1]Developed by J. Reuter, Universität Stuttgart, and D. Rempfer, Illinois Institute of Technology.

Simulation of shock waves dynamics in ICF capsule implosion

Bernard Rebourcet*

The present work is devoted to shocks simulation when one uses pure lagrangian 2D codes [1] for the study of Rayleigh-Taylor instabilities occuring in Inertial Confinement Fusion [2]. In the framework of standard finite volume scheme applied to compressible fluid dynamics coupled to conduction[3], the usual way to both stabilize the numerical solution and get a physical entropy deposition is to mimic a 2D Riemann solver in terms of a stress-strain-like modelling of the shock structure inside a control volume[4]. The definition of that additional pressure, the so-called artificial viscosity term q, can be guided by different criteria :

1. the respect of the multidimensional characteristics of the flow : a tensor formulation analogous to a non-linear stress tensor is suitable,

2. the use of an approximated solution of the Rankine-Hugoniot relations : the 2D formulation is then a compound of a several 1D face centered expressions,

3. the respect of monotone profiles inside the shock depth : TVD ingredients are added.

For meshes composed by a set of quadrilateral cells, the second category corresponds to four degrees of freedom for q instead of only one d.o.f. in the usual underintegrated quadrilaterals. That could lead to non-physical stiffness counteracting the growth of perturbation modes. We define a way to reduce the number of these additional d.o.f.

After having introduced the basis of the physical modeling and the usual choice of numerical framework, we compare results obtained with several types of these formulations on an initially one mode perturbation convergent problem. Attempts are proposed to explain the discrepancies and define a good practice on the subject.

*CEA/DIF, 91 690 Bruyres-le-Chatel, France.

[1] Benson, *Comp. Meth. in Appl. Mec. and Eng.* **99**, (1992).

[2] Lindl, Inertial Confinement Fusion, *AIP Press Springer*, (1998).

[3] Bowers and Wilson, Numerical Modeling in Applied Physics and Astrophysics, *Jones and Bartlett*, Boston, (1991).

[4] Campbell and Shashkov, *J. C. P.*, **172**, (2001).

Barotropic flow modelling of sheet cavitation

A.H. Koop*, H.W.M. Hoeijmakers* and G.H. Schnerr†

Cavitation has a dominant effect on the performance of ship propellers, pumps and hydrofoils. In the proposed paper a computational method is described for numerically simulating three-dimensional cavitating flows.

The basis of the present computational method is a finite-volume unstructured-grid method solving the Euler equations for three dimensional compressible flows developed at the University of Twente by F. Put[1] and P. Kelleners. The new method for cavitating flows employs the Jameson-Schmidt-Turkel scheme[2] with the preconditioning method of Weiss & Smith[3] to cope with low-speed flows. The energy equation is replaced by a barotropic law[4] to model cavitation.

In collaboration with the group Maritime Technology at Delft University of Technology and with Gert Kuiper from Marin, a hydrofoil has been designed to have a sheet cavity with a triangular shaped planform corresponding to sheet cavitation on ship propellers. Furthermore, the interaction of the sheet cavity with the tunnel walls should be avoided. The hydrofoil spans the full width of the tunnel, is symmetric with respect to the mid-plane of the tunnel and has a twist distribution that increases the local angle of attack in the central part of the hydrofoil.

Numerical simulations have been carried out for two hydrofoils: the Twist-08 and the Twist-11, with a twist angle of 8° and 11° at midsection, respectively. The Twist-11 hydrofoil is set at $-3°$ angle of attack to counteract the upwash near the wall caused by the vortical wake of the hydrofoil.

In figure 1 the $-Cp$ distribution on the upper surface of the two hydrofoils are compared. At $Cp = -1.2$ the phase transition from liquid to vapor occurs. This result illustrates that the Twist-11 hydrofoil indeed shows the desired triangular region with sheet cavitation in the central part of the hydrofoil and that the sheet cavity does not reach the tunnel wall. In the full paper results of the present computational method will be compared with experimental results of the Delft group.

*University of Twente, P.O. Box 217, 7500 AE Enschede, the Netherlands
†Technical University of Munich, Germany

[1] Put, *PhD-thesis, University of Twente* (2003)
[2] Jameson et al. , *Proceedings of 14th Fluid and Plasma Dynamics Conference*, **81-1259**, (1981).
[3] Weiss and Smith, *AIAA Journal* **33**, 2050 (1995).
[4] Veldhuis, *MSc-thesis, University of Twente* (2002)

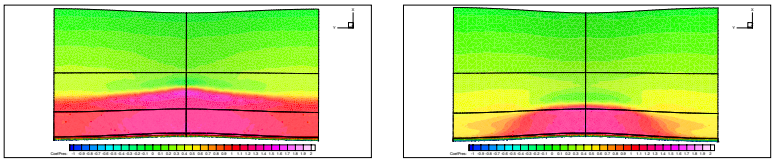

Figure 1: $-Cp$ distribution on upper surface of Twist-08 hydrofoil at 0° incidence (left) and Twist-11 hydrofoil at $-3°$ incidence (right). The cavitation number is $\sigma = 1.2$, i.e. Cp-values below -1.2 indicate regions with vapor.

3D RANS Modeling of Bottom and Bank Stability Subjected by Ship Propeller Jets

I. Brovchenko[a,b], S.Fenical[c] , Yu. Kanarska[b], V. Maderich[a,d], K. Terletska[a]

In coastal engineering practice, strong currents generated by ship propellers jets are known to affect biological resources, sediment quality in marine industrial areas, and in some cases are the design condition for bank/slope protection near marine terminals. The Vessel Hydrodynamics Propwash Unsteady (VH-PU) model is a 3-D, non-hydrostatic free-surface model linked with Lagrangian model of sediment transport. Unlike previous propeller wash models, it describes three-dimensional fields of velocities generated by ship propellers, turbulence intensity and length scale in the given domain of arbitrary bottom and coastal topography. The time and space varying bottom shear stresses that cause bottom erosion are calculated, as well as forces due to pressures on submerged boundaries and sediment erosion processes.

The model was developed based on the non-hydrostatic model of Kanarska and Maderich[1] (2003) and uses the 3-D Reynolds-Averaged Navier-Stokes equations. The model of turbulence is a q-q^2l model. The model uses the terrain-following sigma vertical coordinate system and orthogonal curvilinear horizontal coordinate system.

The simulations agree well with the laboratory experiment of Schokking[2] (2002) with propeller jet impacting on an inclined laboratory tank bottom (Figure 1 (a)) and field experiment in (Figure 1 (b)) where bottom velocities predicted by the model shown for a ferry landing at the Port Townsend Ferry Terminal, Puget Sound, WA.

[a] Ukrainian Center of Environmental and Water Projects, Glushkov av. 42 Kiev 03187 Ukraine
[b] Institute of Mathematical Machine and System Problems, Glushkov av. 42 Kiev 03187 Ukraine
[c] Coast & Harbor Engineering, Inc., 388 Market Street, Suite 500 San Francisco, CA 94111
[d] Institute of Geophysics and Planetary Physics UCLA 405 Hilgard Ave. Los Angeles, CA 90095
[e] Hankuk University for Foreign Studies, Yongin Shi, Kyoungki Do, Korea 449-791

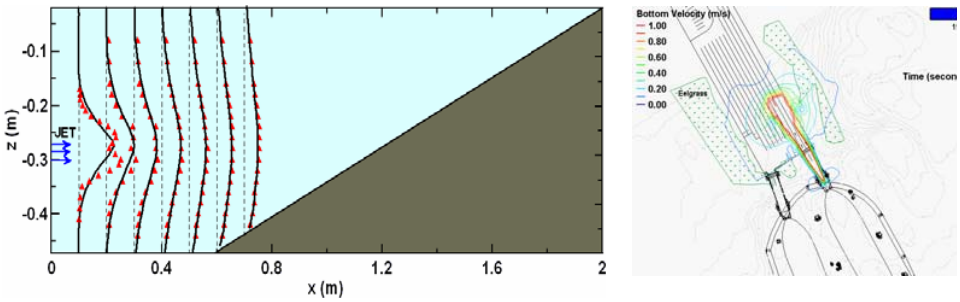

(a) **(b)**

Figure 1. Computed and measured (Schokking 2002[2]) profiles of mean velocities along the jet axis (a). Calculated bottom velocities generated by the ferry (b)

[1] *Kanarska Y, Maderich V.,* Ocean Dynamics **53,** 176 (2003).
[2] *Schokking L.* MS thesis, TUDelft (2002).

Low-order modeling of 3D laminar flows past a con ned square cylinder

M. R. Buffoni*, S. Camarri†, A. Iollo‡and M.V. Salvetti†

In the present work we analyze the capability of a low-order model,based on proper orthogonal decomposition (POD),in reproducing the dynamics of the flow around a confined square cylinder in laminar regime. The considered flow configuration is the same as in Galletti et al. (2004)[1], i.e. a square cylinder between two parallel walls with a blockage ratio equal to 12.5%. The considered Reynolds numbers, based on the the maximum velocity of the incoming flow and on the cylinder side length, L, range between 100 and 300. The numerical solver is based on P1 finite-element discretization of the viscous terms and on a finite-volume treatment of the convective ones on unstructured tetrahedrical grids. Time advancing is implicit. The numerical method is second-order accurate both in space and time. Validation has been performed [2] by comparing the results of 2D simulations with those of previous 2D simulations in the literature. 3D simulations have then been carried out at Re=200 and 300. In spite of the low considered Reynolds numbers, the flow is complex, as shown for instance in Fig. 1a for $Re = 300$.

Low-order models, obtained by Galerkin projection of the Navier-Stokes equations on a POD functional basis, gave satisfactory results for laminar **2D** flows around bluff bodies (see, for instance, Galletti et al. (2004)). Ma & Karniadakis (2002) found that, by combining two sets of POD modes, it was possible to accurately reproduce the onset of three-dimensional instability in a **unconfined** circular cylinder wake. The aim of the present work is to investigate the capabilities of the POD approach for a similar 3D flow, but containing an additional complexity, i.e. the effect of the confining walls. Moreover, a recently proposed calibration technique[1] will be used and assessed for the considered flow. This technique allows the behavior of the low-order model to be improved both in the transient (after an impulsive start-up) and in the fully-developed flow regime. Furthermore, it will be shown that, through calibration, the transitional Reynolds number for the onset of wake three-dimensionalities can be estimated from only two sets of POD modes, obtained for two different Reynolds numbers.

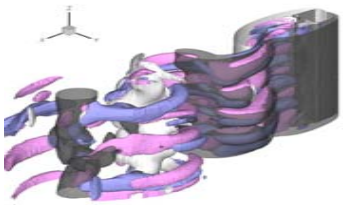

Figure 1: (a) Isosurfaces of the streamwise (pink and blue) and spanwise (black and gray) vorticity components in the wake obtained at $Re = 300$ after the transient.

*Politecnico di Torino, C.so Duca degli Abruzzi, 24, 10129, Torino, Italy.
†Dip. Ingegneria Aerospaziale, Universit'a di Pisa, Via G. Caruso, 56122, Pisa, Italy.
‡MAB, Université Bordeaux 1, 351, cours de la Libération, F-33405 Talence, France
[1]Galletti et al., *J. Fluid Mech.*, **503**, 161 (2004).
[2]Camarri et al., *Proc. of XVII AIMeTA Congress, Florence, Italy*, (2005).

TWO AND THREE DIMENTIONAL COMPUTATION OF HIGHLY SWIRLING FLOW IN A HIGH ASPECT RATIO HYDROCYCLONE WITH REYNOLDS STRESS TURBULENCE MODELS

M. Besharati-Givi[a], J. Ko[b], O. Macchion[a], S. Zahrai[c]

Hydrocyclones are devices widely used for separation of particles from a fluid in industry. In particular, for fractionation of fibers, high aspect ratio hydrocyclones have been suggested to achieve a higher efficiency. Although cyclones have been subject to many theoretical and experimental studies, a complete understanding for influence of different parameters on the efficiency of the cyclone is not at hand. The present study focuses on a hydrocyclone at an aspect ratio of 15 and uses two- and three-dimensional computations of the flow to provide a detailed picture of the internal flow. It should be noted that the ratio between the modeled hydrocyclone length and diameter of 15 is approximately three times more than common hydrocyclones investigated and reported on in literature.

To understand the phenomena occurring in such a hydrocyclone, it is necessary to investigate fiber-free flows. Even without fibers, the flow, including the air core, is very complex and the high aspect ratio geometry increases the difficulty of modeling such flows. To simplify the problem the air core is neglected. Linear and quadratic Reynolds stress models were used to predict the water flow inside the hydrocyclone. The hydrocyclone swirl number is approximately four, which is close to the limit for the accurate modelling of swirling flows with the linear Reynolds stress model.

Both two dimensional and three dimensional models give a good agreement with tangential velocities obtained from experimental data. Additional information regarding the structure of the flow field in the axial and radial directions is extracted from the study. Recommendations for improvement of the hydrocyclone design are given.

[a] KTH Mechanics, Faxénlaboratoriet, OB 18, S-100 44 Stockholm, Sweden
[b] Université Paris VI, Laboratoire de Modélisation en Mécanique, 75252 Paris, France
[c] KTH Mechanics, Faxenlaboratoriet, OB 18, S-100 44 Stockholm, ABB, Corporate Research, S-721 78 Västerås, Sweden

Hybrid modelling of flow around a wind turbine rotor in yaw

I.DOBREV[a], F. MASSOUH[a]

In this paper the authors develop a hybrid model able to solve the flow around a wind turbine rotor in yaw. A 3D RANS code is loosely coupled to blade element method (BEM) in a similar manner as in other studies[1, 2].

In the grid model, which represents flow field around the wind turbine, the blades are replaced by surfaces following the chords of the airfoil sections. The "pressure jump" boundary condition is applied to these surfaces. This boundary condition corresponds to an imposed pressure difference between adjacent grid cells, located at the opposite sides of the boundary. To calculate the "pressure jump" the distribution of the lift and drag forces along blade span is used and the blade element theory is applied. Hence, the forces acting on a blade element are evaluated using upstream velocity and airfoil performance of the considered blade element. Then for each blade element the obtained forces are distributed along the chord using a shape similar to a flat plate pressure distribution. Subsequently the RANS solver calculates flow field around the rotor, which is issued of assigned "pressure jump". The iterative process for each time step stops, when the difference of flow parameters in two consequent iterations is less than a given value.

The RANS code used in the proposed hybrid model is CFD Fluent and the BEM solver plays the role of a user-defined C language function - UDF. This function has access to all grid variables needed to calculate the rotor inflow and it is executed at the beginning of each iteration. To validate the proposed model a three blade-rotor in yaw is investigated. The choice of this case is motivated by the presence of experimental results[3] obtained with phase-locked PIV technique in case of yaw of 0° and 30°. The flow field in the wind tunnel around the turbine is represented by a rectangular volume with a cross-section of 3.3D by 2.5D and a length of 3D upstream and 10D downstream of the rotor plane. This rectangular volume contains a cylindrical volume with surfaces of pressure discontinuity representing the wind turbine blades. The angle between the cylinder axis and the rectangular volume is 30° and the cylinder is rotated with the same angular velocity as the studied rotor. To allow adjacent grids to slide relative one to another the sliding mesh model is applied.

The obtained numerical results show the capability of the proposed hybrid model to represent the velocity field downstream of the wind turbine rotor

[a] Laboratoire de Mécanique des Fluides, ENSAM, 151, Bd de l'Hôpital, 75013 PARIS.

[1] Sørensen and Shen , *J. Fluids Engineering*, vol. 124, no. 2, (2002)
[2] Massouh and all, *AIAA Paper 2006-0782*,(2006)
[2] Massouh and Dobrev, *ICJWSF-2005*, Japan (2005)

Optimization of geometry and chaotic mixing protocol in DNA chip technology

A. Beuf*, F. Raynal*, J.-N. Gence* and Ph. Carrière*.

The DNA chip is a core technology in genetic research. It is composed of an array of biological probes (single-stranded DNA fragments), fixed on a solid surface (typically $1cm^2$). The array is exposed to a solution containing targets (single-stranded DNA to analyze); the latter have a tendency to hybridize with the complementary probe on the chip, if present, which leads to the determination of the genetic sequence of the DNA samples. For a highly reliable and rapid response, each target should rapidly visit the whole surface of the chip. An efficient mixing is thus needed to enhance hybridization. We show that, whereas the transport of the targets by pure diffusion leads to very long characteristic times (up to 300h), chaotic advection allows mixing within the minute. We propose two protocols of chaotic mixing based on a time-periodic pulsed source-sink system (period T). 'Protocol A[1]' uses four syringes, while 'protocol B' operates with two pumps. We present here numerical simulations of Poincaré sections (fig. 1) for the two protocols, computed with a bidimensional velocity field, in agreement with the flow of Hele-Shaw type in a very shallow cavity. The flow-field is known analytically, which allows to change easily the shape of the hybridization chamber. A complete parametrical study is thus carried out for protocols, in a square and a rectangular chamber. The numerical Poincaré sections as well as experimental visualizations show that the best mixing is achieved with protocol B in a rectangular chamber. This study illustrates the potential for optimization of such devices based on numerical simulations.

*Laboratoire de Mécanique des Fluides et d'Acoustique, UMR CNRS 5509 - Ecole Centrale de Lyon, Université Claude Bernard Lyon 1, INSA Lyon, France.

[1]Raynal et al., *Phys. Fluids* **16**, 9 (2004).

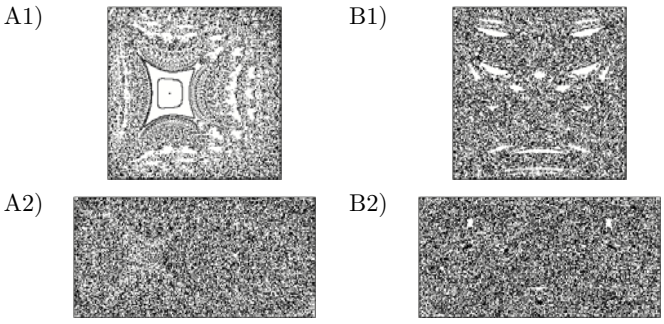

Figure 1: Poincaré sections with period $T = 4$s for protocol A ((A1) and (A2)) and protocol B ((B1) and (B2)) in a square and a rectangular geometry.

Turbulent flow investigations in a micro-channel

T.A. Kowalewski[a], S. Błoński, P. Korczyk

Turbulent flow of water in a narrow gap of an emulsifier is investigated experimentally using micro-PIV technique and compared with numerical predictions performed using the commercial code Fluent. The purpose of the investigations is to develop procedure for well-controlled generation of mono-dispersed suspension of micro droplets. These droplets will form a matrix for collection of nano-particles into well-structured configuration.

The micro-flow measurements are based on epi-fluorescence illumination and high speed imaging. The experimental set-up consists of the experimental emulsifier cell, epi-fluorescence microscope, high resolution PIV camera, double pulse Nd:YAG laser (5ns pulse) and pressure system for flow acceleration. The micro-PIV velocity measurements are performed in a 0.4mm high and 1mm long channel formed between two glass plates. The Reynolds number in the gap is 8000. Fluorescent polystyrene spheres, 2μm in diameter (Duke Scientific Inc.) are used for the flow seeding. The flow is observed through the upper window. By traversing the field of observation in the horizontal and vertical direction, the position of the interrogated flow plane is selected. The vertical resolution depends on the depth of field of the objective. In the micro-PIV experiments performed the vertical resolution is estimated to be 10μm and the horizontal resolution of the velocity field measurements is about 0.5μm. The accuracy of the velocity measurement depends on several experimental factors (quality of images, seeding concentration, particle displacement), as well as on the vector evaluation procedure. Using in house developed software the error of velocity measurement is estimated to be below 5%. The full field flow data are used to evaluate local velocity gradients, necessary to estimate conditions for the droplet break-up.

The experimental data are compared with the numerical results obtained using both turbulent and laminar flow models. It was found that due to small channel dimensions and very short flow development length the turbulent energy dissipation takes place mainly in the gap and shortly behind it. The estimated value of mean energy dissipation is used to predict mean droplets diameter. These predictions are validated using experimental data for the emulsion.

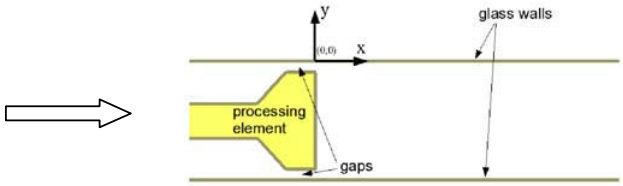

Schematic view of the investigated emulsifier.

[a] IPPT PAN, Swietokrzyska 21, PL 00-049-Warszawa, Poland.

Stokes flow around a micro cylinder rolling on a plane. Application to peristaltic microchannels.

A. Merlen*

One of the technological solution possible for realizing micropumps is the microfluidic equivalent of peristaltic pumps. It is possible to built microchannels of rectangular section where the motion of the fluid is obtained by a sequential contraction of one wall and a continuous displacement of the striction point [1]. Such channels can be realized in PDMS or SU8 with sizes between 2 to 50 microns high, 10 to 500 microns wide and 2cm long. The contraction is obtained by electrostatic forces produced by a set of metallic electrodes along the length of the channel. The field of application of 3D net of such channels is very wide (lab on chip with selection of fluids, etc.). In order to obtain reliable hydrodynamic models for the contraction area the 2D stokes flow in a schematic configuration has been studied. This paper presents the analytical solution describing such 2D Stokes flow near the contraction considering the case of a curved corner of fluid between a cylindrical wall and a planar one. Both walls are considered in contact, the cylindrical one rolling on the plane. Extending the domain far from the contact, the analytical solution of the problem appeared to be exactly the solution of the Stokes flow around a micro cylinder rolling on a plane. As a subproduct, the forces on the cylinder are obtained and it can be shown that the contact induces an infinite lift force. A perfect contact is then impossible. Removing the contact condition between both walls, the squeezed flow can be studied with Rayleigh equations and the effect of the cylinder rotation and the pressure gradient can be discussed. The local flow in the vicinity of the minimum section can illustrate not only microchannel situation, but address also the problem of wheel-road contact.

*Laboratoire de Mécanique de Lille UMR CNRS 8107, Cité Scientifique, Bât M3, 59655 Villeneuve d'Ascq, Cedex

[1] Merlen, *Euromech Microfluidics and transfers* **472** Grenoble (2005).

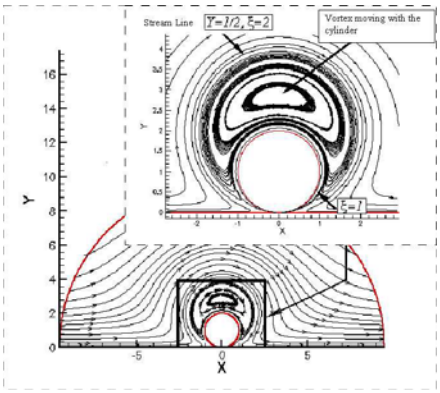

Figure 1: Stream lines for the rolling micro cylinder with a contact condition.

Liquid flow over a regular array of shear free interfaces

C. Pirat*, N. Bremond*†, C.-D. Ohl* and D. Lohse*

The boundary conditions in hydrodynamic systems play a major role when the volume to surface ratio goes down. Indeed, the no-slip boundary condition for a liquid flowing over a solid surface seems to be violated in numerous experiments[1]. The presence of nanobubbles sitting on hydrophobic surfaces revealed by AFM is a candidate to explain such a behavior since they provide a quasi zero shear stress boundary condition leading to an average reduction of the liquid friction on the walls, a wanted phenomenon to reduce hydrodynamic resistance.

The role played by bubbles sitting on the walls in drag reduction in microfluidics is investigated through an experiment allowing for a fine measurement of liquid flow over a well controlled heterogeneous surface (gas and solid) sketched in figure 1 (a). Parallel grooves are etched on a silicon plate and then coated with a silane. These hydrophobic grooves can sustain liquid/gas interfaces, thus providing a slip condition.

A micro-PIV (Particle Image Velocimetry) system has been developed and is used for measuring the velocity field in such microchannels. An example of the expected velocity profile is presented in figure 1(b) for a shear free strip longitudinal to the flow direction with $h = 50\,\mu m$ and $d = 12\,\mu m$ [2] . The velocity is normalized by the maximum velocity U_m of a flow with no-slip condition showing an overall increase of the flow rate.

*Physics of Fluids, University of Twente, The Netherlands.
†Lab. Colloïdes et Matériaux Divisés - ESPCI, Paris, France.
[1]Lauga et al.,*Handbook of Exp. Fluid dynamics, C.Tropea & A.Yarin, Springer* at press (2005).
[2]Philip, *Z. Angew. Math. Phys.* **23**, 353 (1972).

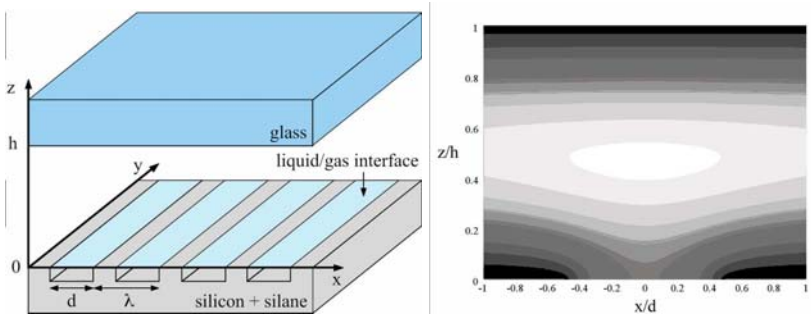

Figure 1: (a) Parallel liquid/gas strips on the microchannel wall. (b) An example of the expected velocity profile. The velocity increases from black to white.

CREATING THIN LAYERS AT THE CONTACT SURFACE OF TWO NONMIXING LIQUIDS

Agnieszka Słowicka[a], Zbigniew A. Walenta[a]

INTRODUCTION

The design of new technologies, making it possible to manufacture the nano – structured materials is one of the most important tasks of the contemporary materials science. The technologies, utilizing the emulsion droplets as templates for producing nanostructures out of solid particles, suspended in the liquid phase, seem very promising; work on developing such technologies is progressing fast[1]. It seems however conceivable, that even smaller structures could be obtained, if instead of solid particles a liquid film was utilized.

In the present research we investigate the conditions necessary for producing a film at the interface of two nonmixing liquids.

In our investigation we used emulsion consisting of water and oil. The assumed diameters of the oil droplets were very small, therefore to simulate the behavior of the liquids we applied the Molecular Dynamics simulation technique, assuming that a liquid is an ensemble of molecules [2]. For the detailed calculations we used the program "MOLDY" [3].

We investigated a number of molecular models of water, oil and the third component, creating the film. Since, at the molecular level, the behavior of the substance depends, in the first place, on the interaction between the molecules, we looked for the combination of the interaction potentials, which might produce the required liquid or solid film at the surfaces of the emulsion droplets. We performed a number of simulation runs for different interaction potentials. Having the information on the required interaction potentials one can look for the real substances, fulfilling these requirements.

PRELIMINARY RESULTS

To test the models of molecules, the formation of water droplet in vacuum and oil droplet in water was simulated. The TIPS2 model of water was used[4]. To simulate interaction of the three liquids we used the third component similar in structure to soap. To obtain a stable film of the third liquid (Fig.1) it was necessary to increase the length of its chain-like molecule.

To test the behavior of solid particles immersed in water, molecules of carbon were used. The carbon molecules form crystalline complexes, which interact with each other through Lennard-Jones and electrostatic potentials. The initial results were not satisfactory; to make the carbon complexes move towards the fluid interface and subsequently stay there we had to remove the electrostatic interactions (Fig.2).

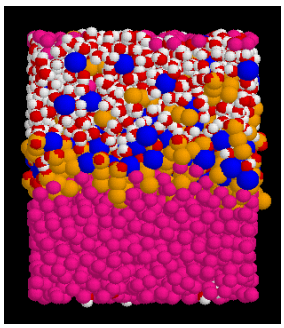

Figure 1: The liquid film at the contact surface.

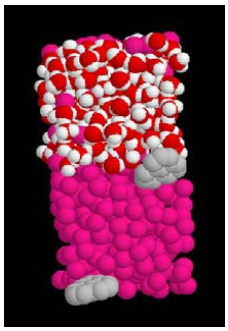

Figure 2: Carbon molecules create the sediment.

[1] Tcholakova et al., *Langmuir,* vol. 19, No. 14 (2003)
[2] Allen, Tildesley, *Clarendon Press, Oxford* (1987)
[3] Refson, *Comput. Phys. Commun.* 126, 3 (2003)
[4] Jorgensen, *J. Chem. Phys.* 77 (1982)

[a] Institute of Fundamental Technological Research, Polish Academy of Sciences, Świętokrzyska 21, 00-049 Warszawa, Poland.

Picoliter droplet formation using a thin fiber

S.Uemura[a], J. Sjödahl[b], M. Stjernström[b],
H. Kawamura[a], G. Amberg[c] and J. Roeraade[b]

Handling of minute droplets of liquid has attracted a great deal of attention in the field of chemistry, bioscience and drug discovery[1]. Volume reduction is associated with numerous advantages related to beneficial reaction kinetics, throughput, space and cost issues. However, droplet manipulation using pins, ink-jet dispensers[2] and microfluidic channels is often associated with problems like fast solvent evaporation and fouling.

In this study, we employed a new technique using thin fibers to generate and transfer picoliter droplets. The process is quite simple. When the fiber is dipped in the aqueous solution and subsequently pulled up, a droplet is formed at the end of the fiber. To avoid evaporation effects, the whole process is carried out under a covering layer of liquid fluorocarbon. With this technique, we can maintain an aqueous picoliter sized droplet for minutes to hours. This method can be applied for micro droplet handling and transfer even if the solution contains particles.

In order to fundamentally understand the nanofluid dynamics occurring at the fiber ends, we examined the snap off process and observed how withdrawal speed and fiber diameter influence the transfer characteristics. Initial experiments show that the droplet volume is strongly dependent on the fiber diameter but not on the withdrawal speed. We also observed that the fiber sidewall wettability is an important parameter influencing droplet dynamics. If the fiber has good wettability, the droplet of the end face will wet the sidewall. Importantly, satellite droplets were observed in the snap off process. Further research will be carried out on the issue of reproducibility of the droplet volume as a function of viscosity and surface tension of the liquid as well as the wettability of the fiber.

---

[a] Tokyo Univ. of Science Dept. Mech. Eng., 2641 Yamazaki, Noda, Chiba 278-8510, JAPAN.
[b] KTH Analytical Chemistry, SE-100 44 Stockholm, Sweden.
[c] KTH Mechanics, SE-100 44 Stockholm, Sweden.

[1] Stone et al., Annu. Rev. Fluid Mech. **36**, 381 (2004).
[2] Basaran, AIChE Journal **48**, 1842 (2002).

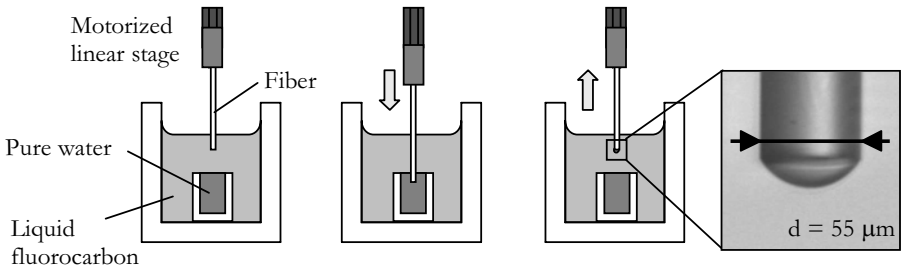

Figure 1: Droplet formation using a thin fiber.

Clustering of inertial particles falling through turbulence

E. Hascoët*and J. C. Vassilicos*

To date, no Direct Numerical Simulations (DNS) have been carried out of polydisperse clouds of falling inertial particles in isotropic homogeneous turbulence with a -5/3 power law energy spectrum. Such simulations are important for many potential applications, in particular clustering of inertial particles/droplets and droplet spectral broadening in warm clouds (e.g. Vaillancourt and Yau [1], Ghosh et al. [2]). Vaillancourt and Yau caution against droplet clustering mechanisms for explaining droplet spectral broadening in warm clouds because the Stokes numbers of cloud droplets are usually too small for them to be flung out of individual vortices and because the resulting concentration fluctuations may not be persistent enough in time. Ghosh et al. consider polydisperse droplet mixtures and argue that enhanced collision rates between large and small droplets can occur as a result of their different sedimentation velocities thus leading to a rapid droplet-size growth. However, they do not take into account the fact that eddies/vortices in turbulence are not isolated but clustered. Chen et al. [3] have shown that inertial particles can cluster as a result of the clustering of zero-acceleration points in two-dimensional inverse cascading DNS turbulence even when the particle Stokes number is small and that the large scales sweep zero-acceleration points and inertial particles together thus implying the kind of persistence in time which might well cause droplet spectral broadening to occur as a result of clustering.

It is therefore pertinent to carry out a study where a mixture of particles of two different sizes is subjected to gravitational acceleration and Stokes drag in a 2D turbulent velocity field with a -5/3 power-law energy spectrum. The results of this study are presented as functions of Stokes number, Froude number and ratio of particle relaxation times and the object of the study is to identify the regimes where nearest neighbours are mostly identical particles brought together by clustering, or distinct particles brought together by differential sedimentation velocities.

*Department of Aeronautics and Institute of Mathematical Sciences, Imperial College London , London SW7 2AZ, United Kingdom.

[1] Vaillancourt and Yau, *Physics Bull. Amer. Meteorol. Soc.* **81**, 285 (2000).

[2] Ghosh et al., *Proc. R. Soc. Lond. A* **461** (2062), 3059 (2005).

[3] Chen et al., *J. Fluid Mech.*, submitted (2005).

See http://www.ae.ic.ac.uk/research/turbmix/Christos/pub-jcv.html.

The intermediate asymptotics of turbulent diffusion*

M. Iovieno†, P.R.Bailey‡, D. Tordella†

A numerical experiment on the interaction of different decaying homogeneous and isotropic turbulence fields is described, see fig.1-left. In the absence of kinetic energy production, the intermediate asymptotics of the turbulent shear-free mixing layer have been observed. A first observation is that the mixing is always highly intermittent. For decaying homogeneous isotropic interacting flows with kinetic-energy ratios far from unity, this result is in contrast to the surmised existence of a Gaussian asymptotic state. The homogeneity of the integral length across the shearless layer – associated to the absence of turbulent energy production – is not a sufficient condition to obtain the Gaussian asymptotic state[1]. If the macroscale gradient is suppressed by considering fields with similar spectra, it is apparent that the intermittency increases with the energy gradient. This increase and the related intermittency behaviour are examined by varying the kinetic energy ratio between the two turbulence fields in the range $[1, \infty]$, fig.1-right.

A second observation is that the intermittency increases/decreases when the kinetic-energy gradients and integral-scale gradients are aligned/opposite. This is found by independently varying the initial energy level and distribution over the wavenumbers of the two turbulence fields. By means of a theoretical analysis, based on the use of the two-point lateral correlation equations and their intermediate-similarity solutions[2], we discuss these two results for which a verification independent of the numerical experiments has been obtained.

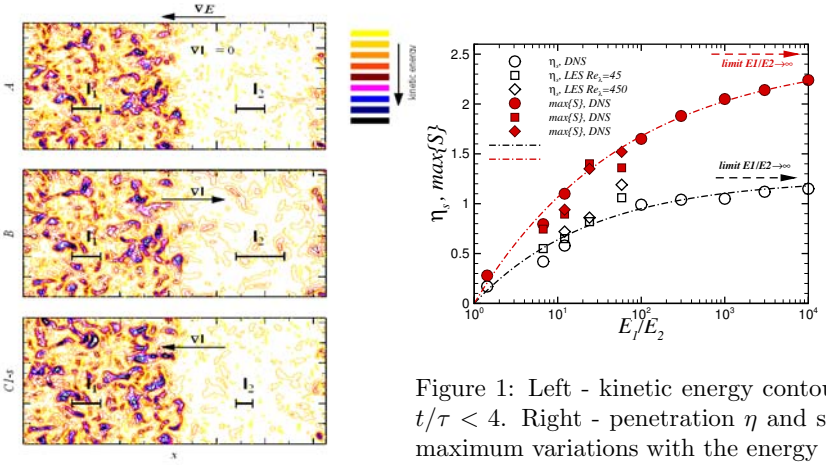

Figure 1: Left - kinetic energy contours, $3 < t/\tau < 4$. Right - penetration η and skewness maximum variations with the energy ratio.

*Work carried out under the HPC-EUROPA project (RII3-CT-2003-506079)
†Politecnico di Torino, DIASP, Italy.
‡Politecnico di Torino, Scuola di Dottorato, Italy.
[1]Tordella and Iovieno, *J. Fluid Mech.*, to appear (2006)
[2]Tordella and Iovieno, *APS-DFD,* 58^{th} *Annual Meeting*, November 20-22, 2005, Chicago, IL.

Evolution of molecular tracer dots in turbulence

M. Pashtrapanska*, T. Elenbaas*, J. Bominaar*, N. J. Dam*,
J. J. ter Meulen* and W. van der Water†

For the experimental study on turbulence small molecular dots are drawn in a strongly turbulent air flow emanating from a jet. The change of the size of these dots and the separation between them with the time gives an insight into complex phenomena like the turbulent mixing. At few times the Kolmogorov time scale τ_η, the squared size of the dots grows linearly, whilst according to Batchelor[1] their squared separation fluctuations increase quadratically in time. Both regimes are accessible in the presented experiment. The measurements are carried out applying a special kind of Molecular Tagging Velocimetry technique, called Air Photolysis And Recombination Tracking[2]. Thin lines of NO molecules with typical size about 60 μm, which corresponds to a few times the Kolmogorov length scale η, are *written* in the air along the waist of a weakly focused pulsed ArF excimer laser beams as result of a non-linear multi-photon photochemical process. The lines move together with the flow and can be *read* at any moment Δt later by laser-induced fluorescence using a pulsed dye laser. By crossing of the NO lines two dots are drawn in the flow. The experiments are carried out in a turbulent jet flow 40 nozzle diameters downstream at $R_\lambda = 420$. The initial separation Δ_0 between the two dots is about 3.5 mm. The measurements are performed for short time delays with a maximum Δt of approximately $3\tau_\eta$. The change of the mean square size of the NO line in still and in turbulent air is shown in figure 1 (a). The relative dispersion changes according to the Batchelor regime as the results in figure 1 (b) show. In a single experiment both mixing regimes are observed, demonstrating the ability of the applied experimental technique to perform Lagrangian measurements. New pathways can be indicated, involving molecular tracers with higher Schmidt numbers, and even reaching out to inertial particles.

*Radboud University Nijmegen, PO Box 9010, 6500 GL Nijmegen, The Netherlands
†Eindhoven University of Technology, PO Box 513, 5600 MB Eindhoven, The Netherlands

[1] Batchelor, *Proc. Camb. Phil. Soc.* **48**, 345 (1952).
[2] Dam et al., *Opt. Lett.* **26**, 36 (2001).

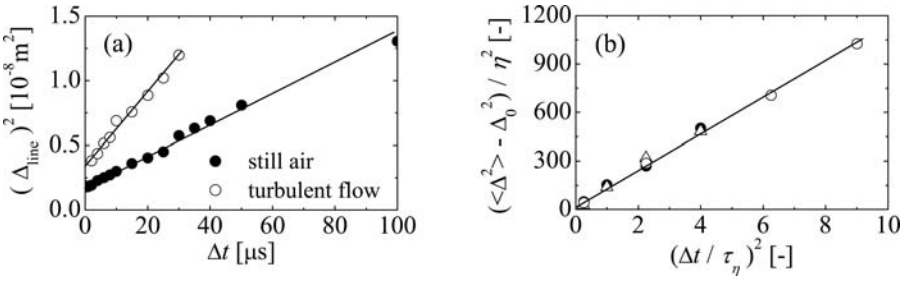

Figure 1: (a) Mean square size of line in still and in turbulent air in time. (b) Mean square dot separation in time.

Depletion of horizontal pair diffusion in vertically stratified turbulence

K. Sung*and J.C. Vassilicos†

Recently, Nicolleau *et al.* (2005)[1] have shown that, in their Kinematic Simulations (KS) of vertically stably and strongly stratified homogeneous turbulence (Froude number smaller than 1), horizontal pair diffusion is significantly depleted by comparison to unstratified isotropic and homogenerous two- and three-dimensional turbulence.

We have found that the probability density function of the horizontal divergence of the velocity field is not a delta function in the presence of stratification but is a gaussian symmetrically spread around 0. This gaussian does not depend on Froude number and neither does the depletion of horizontal pair diffusion, but they both disappear in the absence of stratification, i.e. infinite Froude number. This observation gives a first insight into why horizontal turbulent pair diffusion may be depleted, particularly because horizontal and vertical velocities in stratified turbulence are coupled by pressure fluctuations (Nicolleau & Vassilicos 2000)[2]. However, this observation does not suffice, and we therefore seek to explain this depletion of horizontal pair diffusion by vertical stratification in terms of the statistics of stagnation points following the recent approach to Richardson pair diffusion by Davila & Vassilicos (2003)[3], Goto & Vassilicos (2004)[4], Goto *et al.* (2005)[5] and Osborne *et al.* (2005)[6].

We measure the number density of stagnation points in the KS of three-dimensional strongly stratified turbulence and find that it is virtually identical to what it is in KS of three-dimensional isotropic turbulence. Also, the root mean square stagnation point velocities in the vertical and horizontal directions scale as $(L/\eta)^{-1/3}$ (where L is an outer and η an inner length-scale of the turbulence) which is identical to their scaling in isotropic homogeneous turbulence. Hence, the stratification does not affect the number and persistence of stagnation points in KS. However, the stratification does lead to a depletion of the average enstrophy and the average square strain rate tensor, as well as a depletion of all average square strain rate eigenvalues. Finally, we present an argument where the depletion of horizontal pair diffusion can be understood as a result of the overall depletion of strain rate and we verify in our KS of stratified turbulence the quantitative predictions of this argument.

*Turbulence & Mixing Group, Dept. Aeronautics, Imperial College London, Exhibition Road, London, SW7 2BY, UK.

†Turbulence & Mixing Group, Dept. Aeronautics, and Institute of Mathematical Sciences, Imperial College London, Exhibition Road, London, SW7 2BY, UK.

[1]Nicolleau, F., Yu, G. & Vassilicos, J.C., Kinematic Simulation for stably stratified and rotating turbulence. *Fluid Dyn. Res.*(submitted December 2005)

[2]Nicolleau, F.& Vassilicos, J.C., *J. Fluid Mech.* **410**, 123-146 (2000).

[3]Davila, J. & Vassilicos, J.C.,*Phys. Rev. Lett.* **91**, (14) 144501 (2003).

[4]Goto, S. & Vassilicos, J.C., *New J. Phys.* **6**, 65 (2004).

[5]Goto, S. *et al.*, *Phys. Rev. E* **71**, 015301(R) (2005).

[6]Osborne, D.R., Vassilicos, J.C., Sung, K.& Haigh, J.D., Fundamentals of pair diffusion in kinematic simulations of turbulence. *Phys. Rev. E*(submitted October 2005)

The effects of solid boundaries on confined 2D turbulence

H.J.H. Clercx*, D. Molenaar* and G.J.F. van Heijst*

The effects of solid boundaries on the evolution of two-dimensional turbulence on a finite square domain, both for the cases of decaying and continuously forced flow will be addressed. Laboratory experiments and numerical flow simulations have revealed the crucial role of the solid no-slip walls as sources of vorticity filaments, which may significantly affect the flow evolution in the interior[1]. In addition, the walls generally provide normal and tangential stresses that may exert a net torque on the fluid, which can change the total angular momentum of the contained fluid. For the case of decaying turbulence this is observed in so-called 'spontaneous spin-up', i.e. a significant increase of the total angular momentum, corresponding with a large domain-filling circulation cell in the organised 'final' state[2]. For the case of moderate forcing this phenomenon may still be observed, although the filamentary vortex structures advected away from the walls may cause erosion and possibly a total destruction of the central cell. A few snapshots of this process, obtained from a direct numerical simulation, are shown in Figure 1. This disordered stage - characterised by a significantly decreased total angular momentum - is usually followed by a re-organisation into a large circulation cell (in either the same or opposite direction) with an increased total angular momentum[3]. The scaling behaviour of vorticity structure functions and the probability distribution function of vorticity increments have been investigated for forced turbulence and indicate a strong anisotropy of the turbulent flow in the range of Reynolds numbers considered[4].

The present contribution will in particular focus on vorticity production at no-slip

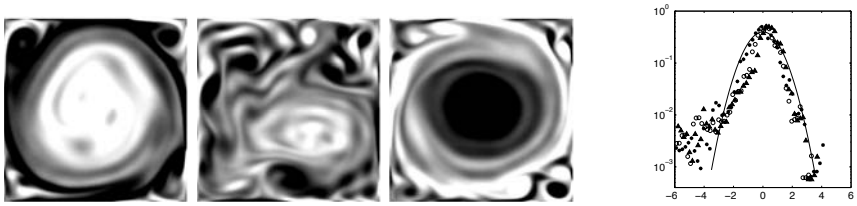

Figure 1: Three snapshots of the vorticity evolution during the sign reversal of a large monopolar vortex structure (left panels). Log-linear plot of the PDF of normalized vorticity increments where the solid line represents a Gaussian normal PDF, near the wall (right panel).

boundaries, the spin-up of the flow and subsequent break-down of a central cell by the presence of strong boundary layers, and the anisotropy of the 2D turbulent flow in square bounded domains (see, e.g., right panel Figure 1).

*Physics Department, TU/e, P.O. Box 513, NL-5600MB Eindhoven, The Netherlands.

[1] Clercx and van Heijst, *Phys. Rev. E* **65**, 066305 (2002).
[2] Clercx et al., *Phys. Rev. Lett.* **80**, 5129 (1998).
[3] Molenaar et al., *Physica D* **196**, 329 (2004).
[4] van Heijst et al., accepted for publication in *J. Fluid Mech.* (2006).

Reconnection of vortices without or with axial flow

Ivan DELBENDE* and Maurice ROSSI†

The Crow instability leads two antiparallel vortices to reconnect one to another on the nonlinear stage. Saffman[1] has described the phenomenology of this process, and suggested that the strain induced by vortex curvature in the reconnnection region be responsible for their collision and subsequent viscous annihilation. The direct numerical simulations by Shelley *et al.*[2] have provided valuable informations about the topology of the process but failed to identify the strain rates prevailing in the reconnection region. Following this latter study, we integrate the Navier–Stokes equations to simulate the reconnection process. At each time, in the symmetry plane normal to the vortex axes, we extract the strain stemming from the three-dimensional structure (i.e. curvature) by subtracting the two-dimensional strain induced in this plane by the dipoles to the total strain. This procedure provides time-dependent space-averaged strain rates. This strain is then enforced externally in a two-dimensional numerical simulation of a vortex dipole evolution: the obtained two-dimensional dynamics is found to follow closely the dynamics of the three-dimensional system in the symmetry plane, thus fully validating the strain extraction procedure. These strain rate values are also compared to the ones obtained by a Biot–Savart integral along the vortex cores.

Finally, we investigate the influence of an axial velocity component inside the vortices on the reconnection dynamics (figure 1).

*University of Paris 6, LIMSI–CNRS, 91403 Orsay Cedex, France
†LMM–University of Paris 6, 75252 Paris Cedex 05, France

[1]Saffman, *J. Fluid Mech.*, **212**, 315 (1990).
[2]Shelley, Meiron and Orszag, *J. Fluid Mech.*, **246**, 613 (1993).

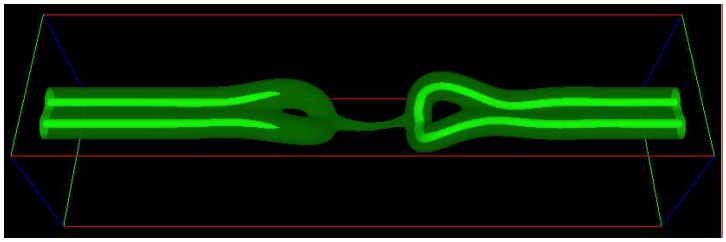

Figure 1: Pressure isosurfaces during a reconnection process involving two vortices with axial flow (flowing from left to right).

Characterization of the fluctuating flow-field in the near-wake of a triangular prism

G. Buresti[a], G.V. Iungo[a],

The velocity fluctuations experimentally detected through hot-wire anemometry in the wake of a prism with equilateral triangular cross-section, aspect ratio $h/w = 3.0$ (where h is the prism height and w the width of its cross-section base), and placed vertically on a plane with its apex edge against the incoming flow, are characterized by using time-frequency signal processing procedures based on the wavelet and Hilbert transforms (see Buresti et al.[1]). The body shape and the direction of the flow are such that two strong counter-rotating vortices detach from the free-end, and significantly influence all the upper-wake flow field.

Fluctuations at three prevailing frequencies are singled out, with different relative intensities depending on the wake regions. In particular, the frequency connected to alternate vortex shedding from the lateral vertical edges of the prism, corresponding to a Strouhal number $St = fw/U \cong 0.15$, dominates for vertical positions below $z/h = 0.9$, and is particularly strong in the regions just outside the lateral boundary of the wake. The related fluctuations are strongly modulated, which is not surprising due to the lower regularity of vortex-shedding with respect to the two-dimensional case.

A lower frequency, at $St \cong 0.05$, is found to prevail in the velocity fluctuations on the whole upper part of the wake, and may confidently be associated, in agreement with previous suggestions, with a vertical, in-phase, oscillation of the vortical structures present in that region, i.e. both the two counter-rotating axial vortices detaching from the body free-end and the upper part of the vorticity layer that originates from the body sides and is dragged around the above-mentioned vortices.

Fluctuations at an intermediate frequency, around $St \cong 0.09$, are also observed, and the region where they prevail is described. In particular, by using as a reference both the numerical results of Camarri et al.[2] and flow-field visualizations using a laser sheet, it is suggested that they may be caused by a flag-like oscillation of the sheet of transversal vorticity shed from the rear edge of the body free-end, and approximately lying along the downstream boundary of the recirculation region in the central part of the near wake.

The amplitudes of the different components are shown to be characterized by time variations that are of comparable relative value. However, the wavelet-Hilbert analysis, applied to velocity signals acquired in positions where all the three frequencies may be detected, does not provide any clear indication of positive or negative correlation between the time variations of the amplitudes of the extracted components. This substantiates the suggestion that they are connected with different physical mechanisms, and in particular with the dynamics of different vortical structures.

---

[a] Dept. of Aerospace Engineering, Univ. of Pisa, V. G. Caruso, 56122 Pisa, Italy.

[1] Buresti et al., *Chaos, Solitons & Fractals* **20**, 149 (2004).

[2] Camarri et al., *J. Wind Eng. Ind. Aerodyn.* (to be published).

The effect of forcing amplitude on vortex strength, drag and Reynolds stresses in the wake of a cylinder in oscillating flow

E. Konstantinidis[a,b] and S. Balabani[b]

The control of the wake flow behind a cylinder is an important problem in fluid mechanics with many practical ramifications. One effective method for controlling the wake and the forces exerted on the cylinder is by periodically forcing the oncoming flow, i.e. by superimposing low-amplitude velocity oscillations.[1,2] This paper reports the effect of forcing amplitude on vortex strength, drag and Reynolds stresses for this kind of flow configuration.

Experiments were made in the range of forcing amplitudes $\Delta U/U_o$ = 0–0.12. The Reynolds number in all experiments is Re = 2150 and the forcing frequency f_e is about two times the natural shedding frequency in the unforced wake f_o ($f_e/f_o \approx 2.0$). Measurements of the wake velocity field were made by a Particle Image Velocimetry system.[3] The mean flow and the Reynolds stresses were computed by averaging the instantaneous fields and the drag force was determined from these distributions. In order to estimate the strength of the shed vorticity a conditional-averaging technique was employed.[3]

Selected results are shown in figure 1. As the forcing amplitude is increased, the magnitude of the Reynolds shear stress, the drag and the vortex strength increase whereas the length of the recirculation bubble behind the cylinder decreases. These effects are associated with a systematic modification of the vortex wake patterns.

---

[a] University of Western Macedonia, Kozani 50100, Greece.

[b] ECLAT, King's College London, Strand WC2R 2LS, United Kingdom.

[1] Konstantinidis et al. *J. Fluids Struct.* 18, 367 (2003).

[2] Konstantinidis et al., *J. Fluid Mech.* 543, 45 (2005).

[3] Konstantinidis et al., *Exp. Fluids.* 39, 38 (2005).

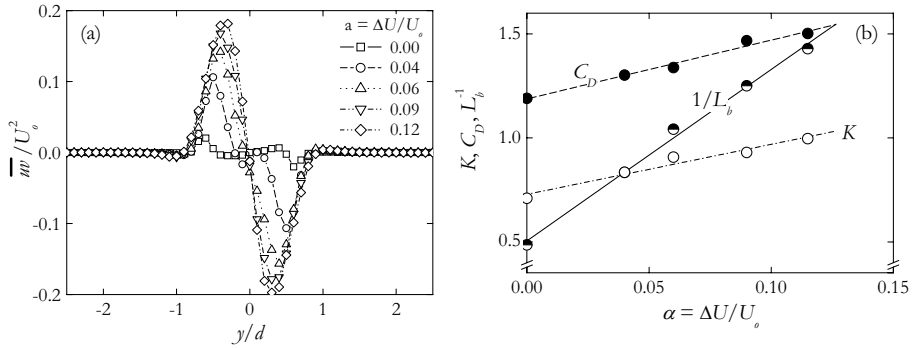

Figure 1: (a) Profiles of the Reynolds shear stress at x/d = 1.0 for different forcing amplitudes. (b) Variation of the vortex strength K, drag C_D, and the inverse of the recirculation bubble length $1/L_b$ with forcing amplitude.

Flows in a rectangular cavity due to symmetric surface forcing LaTeX

John McHugh*, Kahar Osman †

Flow of a constant density fluid in a finite container with surface forcing is considered. The problem is motivated by oceanic flow, as well as the flow in lakes, where the forcing is wind blowing over the free surface. The problem is idealized by considering rectangular geometries, restricting the Reynolds number to small values, and imposing sinusoidal forcing such that the net force is zero. Present results focus on the steady flows that emerge. The symmetric driven cavity [1] is a two-dimensional example. Present results are obtained via numerical computations of the Navier-Stokes equations. The numerical algorithm is a splitting method, and spatial operators are approximated with finite differences. The forcing wavelength is allowed to vary in subsequent trials. The two dimensional results with 2, 4, and 6 oscillations in the forcing show a subcritical bifurcation to an asymmetric solution, with the Reynolds number as the important parameter. The symmetric solution is found to have vortex flow with streamlines that conform to the boundary shape. The asymmetric solution has vortex flow with streamlines that are approximately circular near the vortex center. Two dimensional results with 8 or more oscillations in the forcing show a supercritical bifurcation to an asymmetric solution. Of particular importance is the asymmetric solution, which includes a large scale flow that fills the domain, as shown in the left figure below. This large scale flow can be seen to be nearly identical to the flow generated by the traditional driven cavity, shown on the right. This result implies that the large scale flow is somewhat insensitive to the character of the surface forcing.

*University of New Hampshire, Durham, NH 03833, USA
†Universiti Teknologi Malaysia, 81310, Skudai, Johor, Malaysia
[1]Farias and McHugh, *Phys. Fluids*, **14**, (2002)

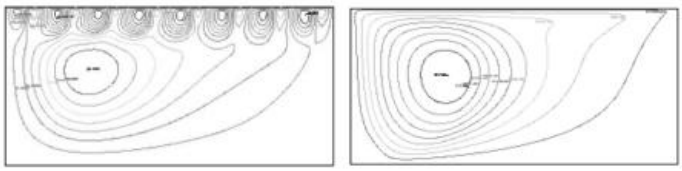

Figure 1: Steady streamlines for n=16 and n=1

Vortical structures generated by a time varying jet flow in a ventilated enclosure

P. Å. Elvsén[a], J. H. M. Fransson[b] and M. Sandberg[a,b]

We consider a momentum driven two-dimensional flow into a ventilated enclosure, where the momentum source is a two-dimensional jet in the lower left corner of a room. The experiments were conducted in a model with water as operating fluid. With a constant supply and extract of fluid the momentum source continuously generates vortices, which cover the whole perimeter of the ventilated enclosure, see the sketch in Figure 1. The region in the neighbourhood of the rotation centre constitutes a stagnation zone.

In a second step we consider a periodic flow rate, $Q_0(t)$, with different frequencies. This generates smaller vortices, in the acceleration phase of the pulsed flow, which are convected into the room by the larger vortices. If the rate of generation of vortices is sufficiently high the stagnation zone disappears.

Particle Image Velocimetry pictures of the flow field were taken and analysed with a vortex detection program based on the approach by Adrian *et al* [1] and developed in the mathematical software Matlab. Statistical results of vortex strength, size, circulation and path will be presented. A time dependent inlet may be desired in ventilation applications, since more vortices and different vortex sizes are generated which enhances the mixing and in turn the room ventilation.

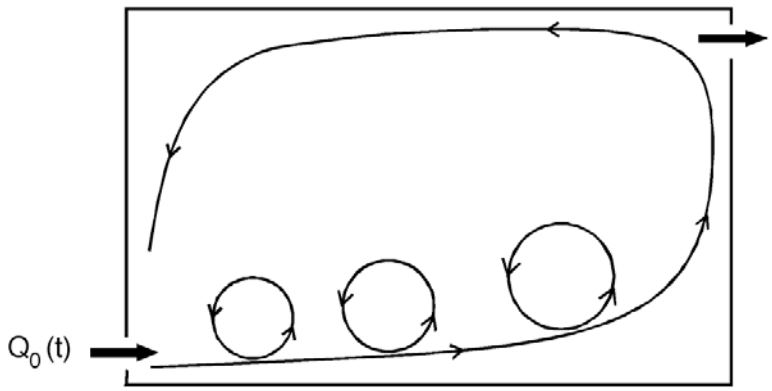

Figure 1: Generation of vortices by a time varying supply of the flow.

[a] University of Gävle, KTH Research School, SE-801 76 Gävle, Sweden.

[b] KTH Mechanics, Osquars Backe 18, SE-100 44 Stockholm, Sweden.

[1] Adrian, R. J. et al., *Exp. Fluids* **29**, 275-290 (2000**)**.

Session 10

Onset and characteristics of the oscillatory motion of axisymmetric bodies rising freely in a low-viscosity liquid

P.C. Fernandes*, F. Risso*, P. Ern* and J. Magnaudet*

Freely-falling or -rising particles in a low-viscosity fluid otherwise at rest can exhibit oscillatory motions along helical or zigzag paths. We have investigated the causes and the characteristics of these periodic motions. The rise of flat cylinders of density close to that of the fluid has been followed by two travelling cameras to characterize the body translation and rotation for Reynolds numbers $100 < Re < 300$ and diameter-to-height ratios $2 < d/h < 20$. The transition from a stable rectilinear rise to a stable oscillatory motion occurs for a critical Reynolds number Re_c that depends on the body aspect ratio d/h, as shown in the figure. To help understanding the role of the wake instability on the body motion, numerical simulations of the flow around the body held fixed have been performed. For all aspect ratios, the wake of the fixed body looses its axial symmetry above a critical Reynolds number Re_{c1} (plain line in the figure) and vortex shedding begins at $Re_{c2} > Re_{c1}$ (dotted line). For thick bodies, the appearance of the oscillatory path coincides with the first destabilization of the fixed body wake ($Re_c \approx Re_{c1}$); the wake instability causes a lift force and a torque able to induce the oscillatory motion. For thin bodies, the oscillations appear at a Reynolds numbers higher than Re_{c2} and PIV measurements have shown that the wake is still stationary for $Re_{c2} < Re < Re_c$. Then, a detailed analysis of the oscillatory regime has been carried out (frequency, amplitudes and relative phases[1] of the velocity and orientation). Finally, the different contributions of the forces and torques acting on the bodies have been analyzed from the Kirchhoff's equations.

*Institut de Mécanique des Fluides, Allée du Prof. C. Soula, 31400 Toulouse, France.

[1]Fernandes et al., *Phys. Fluids* **17**, 098107 (2005).

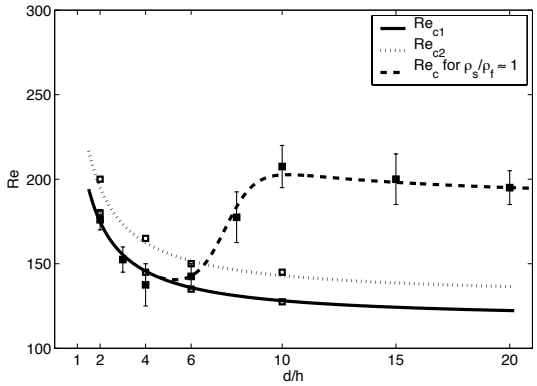

Figure 1: Onset of the oscillatory motion for a freely-rising body compared to the thresholds of the two successive wake instabilities of the fixed body.

A synthetic perturbative hypothesis for multiscale analysis of bluff-body wake instability

D. Tordella*, S.Scarsoglio†, M.Belan‡

A nonparallel stability analysis of the intermediate region of the two-dimensional wake behind a bluff body is performed using a WKBJ method on a basic flow previously derived from intermediate asymptotics[1]. The multiscaling is carried out to explicitly account for the effects associated to the lateral momentum dynamics. These features of the base flow can be included in the perturbative equation as well as in the associate modulation equation through a spatial multiscaling[2] or, more generally, through a spatio-temporal multiscaling[3]. At the first order, the disturbance is locally tuned to the property of the instability, as can be seen by the zero order theory. This leads to a very synthetic analysis of the nonparallel correction on the instability characteristics. The system is perturbed by disturbances with a wave number that varies along the wake and which is locally equal to the wave number of the dominant saddle point of the zero order dispersion relation, taken at different Reynolds numbers. In this way, the Reynolds number is the only parameter, in contrast with the more classical parametrization with respect to both the wave number and the Reynolds number[3]. It is shown that the corrections to the frequency, temporal and spatial growth rate are remarkable in the first part of the intermediate wake and lead to absolute instability in regions that extend to 10 body scales, see Fig.1a. The correction increases with the Reynolds number and agrees with data from laboratory and numerical experiments in literature, see Fig.1b.

*Politecnico di Torino, DIASP, Cso Duca Abruzzi 24, 10129 Torino, Italy.
†Politecnico di Torino, Scuola di Dottorato, Cso Duca abruzzi 24, 10129 Torino, Italy.
‡Politecnico di Milano, DIA, v. la Masa 34 - 20156 Milano, Italy
[1]Tordella and Belan, *Phys. Fluids* **15**, 7, 1897 (2003).
[2]Tordella and Belan, *ZAMM* **85**, 1, 51 (2005).
[3]Belan and Tordella, *J. Fluid Mech.*, revised (December 2005).

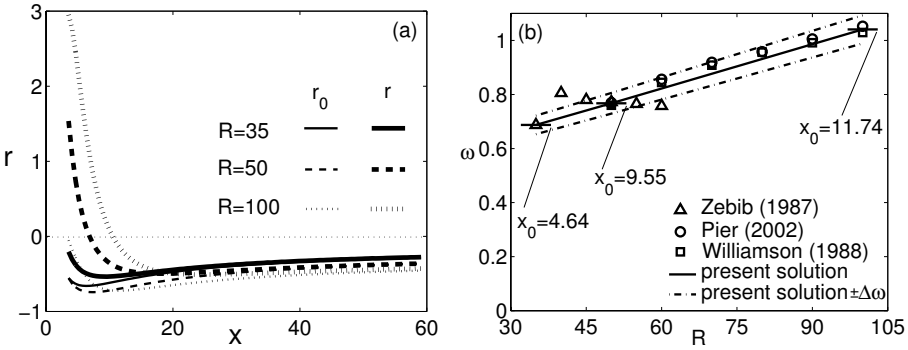

Figure 1: (a) Temporal growth rate 0-order (r_0) and (0+1)-order (r), R = 35, 50, 100; (b) Pulsation: present solution ($\Delta\omega = 0.05$) and global results in literature.

Local and global instabilities in the wake of a sphere

Benoît PIER*

The wake of a sphere is known to display the following behaviour at moderate Reynolds numbers: the steady axisymmetric wake is stable for $\mathrm{Re} < \mathrm{Re}_1 \simeq 210$; a steady planar-symmetric flow is observed for $\mathrm{Re}_1 < \mathrm{Re} < \mathrm{Re}_2 \simeq 270$; at Re_2 a periodic régime takes over with a vortex shedding Strouhal frequency of $\mathrm{St} \simeq 0.14$ near onset.

The present investigation revisits this flow and compares the global behaviour, reproduced by direct numerical simulations, to the local stability characteristics, computed for the basic flow under a quasi-parallel flow assumption. It is shown that the time-periodic régime may be interpreted as a nonlinear global mode and its naturally selected frequency derived from local stability considerations.

For a given Reynolds number, the local linear stability characteristics are determined using the corresponding basic wake flow, defined as the time-independent solution of the Navier–Stokes equations. The axisymmetric and non-axisymmetric base flows are obtained by direct numerical simulation or, when they are gobally unstable, by a Newton–Raphson iterative scheme.

After computation of these time-independent basic flow fields, the local linear dispersion relation is derived from two-dimensional eigenproblems based on the velocity fields prevailing at each streamwise station z. The essential feature of the frequency selection mechanism is the complex local absolute frequency $\omega_0(z)$ shown in Figure 1 for $\mathrm{Re} = 300$. According to the theory of "elephant global modes"[1], a self-sustained nonlinear oscillating structure is triggered by a front at the transition station z^{ca} from convective ($\omega_{0,i} < 0$) to absolute ($\omega_{0,i} > 0$) local instability. This front acts as a wavemaker and imposes its frequency on the entire system. The front frequency equals the (real) local absolute frequency $\omega_0^{ca} = \omega_0(z^{ca})$ prevailing at its location. At $\mathrm{Re} = 300$, this frequency selection criterion yields a prediction of $\mathrm{St} = \omega_0^{ca}/2\pi \simeq 0.17$, in reasonable agreement with the observed $\mathrm{St} = 0.14$. Bearing in mind that the present flow is rather far from parallel, one may consider that this establishes the validity of the proposed underlying frequency selection mechanism.

*LMFA, École centrale de Lyon, 36 avenue Guy-de-Collongue, F-69134 Écully.

[1] Pier et al. *Physica D*, **148**, 49 (2001).

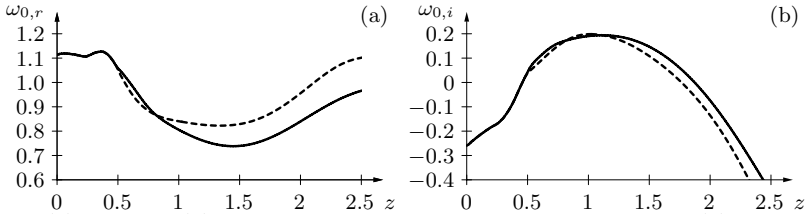

Figure 1: (a) Real and (b) imaginary parts of local absolute frequency $\omega_0(z)$ computed for the two most unstable modes of the non-axisymmetric basic wake flow at $\mathrm{Re} = 300$ for a sphere of radius 0.5 with center at $z = 0$.

Linear stability and receptivity analysis of the vortex shedding in flows past confined square cylinders

S. Camarri*, F. Giannetti†

The flow around two-dimensional bluff bodies confined between two parallel walls may have, depending on the value of the blockage ratio, very peculiar characteristics. Systematic studies on circular cylinders, for instance, have revealed that, for certain values of the parameters, the positions of clockwise and counter-clockwise vortices in the Karman street are reversed with respect to the unconfined case [1,2]. Moreover, the steady flow at the critical Reynolds number at which the vortex shedding sets in may be asymmetric, even if the cylinder's center is located on the centerline of the channel[2]. Compared to the large number of publications on the flow past circular cylinders, the square counterpart has not been investigated to the same extent, although it plays a dominant role in many technical applications such as building aerodynamics. Only a few studies have dealt with the influence of confining walls on the flow phenomena around square cylinders. Recent numerical simulations for a blockage ratio 1:8 [3,4] have shown interesting phenomena similar to those observed in the circular case. For instance, the wake vortices appear in a reversed order with respect to the unbounded problem [5], while the vortex shedding frequency seems to be very sensitive to the oncoming flow.

In the present work, the flow past a square cylinder located in the center of a channel with one face orthogonal to the direction of the incoming flow is analyzed for different values of the Reynolds number and blockage ratio. An immersed-boundary technique and a second-order central finite-difference scheme on a staggered mesh are used both to evaluate the steady base flow and to perform a linear stability analysis. The possible existence of stable asymmetric steady configurations is investigated and the value of the critical Reynolds number at which the vortex shedding first sets in is determined by solving numerically the eigenvalue problem derived from a normal mode expansion. The results are then compared with data available in the literature [4]. The characteristics of both direct and adjoint eigenfunctions are analyzed to study the receptivity of the flow to initial conditions and to external forcing and to better understand the occurrence of the vortex reversal. The receptivity to localized feedback and the sensitivity of the shedding frequency to the inflow and outflow conditions are studied by determining the stability of the system to perturbations of the differential operators, a technique originally introduced to analyze the wake behind a circular cylinder [6 7] .

*Dip. Ingegneria Aerospaziale, Università di Pisa, via G. Caruso, 56121 Pisa, Italy
†DIMEC, Università di Salerno, via Ponte don Melillo, 84084 Fisciano (SA), Italy
[1] Zovatto and Pedrizzetti, *J. Fluid Mech.* **330**, 1 (2003).
[2] Sahin and Owens, *Phys. Fluids* **16:5**, 1305 (2004).
[3] Galletti et al., *J. Fluid Mech.* **503**, 161 (2004).
[4] Breuer et al., *Int. J. Heat and Fluid Flow***21**, 186 (2000).
[5] Camarri et al., *Proceedings of the XVII Congress AIMeTA*, 11-15 September 2005, Florence
[6] Giannetti and Luchini, *V Euromech Fluid Mechanics Conference*, Toulouse, August 24-28, 2003.
[7] Giannetti and Luchini, *Journal of Fluid Mechanics*, (submitted) .

An experimental and theoretical study of flag flutter

C. Souilliez*, C. Eloy* and L. Schouveiler*

The study of flag flutter or the vibration of flexible plates is of critical importance in the understanding of many industrial problems (e.g. aeroelasticity of airplane wings or paper printing) or biological subjects (fish swimming, snoring, etc). Since the pioneering work of Lord Rayleigh in 1879, there has been several studies both experimental and theoretical (see Paidoussis[1] and references therein). But so far, experiments showed that the system is much more stable than the theoretical predictions.

We present an experimental work performed in a horizontal wind tunnel. In its test section, we have positionned a flag clamped to a profiled and vertical mast. The flags tested are made of several materials (paper, plastic,...) of different flexural rigidity. At low velocities, the flag is parallel to the flow and motionless. Above a critical wind velocity U_c, the flag exhibits periodic oscillations (see figure 1(a)). We particulary focus on the variation of the instability threshold with respect to the aspect ratio H/L where H is the flag span and L its length.

We have also developed a linear model of 2D fluttering coupled to a 3D flow for a flag of finite aspect ratio. An asymptotic theory is carried out to express the fluid load on the flag as powers of L/H. At first order, we recover the results of existing theories for flags of infinite span. The second and third orders are found to lower the pressure on the flag, resulting in a stabilizing effect. The predicted critical velocity compares well to experimental results as shown on figure 1(b).

*IRPHE, Technopôle de château Gombert, 49, rue F. Joliot Curie, Marseille, France.

[1]Paidoussis, *Fluid-Structure Interactions, Slender Structures and Axial Flow, Vol 2*, Elsevier (2004).

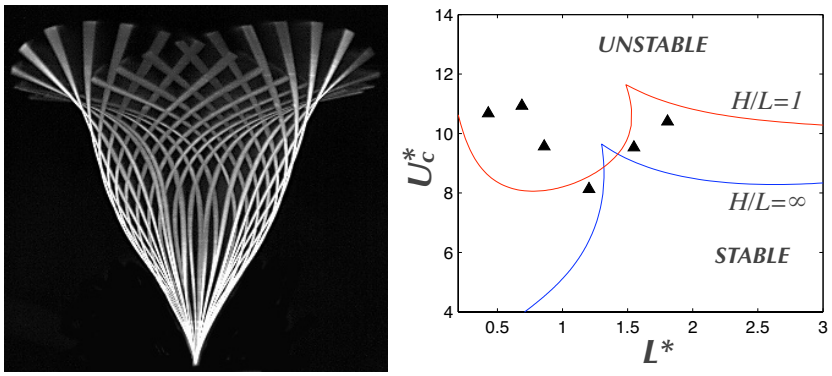

Figure 1: (a) Superimposed views of the side edge of the flag during flutter (flow is upwards). (b) Dimensionless critical velocity as a function of the dimensionless length $L^\star$. Curves show predictions for two aspect ratios. Triangles are experiments for $H/L = 1$.

Laboratory and numerical modelling of far wake flow in a stratified fluid

Yu.I.Troitskaya[a],O.A. Druzhinin, D.A. Sergeev [a]

A laboratory study and direct numerical simulation (DNS) of far wake flow in a stratified fluid are performed. The laboratory study employs the PIV technique to measure the velocity field in a wake behind a sphere towed under a picnocline with high Reynolds and Froude numbers. The DNS parameters and initialization are prescribed in accordance with the experimental data which allow a direct comparison between DNS results and experimental data. Good qualitative as well as quantitative agreement is obtained between the numerical and experimental results, such as the temporal development of the flow integral parameters (wake width and axis velocity) and characteristic spatial scale of the instantaneous velocity distribution.

A simplified theoretical model to describe the far wake evolution is proposed and verified by direct numerical simulation and laboratory investigation. Within the model, the wake is considered as a quasi-two dimensional turbulent jet flow, for which the main mechanism of spreading and decay is associated with transfer of momentum from the mean flow to quasi-two dimensional disturbances growing due to hydrodynamic instability. The calculation of the wake evolution is performed in quasi–linear approximation taking into account only development of the most unstable bending mode is considered.

The results of the DNS and the laboratory experiment are compared with conclusions of the quasi-linear quasi-two-dimensional theory. The time evolution of the wake axis velocity and its width, obtained within the model is in very good agreement with the experimental data (fig.1).

This work was performed under financial support of the Russian Foundation for basic research (project codes 04-05-64264)..

[a] Institute of Applied Physics, Nizhny Novgorod, RussianFederation.

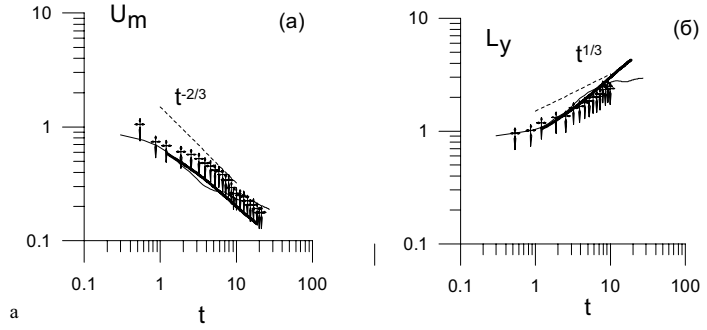

Figure 1: (a) Time dependencies of (a) wake axis velocity и (b) wake width. Symbols correspond to experimental data, thin curves – to DNS, thick lines – to the quasi-linear model.

Experimental observation of the periodical solutocapillary Marangoni convection

K. G. Kostarev[a], A. Viviani[b] and A. L. Zuev [a]

The solutocapillary and thermocapillary Marangoni phenomena, despite an obvious similarity of the driving forces, are found to be not completely analogous. The key difference is that the characteristic times of the admixture diffusion are hundred times longer than times of heat diffusion. As a result, the concentration inhomogeneities in liquids persist much longer than thermal ones, and the intensity and duration of the capillary phenomena at the interface increase many times. Furthermore there is a drastic change in the ratio of contributions to mass transfer made by competing mechanisms of gravitational and solutocapillary convection. The other marked distinction of the solutocapillary convection is that the mechanism of surfactant emergence to the interface (adsorption) also differs from the mechanism of the interface temperature formation. These differences can be viewed as the main reasons of new phenomena that cannot occur in thermocapillary situation.

The paper presents the results of the experimental studying the two-dimensional solutocapillary flow generated around an air bubble in heterogeneous aqueous solutions with vertical surfactant concentration gradient. A stationary bubble having the shape of a short cylinder with free lateral surface was placed in a vertically oriented thin layer of the stratified liquid — the Hele-Shaw cell. The structure of convective flows and the evolution of the concentration field around the bubble were investigated with the help of Fizeau interferometer. It has been found that in contrast to thermocapillary convection, which is generally stationary, the solutocapillary flow is of the oscillatory character since the concentration field around the bubble experiences quasiperiodic disturbances. The time dependences of the oscillations period has been analyzed in relation to the average concentration of the solution, the concentration gradient and the concentration Marangoni number. A reasonable explanation of the discovered effect, manifesting itself as the specific interaction of the diffusion and convective mechanisms, is proposed.

The work was supported by RFBR Grant № 06-01-00221.

[a] Institute of Continuous Media Mechanics UB RAS, 614013 Perm, Russia.
[b] Seconda Universita di Napoli, I-81031 Aversa, Italy.

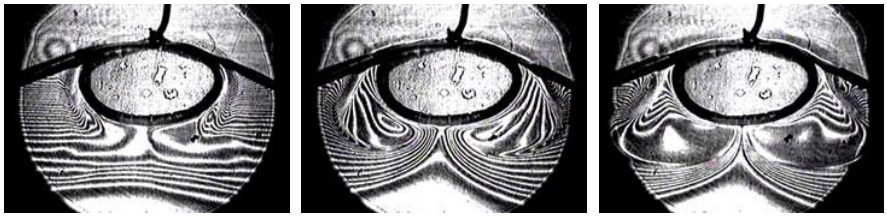

Figure 1: Typical interferograms of the concentration distribution.

Pendular thermovibrational convection

A. Ivanova[a], V. Kozlov[b] and N. Selin[a]

The report summarizes the results of theoretical and experimental investigation of thermovibrational convection in cavities subject to high frequency pendular vibration. As follows from the theory[1] the effect of combined translational-rotational vibrations (pendular is the typical one) qualitatively differs from the case of translational vibration (classical thermovibrational convection) due to additional mechanism of averaged convection excitation. Theoretical and experimental studies[1,2] demonstrate this vibrational mechanism to play the governing role in many cases. This mechanism is of especial importamce because the vibrations usually contain some nontranslational component. In plan layers, due to specific form of pulsating velocity component connected with the rotary cavity oscillations, the action of this mechanism is similar to static force field and results in renormalization of gravity (imitates the gravity in weightlessness, increases or compensates its role on the Earth).

The new investigations concern the theoretical and experimental study of thermovibrational convection in plane layer of liquid with uniform internal heat release subject to three dimensional oscillations of spherical pendulum. The experiments include also the limiting cases of indefinitely long pendulum (it corresponds to translational vibrations of circular polarization) and the case of zero pendulum length (3D rotational oscillations about the cavity center). The experimental results of vibrational convection excitation are in good agreement with theoretically predicted in high frequency case. At moderate dimensionless frequencies of vibration, when the thickness of Stokes boundary layers is relatively large, the critical intensification of heat transfer below the threshold of thermovibrational convection is found in experiments. It is proved to be connected with the instability of Stokes layers and formation of regular 3D system of vortexes.

The role of the ends of the cavities in case of nontranslational vibrations, mean flows generation and heat-mass transfer intensification in the end areas[3,4], are also analyzed. Experimental studies were performed in wide interval of dimensionless frequencies including the limiting cases of low and high frequencies and found the excitation of intensive mean flows due to Schlichting mechanism of mean vorticity generation in nonuniform Stokes layers.

Acknowledgement: support of Russian Foundation for Basic Research is thanked.

---

[a] Perm State Pedagogical University, 614990, Sibirskaia 24, Perm, Russia.

[b] Institute of Continuous Media Mechanics RAS, 614013, akad. Koroleva 1, Perm, Russia.

[1] Kozlov, *Fluid Dynamics* **23**, 437 (1988).
[2] Ivanova and Kozlov, *Fluid Dynamics* **38**, 372 (2003).
[3] Ivanova and Kozlov, *Fluid Dynamics* **38**, 186 (2003).
[4] Ivanova et al., *Fluid Dynamics* **40**, 369 (2005).

On existence of stationary 3-D waves on falling liquid films

S. V. Alekseenko[a], V. A. Antipin[a], V. V. Guzanov[a], S. M. Kharlamov[a] and D. M. Markovich[a]

3-D wavy regimes are the last stage of wave evolution for falling liquid films at low and moderate Reynolds numbers (Re ≤ 100). Here Re = q/ν, where q is the specific volumetric flow rate, ν - the kinematic viscosity. In case of such regimes the film surface is covered by numerous nonlinear horseshoe-shaped waves, which interact with each other in a random fashion.

Theoretical solution in the form of traveling stationary 3-D solitary wave was obtained first by Petviashvili and Tsvelodub[1] on the basis of Kuramoto-Sivashinsky (KS) equation valid for Re~1 and recently by Chang and Demekhin[2] on the basis of the generalized Kuramoto-Sivashinsky (gKS) equation valid for moderate Reynolds numbers. The last results indicate that for vertically falling film there exist numerous branches of stationary solutions in the form of one- and multi-humped solitary waves. Experimental evidence of stationary solitary 3-D waves existence is given in this report.

Experiments were carried out on the film flowing down vertical glass plate. 3-D solitary waves were excited and investigated in the region of waveless film flow, above the boundary of natural waves inception. Fluorescence imaging method[3] realized on the basis of standard equipment of PIV-systems was used to measure instantaneous spatial form and velocity of exited 3-D wave. For a few cases stationary solitary 3-D waves (i.e. waves which travel without changing their form and velocity) were registered. Experimental data on amplitudes and velocities of stationary 3-D waves turn out to be in agreement with values predicted on the basis of KS equation.

---

[a] Institute of Thermophysics, Lavrentiev Ave. 1, 630090 Novosibirsk, Russia

[1] Petviashvili and Tsvelodub, *Dokl. Acad.* Nauk. SSSR **238**, 1321 (1978).

[2] Chang and Demekhin, *Complex wave dynamics on thin films*, Elsevier (2002.)

[3] Liu et al., *J. Fluid. Mech.* **250**, 69 (1993).

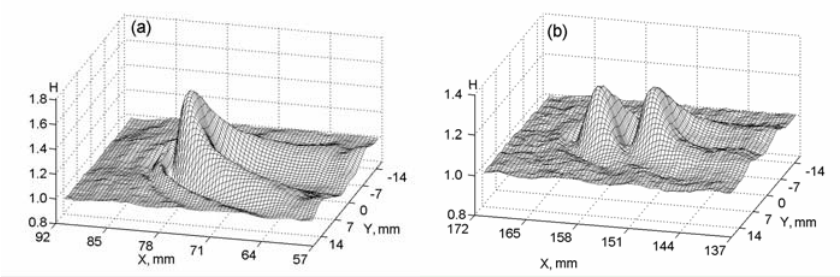

Figure 1: (a) One-humped stationary 3-D wave at Re =3.9 (b) Two-humped stationary 3-D wave at Re =2.2. H – film thickness normalized to thickness of undisturbed film.

Wave flow regimes on a film of a non-Newtonian fluid

O. Yu. Tsvelodub*

The flow of a thin film of a rheological fluid falling down on a vertical wall by a gravity is considered. The equation of state for "a power law" fluid is used as a rheological model. The stress tensor τ_{ik} links with the strain-rate tensor D_{ik} by equality:

$$\tau_{ik} = -p\,\delta_{ij} + \mu_n\, I_2(v)^{(n-1)/2}\, D_{ik}.$$

Here $I_2(v)$ is the second invariant of the strain-rate tensor D_{ik}. The constant μ_n is an indicator of the fluid consistency, and the parameter n characterizes the degree of non-Newtonian behavior. The greater the deviation of n from unity, the more pronounced the viscosity anomaly in such a medium. The values $0 < n < 1$ refer to pseudoplastic fluids whose apparent viscosity degreases with increasing shear rates, and the values $n > 1$ correspond to dilatant fluids whose apparent viscosity increases with increasing shear rates.

For a case of small flowrates in a long wavelength approximation an equation describing evolution of perturbations of a film surface is obtained[1]:

$$\frac{\partial H}{\partial \tau} + 4H\frac{\partial H}{\partial x} + \frac{\partial^2 H}{\partial x^2} + \left(\frac{\partial^2}{\partial x^2} + \frac{\partial^2}{\partial z^2}\right)\left(\frac{\partial^2}{\partial x^2} + n\,\frac{\partial^2}{\partial z^2}\right) H = 0. \qquad (1)$$

Here H is the dimensionless and transformed deviation of films thickness from undisturbed level.

For $n = 1$, the equation (1) coincides with the equation that describes the waves on the surface of a Newtonian fluid. In the case of two-dimensional disturbances ($H = H(x,t)$), for all n the equation (1) transforms to the well known Kuramoto–Sivashinsky equation.

The area of a linear instability of a trivial solution is defined. In the vicinity of the neutral curve the steady-state solutions of the equation (1) are analytically obtained. It is shown, as there is branching sets of solutions in vicinity of a singular point of the neutral curve. For different values of n some typical solutions of the equation (1) are found numerically. Especially, there are define how non-newtonian properties of fluids influence on a coherent structure in wavy films (horse-shoe waves). At first, for films of Newtonian fluids these structures were obtained in the paper[2].

This work was supported by the Russian Foundation for Basic Research (Grant 04-01-00183) and by the Siberian Branch of the Russian Academy of Sciences (Basic Grant 4.2-04).

*Dept of Phys. Hydrodynamics, Institute of Thermophysics SB RAS, 630090 Novosibirsk, Russia.

[1]Tsvelodub and Shushenachev, *J of Appl. Mech. and Tech. Phys.* **46**, 365 (2005).

[2]Petviashvili and Tsvelodub , *Sov. Phys. - Dokl.* **23**, 117 (1978).

Statistical analysis of coherent structures in transitional pipe flow

Tobias M. Schneider*, Jürgen Vollmer* and Bruno Eckhardt*

The transition to turbulence in pipe flow is an outstanding problem in fluid dynamics. Although linear stability theory suggests that the laminar state always remains stable, the transition to turbulence occurs at rather moderate flow speeds. Recently, computer simulations and the numerical discovery of unstable travelling waves have supported a transition scenario that is inspired by ideas from dynamical systems theory. According to these ideas, the transition is connected with a strange saddle that forms in the state space of the system in the neighborhood of the travelling waves. One indicator for this saddle are exponential lifetime distributions, as reported in another contribution to this meeting. A second indicator are the travelling waves, which should appear transiently in the dynamics of the flow field, as confirmed in the experimental study[1]. The current study focuses on the statistics of the appearance of travelling waves in numerical simulations of the flow.

As in[1] we use azimuthal correlation functions to pick out periodicities in downstream or normal velocities as indicators of vortices. Time traces of correlation functions clearly show regions dominated by four or six vortices, in agreement with the experimental observations. In addition, we can study the time spend near each travelling wave and can characterize the dynamics in a statistical sense by transition probabilities between the states. This is a first and empirically feasible step towards an analysis of the turbulent characteristics in terms of travelling waves.

*Philipps-Universität Marburg, Fachbereich Physik, 35032 Marburg, Germany.

[1]B. Hof, C. van Doorne et al, Science, **305**, 1594 (2004)

Selection of the convective rolls in a thin layer of evaporating liquid blown up by an air current

G. V. Rybushkina[a], V. P. Reutov[a]

The paper is concerned with the problem of pattern selection for roll convection in a thin layer of evaporating liquid, the surface of which lies under a turbulent boundary layer of an air current. Such a convection is widely encountered in natural conditions (convection in a «cold film» on a surface of open basins[1]), and also observed in experiments with evaporating liquids[2].

The analysis is constructed within the framework of a two-dimensional model for the flow in a liquid layer. Numerical simulation of the onset and development of convective rolls is made for a set of initial and boundary conditions. It is found that at large Rayleigh numbers a quasistationary system of rolls occurs, which is characterized by slow fluctuations of the sizes of rolls and modulation of their period along a chain (Fig. 1). Time dependence of mean roll scale and its dispersion is obtained. The temporal behaviour of the individual vortex scale is investigated.

It is revealed, that the system demonstrates the property of multistability, that is the scale of the selected rolls depends essentially on the initial conditions. However, it occurs only when the initial disturbances are large enough for a certain scale. If the initial fluctuations are small and random, the result of selection is determined by the dynamics of the system and does not depend on the initial conditions. In this case the characteristic size of the rolls calculated for Ra=60140, Pr=16.6, coincides well with the results of experiments earlier performed with ethanol[2]. The preferable wave number decreases with the growth of the Rayleigh number that also agrees well with the experimental data[3]. Thus, for the system considered a correct description of convective roll selection is obtained within the framework of the two-dimensional model.

The work was performed with financial support from the Russian Foundation for Basic Research (project No. 04-05-64627).

---

[a] Institute of Applied Physics RAS, Ulyanov str., 46, Nizhny Novgorod, 603950, Russia.

[1] Polezhaev et al., *Mathematical Modeling of the Convective Heat and Mass Transfer on the Basis of Navie - Stokes Equations,* Nauka, Moscow (1987) (in Russian).

[2] Reutov et al., *Preprint LAP RAS* **680**, Nizhny Novgorod (2005) (in Russian).

[3] Getling, *Rayleigh - Benard Convection,* Editorial URSS, Moscow (1999) (in Russian).

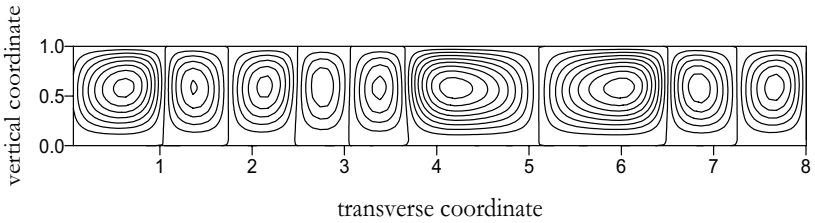

Figure 1: The modulated chain of convective rolls in a thin layer of ethanol.

Mixed turbulent convection in an asymmetrically-heated isothermal plane channel

M. M. H. Khalil[†*], A. Vernet[†] and J.A. Ferré[†]

Heat transfer by turbulent convection plays a major rule when it comes to cooling of a wide range of industrial equipments. Convection can be natural, forced or mixed. Probably the most common type of convection, mixed convection is the least studied. This is due to its complexity, since it involves the interaction of both buoyancy and externally imposed forces. Mixed convection occurs in a selection of industrial and technological applications. For example, it is of great interest to thermal designers in the field of electronics cooling [1, 2]. It can also be relevant to heat exchangers and stratified atmospheric boundary layers, among other applications. As a result, there is a necessity to understand the physics of this fundamental mechanism in a way that enables better design of engineering equipment and better prediction of natural phenomena.

The combined effect of buoyancy and mean shear on the wall bounded incompressible turbulent flows is emphasized in this study. Direct Numerical Simulation (DNS) of turbulent mixed convection in horizontal asymmetrically-heated isothermal channel under unstable density stratification, is performed. Second order finite volume code, with operator splitting to handle velocity-pressure coupling, is used. A domain of size $(5\pi\delta, 2\delta, 2\pi\delta)$ is discretized with $(128, 96, 128)$ cells in the stream-wise, wall-normal and span-wise directions, respectively, where δ is half channel height. Cyclic boundary condition is applied in stream-wise and span-wise directions.

Iida et al. [3] have tackled this problem at $Gr/Re_\tau^2 \approx 58$, where, Gr and Re_τ are Grashof number and Reynolds number based on the friction velocity and half the channel height. Our contribution is to perform a set of simulations for a range of Gr/Re_τ^2 that focus on mixed convection. This will help improve our understanding of the heat transfer processes that exist in a range of practical applications.

The effect of buoyancy on mean quantities, Reynolds stresses, temperature variance, turbulent heat fluxes and budgets of Reynolds stresses and turbulent heat fluxes will be reported. Instantaneous flow and thermal fields are visualized to highlight buoyancy effects on flow structures.

[*]Automotive Eng. Dept. Ain Shams University, 1 Al-Sarayat St., Abbassia, Cairo. Egypt.
[†]Mech. Eng. Dept., Univ. Rovira i Virgili, Av. Països Catalans, 26, 43007-Tarragona. Spain.
[1]Kehoe et al., *IEEE transactions on components and packaging technologies* **26**, 126 (2003).
[2]Teertstra et al., *Journal of Electronics Manufacturing* **7**, 79 (1997).
[3]Iida and Kasagi, *Journal of heat transfer-transactions of the ASME.* **119**, 51 (1997).

Solutions of the Boltzmann equation for microflow problems

V.V. Aristov[a], S.A. Zabelok[a]

The need to solve the Boltzmann kinetic equation in microfluid problems is caused by several reasons. Accurate simulation of microflow problems is important for a number of modern practical applications and it is interesting from the theoretical point of view. Direct methods for solving the Boltzmann equation possess attractive features intrinsic to low speed flows (it is known that traditional DSMC methods have large statistical noise for such slow flows). There are some appropriate solutions by means of the model kinetic equations but reliable solutions by the Boltzmann equation itself (which is a more adequate physical model) are necessary. Kinetic treatment can be crucial for studies of gas flows in micro-electro-mechanical systems (MEMS) that can operate in a transitional regime (in the range of Knudsen number $0.1<Kn<10$) where the rarefied gas effects can be significant, and the Navier-Stokes solver with a velocity slip boundary conditions and the Lattice Boltzmann can be inadequate.

Recently direct numerical methods (see[1]) have demonstrated their possibilities in study of some complex problems of the kinetic theory of gases. Now we develop a Unified Flow Solver (UFS) for a hybrid scheme with the decomposition of a flow region into kinetic and continuum domains where respectively the direct Boltzmann solver and kinetic schemes approximating the continuum equations are used (the method has been first demonstrated in[2] for supersonic aerodynamic problems). Since then, we have further developed this technology using dynamically adaptive Cartesian mesh and the parallel version of the UFS. In the present paper, the application of the direct Boltzmann approach to low speed internal microflow problems is described. Simulations of gas flows through an orifice and a slit for a wide range of pressure ratios including small values of a pressure drop of the order of 1% for isothermal and non-isothermal regimes are considered. Flows in channels of the wide range of the height-to-width ratio are also simulated. Calculations are performed for channels at different outlet Knudsen numbers and for different molecular potentials including the Lennard-Jones model (the influence of intermolecular potentials is considered). The behaviour of gas flow characteristics, in particular, the mass flow rate is studied. A special attention is paid to the Knudsen effect for long channels.

This work was supported by the Russian Foundation for Basic Research (grant No. 04-01-00347), by the project of the Presidium of the Russian Academy of Sciences (grant No. 17) and by the Russian Science Support Foundation.

---

[a] Dorodnicyn Computing Center, Russian Academy of Sciences, Vavilova 40, 119991, Moscow, Russia

[1] Aristov, Direct Methods for Solving the Boltzmann Equation and Study of Nonequilibrium Flows. Kluwer Academic Publishers, Dordrecht (2001)

[2] Kolobov, Bayyuk et al., AIAA J. Spacecraft and Rockets **42**, 598 (2005)

Modeling of complex fluid dynamics with phase transitions

G. V. Sandrakov*, D. I. Cherniy* and V. V. Meleshko*

Method of direct numerical simulation for some heterogeneous fluid dynamics is presented. It is supposed that the fluids are compressible and inviscid (non-viscous). Heterogeneities of the fluids are considered as small drops or particles of one fluid within other fluid. Total number of the drops can be large enough and the drops can have phase transitions. Thus simulations of the main fluid (or gas) with small transited drops dynamics are discussed. These are dynamics of multiphase flows really. Therefore it is possible to use general multiphase flow models in the case. But standard multiphase equations are not complete as a rule and various physical experiments are necessary for solving of the problem in concrete cases. The situation is more difficult whenever phase transitions are possible.

Presented method is a combination of the Harlow's method of particles in cells and the Belotserkovskii's method of large particles and is based on a discretization of conservation laws for masses, momentums, and energies in integral forms. The discretization is natural and numerical simulations are realized as direct computer experiments for the dynamics of main fluid together with transited drops without use multiphase flows approach. The method seems to be much more adequate to the mechanical and mathematical essence of the dynamics because conservation laws are correct on the discrete level at least.

The method is designed to numerical modeling of following physical processes. Let us consider graphite drops distributing uniformly in some fluid. More exactly there is medium with graphite particles and the medium can be considered under high pressure as "fluid" with corresponding state equation. Inducing conical shock waves in the heterogeneous medium it was possible to observe dynamics and phase transitions of the graphite particles in computer experiments by the method, where the transitions are realized if the pressure or temperature is more (or less) than the critical pressure or temperature by relevant phase diagrams. Results of the computer experiments were in agreement with results of physical experiments. The results were greatly depending on density of graphite particles and intensity of the shock waves.

The method was applicable to numerical simulations of plasma dynamics also. The plasma can be considered as gas with ionized particles. The gas and particles were defined by corresponding state equations. Conservation laws were coupled with Maxwell's equations. Inducing motions of the heterogeneous plasma in some region it was possible to observe dynamics and absorption of the ionized particles on relevant boundaries in computer experiments by the method coupling with appropriate method for Maxwell's equations. Results of the computer experiments were in agreement with results of physical experiments also in the case.

The method seems to be perspective for numerical simulations of other absorption and diffusion processes in complex fluid and gas dynamics.

*Kyiv National T. Shevchenko University, Volodymyrska 64, Kyiv 01033, Ukraine.

Gas-Enrichment at Liquid-Wall Interfaces

S. M. Dammer* and D. Lohse*

Molecular dynamics simulations are performed to study the effects of dissolved gas on liquid-wall interfaces. The systems are composed of different particle species (liquid/gas/wall) that interact via Lennard-Jones potentials. Liquid-gas mixtures in contact with walls exhibit gas enrichment at the walls, which increases with increasing hydrophobicity, quantified by the contact angle which is obtained from additional simulations of droplets at walls, figure 1(a). When compared to the gas concentration in the bulk of the liquid, for atomically smooth hydrophobic walls the observed gas enrichment can exceed more than two orders of magnitude, figure 1(b)[1]. In the case of nanometric wall roughness gas accumulates in nano-crevices on hydrophobic walls. Close to the walls the liquid shows a layered structure which is less pronounced for increasing contact angle and which for large contact angle is considerably altered by the presence of a gas. Furthermore, we investigate the influence of the gas enrichment at hydrophobic walls on dynamical properties, such as the slip length, by nonequilibrium molecular dynamics simulations.

*Physics of Fluids Group, University of Twente, 7500 AE Enschede, The Netherlands.

[1] Dammer and Lohse, *cond-mat*/**0510687**.

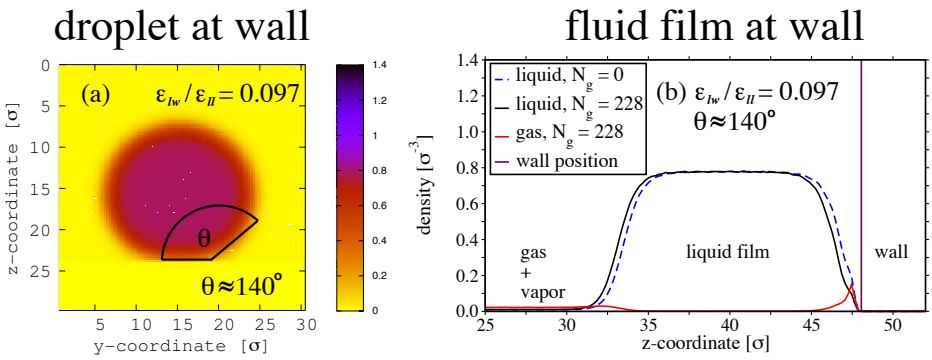

Figure 1: (a): Density profile for a droplet at a hydrophobic wall, to characterize the hydrophobicity through the contact angle. (b): Corresponding density profile for a fluid film in contact with a wall and in coexistence with its vapor(-gas) phase. The fluid film is either a pure liquid (number of gas particles $N_g = 0$) or a liquid-gas mixture ($N_g > 0$). Note the tremendous increase of the gas density at the hydrophobic wall. ϵ_{ll} is the energy scale for interactions between liquid particles and ϵ_{lw} is the energy scale for interactions between liquid and wall particles. σ is the characteristic length scale (molecular diameter) and θ is the measured contact angle.

Granular micro ripples in a capillary tube

F. Zoueshtiagh*, V. Thomy†, P. J. Thomas‡

The effect of an alternating direction of flow on a fluid carrying micron sized-particles inside a capillary tube is studied experimentally. The experimental setup is illustrated in figure 1. It consists of a capillary tube of 288 μm diameter connected to a 25 μl Hamilton syringe. The syringe is connected to the capillary tube by means of a teflon PTFE tube of 300μm internal diameter. The tubes and the syringe are fully filled with water which was previously seeded with microspheres of 10 μm diameter. The syringe is then placed on an electronic pump which enables a continuous and controlled, alternating injection and withdrawal of defined volumes of liquid. The syringe motion is computer controlled giving exact control over the flow speed, S, and the amount, A, of the liquid injected/withdrawn. The system creates then an alternative flow in the capillary tube. The response of the particles to this flow and its dependency on S and A is investigated. The motion of the particles is observed through a microscope as indicated figure 1.

The experiments show that patterns can form for a certain range and combination of S and A. They typically form after, approximately, a few tens of seconds and settle on a stable size and wavelength after roughly 300 to 400 seconds. The wavelengths are found to be of the order of hundred microns. Figure 2 shows a typical photograph of patterns observed in the experiments.

In order to investigate the physical origin of the present patterns we have compared our data to scalings found for the formation of sand ripples[1] such as those observed on the bottom of the ocean. The comparison reveals that the micrometric patterns formed in the present system display the same type of scaling behaviour as the centimetre-scale ripples observed on the bottom of oceans.

*Laboratoire de Mécanique de Lille CNRS 8107, Bd P. Langevin, 59655 Villeneuve d'Ascq, France.
†Institut d'Electronique et de Microélectronique du Nord CNRS 8520, Avenue Poincaré, 59652 Villeneuve d'Ascq, France
‡Fluid Dynamics Research Centre, School of Engineering, University of Warwick, Coventry CV4 7AL, United Kingdom

[1]Zoueshtiagh and Thomas, *Phys. Rev. E* **67**, 031301-1 (2003).

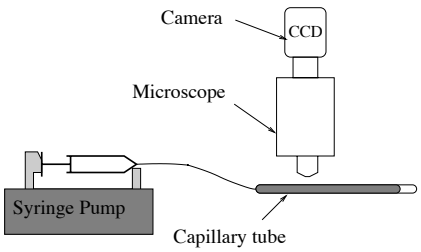

Figure 1: Experimental setup.

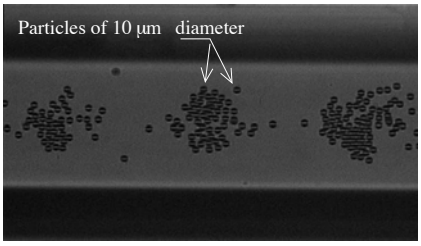

Figure 2: Ripple patterns observed in a capillary tube.

Fluctuation decay in a sedimenting suspension

E. S. Asmolov*

Velocity fluctuations in a dilute sedimenting suspension with random particle locations grow linearly with container size[1]. Disturbance field induced by a particle in low-Reynolds-number limit decays at large distances like r^{-1}. A slow decay of long-range interparticle interactions is the cause of the divergence of fluctuations for infinite system. In the experiments[2] the fluctuations converge to finite values as the container sizes increase. Other interesting observations are large-scale vortex structures in particle motion. The effect is due to the hydrodynamic interactions of many particles. Different numerical approaches, Stokesian dynamics, lattice-Boltzmann model and point particles, were applied to simulate the particle motion. Simulations based on the lattice-Boltzmann model[3] found that the fluctuations in a container bounded at the top and bottom by rigid walls saturate with increasing container width. The simulation methods are computationally demanding, so that the maximum particle number N is usually less than $10^4 - 10^5$.

The continuum model of sedimentation appears suitable for large containers since the calculation procedure does not depend on N. Central to the approach is the assumption that large-scale disturbances with lengthscale compared to the container width play a key role in the fluctuation evolution while the hydrodynamic interactions at the distances of the order of interparticle distance or less are of no importance. It was applied previously[4] for a linear case only, when velocity fluctuations are small compared with the Stokes settling velocity. In the present work the non-linear case is considered. The cell is bounded by two rigid horizontal walls and periodic in two horizontal directions. Equations governing disturbances of volume concentration and front position are derived from the continuity equation for particulate phase using perturbation methods with $\varepsilon = N^{-1/2} \ll 1$.

The front variation relative to the average vertical position is $O(\varepsilon)$ and damps volume inhomogeneities. The front holds position ensuring the dimensionless vertical fluid velocity across the front to be $O(\varepsilon)$. So the front acts approximately as the no-slip wall. The particle distribution becomes more ordered especially for horizontal long-wave inhomogeneities. Decay of velocity fluctuations is due mainly to convection of large-scale concentration disturbances. The decay rate is greater for large blobs as they migrate relative to the average concentration field and attain the top and bottom boundaries of suspension faster. The lighter and heavier clusters accumulate near the front and the bottom wall respectively. So the non-linear convective effects also cause the vertical stratification.

The research was supported by Russian Foundation for Basic Research (Grant No. 05-01-00847).

*Central Aero-Hydrodynamics Institute, Zhukovsky, Moscow region, 140180, Russia

[1]Caflisch and Luke, *Phys. Fluids* **28**, 759 (1985).
[2]Segrè et al., *Phys. Rev. Lett.* **79**, 2574 (1997).
[3]Nguyen and Ladd, *J. Fluid Mech.* **525**, 73 (2005).
[4]Asmolov, *Phys. Fluids* **16**, 3086 (2004).

Modelling of turbulence with strong intermittency "seen" by light solid particle; LES with stochastic process at sub-grid scales

A. Chtab[a] and M. Gorokhovski[a]

Our study was motivated by recent experimental observations[1]. In this experiment, the Lagrangian statistics of polystyrene particle in the high Reynolds number stationary turbulence of water flow has been measured across the inertial range of scales. The measurements showed that the velocity auto-correlation function and the time spectrum agreed to Kolmogorov, 1941 phenomenology. However, the distribution of velocity increment revealed the strong intermittency at small scales. For numerical simulation of such high Reynolds number flow, the DNS approach requires the significant CPU resources, while LES approach has no access to the strong inhomogeneity of the flow at small scales. At the same time, these effects may be crucial in simulation of multiphase high Reynolds number flows.

Our objective was to propose the numerical model, which allows to predict observations from [1]. In our paper, the flow was simulated in Lagrangian way. The velocity of fluid particle was considered to have a large-scale part (resolved by LES approach) and a modelled stochastically small-scale part, in order to represent the sub-grid acceleration. The polystyrene particle was dragging in such a flow and its Lagrangian statistics has been compared with measurements. Two stochastic models have been proposed for small-scale intermittent turbulence. The first one was based on the symmetry scaling assumption for turbulent cascade with intermittency[2,3,4]. The second one represented the stationary log-normal stochastic process written for the norm of Lagrangian acceleration (with randomly chosen direction). With both proposed models, the results of computation agreed with measurements. At small scales, the second-order structure function had, practically, quadratic dependency on time lag with evolution towards twice of variance of the Eulerian velocity field. The computed velocity spectrum proofed the Lorentz form. However, the computed statistics of the velocity increment displayed a strong non-gaussianity at small scales: when scale was getting smaller, the distribution exhibited a growing central peak with stretched tails. At the same time, at integral times, the velocity increment was normally distributed. This numerical approach can be easy applied to computation of non-homogeneous flows. The computation of turbulent boundary layer over a rough wall are envisaged in comparison with experiment.

---

[a] CORIA – UMR 6614 CNRS / University of Rouen, Site Universitaire du Madrillet BP 12, 76801 Saint Etienne du Rouvray, France.

[1] Mordant et al., *New Journal of Physics*, **6**, 116 (2004).
[2] Saveliev and Gorokhovski, *Physical Review E* **72**, 016302 (2005).
[3] Gorokhovski and Saveliev, *J. Physics of Fluds* **15**(1), 184 (2003).
[4] Gorokhovski, *Annual Research Briefs-2003*, 197, (2003).

Bursting of a fluid film in a viscous environment

E. Reyssat*, D. Quéré*

Owing to its high surface area, a fluid sheet is not stable. The nucleation of a hole in such a film leads to its bursting. We present experimental results about the bursting of fluid sheets in a viscous atmosphere. We show different setups that lead to films in viscous atmospheres (antibubbles, impact of a jet on a bath of viscous oil...), and describe the properties of such films. Opposing the case of a soap film in air, the environment plays here a dominant role in the opening process of a hole in the film. A simple model is provided to explain the observed bursting speeds. We also describe different hydrodynamic instabilities that occur during the bursting of films in a viscous atmosphere.

*PMMH, ESPCI, 10 rue Vauquelin, 75005 Paris, France.

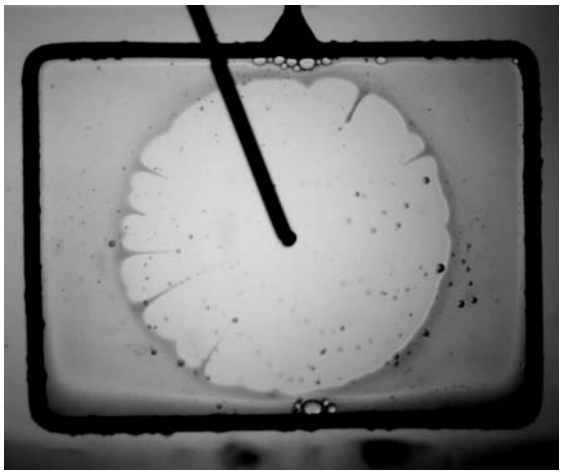

Figure 1: Hole opening in a water film plunged in a bath of silicon oil.

Spreading and evaporation of liquid droplets on heated surfaces

C.Sodtke*, V.S.Ajaev†, and P.Stephan*

We carry out combined theoretical and experimental studies of spreading of thin volatile liquid droplets on heated surfaces. The theory accounts for the effects of surface tension, evaporation, thermocapillarity, gravity, and disjoining pressure for both perfectly wetting and partially wetting liquids. Previous studies of non-isothermal spreading did not include the effects of disjoining pressure and therefore had to address a difficult issue of imposing proper boundary conditions at the contact line where the droplet surface touches the heated substrate. We avoid this difficulty by taking advantage of the fact that dry areas on the heated solid surface are in fact covered by a microscopic adsorbed film where the negative disjoining pressure suppresses evaporation. We use a lubrication-type approach to reduce the coupled fluid flow and heat transfer problem to a single partial differential equation capable of describing both the time-dependent macroscopic shape of the droplet and the microscopic adsorbed film; the contact line is then defined as the transition region between the two. In the framework of this model we investigate competition between capillary spreading and evaporation, as well as the effect of Marangoni stresses. Evaporation is shown to effectively prevent surface-tension driven spreading for sufficiently intense heating. Thermocapillary stresses are typically not very large and also tend to prevent spreading. Apparent contact angle, defined by the maximum interfacial slope in the contact-line region, is investigated as a function of time and heating conditions. The angle decays with time as predicted by several related models available in the literature, but the characteristic time of this decay is different from that predicted in the earlier studies. We attribute the difference to a nonlinear coupling between different physical effects contributing to the value of the contact angle; previous studies of spreading of volatile droplets used a linear superposition of these effects.

The experimental part of the study involves thin water droplets on heated surfaces in a closed container filled with saturated vapor. The droplets are deposited on an electrically heated stainless steel foil. Evolution of droplet shapes is studied by optical methods simultaneously with high-resolution temperature measurements under the droplet using thermochromic liquid crystals. Good agreement is shown between theory and experiment.

*Technical University of Darmstadt, 64287 Darmstadt, Germany
†Southern Methodist University, Dallas TX 75275, USA

Interaction of a pair of bubble in Hagen-Poiseuille flow

Debopam Das[a], Deepak K Choudhary[b], Gopal K. Choudhary[b]
Indian Institute of Technology, Kanpur, India

Fundamental research on bubbly flows are important in understanding flow characteristics in wide range of applications such as oil transportation, mixing in chemical processes, aeration processes, ship hydrodynamics, two phase heat exchanger, and atomizers. Few fundamental questions are

1. How the bubble moves within the flow?
2. What are the forces acting on the bubble in steady and unsteady state?
3. How the continuous phase is affected by the disperse phase in terms of momentum and energy transport?
4. How the dispersed phases interact?

Several researches have been carried out to study the first three issues[1&2] but very little on the fourth[3]. A few numbers of theoretical studies on interacting bubbles exist but very little experimental evidences are available because of the difficulty in creating two or multiple bubbles in equilibrium in a flowing system. In this paper simple experimental techniques are used to create two interacting bubbles when the drag and buoyancy of the air bubble are in equilibrium. Two levitated bubbles are created in close proximity. When the bubbles are close to each other there is slight decrease on the drag on the down stream as it reaches in the wake of the upstream bubble, thus the lower bubble moves upstream and interact with the upper bubble and set up an oscillating motion as shown in figure1. The created bubbles are drifted slightly (approximately 10 mm) as the precise control is difficult as shown in first subplot of figure1. But the drift being linear is subtracted from the motion and the oscillating pattern of interacting motion is shown in the second subplot of figure 1. The corresponding flow visualization picture is shown in figure 2. The paper will highlight on the following: (i) variation of frequency of oscillation with Reynolds number (ii) with ratio of bubble diameter to pipe diameter, (iii) dependence of amplitude of oscillation with different parameters and (iv)how drag on unsteady oscillating bubble can be obtained experimentally.

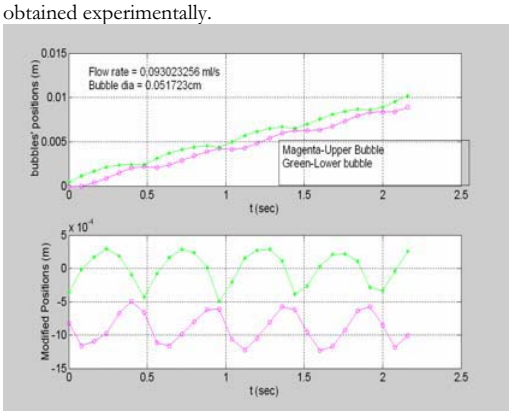

Figure:1 Trajectory of oscillating bubble pair.

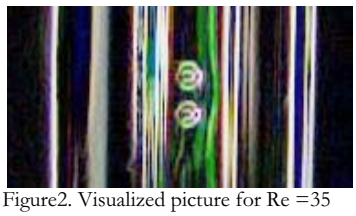

Figure2. Visualized picture for Re =35

[a] Department of Aerospace engineering.
[b] Department of Chemical engineering.

[1] Mei & Klausner, *Physics fluid* **63**,4(1992).
[2] Takemura et al, *J Fluid Mech.***277** 461(2002).
[3] Tsao & Donald, *Physics Fluids*, **2591** 6(1994)

Surface modes and sound emitted by bubbles in an acoustic field

B. Dollet*, P. Palanchon†, D. Goertz†, S. van der Meer*, I. Heitman*, M. Versluis*, N. de Jong† and D. Lohse*

We investigate the non-spherical oscillations, or surface modes, of bubbles within an acoustic field. The amplitude of such oscillations is slaved to the radial dynamics, determined from a modified Rayleigh-Plesset equation[1]. For free gas bubbles of radius between 10 and 60 μm and a given frequency of 130 kHz, the numerical calculations of the parametric instability leading to surface modes and the existing experimental results are in excellent agreement[2]. We find that the observed mode number n ($n = 2$ to 6) is linearly related to the resting radius of the bubble. In particular, we show that the critical threshold in acoustic pressure for shape oscillations is minimum at the resonance of the volumetric radial mode, and that the mode number is independent of the forcing pressure amplitude, as observed in experiments.

We then present the calculations of surface modes for bubbles used as ultrasound contrast agents in medical imaging (typically, radius between 1 and 10 μm and frequency of 1.7 MHz). We report new results about the sound emission associated with surface modes in a therapeutic context. For free oscillations, these modes are known to produce monopole sound as a second-order effect[3]. We show that this is also the case when the dynamics is forced by an acoustic pressure, and we predict the emitted sound. We study the frequency spectrum of the emitted sound and clarify the origin of the subharmonic response, which is often used in medical ultrasound imaging. To better fit to the medical conditions, we also discuss modifications due to bubble coating[4] and the effect of a confining wall.

*Physics of Fluids, University of Twente, PO Box 217, 7500 AE Enschede, The Netherlands.
†Experimental Cardiography, Erasmus MC, Rotterdam, The Netherlands.

[1] Tögel and Lohse, *J. Chem. Phys.* **118**, 1863 (2003).

[2] Versluis, van der Meer, Heitman, Lohse, Palanchon, Goertz, de Jong, submitted.

[3] Longuet-Higgins, *J. Fluid Mech.* **201**, 525 (1989).

[4] Marmottant, van der Meer, Emmer, Versluis, de Jong, Hilgenfeldt, Lohse, to appear in *J. Acoust. Soc. Am.*

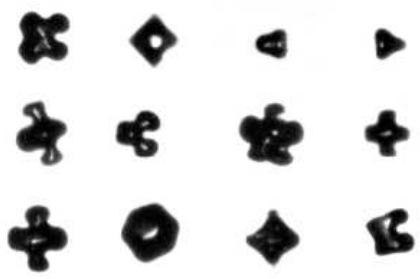

Figure 1: Examples of surface modes as experimentally observed through high-speed imaging at 1 million frames per second (resting radius of the bubble: 40 μm).

Bouncing droplets trajectories

S. Dorbolo*, D. Terwagne * and N. Vandewalle*

Silicon oil droplets are deposited on a vibrated layer of oil. Their lifetime has been studied with respect to the amplitude and to the frequency of the layer for acceleration greater or lower than the gravity. Using a high speed video camera and some imaging algorithms, the trajectory of the droplet has been measured. The phase of the bounce has been deduced with respect to both amplitude and frequency parameters. The deformation of the droplet may be related to the viscosity and an effective restitution coefficient is defined.

Within the range of frequency we tested, the droplet has been found to bounce synchronously with the plate exactly as an inelastic bouncing ball. The analysis of the trajectory gives interesting information about the interaction of the droplet with the air. Several viscosities of the silicon oil has been tested.

*GRASP - University of Liège - Dept. of Physics B5 - 4000 Liège

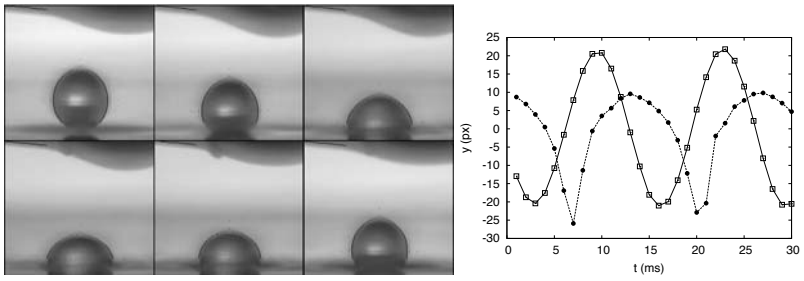

Figure 1: (left) Image sequence of a silicon oil droplet boucing on a vibrating plate. The plate oscillates at a frequency of 75 Hz. (right) Temporal evolution of the position of the droplet center of mas (full circles). The position of the plate is also illustrated.

Sound absorption of bubbles in inkjet-printer microchannels

R. Jeurissen* J. de Jong* H. Borel* M. Versluis*
M. van den Berg† H.Wijshoff† H. Reinten† A. Prosperetti*
D. Lohse*

A major problem in piezo-acoustic inkjet printing is nozzle failure, caused by an entrained $5 - 20\,\mu m$ radius bubble in the nozzle. When applying pressure pulses, a considerable part of the pulse results in bubble compression, and not in the desired jetting process of ink-droplets out of the nozzle. The entrained bubbles grow by rectified diffusion and remarkably, due to a resonance phenomenon, first lead to an enhanced droplet velocity, see figure 1.

We have developed a simple one-dimensional, quantitative model for this phenomenon, based on a narrow gap approximation and a slice-of-gas bubble. The main ingredients of the model are as follows:

- acoustics in the channel sections, with deforming walls and viscous friction
- volume oscillations of the bubble, causing rectified diffusion
- free surface flow at the meniscus, with variable mass effect
- viscous incompressible flow in the nozzle, with micropump effect

This model captures the measured droplet velocity as a function of the bubble size.

*University of Twente, Applied Physics, P.O. Box 217 7500 AE Enschede, The Netherlands.
†Océ technologies B.V., P.O. Box 101 5900 MA Venlo, The Netherlands.

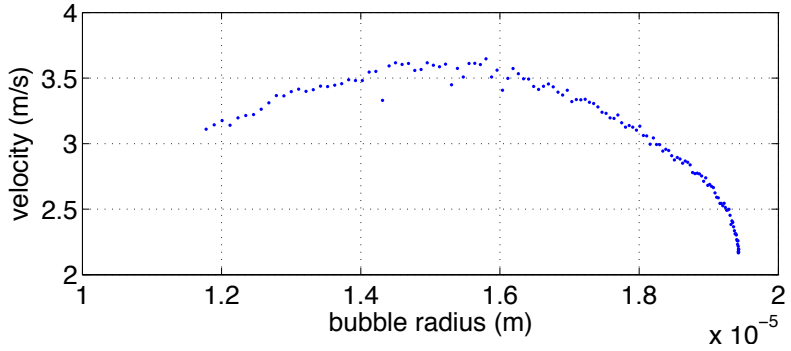

Figure 1: Measured droplet velocity as a function of the radius of the bubble in the channel.

Characterization of Nanobubbles by Atomic Force Microscopy

S. Yang[a], N. Bremond[c], H. J. W. Zandvliet[b], S. M. Dammer[a], E. S. Kooij[b], B. Poelsema[b] and D. Lohse[a]

Recent studies suggest that the deviation from no-slip hydrodynamic boundary conditions and the long-range attractive force on hydrophobic surfaces may be connected to *nanobubbles* attached on the surfaces. In this work here we characterize the surface nanobubbles through AFM (atomic force microscopy) operated in tapping mode. Our experimental results are as follows: (i) We confirm that the surface nanobubbles can stay stable for hours, which is surprising, given large Laplace pressure in the bubbles. A possible explanation for this unusual behavior may be connected to the topography of the substrate surface, as we see strong correlations between the size of nanobubbles and the substrate topography. (ii) The density of the nanobubbles is strongly affected by the relative gas-saturation in water: On a certain surface, no nanobubbles form at 20^{0}C and 25^{0}C, which corresponds to low gas saturation. At moderate gas saturation (corresponding to 30^{0}C and 35^{0}C) very few nanobubbles form. At 40^{0}C and 45^{0}C the nanobubble density achieves a considerable density, as shown in figure 1. (iii) Finally, the resulting nanobubble density is much higher on initially dry surfaces as compared to pre-wetted surfaces. This suggests that nanobubbles form directly after the substrate is immersed in water.

[a] Physics of Fluids Group, University of Twente, 7500AE Enschede, The Netherlands.

[b] Solid State Physics Group, University of Twente, 7500AE Enschede, The Netherlands.

[c] Lab. Colloides et Materiaux Divises, ESPCI, 75005 Paris, France.

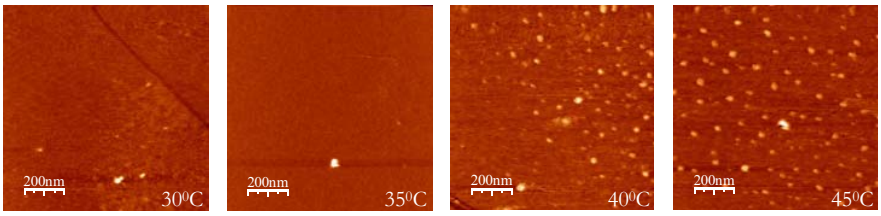

Figure1: AFM topography images of a hydrophobic substrate immersed in water at different temperatures, corresponding to different relative gas concentrations. The nanobubble density (white spots) increases with increasing relative gas concentration.

Active mixing control in a small-scale channel

S. Izawa*, T. Kaneko†, K. Kokunai*, A.K.. Xiong*, and Y. Fukunishi*

Mixing enhancement of two liquids by an active flow control in a millimeter-scale channel is carried out[1]. As shown in figure 1, both liquids, blue and clear water, are alternately injected using two syringe pumps, which are controlled by a computer. The effects of the channel geometry and the period of sinusoidal alternate injection on the mixing enhancement are examined experimentally and numerically.

In the simulation, first the flow field is computed by a finite difference method, and after the velocity field is obtained, the two-dimensional diffusion-convection equation is solved using the data.

The experiment is carried out using a straight channel shown in figure 1. The flow channel is inscribed into an acrylic resin plate surface using a milling machine. The size of basic straight channel is 115mm long, 1mm wide and 0.4mm deep. The photographs of the downstream region taken by a digital camera attached to a microscope are analyzed to evaluate the mixing effect. A clear interface between the two liquids can be observed when there is alternate injection. However, when the two syringe pumps are used to inject the liquids at a sinusoidal flow rate, the interface at the junction starts to show a wavy motion. This wavy pattern, which travels downstream, leads to an increase in the contact area, and hence, more mixing.

When a cavity is attached to the straight channel, the mixing effect further increases, which is shown in figure 2. The figure compares the flow pattern obtained in the experiment and the numerical simulation. The agreement is good. Because the wavy pattern piles up and thin laminated layers are generated inside the cavity, very effective mixing between the two liquids can be achieved by this method.

A new method for an advanced evaluation of the mixing effect is also proposed.

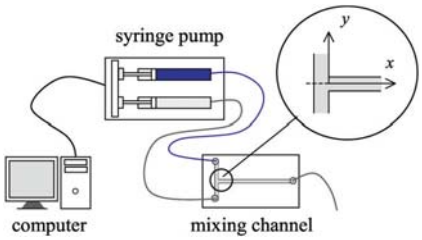

Figure 1: Experimental setup.

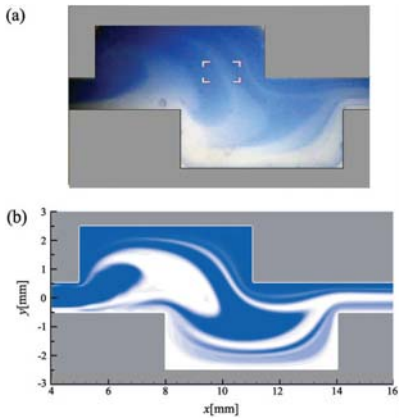

Figure 2: Comparison of flow patterns, (a) experiment and (b) computation.

*Department of Mechanical Systems and Design, Tohoku University, Sendai 980-8579, Japan.
†Nippon Petrochemicals Company, Ltd., Kawasaki 210-8545, Japan

[1]Kaneko et al., *ACFMX*, CD-ROM (2004).

Tracer particles in turbulent superfluid helium II

Y. A. Sergeev*, C. F. Barenghi†, D. Kivotides†

Much of the interest in the turbulence of superfluid helium is motivated by the simplicity of the vortex structures: the core of a vortex line has atomic thickness, the circulation is quantized, and the superfluid has zero viscosity. The recent success of implementing the Particle Image Velocimetry (PIV) technique in liquid helium has opened up the possibility of visualizing flow patterns. This technique consists of tracking the motion of small, micron-size inertial particles using lasers. However, the interpretation of PIV data is complicated by the presence in helium II of two separate fluid components: the normal fluid and the actual superfluid.

After setting up the governing equations of motion, we first solve them in some simple cases in order to gain physical insight, and then we formulate semi-quantitative general arguments relating to turbulent flow, with the assumption initially that particle trapping by vortex lines does not occur. We find that a number of different but simple regimes can be identified if the particles are neutrally buoyant: in some regimes the particles trace the normal fluid, in others the superfluid, in others the total mass current. An analysis of two-dimensional flow reveals an instability of particle motion that requires some modification of these conclusions. It is then shown that particle trapping on vortex lines can be important and can lead to serious modification of our conclusions. The results of our analysis are used to discuss what types of superfluid flow can usefully be studied by PIV, and to suggest the most appropriate size and mass of the tracer particles.

To illustrate our approach, we consider first the limit of pure superfluid in the case of low temperatures ($T < 1\,\mathrm{K}$). We show that, due to the instability and the mismatch of initial velocities of particles and the fluid, small particles cannot realistically be used to visualize the full superfluid velocity field at very low temperature. This does not mean that such particles cannot be used to visualize time-dependent, but spatially-independent (vortex-free) superflows at low temperatures. Furthermore, it does not mean that important information about low-temperature superfluid cannot be obtained from the observation of particles that are trapped on vortex lines. We present the results of calculation of statistical properties of the superfluid and particles and show that the particle velocity spectrum obeys a simple scaling law.

In the case of finite temperature superfluid, we performed numerical calculations of superfluid vortex ring propagating against a particulate sheet and show that the solid particle trajectories collapse to a very good approximation to the normal-fluid path lines. We propose an experiment in which, by measuring velocities of solid particles, direct information could be obtained about the instantaneous normal-fluid velocity. We also calculate the statistical properties of the particulate motion in the thermal counterflow in superfluid helium II.

*School of Mech. and Syst. Eng., University of Newcastle, Newcastle upon Tyne NE1 7RU, U.K.
†School of Math. and Stats., University of Newcastle, Newcastle upon Tyne NE1 7RU, U.K.

Recent developments in superfluid turbulence

C. F. Barenghi [*], Y. A. Sergeev[†] and D. Kivotides[‡]

Quantum fluids are particularly interesting because of the property of superfluidity (flow without viscosity). This phenomenon occurs in liquid helium (a substance used by engineers to cool devices such as superconducting magnets and infrared detectors) and in ultra–cold gases (atomic Bose–Einstein condensates).

Besides the absence of viscosity, what makes the motion of a superfluid special is that any rotation is constrained by quantum mechanics to thin vortex filaments. Whereas in a classical fluid eddies can be of any size and strength, the circulation Γ around a superfluid vortex and its core radius ξ are both fixed. For example, $\Gamma = 9.97 \times 10^{-4}\mathrm{cm}^2/\mathrm{sec}$ and $\xi \approx 10^{-8}\mathrm{cm}$ in superfluid ^{4}He. Another non–classical effect is that, when superfluid vortices come close to each other by a distance less than ξ, they can reconnect without the need of viscosity, unlike classical vortices.

Although the core of a superfluid vortex filament has microscopic size, the length of the filament is macroscopic; vortices can be as long as the experimental cell or channel which contains them, typically 0.1cm to 10cm. This is why superfluid vortices are well described by the classical theory of inviscid vortex lines in an Euler flow.

Superfluid turbulence is easily excited by stirring liquid helium with grids or propellers, or by making it to flow along channels at speeds of the order of few cm/sec. This kind of turbulence, which consists of an apparently disordered tangle of vortex filaments, has been the subject of recent experimental[1] and theoretical[2] investigations, which have also stimulated the progress of better flow measurement techniques near absolute zero [3]. Recent experiments have shown remarkable similarities between superfluid turbulence and classical turbulence. For example, the classical $k^{-5/3}$ Kolmogorov energy spectrum has been observed in superfluid helium; this is at first surprising, given the lack of a viscous kinetic energy sink.

The aim of this talk is to discuss the relation between superfluid turbulence and classical turbulence. Particular attention will be devoted to the nonlinear interaction of large amplitude Kelvin waves (helical displacements of vortex cores). Kelvin waves arise from the relaxation of the vortex cusps left over by vortex reconnection events. The interaction of Kelvin waves can generate a "Kelvin wave cascade", in which kinetic energy is transferred to higher and higher wavenumbers until it is eventually dissipated as sound (which, in a quantum fluid, means phonons, hence heat). The process is similar to the classical Richardson cascade, in which kinetic energy is transferred to smaller and smaller scales until it is dissipated by viscous forces into heat.

[*]School of Mathematics, University of Newcastle, Newcastle upon Tyne, NE1 7RU, United Kingdom.

[†]School of Mechanical and Systems Engineering, University of Newcastle, Newcastle upon Tyne, NE1 7RU, United Kingdom.

[‡]School of Mathematics, University of Newcastle, Newcastle upon Tyne, NE1 7RU, United Kingdom.

[1]Finne et al., *Nature* **424**, 1022 (2003); Bradley et al., *Phys. Rev. Lett.* **95**, 035302 (2005).

[2]L'vov et al., *JETP Lett.* **80**, 479 (2004).

[3]Zhang and Van Sciver, *Nature Physics* **1**, 36 (2005); Kivotides et al., *Phys. Rev. Lett.* **95**, 215302 (2005).

LES modeling of decaying compressible MHD turbulence

A. A. Chernyshov[a], K.V. Karelsky[a], and A.S. Petrosyan[a]

Numerical simulation of turbulent magnetohydrodynamic (MHD) flows is an effective tool for study of flows of charged fluid of astrophysical, helio and geophysical plasma (for instance, solar corona expansion, solar wind, flows in the solar convection zone, turbulence in interstellar matter), that is beyond the reach of direct experimental study. Complete information about turbulent fuid flow can be obtained by means of direct umerical simulation (DNS) that lies in numerical solution of full nonstationary system of equations. That approach allows resolving all scales of charged fluid flows and does not require special closures for magnetohydrodynamic equations. However, direct numerical computation of MHD-turbulence faces fundamental difficulties concerned with large hydrodynamic and magnetic Reynolds numbers typical for studied processes, because in that case the number of degrees of freedom of turbulent flow is large and minimal number of mesh points must be so large that application of direct numerical simulation for study of turbulent flows with real Reynolds numbers is limited by available computational resources. Large eddy simulation (LES) approach describes approximate turbulence dynamics, where the large-scale part of turbulent fowl is computed directly, while the small-scale one is simulated. In present work large eddy simulation technique for study of compressible magnetohydrodynamic turbulence is developed. The filtered equations of magnetohydrodynamics of compressible fluid are obtained with use of mass-weighted filtering procedure (Favre filtering). Favre filtered equations for large-scale component of turbulence include subgrid scale terms describing subgrid phenomena. For the case of polytropic fluid these terms represent combination of subgrid stresses already known from studying incompressible magnetohydrodynamic turbulence and compressible turbulence of neutral fluid. Different models of closures for subgrid terms appearing after filtration of initial equations of magnetohydrodynamics of compressible fluid are developed. The results of numerical DNS computations and different subgrid closures for LES are demonstrated; analysis and comparison of obtained results are carried out. It is shown that subgrid scale closure models suggested in this work provide suffcient dissipation of kinetic and magnetic energy and reduce computational efforts at simulation of compressible magnetohydrodynamic turbulence. The three subgrid closures are compared: Smagorinsky model, Kolmogorov model and cross-helicity model. Smagorinsky model and cross-helicity model represent more accurate results than Kolmogorov model. Results presented in the paper allow drawing conclusion that LES is a convenient tool for simulation of compressible magnetohydrodynamic turbulence.

[a]Space Research Institute, Russian Academy od Sciences, Moscow, RUSSIA

Master-modes of the 3D turbulent channel flow

Bondarenko, M.E. and Chernyshenko, S.I.
School of Engineering Sciences
University of Southampton
Southampton, UK.

Using Chebychev-Fourier representation of Direct Numerical Simulation solution we determine the so-called master modes, that is those modes which contain all essential information about the flow. The method used by E. Olson and E.S. Titi for 2D case is applied for 3D turbulent channel flow (i.e. Determining modes for continuous data assimilation in 2D turbulence, Journal of Statistical Physics, 113 (2003), 799-840). Initial simulation performed with 32786 Chebychev-Fourier modes using a spatial domain with streamwise and spanwise periods of 1.6π revealed that the number of master-modes for Re_τ=85 is $N \leq 650$. Number of master-modes is not the same as but may be related to the fractal dimension of the attractor. For the comparison, L. Keefe, J. Kim and P. Moin estimated the fractal dimension as D_λ=780 for Re_τ=80. (i.e. The dimension of attractors underlying periodic turbulent Poiseuille flow, J. Fluid Mech (1992), vol. 242, pp.1-29). Results for higher Re_τ will be obtained, analysed and reported at the conference. In particular we are interested in what organised structures will appear in the master modes.

The decay of turbulence generated by fractal grids.

D.Hurst*, R.E. Seoud* and J.C. Vassilicos*

21 different fractal grids pertaining to three fractal-pattern families were tested in two different-sized wind tunnels. Most grids have 25% blockage. The fractal dimension D and the ratio tr of max to min bar thicknesses are amongst the most important parameters characterising the grids. We report results from 5 grids pertaining to one family with fractal-generating square motif, all with the same $D = 2$, but different tr.

Results from fractal grids of same blockage but different D have shown that best homogeneity in the mean flow and the turbulence is for a maximal $D = 2$. Large- and small-scale isotropy indicators are similar to those in turbulence generated by classical and active grids [1,2]. The Reynolds number Re_λ is 2 to 3 times larger than for classical grids of higher blockage ($\approx 35\%$) in similar wind tunnels and flow conditions.

The turbulence intensity u'/U grows with streamwise distance x from the grid until it reaches $x = x_{peak}$. From there on, the turbulence decays freely and is approximately homogeneous isotropic. For all grids, integral length-scale, L, Taylor microscale, λ, remain near constant and their ratio constant during decay in agreement with the self-preserving decay solutions of [3] [3]. L is 10 times smaller than the tunnel width T and $L/\lambda = O(10)$. Attempting to fit power-law growths to L and λ, in particular the classical square root growth for λ, requires virtual origins x_0 about 9m behind the grid. Attempting to fit corresponding power-law decay laws for u', requires either a virtual origin an order of magnitude smaller than required for λ or a power-law exponent two to three times larger than anything observed or predicted by previous laboratory, numerical and experimental studies. A power-law decay is also ruled out by our finding $\lambda \propto U^{-0.2}$ inconsistent with $\lambda \propto \nu(x - X_0)/U$.

A special case of decay solutions[3] exists where L and λ are constant during decay[4]. In this case, u' decays exponentially with x. We find that

$$u'^2 = u_0'^2 \exp[-10\nu(x - x_{peak})/\lambda^2 U]$$

with $x_{peak} = 75(t_{min}/l_{min})T$ (t_{min} and l_{min} are minimum bar thickness/length on fractal grid) fits and collapses the decay data of all 5 grids. Energy spectra at different distances downstream from x_{peak} will also be presented in collapsed form for all grids. They show well-defined intermediate power-law ranges approaching -5/3 for higher Re_λ.

*Dept. Aeronautics, Imperial College London, Exhibition Road, London SW7 2BY, UK.

[1]Comte-Bellot et al., *J. Fluid Mech.* **25**, 657 (1966).
[2]Mydlarski et al., *J. Fluid Mech.* **320**, 331 (1996).
[3]W.K. George, *Phys. Fluids A* **7**, 1492 (1992).
[4]Wang et al., Unpublished preprint (2002).

An experimental and numerical study of gas turbine combustion

C. Fureby[a], G. Li[b], E. Gutmark[b], F.F. Grinstein[c]

The turbulent flow and flame dynamics within a Lean Direct fuel Injection (LDI) multi-swirl gas turbine combustor[1] is examined using a combination of state-of-the-art diagnostic methods, such as LDV, PIV and fine bead thermocouples, and modern computational methods, such as Large Eddy Simulations (LES). The LES model used in the present study is based on a propagation-based flamelet model[2,3], together with a passive scalar representing mixing. The LES computations provide unsteady field data of any quantity of interest, but are to some extent model dependent, whereas the experiments describe the real processes but often only at a few discrete locations. The combined results thus provide, besides mutual validation of the methods and models, a more complete understanding of the physical and chemical processes involved, including also interdependencies between processes that are very difficult to measure. In turn, this will aid in modification of present gas turbine combustors and design of future generations. The flow is affected by the exothermicity through the volumetric expansion, increased molecular viscosity and baroclinic torque, resulting in flow acceleration and the development of wall jets. The compact wrenched flame is anchored just downstream of the multi-swirler exit, figure 1a, due to the combined effects of recirculation, swirl and vortex formation. Good agreement is obtained when comparing LES and experimental data, figures 1b and 1c. The unsteady characteristics are dominated by longitudinal modes at ~400 Hz as observed both computationally and experimentally. Comparing predicted and measured NO_X emissions show very good agreement, suggesting that LES can be used to predict emissions.

---

[a] FOI, Div. of Weapons & Protection, Warheads & Propulsion, SE-147 25 Tumba, Sweden.
[b] Aerospace Engineering & Engineering Mechanics, University of Cincinnati, Cincinnati, OH 45220
[c] Applied Physics Division, MS-F699, LANL, Los Alamos, NM 87545, USA

1 Li G. & Gutmark E.; 2006, AIAA.J, In press.
2 Duwig C. & Fureby C.; 2005, "LES of Unsteady Stratified Combustion", Submitted to the 31st Int. Symp. on Comb.
3 Fureby C.; 2004, Proc. of the Comb. Inst., **30**, p 593.

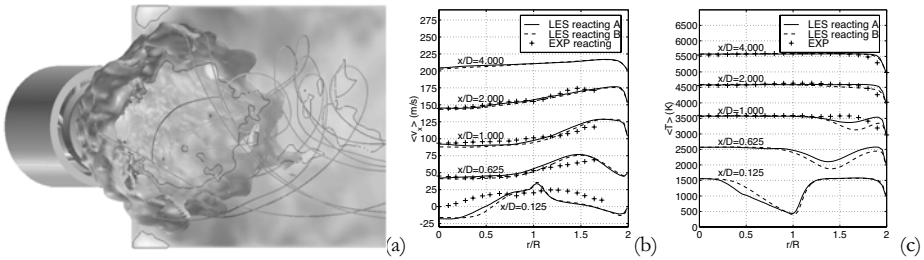

Figure 1. (a) Perspective view in terms of velocity contours, a line representing zero axial velocity, the flame and streamlines released at the inflow boundaries. (b) computed and measured profiles of the time- and circumferentially averaged axial velocity and (c) temperature along radial lines across the combustor.

Large Eddy Simulation of a swirling flame during Flashback

C. Duwig[a], L. Fuchs[b]

Today clean industrial combustion devices operate under premixed fuel lean conditions. Consequently, pollutant emissions are reduced but combustion instabilities may occur[1]. We use Large Eddy Simulation together with a flamelet model[1] for capturing flame instabilities and understanding underlying mechanisms.

We consider a model gas turbine combustor. Figure 1 (left) shows the swirl generator. The premixed fuel/air mixture enters the cone tangentially through four rectangular slots inducing a swirling motion. Further downstream, the swirling jet enters into the chamber where vortex breakdown takes place. The breakdown results in a central recirculation that brings burnt gases towards the incoming fresh mixture and stabilizes the flame. Figure 1 (left) shows a snapshot of the recirculation shape (iso-axial velocity surface) during isothermal operations. The shape of the recirculation is irregular both in space and time. However, under some circumstances, the back flow velocity might be such that the central recirculation enters the premixing tube leading to an upstream propagation of the flame (so called flash-back). Figure 1 (right) depicts a snapshot of the flame surface during flash-back. The flame is wrinkled by turbulence and exhibits highly irregular pattern. The flame enters the premixing tube along the axis. It propagates upstream and eventually stops where the flow axial velocity balances the flame propagation speed. This paper focuses on the interaction between the upstream propagating flame and the swirling pipe flow. In particular, we show how the swirl generated turbulence enhances the flash-back by increasing the flame area, and thereby the flame propagation speed.

---

[a] Div. Fluid Mech., LTH, 22100 Lund, Sweden.

[b] Div. Fluid Mech., LTH, 22100 Lund, Sweden.

[1] Duwig & Fuchs, *Combust. Sci. Tech.* **177**, 1485 (2005).

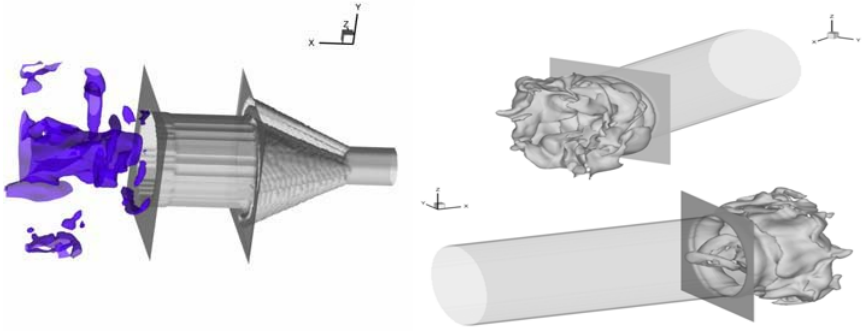

Figure 1: (Left) Conical swirl generator (light grey) and snapshot of the breakdown induced recicurculation bubble (blue). (Right) Two unsteady views of the flame surface during flashback.

Effect of the reversibility of the chemical reaction on planar premixed flames and their stability

J. Daou* and P. Sparks*

The reversibility of the chemical reactions is known to be an important ingredient in the chemical modelling of many combustion problems such as the burning of hydrocarbons or high-caloric fuels in oxygen, both in unpremixed and premixed reactive gases. Despite this importance, few analytical results are available to clarify the role of reversibility in the study of flames and their stability. In this work, we investigate the effect of the reversibility of the chemical reaction on planar premixed flames both when these are freely propagating (deflagrations) or strained (twin-flames); in doing so we also account for heat-loss and preferential diffusion. The investigation is carried out in the simple framework of a single *reversible* reaction of the form $F \rightleftharpoons P$ whose forward and backward rates are assumed to follow an Arrhenius law. Non-unit Lewis numbers for both the fuel F *and* the product P are allowed. An asymptotic analysis is conducted in the limit of infinitely large activation energy of the forward reaction, which provides an analytical description of the propagation of deflagrations, of their dependence on preferential-diffusion and heat-loss, and of their stability (within a constant density model). A detailed analytical description of the twin-flames is also given for arbitrary values of the strain rate. In all the situations considered, it is shown that the results corresponding to the reversible chemistry model can be reduced to those of the irreversible standard model by defining an effective Lewis number and an effective heat-loss parameter. Analytical explicit formulae for these effective parameters are derived which significantly simplify the discussion and understanding of the findings, e.g. the coupled effect of reversibility, preferential-diffusion, heat-loss and strain on twin-flames. In the latter case, the domain of existence of solutions and their multiplicity is systematically determined in terms of the effective parameters, a synthesis which significantly complement the results of the literature.

In short, the findings provide a clear insight into the combined effect of reversibility, heat-loss, and non-unit Lewis numbers, and a simple way to account for them in combustion studies. This can be useful in improving current combustion models such as flamelet models in turbulent combustion, or in understanding multiple solutions in studies concerned with flammability limits or premixed edge-flames[1].

*School of Mathematics, University of Manchester, Manchester M601QD, UK.

[1]Daou et al., *Combustion Theory and Modelling* **7**, 221 (2003).

Water Mist Effects on Flame Mitigation

M. T. Parra[a], F. Castro[a] and M. A. Rodriguez[a]

The present numerical work focuses on the interaction of a premixed methane/air flame with a water mist in order to provide its mitigation. Water spray barriers of fine droplets can be very effective in quenching flames[1]. When water droplets change from liquid to steam, there is an important reduction of both gas mixture temperature and oxygen concentration in the flame front surroundings.

The code SECIBA[2] (Simulator of Confined Explosions and its Interaction with Barriers of Water) was developed by the authors to carry out this research.

The gas flow behaves according to the Navier-Stokes equations expressed for a transient, compressible and reactive flow. The conservative equations are solved using a Flux Corrected Transport algorithm. The chemical kinetics of the simplified mechanism of reactions are solved using the CHEMQ solver developed by Young[3].

The monodispersed water barrier is modelled using an eulerian description. Main interaction effects of the gas mixture on the water droplets are drag, break-up, heating and vaporization of the water droplets[4]. The interaction between liquid and gas phases is represented by source terms.

An extinction criterion based on the Damköhler number is analyzed as well as the conventional criterion of the propagation velocity. The analysis reveals the important decrease of the flame propagation velocity for water barriers of 0.05 % liquid volume and droplets of 100 microns of mean diameter. See figure 1.

---

[a] Energy and Fluid Dynamics Engineering, University of Valladolid, Spain.

[1] Grant et al., *Progress in Energy and Combustion Science* **26**, 79 (2000).

[2] Parra et al., *Fire Safety Journal* **39**, 581 (2004).

[3] Oran and Boris *Numerical Simulation of Reactive Flow* Ed. Elsevier (1987).

[4] Sirignano, *Journal of Fluids Engineering* **115**, 345 (1993).

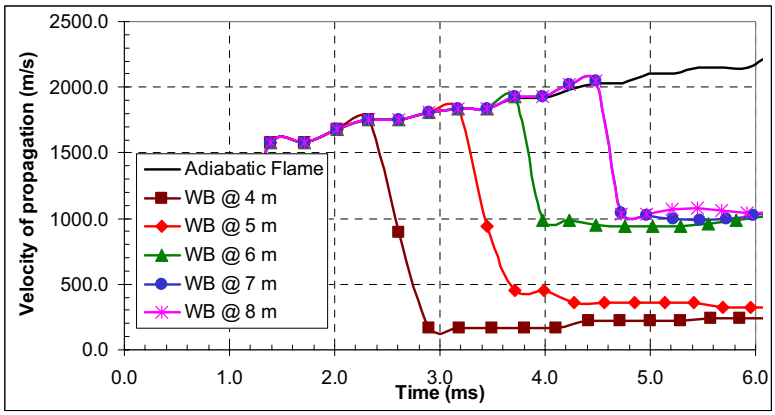

Figure 1: Influence on the velocity of propagation of the distance between the water barrier and the ignition region (water barrier of 0.05 % liquid volume and 100 micrometers of diameter).

Viscous Oscillation of a Liquid Shear Flow in an Exothermic Reacting Pipe

S. Fujioka*, H. Matsumoto* and C. Kuroda*

In this study, viscous oscillation in an exothermic reacting flow is experimentally investigated using narrow rectangular pipes. This oscillatory phenomenon occurs near the boundary between two miscible reacting fluids and it easily occurs near the wall where shear stress is large. A qualitative model of occurrence of that oscillation based on the interaction among reaction, molecular momentum transfer, molecular heat transfer, molecular mass transfer and forced convective transfer was proposed by Kuroda and Ogawa[1]. It is experimentally shown in our study that the oscillatory flow patterns change in the flow direction. Effects of viscosity on transition process of oscillatory flow patterns are investigated. Using fractal analysis, the relationship between flow patterns and process factors e.g., the entire viscosity(viscosity of main flow), the viscosity ratio, the flow rate and the flow rate ratio is quantitatively investigated based on visualized flow images.

Viscosity is a coherent variable among momentum, heat, and mass transfer, therefore change of viscosity is considered to make effects on both oscillation of flow and temperature. Effects of viscosity on thermal oscillation is investigated by the measurement of temperature fluctuation near the boundary between two fluids. Experiments are implemented with keeping the viscosity ratio of two fluids unity and effects of the entire viscosity is examined. It is shown by both frequency analysis and fractal analysis for time-series data that typical signals of thermal oscillation decrease as the increase of the entire viscosity. Moreover, the relationship between oscillatory patterns of flow and temperature is investigated by using fractal dimension in this reactive flow system.

Figure 1(a) shows an example of oscillatory flow pattern visualized by using dye. In figure 1(b) it is shown that fractal dimension of temperature fluctuation gradually approaches to 2, which means that characteristic patterns of oscillation become obscure with increase of the entire viscosity.

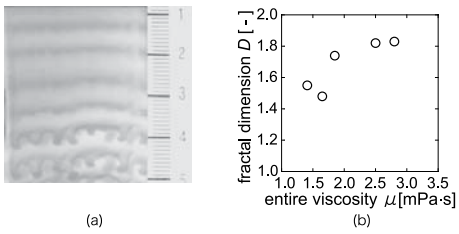

Figure 1: (a)An example of visualized oscillatory flow pattern (b)Characteristics of thermal oscillation depnding on the entire viscosity shown by fractal dimension

*Dept. of Chemical Engineering, Tokyo Institute of Technology, Japan

[1]Kuroda and Ogawa, *Chem. Eng. Sci.* **49**, 16 (1994).

Mini-symposium

New developments in hydrodynamic stability

Hydrodynamic stability theory - a modern approach

P. J. Schmid*

Hydrodynamic stability theory is one of the central disciplines of fluid dynamics. It is concerned with the quantitative description of disturbance behavior in the presence of external excitations or noise, and its important role in the study of transition to turbulent fluid motion has been confirmed in physical experiments and numerical simulations.

After a brief historical introduction, a general mathematical framework will be developed which allows the accurate description of disturbance behavior that extends beyond the dynamics of the least stable (Tollmien-Schlichting) mode. Special emphasis will be directed toward a robust definition of stability, and tools for the analysis of the response behavior of fluid systems (to both harmonic and impulsive excitations) will be given. The quantitative description of disturbance behavior in the presence of noise in the forcing and in the operator will be addressed, and extensions to time-dependent flows, spatially varying flows and complex geometries will be discussed.

The presentation is intended as a general introduction to modern hydrodynamic stability theory and will serve as the foundation for subsequent, more specialized, talks in this mini-symposium.

*Laboratoire d'Hydrodynamique (LadHyX), CNRS-École Polytechnique, F-91128 Palaiseau, France.

Edge states in the transition to turbulence in pipe flow

Bruno Eckhardt, Tobias M. Schneider*

We study the boundary of the laminar region in pipe and other shear flows near the onset of turbulence. Approaching the boundary from the laminar side, the lifetime of perturbations increases, and it diverges when the boundary is reached. Once this critical amplitude is exceeded the trajectory swings up to the turbulent regime, but its lifetime varies sensitively with amplitude, consistent with the strange saddle picture of the turbulence proposed earlier. The edge trajectory is asymptotic to a single well defined state, independent of the type of perturbation. The edge then becomes the stable manifold of this structure. In the case of a model shear flow, the edge states are simple or period doubled or chaotic trajectories. The case of pipe flow shows less variability and the edge state seems to be dominated by a simple vortical structure.

*Philipps-Universität Marburg, Fachbereich Physik, 35032 Marburg, Germany

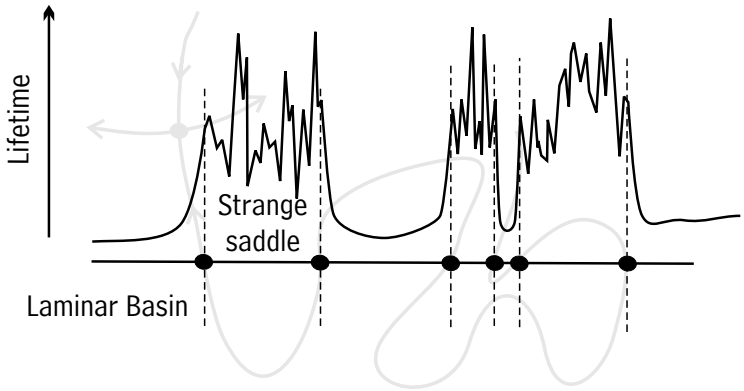

Figure 1: The saddle state in the upper left and its stable manifold separates turbulent and laminar regions. Whenever variations in initial conditions cross the stable manifold, the lifetime diverges. To one side of the crossing the lifetime variations are smooth, on the other they are irregular due to the presence of a chaotic saddle.

Finite amplitude stability curves in the transition to turbulence in pipe flow

J. Peixinho* and T. Mullin*

We present the results of an experimental investigation of the transition to turbulence in a long pipe. Transition in a fully developed Hagen–Poiseuille flow is probed by the introduction of an amplitude boxcar pulse emanating from holes in the wall. The duration and amplitude of the perturbation can be varied independently. Different holes sizes and spatial configurations around the circumference and along the pipe have been used in order to test the effects of symmetry and spatial distribution of the perturbations.

Below a critical Reynolds number, Re_c, a large finite amplitude perturbation will produce a localised disordered patches of fluid which will relaminarize as it progresses along the pipe. When the flow rate is increased in the pipe such that Re_c is approached, the distance of propagation of large amplitude disturbances increases exponentially. There is now a threshold amplitude of perturbation which if crossed, will produce a sustained puff of turbulence. Above Re_c, all the patches of disordered fluid systematically passed beyond the end of the pipe.

For larger Re, the threshold amplitude for transition to turbulence varies with Re. It is observed that perturbations with different spatial distributions can change the threshold level and may produce different scaling laws of the amplitude of perturbation required to produce turbulence. In Figure 1 the results are presented for two perturbations. These are a six azimuthal jet injection and a two point push and pull perturbation. The six jet perturbation gives a -1 scaling in accord with previous results[1]. However, the two point push/pull perturbation produces a -1.3 scaling. These results will be discussed and compared with previous work[2,3].

*Manchester Center *for* Nonlinear Dynamics, The University of Manchester, UK

[1]Hof et al., *Phys. Rev. Lett.* **91**, 244502 (2003).
[2]Darbyshire and Mullin, *J. Fluid Mech.* **289**, 83–114 (1995).
[3]Draad et al., *J. Fluid Mech.* **377**, 267–312 (1998).

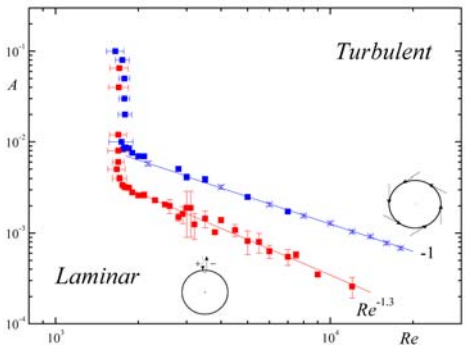

Figure 1: Finite amplitude stability curve for different perturbations.

Receptivity and transient growth in wakes

Jean-Marc Chomaz[a], Claire Donnadieu[a], Sabine Ortiz[a] and Paul Billant[a]

We investigate numerically the transient growth of three-dimensional (3D) secondary instability of wakes forming behind a thin flat plate (von Karman vortex street) and an aircraft (vortex dipole).

In the flat plate case, the primary flow, known as the von Karman vortex street has been previously numerically computed by Julien et al.[1]. The maximum growth rate and the wavelength at which it occurs as well as the cut off wavelength are well predicted by the local elliptic instability of the vortex cores of the vortices. The local hyperbolic instability theory would predict a five times larger growth rate and two times higher cut off than the ones computed. However eigenmodes are mostly localized in the braid region. As recently discussed in the case of the mixing layer by Caulfield and Kerwell[2], the finite hyperbolic region localized in the braid between the vortices generates intense transient growth but cannot sustains long time perturbation energy growth. By analysing the optimal perturbations using a direct-adjoint technique[3], we discuss the existence of amplified transients and their link with the hyperbolic instability. At short time, the energy gain is well predicted by the maximum strain that occurs close to the hyperbolic point. Initially, the spanwise perturbations nucleate and grow in the braid before being eventually amplified by the instability of the core region. Amazingly, all the spanwise wavelengths are initially strongly amplified whereas ultimately, only very narrow band of spanwise wavelengths will sustain growth due to the selective resonance condition imposed by the elliptic instability.

An aircraft wake is made of counter-rotating vortices and is known to be affected by a long (Crow) and a short (elliptic) wavelength instabilities. With the same numerical techniques developed on the von Karman vortex street, we recover instability peaks corresponding to Crow and elliptic modes but also observe less unstable oscillatory instabilities with very broad picks that seems to correspond to higher order elliptic instability. The study of the transient growth demonstrates the crucial role of the region of maximum strain that, for a vortex dipole, is mot located close to the hyperbolic point but inside the cores of the vortices.

Further investigations on the dynamics of trailing vortices in stratified fluids will be performed. Indeed, as such dipoles propagate downwards, they evolve under the influence of the stratification of the atmosphere. This unsteadiness of the flow makes standard stability theory ineffective whereas the optimal perturbations are still accessible via direct-adjoint technique[3] taking into account the evolution of the base flow. This optimal perturbation analysis allows us to discuss the effect of both inertial effects: the elliptic and hyperbolic instabilities, and buoyancy effects: the overturning instability.

---

[a] LadHyX, Ecole polytechnique, 91128 Palaiseau cedex, France

[1] S. Julien, S. Ortiz & J.M. Chomaz, Eur. J. Mech. **23**, 157 (2004).
[2] C. P. Caulfield & R.R. Kerswell, Phys. Fluids **12**, 1032 (2000).
[3] P. Corbett & A. Bottaro, Phys. Fluids **12**, 120 (2000).

Recent advances in the computation of BiGlobal linear instability of flows over complex configurations

V. Theofilis*, J. de Vicente*, E. Valero*, N. Abdessemed† and S. Sherwin†

The present contribution highlights aspects of the numerical solution of the three-dimensional BiGlobal eigenvalue problem (EVP) in incompressible steady and time-periodic flows developing over complex geometries. Two applications are analyzed in some detail with respect to their linear instability, namely flow over an open cavity[1] which contains a model store, and flow over a periodic row of blades in a low-pressure turbine (LPT) passage. Challenges encountered include geometric complexity (and fidelity of geometry representation), accurate description of periodic orbits, and the associated size of the respective EVPs. State-of-the-art algorithms for both the spatial discretization and the numerical solution of the BiGlobal EVP have been designed and applied. In the open cavity case we take advantage of the regularity of the geometry and solve the three-dimensional BiGlobal EVP using a novel non-conforming spectral multidomain method, of the mortar element class. On account of the sparsity of the discrete matrix, its non-zero entries are formed and stored exlicitly. The LU-decomposition within the Krylov subspace iteration used for the solution of the EVP is performed using sparse matrix techniques on a large number of processors (of the order of hundreds); currently scalability and resulting timings for the solution of the EVP are being optimized. In the LPT case the aforementioned challenges are compounded by the need to employ Floquet theory in order to analyze the time-periodic orbits. Here spectral/hp element methods are used in order to deal with the very large memory requirements, which prohibit explicit formulation of the discretized EVP matrix. Techniques used for the time-advancement in direct numerical simulations are then utilized for the solution of the Floquet-EVP. Further details, from both a numerical and a physical point of view, will be provided at the meeting.

*School of Aeronautics, Universidad Politécnica de Madrid, E-28040 Madrid, Spain
†Department of Aeronautics, Imperial College London, London SW7 2AZ, UK

[1] Colonius and Lele, *Prog. Aero. Sci.* **40**(6), 345 (2004).

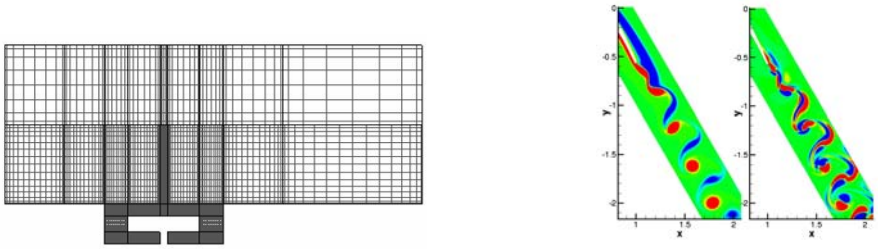

Figure 1: (a) The non-conforming spectral multidomain decomposition of a rectangular *T-Store* model. (b) Basic state in the wake of a T-106/300 LPT blade (left) and amplitude function of the associated leading Floquet eigenmode (right).

Global modes and streamwise non-normality in the flat-plate boundary layer flow

U. Ehrenstein*, F. Gallaire*, E. Åkervik†and D. Henningson†

Temporal linear stability modes depending on two space directions are computed for a two-dimensional unstable boundary-layer flow along the flat plate. The linearized Navier-Stokes system is discretized using Chebyshev-collocation in both the streamwise and wall-normal direction and the resulting eigenvalue problem is solved by means of a Krylov-Arnoldi method. It is shown that for appropriate inflow and outflow conditions, the spatial structure of each individual temporally stable mode is reminiscent of the spatial exponential growth of perturbations along the flat plate, as predicted by local stability analyses. In this approach the flow velocity perturbation is of the form $\mathbf{u} = (\hat{u}(x,y), \hat{v}(x,y))\, e^{-i\omega t}$ and the mode structure for two different frequencies ω is shown in figure 1.[1]
A finite subset of these modes is then considered for model reduction and used for an optimal temporal growth analysis. It is demonstrated that a suitable superposition of a moderate number of those non-normal temporal modes gives rise to a spatially localized wave packet, starting at inflow and exhibiting transient temporal growth when evolving downstream along the plate. In this way both Tollmien-Schlichting type instability waves at moderate convective time scales and the transient Orr mechanism at short time scales are retrieved. The dynamics of the reduced system is shown to be in qualitative agreement with the instability dynamics of the Navier-Stokes system, for equivalent initial conditions. In particular, the reduced system provides reliable results, when considering the signalling problem aimed at triggering spatially growing Tollmien-Schlichting instabilities.

*Laboratoire J.A. Dieudonné, UNSA, Parc Valrose, F-06108 Nice Cedex, France.
†KTH Mechanics OB 18, SE-100 44 Stockholm, Sweden.
[1]Ehrenstein and Gallaire, *J. Fluid Mech.* **536**, 209 (2005).

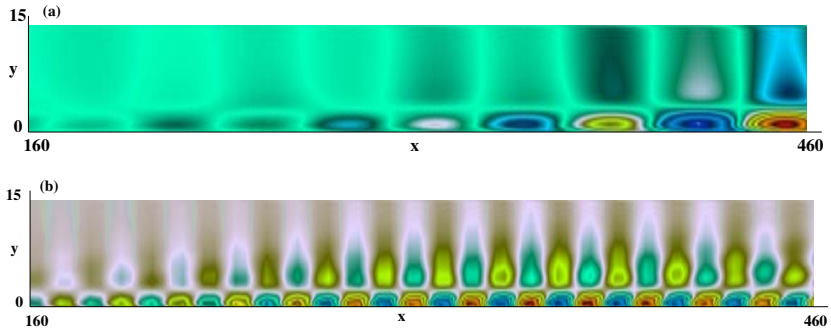

Figure 1: Global mode structure, real part of streamwise velocity component, with frequency: (a) $\omega = 0.03 - 0.005i$, (b) $\omega = 0.1 - 0.006i$.

Influence of crossflow vortices on the instability of a 3-d APG boundary-layer flow with preceding FPG

Markus J. Kloker[a]

The laminar breakdown of a three-dimensional flat-plate boundary-layer flow with favourable and ensuing adverse pressure gradient (FPG/APG), generic for an infinite swept wing, is investigated in detail by means of spatial direct numerical simulations (DNS). Emphasis is on instability and transition mechanisms in the region of adverse pressure gradient where primary linear stability theory (LST) predicts the naked laminar base flow to be also unstable with respect to Tollmien-Schlichting waves that are most amplified if two-dimensional with respect to the local streamwise direction (fig. 1). The influence of finite-amplitude crossflow (CF) vortices, coming from the region of favourable pressure gradient, on the TS instability properties is investigated. It turns out that crossflow-vortex-induced secondary instabilities are the most amplified disturbances even for low-amplitude vortex modes. The TS waves act as generators of fundamental, low-frequency secondary modes but are neither important for their growth nor for breakdown. For low CF amplitude the low-frequency TS-generated secondary modes form obliquely oriented, contra-rotating secondary vortices seemingly similar to a Λ-vortex (fig. 2) but their tips are split by the primary CF vortex (not visible) in-between them. Breakdown is not of K-type, rather tertiary vortices twining around the secondary structures appear. For higher CF amplitude a (crosswise) localized secondary instability mode of `z´-type prevails, with five times the TS-frequency, leading to localized secondary vortices. Finally also arc-type vortices on top of the primary CF vortex appear, an indication of an additional `y´-mode instability (fig. 3). As for active disturbance control, any method aiming at attenuating flow-aligned two-dimensional TS waves must fail. On the other hand, forcing tightly spaced, benign CF vortices is shown to delay transition also in the APG region[1, 2].

In the second part results of secondary stability theory are quantitatively compared with several adulterated DNS to elucidate differences found in the prediction of mode types and growth rates for a 3-d FPG boundary layer.

---

[a] Institut für Aerodynamik und Gasdynamik, Universität Stuttgart, 70550 Stuttgart, Germany

[1,2] Wassermann and Kloker, *J. Fluid Mech.* **456,** 49-84 (2002), **530,** 265-293 (2005).

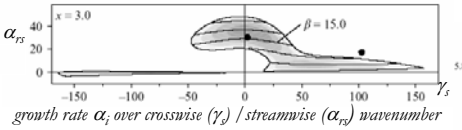

Figure 1: Instability diagram (LST, α_i) at a downstream position with slight APG, showing the appearance of TS instability in addition to CFI.

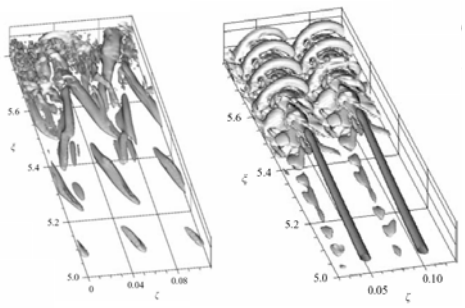

Figure 2 (middle) and 3 (right): snapshots of vortex structures during breakdown with low and medium primary CF vortex amplitude.
λ_2-isovalues: -50 (middle) and -5 (right).

Delaying transition to turbulence by a passive mechanism

J. H. M. Fransson*, A. Talamelli*†, L. Brandt* and C. Cossu‡

Reducing skin friction is important in nature and in many technological applications. This reduction may be achieved by reducing stresses in turbulent boundary layers, for instance tailoring biomimetic rough skins. Here we take a second approach consisting in keeping the boundary layer laminar as long as possible by forcing small optimal perturbations. Due to the highly non-normal nature of the underlying linearized operator, these perturbations are highly amplified and able to modify the mean velocity profiles at leading order. We report results of wind-tunnel experiments in which we implement this concept by using suitably designed roughness elements placed on the skin to enforce nearly-optimal perturbations. The aim of this investigation is to prove that controlled low energy optimal perturbations can, due to their large transient amplification in a non-normal system, effectively *stabilize* that system even in the non-linear regime and can indeed be used for control purposes.

The experiments were performed in a flat plate boundary layer positioned in the MTL wind tunnel at KTH Mechanics. The 3D modulated base flow was generated by placing roughness elements, small standing coin-like cylinders, in an array in the spanwise direction. This array generates a sinusoidal spanwise distribution of alternating high and low speed streaks some distance downstream the array. Smoke visualizations and hot-wire anemometry measurements are used to quantify the transition delay by means of this passive control method. Figure 1 show visualization images (210×168 mm^2), with and without streaks and 2D forced disturbances, located 1434 mm downstream of the leading edge. Flow is from left to right.

*KTH Mechanics, SE-100 44 Stockholm, Sweden.
†II Facoltà di Ingegneria, Università di Bologna. I-47100 Forlì, Italy.
‡LadHyX, CNRS Ecole Polytechnique, F-91128 Palaiseau, France.

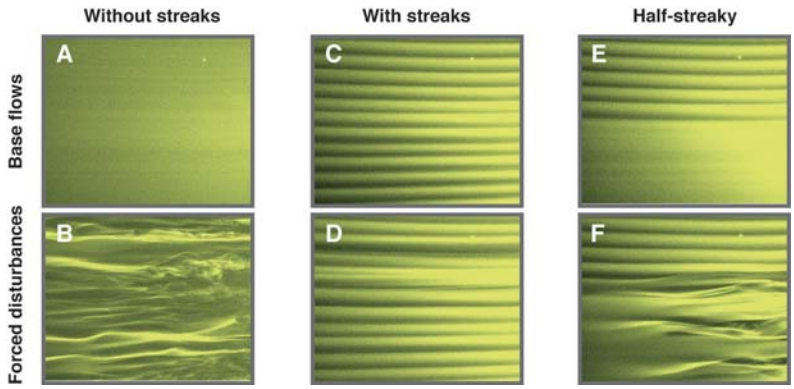

Figure 1: A and B without streaks, without and with excitation ($\mathcal{V}$), respectively. C and D with streaks, without and with excitation ($> 2\mathcal{V}$), respectively. E shows a half-streaky boundary layer without and with excitation ($\simeq 0.8\mathcal{V}$), respectively.

Stochastic excitation of streaky boundary layer

J. Hœpffner*, L. Brandt* and D. S. Henningson*

Boundary layers subject to free-stream turbulence of moderate amplitude are characterised by the growth of perturbation elongated in the streamwise direction. These structures are usually referred to as streaks or Klebanoff modes. The mechanism of their growth is related to the non-normality of the linearised Navier-Stokes equations in the presence of shear of the basic flow (transient or non modal growth).

When the streaks grow to finite amplitudes, secondary instability can occur, leading to the appearance of turbulent spots. The secondary instability of steady spanwise periodic streaks has been studied in[1]. However, recent studies[2] suggest the possibility of a secondary transient growth mechanism responsible for the breakdown of subcritical streaks. By computing the initial condition leading to the largest possible energy growth, we found that, indeed, significant growth could be achieved well below the streak amplitude threshold for modal instability[3].

The aim of the present study is to quantify the realizability of this optimal secondary transient growth and the streak sensitivity in the presence of physically relevant external disturbances, in particular free-stream turbulence and wall roughness. To do this, a stochastic approach is followed. In particular, we will compute the evolution of a stochastic initial condition and the response to stochastic forcing.

In the former case, the statistics needed to describe the initial disturbance are the two point correlations in the flow domain. By assuming homogeneous isotropic turbulence in the free-stream, it is possible to obtain the correlations directly from the turbulence energy spectra (we assume as analytical expression for it the Von Karman spectrum). The covariance of the initial condition P_0 is obtained by enforcing zero perturbation inside the boundary layer. The subsequent time evolution of the flow perturbation can be computed by means of the Lyapunov equation

$$\dot{P} = AP + PA^H, \quad P(0) = P_0, \tag{1}$$

where A represents the Navier-Stokes equations, linearised about the streaky nominal flow profile, and the equation variable $P(t)$ is the covariance matrix of the flow fluctuations for each instant of time. Significant growth of the stochastic initial condition modelling isotropic homogeneous turbulence is observed: about 20% of that of the optimal perturbations. To gain insight into the growth mechanism, coherent structures from the flow covariance, by means of Proper Orthogonal Decomposition, are extracted. The same structures as in the case of optimal initial condition are observed.

Two types of forcing will be considered in the study of the streak sensitivity to stochastic excitation. To mimic the effect of wall roughness, forcing by non-homogeneous boundary condition at the wall will be introduced. The forcing due to free-stream perturbations will be modelled by assuming isotropic homogeneous turbulence.

*KTH Mechanics, SE-100 44 Stockholm, Sweden.

[1]Brandt and Henningson, *J. Fluid Mech.* **472**, 229 (2002).
[2]Schoppa and Hussain, *J. Fluid Mech.* **453**, 57 (2002).
[3]Hœpffner et al., *J. Fluid Mech.* **537**, 91 (2005)

Secondary optimal growth in channel flow

C. Cossu*, M. P. Chevalier† and D. S. Henningson‡

We compute the linear 'secondary' optimal transient energy growth supported by an unsteady primary optimally growing basic flow in a plane channel at $R = 1500$. The primary flow is generated by giving as initial condition the Poiseuille solution plus 'primary' optimal spanwise periodic vortices of finite amplitude A_v which then evolve into transiently growing streaks. The secondary optimal initial condition is given at $t = 0$, like the primary one, and is computed on the unsteady basic flow by using an adjoint technique. For small amplitudes A_v of the primary initial vortices, the secondary optimal perturbation and energy growth are almost identical to the primary one and respectively consist in $\alpha = 0$ streamwise vortices and streaks. For larger A_v, however, two distinct secondary growth mechanisms set in. The first one is related to the one recently observed on frozen boundary layer streaks[1] and consists in a modified lift-up mechanism leading to a large wavelenght bending of the primary streaks. The second acts on shorter wavelengths and is related to the local (in time) modal secondary instability of the streaks. Sample associated optimal perturbations are shown in figure 1. We conclude that for sufficiently large amplitudes of the primary optimal vortices, the optimal perturbations leading to maximum transient growth in a plane channel flow have $\alpha_{opt} \neq 0$.

*LadHyX, CNRS-École polytechnique F-91128 Palaiseau, France.
†Swedish Defence Research Agency (FOI) SE-164 90 Stockholm, Sweden.
‡KTH Mechanics OB 18, SE-100 44 Stockholm, Sweden.
[1]Hoepffner *et al.*, J. Fluid Mech. **537** 2005

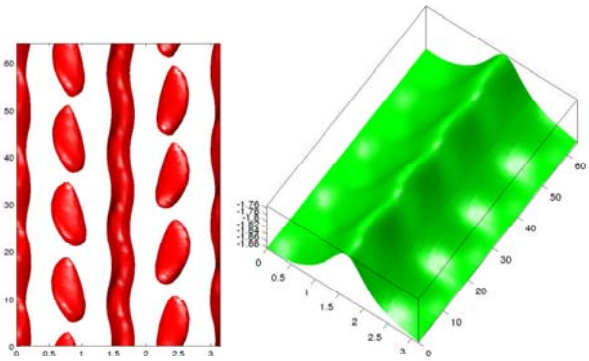

Figure 1: Optimal secondary perturbations added, with an arbitrary constant, to the primary optimal basic flow with $A_v = 0.02$. Left: iso-level surface of $\left[v^2 + w^2\right]^{1/2} = 0.9\left[v^2 + w^2\right]^{1/2}_{max}$ for the optimal initial condition. Right: iso-level surface of $u = 0.4u_{max}$ for the optimal response.

Mini-symposium

Microfluidics

Optical micromanipulation takes hold for microfluidics

K Dholakia[a], S. Neale[a], S. McGreehin[a], L. Paterson[a], M. MacDonald[a], V. Garces-Chavez[a], P. Jess[a], P Zemanek[b], T Cizmar[b] and T.F. Krauss[a]
[a]School of Physics and Astronomy, University of St Andrews, Fife KY16 9SS
[b]ISI Brno, Academy of Sciences of the Czech Republic, Kralovopolska 147, 612 64 Brno, Czech Republic

Optical tweezers is a powerful non-contact technique where micrometre sized particles can be grabbed, moved and generally manipulated solely with light. Optical tweezers have forged an important bridge between physics, chemistry and biology [1]. In recent years there has been a proliferation of activity in this area, fuelled, in part, by the recognition that we need to advance the "optical toolkit" particularly for microfluidic environments. This essentially means enhancing our ability to move, rotate particles and importantly, create 2D and 3D arrays of particles. Rotation of particles can lead to the development of optically driven micromachines to pump microscopic volumes of fluid from one chamber to another and indeed in mixing at a microscopic level. Trapping in microfluidic environments offers prospects for particle sorting and selection as well as novel studies.

In this talk I will give an overview of a host of novel methods for enhanced micro-manipulation for microfluidics, including the use of specialist light beams and interference patterns. In particular I will discuss methods for particle and cell sorting in microfluidic environments using optical lattices [2], motional light patterns [3] and static light patterns [4]. Additionally I will discuss the development of micro-cogs and components using the concept of form birefringence. Raman spectroscopy may then be used in a trapping environment to analyse cells [5]. Finally I will describe the development of the first ever integrated optical trap which incorporates lasers adjacent to a microfluidic channel. This is a truly portable microtrap and may be adapted in a number of ways

[1] Dholakia and Reece, to appear in Nano Today (Feb 2006)
[2] MacDonald et al., Nature **426**, 421 (2003)
[3] Cizmar et al., submitted to Phys Rev Lett (2005)
[4] Paterson et al. Appl. Phys. Lett. **87** 123901 (2005)

Laser induced thermocapillary driven flow in Hele-Shaw geometry

F. Gallaire*, J.-P. Delville† and C. Baroud‡

Recent experiments[1] have demonstrated how to block of a water drop entrained in a silicon oil flow in a microchannel by the use of a focused laser-beam. The heat from the laser beam released at the interface between the two immiscible fluids produces thermocapillary stresses along the interface at the origin of a secondary flow opposing the entraining flow.

The aim of the study is to numerically determine the flow induced by these Marangoni stresses by considering the Stokes equations around the drop of radius R with a small gap $h/R = 0.1 \ll 1$ Hele-Shaw type approximation[2]. The averaged two-dimensional equations are then discretized by a Chebyshev-Fourier method in the radial and azimuthal directions A typical solution is displayed in figure 1. The force distribution on the drop interface is then evaluated so as to examine the possibility of stable equilibrium solutions. The obtained force balance is compared with the asymptotic estimates of Nadim *et al.* (1996)[3].

*Lab. J.-A. Dieudonné, UNSA-CNRS, Nice, France
†CPMOH, Université de Bordeaux-CNRS, Talence, France
‡LadHyX, Ecole Polytechnique-CNRS, Palaiseau, France

[1] Baroud and Delville, Localized laser forcing for breaking, sorting or blocking droplets in a microchannel APS DFD 2005, Chicago

[2] Boos and Thess, Themocapillary flow in Hele-Shaw cell" J. Fluid. Mech. **352**, 305-330, 1997

[3] Nadim, Borhan and Haj-Hariri, Tangential stress and Marangoni effects at a fluid-fluid interface in a Hele-Shaw cell" J. Colloid Interface Sci. **181**, 159-164, 1996

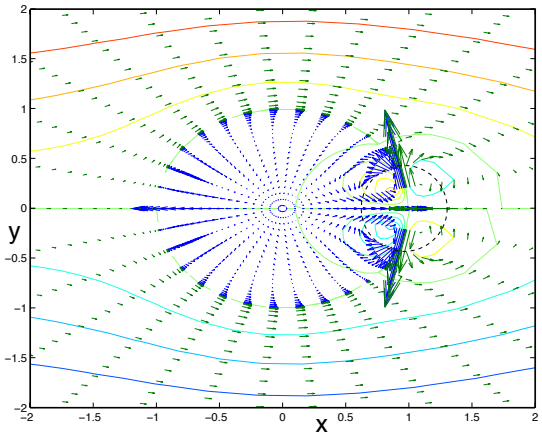

Figure 1: Velocity field around the drop with $h/R = 0.1$ and a Laser beam focused at $x = 1, y = 0$.

Numerical Simulation of Dielectrophoresis

Yuan Lin*, Gustav Amberg*, Fredrik Aldaeus† and Johan Roeraade†

The subject of separating micro-size particles with different properties is always of great interest. Among those methods, dielectrophoretic separation devices are most commonly used as trap-and-release filters or particle sorters.Dielectrophoresis is the phenomenon that a particle moving in a converging electrical field.If the motion is in the direction towards higher field strength, it is referred to as positive dielectrophoresis (pDEP), while the case of motion towards lower field strength is called negative dielectrophoresis (nDEP).The dielectric force is determined by the electric properties parameters of the particle and the medium and it is frequency dependent.

We have set up a highly simplified model to calculate spherical particles movements in different geometries and with various conditions[1].In this model, the hydrodynamics force and interactive dielectrophoresis forces have been neglected, and we regard the particle interface as a hard interface. In principle, this model is enough for providing some useful information for design optimization.

For example, superpositioned electrical fields have been used for trapping particles more efficiently. Because the polarization factor is dependent on the frequency of AC, and it could be pDEP in one frequency, and nDEP in another frequency. If both sequences of AC are used at the same time, the trapping efficiency could be enhanced greatly. Also, we simulated separation of particles with different sizes and electric properties. Multi-step separation is used to increase the separation efficiency[2]. This work was done in collaboration with analytic chemistry, KTH.

However, in actual situation, hydrodynamics force between particle and fluid, the interactive dielectrophoresis between the polarized particles play important roles. We now focus on simulating the hydrodynamics force and interactive dielectrophoresis forces. Flexible interface may be taken into account since our aim is to simulate cells dielectrophoresis separation,which is quite challenging. Besides, since cells are usually of elliptic shape, we also would simulate elliptic particles instead of spheric particles in our near future work. The simulation calculation work was done with the help of FemLego[3].

*KTH Mechanics OB 18, SE-100 44 Stockholm, Sweden.
†KTH Chemistry TR 36, 100 44 Stockholm, Sweden.

[1]Fredrik A., Yuan L., Johan R. and Gustav A.*J. Electrophoresis.* **4252-4259**, 26 (2005).
[2]Fredrik A., Yuan L., Johan R. and Gustav A.*Multi-stepped Dielectrophoretic Separation* **to be submitted**
[3]Amberg,G.,Tönhardt,R.,Winkler,C.*Math.Comp.Simulation* **257-274**, 49 (1999).

Surfactant effects on drop detachment

F. Jin[1], N. R. Gupta[2], K. J. Stebe[3]

In microfluidics, the creation of drops of well-defined dimensions in a continuous external phase is achieved by use of flow configurations that impart strong local extension to elongate the drop phase and drive pinch-off. Typically, the drop phase contains analytes or reagents that are surface active. Similarly, surfactants are often added to the continuous phase to reduce the surface tension and lower the work required to create new interface. The presence of surface active components can significantly alter drop detachment modes. Surfactant effects on drop deformation and detachment are studied numerically in a model problem of a buoyant viscous drop in an external viscous fluid. As the drop is injected, it deforms to assume a distended shape. A neck forms and thins rapidly in a rapid surface-tension driven pinch-off mechanism. In the absence of surfactants, surface contraction is fastest just above the neck. When surfactants are present on the interface, they are drawn to this region and accumulate if the desorption of surfactant off of the interface, or bulk diffusion flux away from the surface are slow. This reduces the local surface tension that drives neck thinning, and can impart Marangoni stresses that also impede outflow from the neck. We demonstrate that surfactant accumulation can lead to a variety of drop detachment behaviours depending upon the surfactant concentration and adsorption/desorption kinetics, including the formation of new neck shapes, or a failure to form necks at all. These results have implications in terms of detached drop dimension and satellite drop management.

[1] Johns Hopkins University, Chemical and Biomolecular Engineering Dept., Baltimore, MD 21218, USA.

[2] University of New Hampshire, Chemical Engineering Dept., Durham, NH, 03824, USA.

[3] Johns Hopkins University, Chemical and Biomolecular Engineering Dept., Baltimore, MD 21218, USA.

Rate-of-flow-controlled Break-up; Formaiton of Bubbles and Droplets in Mirofluidic Systems.

Piotr Garstecki[a]

Microfluidic systems offer highly controlled methods of emulsification. In contrast to the dynamics of break-up in unbounded fluids, where one typically observes two distinct regimes of break-up: dripping and jetting; microfluidic systems exhibit an additional mode of break-up which is dominated by the normal—and not tangential—stresses exerted on the emerging droplets. I will describe this new mechanism in detail for two most popular microfluidic devices used for emulsification: flow—focusing[1,2] and T-junction geometries. I will also briefly review how this dynamics and controlled formation of bubbles and droplets can be used in construction of microfluidic systems exhibiting surprising non-linear phenomena[3], and in applications, including micro-mixing[4], formation of particles[5] and microcapsules[6], and in fluidic optical systems.

[a] Institute of Physical Chemistry, PAS, Kasprzaka 44/52, 01-224 Warsaw, Poland.

[1] Garstecki, et al., *Appl. Phys. Lett.* **85**, 2649 (2004)
[2] Garstecki, et al., *Phys. Rev. Lett.* **94**, 164501 (2005)
[3] Garstecki, et al., *Nature Physics*, **1**, 168-171 (2005)
[4] Garstecki, et al., *Appl. Phys. Lett.* **86**, 244108 (2005)
[5] Xu, et al., *Angew. Chem. Int. Ed.* **44**, 724 (2005)
[6] Takeuchi, et al. *Adv. Mater.* **17**, 1067 (2005)

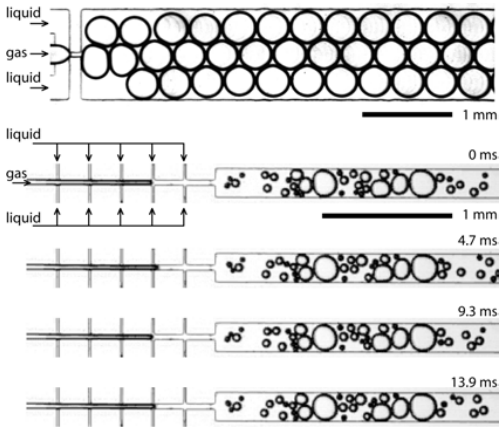

Figure 1. Top panel – single flow- focusing bubble generator reproducibly forms bubbles of uniform size. Bottom panel – the device comprised of five flow-focusing bubble generators coupled in series. The generators interact and produce complex series of bubbles of different sizes (here 29 bubbles in a single series is shown). Surprisingly, this intricate behavior is stable – the system continuous to produce bubbles in this complex manner for minutes and hours. Consecutive micrographs illustrate the system 4.7, 9.3 and 1.9 milliseconds after the first micrograph was taken.

Handling microfoams

P. Marmottant[a], J.P. Raven[a] and F. Graner[a]

A useful characteristic of foams is the abundance of interfaces and low volume contents of liquid. The control of microscopic foams, microfoams, would provide applications like transporting amphiphilic molecules on interfaces, and the individual handling of gas pockets or small amounts of liquid.

We will present how to produce a foam in situ on a microfluidic chip. Using a flow focusing method, quasi-monodisperse bubbles can be generated in thin channels. Their assembly generates 2D foams with a large range of liquid fractions, depending on the applied liquid and gas flow rates (figures a and b). Microscopic imaging allows monitoring the transition from separated bubbles into the desired foam in which bubbles are closely packed.

The foam flowrate in the microchannel displays a threshold pressure due to capillarity, and depends non-linearly on the applied pressure, a consequence of the friction of bubbles on walls. The drag is very dependent on the arrangements of bubbles in the foam, and bubble volume variations can induce sudden discontinuous increase in the drag. We can obtain ultraflat foams, reducing the channel height to about 8 micrometers, with a bubble thickness to diameter ratio down to 0.02; we then observe a marked change in bubble shape during the flow (figure c).

The deformation of foams by various channel geometry, like obstacles, bifurcations, or constrictions, will be discussed in the scope of microrheometry experiments designed to learn more on the elasto-plastic behaviour of foams.

[a] Laboratoire de Spectrométrie Physique, CNRS-Université Joseph Fourier, 140, Avenue de la Physique, BP 87, 38047 Grenoble, France

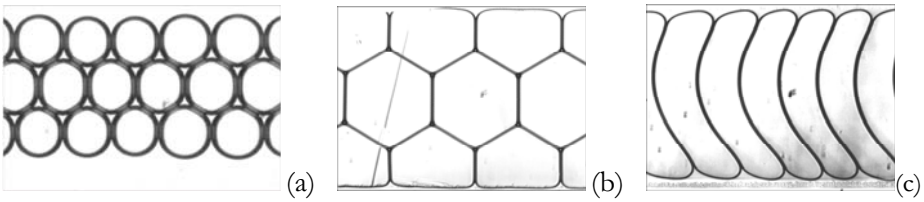

(a) (b) (c)

Figure: Foams in a 400 micrometer wide microchannel: (a) wet microfoam, (b) dry microfoam and (c) distorted bubble shapes during flow.

Disturbing bubbles in piezo-acoustic printing

D. Lohse*, J. de Jong*, M. Versluis*,
M. van den Berg†, H. Wijshoff† and H. Reinten†

In piezo-electric ink-jet devices voltage pulses applied to a piezo-electric element cause an ink-filled channel to deform, thereby creating a pressure waveform in the ink and ultimately ink-drops flying out of the channel. Typically the ink-drop diameter is presently about $30\mu m$ and the frequency is about 20kHz. The ink-jetting process however is known to be vulnerable to spontaneous break down. By a combination of high-speed imaging and acoustic response measurements we can show that the origin of the breakdown is an entrainment of a bubble at the nozzle. By designing a nozzle plate out of glass we are able to follow the bubble in the nozzle with high-speed imaging, including the bubble's growth by rectified diffusion. The bubble is first pulled into the nozzle's interior by the Bjerknes forces and then pushed towards the edge, once it is beyond resonance size. A numerical model, based on the insight gained into bubble dynamics from single bubble sonoluminisence, is applied to the bubble in the inkjet channel and is able to catch the essentials of the observations.

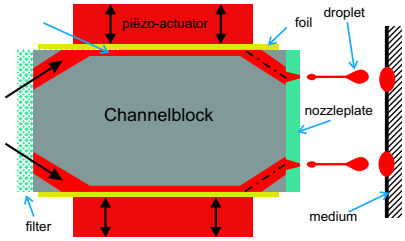

Figure 1: Cross section through the printer head with two ink channels and the piezo-actuator which acoustically drives out the molten ink. The nozzle plate determines the width of the nozzles. On the right hand side the drop formation is sketched.

*Faculty of Science and Technology, University of Twente, Enschede, The Netherlands.
†Océ Technologies B.V., Venlo, The Netherlands.

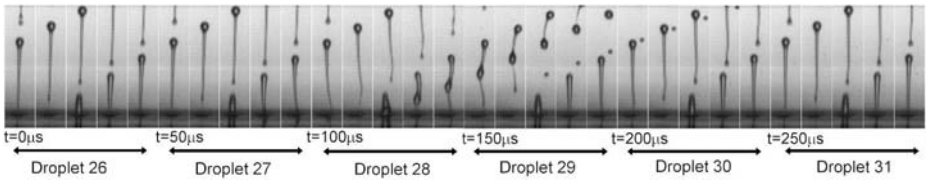

Figure 2: Droplet formation recorded at 100 kfps showing the disturbance which is connected with the entrainment of an air bubble.

Universality in microfluidic phenomena inside microchannels with arbitrarily shaped cross-sections

H. Bruus*, N. A. Mortensen*, F. Okkels* and L. H. Olesen*

The rapid development in the field of lab-on-a-chip systems during the past decade has put emphasis on laminar flow in microfabricated channels. Depending on the fabrication technique in use, the microchannel cross-sections come in a variety of shapes.

We present a theoretical study of three microfluidic phenomena in straight microchannels with arbitrarily shaped cross-sections: edge source diffusion[1], on-set of Hagen–Poiseuille flow[2], and electro-osmosis[3]. Using eigenfunction expansions and a Hilbert space formulation, we demonstrate the existence of universal, i.e. shape-independent, features in all three cases.

For edge-source diffusion, we consider a concentration field $c(\mathbf{r},t)$, which initially is zero inside the microchannel, and always kept at the value c_0 at the walls. Solutions of the diffusion equation $D\nabla^2 c = \partial_t c$ is written as the eigenfunction expansion $c(\mathbf{r},t)/c_0 = 1 - \sum_n f_n \phi_n(\mathbf{r}) \exp(-\alpha_n t/\tau)$, which upon substitution into the diffusion equation yields a Helmholtz eigenvalue problem for ϕ_n and α_n of the form $-\nabla^2\phi_n(\mathbf{r}) = \frac{4}{\pi}(\mathcal{P}/\mathcal{A})^2\alpha_n\phi_n(\mathbf{r})$. Here $\mathcal{A}$ and $\mathcal{P}$ is the area and perimeter of the channel cross-section, respectively, and the time-scale is $\tau = (\mathcal{A}/\mathcal{P})^2\,\pi/(4D)$. Based on this result we study the integrated concentration and find $N(t)/N_0 = 1 - \sum_n \beta_n \exp(-\alpha_n t/\tau)$. For short times $t \ll \tau$ we obtain $N(t)/N_0 = \sqrt{t/\tau}$, while for long times $t \gg \tau$ the lowest eigenvalue dominate hence $N(t)/N_0 \approx 1 - \beta_1 \exp(-\alpha_1 t/\tau)$. Remarkably, for a wide range of different shapes the parameters α_1 and β_1 only vary a few percent. We find $\alpha_1 \approx 1.1$ and $\beta_1 \approx 0.66$ and conclude that edge-source diffusion is universal in the sense that essentially all shape dependence is captured by the rescaling of time using the time-scale τ.

A similar analysis is carried out for the onset of Hagen–Poiseuille flow by abruptly imposing a pressure difference on a liquid initially at rest inside a microchannel. Here the governing equation is the Navier–Stokes equation, i.e., a diffusion equation for momentum density, where the diffusion constant is the kinematic viscosity ν. The flow rate, denoted $Q(t)$, is found to have the form $Q(t)/Q(\infty) \approx 1 - \exp(-\alpha_1 t/\tau)$, where the time-scale now is given by the kinematic viscosity as $\tau = (\mathcal{A}/\mathcal{P})^2/\nu$.

Finally, we analyze the problem of a microfluidic channel with a combined pressure driven and electro-osmosis driven flow in steady state. The flow rate Q and the electric current I are related to the applied pressure drop Δp and voltage drop ΔV through the 2×2 conductance matrix G as $(Q, I) = G\cdot(\Delta p, \Delta V)$. Applying the eigenfunction expansion leads to expressions for G as a function of the eigenvalues α_n and the effective areas $\mathcal{A}_n$ occupied by the eigenfunctions. One example is the off-diagonal elements in the Debye–Hückel approximation, $G_{12} = G_{21} \approx -(\epsilon\zeta\mathcal{A}_1/\eta L)/(1+\alpha_1\lambda_D^2)$, which shows the same shape independence as in the previous examples.

*Dept. Micro and Nanotechnology, Technical University of Denmark, DK-2800 Lyngby, Denmark.

[1] N.A. Mortensen, F. Okkels and H. Bruus, *Phys. Rev. E* **73**, in press (2006) [cond-mat/0510627].

[2] N.A. Mortensen and H. Bruus, *http://arxiv.org/abs/physics/0511056* (2005).

[3] N.A. Mortensen, L.H. Olesen and H. Bruus, *http://arxiv.org/abs/physics/0511183* (2005).

Water behavior in fluidic systems described using the water potential

J.C.T.Eijkel[a], A. van den Berg[a]

Micro- and nanofluidic systems have become very popular for (bio)chemical analysis, chemical synthesis and increasingly for studies of the living cell. Very often aqueous solutions are used in these systems, and pumped around by e.g. pressure-driven flow and electroosmotic flow. In the modeling of these systems the boundaries of the aqueous solution to the walls and to the atmosphere are often considered to be impermeable, i.e. no transport takes place through them. Interfacial forces are often neglected as well. In this contribution we will show that many interesting phenomena take place because the boundaries are permeable, and also because the interfacial forces are not negligible. Examples will be shown of evaporation-driven flow in microfluidic chips[1], of capillary condensation in nanochannels (see figure 1)[2], of osmosis and pervaporation through the walls of polyimide nanochannels[3], of pumping and strongly accelerated drying by capillary forces[4] and of capillarity-induced negative hydrostatic pressures[5].

Researchers in the soil science and in plant science have been investigating these phenomena for more than a century, for example to explain the ascent of sap in trees. As a unifying concept to understand why water moves from the soil to the atmosphere, thereby sometimes passing through the tree on its way, they employed the water potential, which is the chemical potential of water per unit volume (J/m^3 or Pa).[2] In this contribution we will apply this concept to the movement of water in micro- and nanofluidic systems, which will enable us to calculate the driving force for water transport in every case, which will be the gradient of the chemical potential. The kinetics of water movement will be different in every case, and will not be treated in detail.

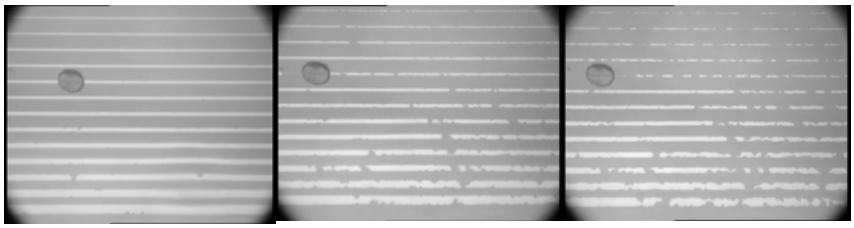

Figure 1 Capillary condensation in an array of 75 nm high Pyrex nanochannels placed in an atmosphere of RH = 95%. Photomicrographs taken at t = 9, 47 and 68 minutes.

---

[a] BIOS/Lab-on-a-Chip group, MESA+ Institute, Twente University, 7500 AE Enschede, Netherlands

[1] Goedecke, Eijkel and Manz, *Lab Chip*, **2** 219 (2002)
[2] Eijkel and van den Berg, *Lab Chip,* **5** 1202 (2005)
[3] Eijkel, Bomer and van den Berg, *Appl. Phys. Lett.* **87**, 114103 (2005)
[4] Eijkel, Dan, Reemeijer, Hermes, Bomer and van den Berg, *Phys.Rev.Lett.*, in press
[5] Tas, Mela, Kramer, Berenschot and van den Berg, *Nano Lett.* **3**, 1537 (2003)

Reaction-diffusion dynamics in a microchannel

J. B. Salmon*, A. Ajdari†, P. Tabeling ‡
Sandrine Charier, Damien Alcor, Ludovic Jullien §
Laurent Servant¶

In the macroworld, chemical reactors usually operate in three dimensional turbulent regimes. Investigating such systems requires the local measurements of the concentrations of the reactants, which is an extremely difficult task. More generally, the coupling between flow and chemical reactions lacks of experimental input at the moment, and this is unfortunate, owing to the considerable importance for chemical industry. We show here that microfluidics allows to improve the situation, by offering the possibility to analyze, on an experimental basis, fundamental chemical diffusion phenomena, under an unprecedented control level. The physical reason is that, by miniaturizing, the laminar nature of the flow is fully guaranteed, whatever the liquid of interest we may use in the experiment.

This paper focuses on a theoretical model used to extract rate constants of chemical reactions down to the millisecond time scale from the observation of reaction-diffusion processes in a microchannel [1]. We validate this theoretical approach by examining an appropriate model reaction in a Y-shaped microchannel. A proton exchange reaction using a fluorescent pH indicator (a coumarin) was chosen to evaluate this theoretical model. The measured rate constant is in excellent agreement with the one obtained from nuclear magnetic resonance relaxation experiments.

In the present work, we also use Raman confocal microscopy to address these microscale phenomena. Raman imaging is a non-intrusive technique that gives the local concentrations of various chemical species in a micrometer-size confocal volume (1-5 μm^3). Thus, Raman microscopy is a powerful tool as compared to classical fluorescence techniques for the study of reaction-diffusion dynamics. We present here a situation commonly encountered in microfluidics: the interdiffusion of two pure liquids [2]. Using models that take into account the difference in viscosities, we were then able to estimate the interdiffusion coefficients during these reaction-diffusion processes.

*LOF, CNRS-Rhodia, 178 av. Schweitzer, 33608 Pessac, France
†PCT, ESPCI, 10 rue Vauquelin 75005 Paris, France
‡Microfluidique, Mems et Nanostructures, ESPCI, 10 rue Vauquelin 75005 Paris, France
§Département de Chimie, École Normale Supérieure, 24 rue Lhomond, 75231 Paris Cedex, France
¶LPCM, Université Bordeaux I, 351 cours de la libération, 33405 Talence cedex, France
[1] Salmon *et al.*, *Anal. Chem.* **77**, 3417 (2005)
[2] Salmon *et al.*, *Appl. Phys. Lett.* **86**, 094106 (2005)

Mini-symposium

Vehicle aerodynamics

Introduction to vehicle aerodynamics: achievements and open issues

G. Buresti[a]

The role of aerodynamics in the design of ground vehicles is analysed, pointing out its evolution, the main established results that were obtained, and the several aspects that still need significant research efforts.

The importance of aerodynamics for the performance (and specially for the maximum attainable velocity) of motor vehicles has been realized since the early years of the 20th century, when efforts were made to reduce aerodynamic drag, using mainly the knowledge deriving from the aeronautical field. However, it was only after the '70s that the growing interest in fuel consumption reduction, and the development of "ad hoc" experimental facilities and investigations, produced a significant and sound progress. For instance, general rules for the design both of the global shape and of the geometrical details of motor vehicles have been established, and drag coefficients of the order of 0.30 or less have now become a standard for family cars.

Moreover, and perhaps more significantly, the importance of aerodynamic research for the improvement of other design aspects has progressively been recognized by the automotive industry. Examples are the management of inner flows (for both the cooling and the air-conditioning systems), and the achievement of satisfactory (and safe) handling qualities, specially for high-performance vehicles. Progress in this field has also been significantly promoted by the development of computational fluid dynamics (CFD) and by the rapid increase in computer power. Indeed, numerical codes are increasingly being used in the preliminary and development stages of the design, as an invaluable tool for reducing the extent of the (still necessary) experimental activities.

Nonetheless, the number of issues in which progress is still needed is also remarkable. Indeed, all ground vehicles are (more or less) bluff bodies, and much is still left to be done to achieve a thorough understanding and control of their aerodynamic features. Open problems are, for instance, the prediction of base drag and, generally, of separated flow features, the assessment of the different types of interference effects, the evaluation of the aerodynamic loads in unsteady conditions, the characterization of the aeroacoustic qualities of a vehicle. Furthermore, significant developments should still be pursued as regards CFD codes, in order to improve their predictive performance and their efficiency, and to possibly allow their introduction in optimization routines. Finally, in order to gain a higher understanding of the potential and of the limits of the various available design procedures, a crucial point still deserving attention is the analysis of the correlation between CFD outputs, wind tunnel data and the results of appropriate road tests.

[a] Dept. of Aerospace Engineering, University of Pisa, V. G. Caruso, 56122 Pisa, Italy.

Flow control in an adverse pressure gradient boundary layer

O. Lögdberg*†

Control of separated flows are of interest in many applications. For example on airplane wings, on cars and trucks and in various internal flows. A common and efficient method to control separation is to introduce longitudinal vortices that transport high momentum flow from the free stream towards the surface. The vortices can be produced either by active or passive devices.

In the present work an array of passive vane type vortex generators (VGs) were applied to produce counter rotating vortices inside the turbulent boundary layer. The experiments were conducted in the set-up shown in figure 1(a). In this wind tunnel the pressure gradient is adjustable by changing the suction rate through the test section ceiling. The flow field is studied by means of PIV.

The three objectives in this work are to investigate the general flow field at different VG/pressure gradient configurations, study how the level of circulation (Γ) necessary to avoid separation depend on the pressure gradient and examine if the effectiveness of the control depend on how far upstream the circulation is generated. An example of the results is shown in figure 1(b), where the shape factor (H_{12}) is plotted against the circulation at three different pressure gradients. The circulation per unit length in the spanwise direction is estimated by $\Gamma = 2hU/D$, where h is the height of the VG, U is the velocity at $y = h$ and D is the distance between the VG pairs.

The circulation is varied by changing the VG size and its position in x. When H_{12} is larger than 3.5–4 the flow was found to be separated. A prominent feature is that the circulation needed to keep the flow attached seem to be constant, regardless of pressure gradient.

*KTH Mechanics, SE-100 44 Stockholm, Sweden.
†Scania CV AB, SE-151 87 Södertälje, Sweden.

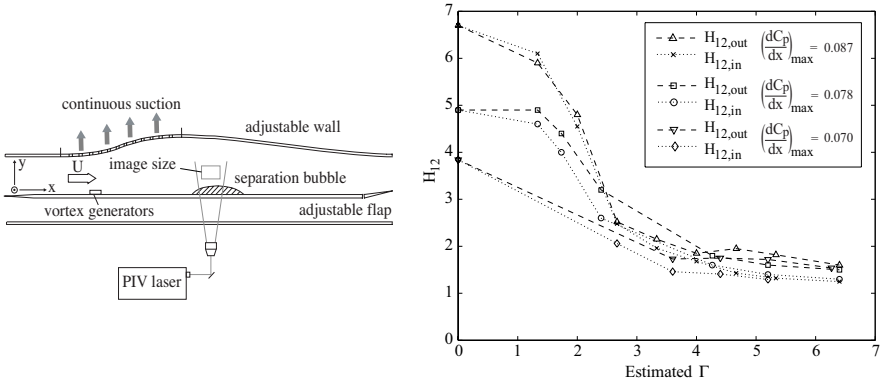

Figure 1: (a) Experimental set-up. (b) The shape factor at the position of maximum separation bubble height is shown for different Γ-values.

Characterization of the flow induced by high amplitude clearance pulsed micro-jets.

F. Harambat[*], J. J. Lasserre [*], J. F. Beaudoin [*] and C. Edouard[†]

With the aim of reducing drag, control of flow separation constitutes a fundamental stake for aerodynamics engineers. Separation is generally induced by adverse pressure gradients within the boundary layer, or by geometrical singularities such as sharp edges on the solid wall. In order to delay separation, a well tried technique is to inject momentum into the near wall flow zones. These two last decades, it was shown that a periodic excitation could bring the same performances as steady blowing, with a required momentum addition weaker of two orders of magnitude [1]. In this context, the recent improvement of micro-actuators technology let foresee important advances in active control of boundary layer detachment [2]. In the present study, we are interested in the performances of a new rectangular slots MEMS type, involving high amplitude clearances. Periodic pulsed flow is experimentally characterized and compared to the continuous blowing configuration. Both time-resolved PIV and hot wire anemometry techniques are employed, giving access to the spatial and temporal flow dynamics, as well in the very close slots vicinity, as within a larger surrounding field of order $10 * 10cm^2$. For an excitation frequency range varying from 0 to 90Hz, spectral analysis enables the measurement of the streamwise oscillations damping. Velocity profiles are measured, and momentum, mass and kinetic energy repartition investigated. Typically, with a 90Hz oscillating blowing and an inlet pressure as low as 3 mBar, mean velocities up to 25m/s are reached. The periodic blowing induces an addition of momentum and mass mean fluxes in the direction normal to the slots plane.

[*]P.S.A. Peugeot Citröen, Route de Gisy, 78943 Vélizy Villacoublay Cedex, France.
[†]Flowdit, Temis Innovation - Unité 17, 18 rue A. Savary, 25000 Besançon, France.
[1]Greenblatt and Wygnanski, *Prog. Aerospace Sci.* **36**, 487 (2000).
[2]Ho and Tai, *J. Fluids Eng.* **118**, 437 (1996).

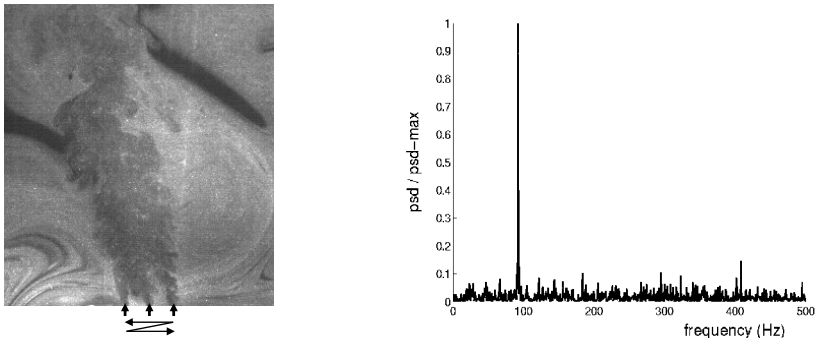

Figure 1: On the left: 3 slots MEMS flow. On the right: normalised power spectral density at 1.4 cm above the middle slot (excitation at 90 Hz).

Closed loop control experiments on a simplified car model using vortex generators and wall pressure measurements

J. F. Beaudoin*, O. Cadot†, J. L. Aider‡and J. E. Wesfreid‡

A control device is generally designed to operate a system in a desired manner. In case of automotive flows one often aims at reducing the drag force by creating small disturbances into the boundary layer. We choose to study the flow around a modified Ahmed body with a curved rear part ($Re = 2.10^6$) and first propose to use a line of vortex generators (fig. 1) that are shown to trigger separation on the one hand, but strongly reduce the tip vortices intensity on the other hand, so that the global effect on the drag is favorable. Next by varying the angle of the VG we observe that the drag reduction is minimum for an optimal value of α. As this optimum value is shown to be Reynolds dependant we use an extremum control strategy[1] to make our system able to identify and reach its optimal set point in real time, and to fit to mean flow velocity modifications. In this set of feedback control experiments, the angle of the VG is a slowly variable function of time that is adjusted thanks to a wall pressure measurement located in the recirculation part of the rear of the model. The feedback law is built using the sinusoidal perturbations method[1]. It consists in a synchronous detection of the response measured in the pressure signal to a modulation of the angle of the VG. It is finally demonstrated that the closed-loop system is robust and reacts successfully to unpredictable changes in the external flow conditions.

*PSA Peugeot-Citroën, Department of Research and Innovation, 2 route de Gisy, 78943 Vélizy-Villacoublay, France.
†Unité de Mécanique, ENSTA, Chemin de la Hunière, Palaiseau, France.
‡PMMH UMR 7636-CNRS-ESPCI, 10 rue Vauquelin, 75231 Paris Cedex 5, France.
[1]Beaudoin et al., *J. Fluids Struc.*, Accepted (2005).

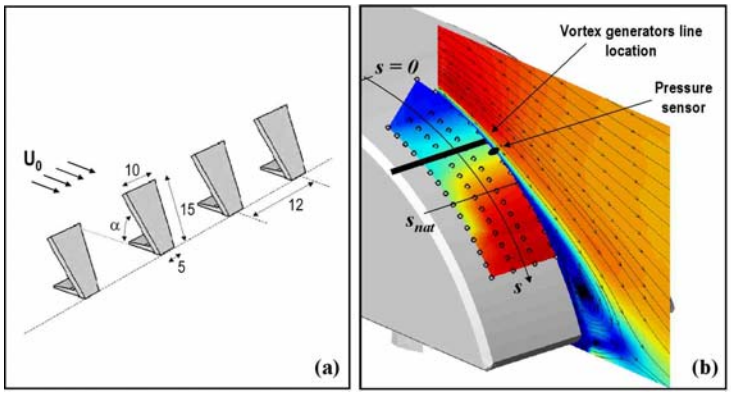

Figure 1: (a) Vortex generators line dimensions (in mm). (b) Wall pressure distribution and mean flow in the symmetry plane on the rear of the model in the uncontrolled case. The arrows indicate the location of the VG line and pressure sensor.

On the role of coherent structures visualization in the numerical analysis of bluff-bodies aerodynamics

R. Rossi*, L. Barbone*, L. Gattei*

Nowadays, the increasing availability of computational resources allows the analysis of the flow field around bluff-bodies of growing complexity. These flows are normally made up of strong separated regions, recirculation zones and turbulent structures of different lengthscales. The development of efficient tools for coherent structures (CS) identification is a key-feature both for results understanding and to highlight strategies for computational models improvement. In this research five different methods have been considered and investigated: static pressure minimum, vorticity magnitude, total pressure drop, second invariant method, Jeong and Hussain method. The Ahmed body has been choosen as a reference bluff body, since it generates different wake structures simply by changing the slant angle of the afterbody without further modifications of the computational model. In figure 1 (a) and (b) the results[1] show that even if the turbulent structures are deeply characterized by strong changes in the flow variables, namely pressure, flow-kinematics based methods allows a better investigation of the relevant features of the flowfield to be performed.

Furthermore, the turbulent structures identificated by means of flow-kinematics based methodologies can be useful to the development of new grid-refinement strategies[2]. Numerical experiments performed on the Ahmed body show that is possible to obtain reliable results in terms of drag prediction, reducing at the same time the total number of cells of the adapted model.

Finally, the identification of coherent structures can be also useful to understand the mechanisms by which the aerodynamics coefficients are influenced by appendages. To further investigate the flow-kinematics based methods, a nolder-like surface placed at the end of the slant plane is considered and investigated.

*Laboratorio di Termofluidodinamica Computazionale, Università di Bologna, Via Fontanelle 40, 47100 Forlì, Italy

[1] L. Barbone, L. Gattei, R. Rossi, *Proceedings of the 2nd European Automotive CFD Conference*, Frankfurt, Germany, (2005).

[2] R. Rossi, L. Barbone, L. Gattei, *Invited talk at the Italian Fluent User Group Meeting*, Milano, Italy, (2005).

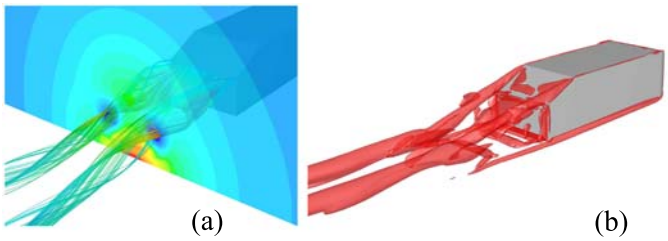

Figure 1: (a) Static pressure field within and around the vortex core. (b) Coherent turbulent structures around the 25° slant angle configuration.

Flow structures and related global forces for a 3D bluff-body in cross-wind

M. Gohlke*†, J.F. Beaudoin*, M. Amielh†and F. Anselmet†

Under the influence of cross-wind, cars tend to loose their driving-stability, even more so as the passenger cab tends to be bigger. This leads to a discomfort and higher concentration of the driver, and consequently to a higher accident risk. Following other researches, i.e. by Howell[1], we try to understand the topology of the flow and shed some light on the interaction of the flow structures on the forces and moments of a car. In a first step, we work on a simplified car model, named "Willy", introduced by Chometon et al.[2]. We apply a commonly used basic cross-wind simulation, which is to turn the 1/5th scale model around its vertical axis at $Re = 2 \cdot 10^6$. Using several different measurement techniques, we have come closer to a global understanding of the flow around this body and we find that the force and momentum results are very similar to standard observations on real cars[3]. This seems to be the case although certain geometrical features are strongly simplified. We observe two counter rotating asymmetrical longitudinal vortices similar to those produced in flows over an ogive at incidence, as demonstrated in 1(a). Figure 1 (b) shows their footprint on the surface by means of static pressure measurements. We observe that the upper vortex becomes dominant with a growing angle of attack. Furthermore, velocity fluctuations in the wake are getting stronger, but are basically limited to the wake.
Our aim is to understand the flow around "Willy" and its impact on forces and moments depending on the angle of attack, to get a better comprehension of the influence of side-wind on cars. In this respect we intend to couple experiments with numerical analyses.

*PSA Peugeot-Citroën, Department of Research and Innovation, Vélizy-Villacoublay, France.
†IRPHE, UMR CNRS 6594, Technopôle de Château-Gombert, Marseille, France.
[1]Howel, *J. Wind. Eng. Ind. Aero.* **139**, 60 (1996).
[2]Chometon et al., *SAE International*, 2005-01-0604, (2005)
[3]Hucho, *SAE International*, 1998

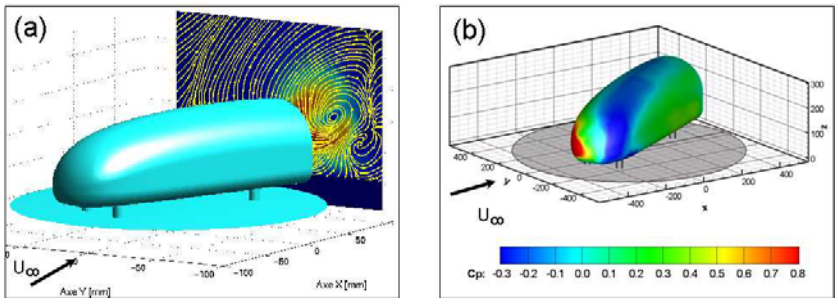

Figure 1: (a)PIV-Measurements in a vertical plane $x/L = 0.3$ (x=constant), colorplot shows U/U_{inf}, (b) Pressure measurements on the body surface: the model is turned to a -20° (a) and +20° (b) angle, airspeed is $U_{inf} = 40m/s$ and the model is $L = 0.857m$ long.

Computational Aerodynamics of Vehicle Passing

A. Filippone*, J. Clarke†

Overtaking on highways occurs at increasingly higher speeds and reduced vehicle separations. The need to improve vehicle efficiency has engendered a trend towards low drag shapes. This often produces an inherent reduction in directional stability. In addition, use of modern materials is reducing typical vehicle masses and increasing sensitivity to aerodynamic inputs.

Thus, it is necessary to acquire a thorough understanding of the aerodynamic phenomena encountered in overtaking. This may yield severe risks, particularly in adverse weather conditions such as crosswinds and gusts, black ice and surface water, reduced visibility from precipitation, glare etc., as well as on poor road surfaces with hills and strong camber, uneven surfaces and oil and loose material.

To date, a thorough analysis of the overtaking process has not been performed. The most recent works on the subject are those by Gillieron & Noger[1], Noger & Szechenyi[2] and Szechenyi[3]. Our aim is to begin to develop a computational simulation of these experiments and thus better understand the flow physics producing the aerodynamic forces on the bodies under test. We acknowledge that similar work has been performed on this subject in the past by Okumura and Kuriyama[4]. However, this is a brief examination focusing on a specific case rather than the effects of varying parameters of lateral spacing and relative velocity which are intuitively of great influence.

The present study focuses on two-dimensional overtaking as a preliminary means of investigating an appropriate simulation strategy. Thus we must make comparisons with the pseudo-2D case of interference between long, slender cylinders of rectangular cross section. A wealth of data is available on interference between square section cylinders. However this almost always focuses on tandem and parallel configurations.

The main thrust of this study is to determine a suitable modelling strategy and obtain some preliminary results for discussion and comparison with experimental data. High drag at the nose passing situation does not seem to have been formally identified elsewhere. The 'squeeze and squirt' effect and associated flow stagnation and separation yield high drag, high side force and high yawing moment at this point. These increase in magnitude with increasing relative velocity and/or decreasing lateral separation.

The 'push-pull' side force seen in 3D tests is seen, although the push is consistently at nose passing and the pull in our case occurs after the parallel configuration. This is in stark contrast to the 3D case where the timings appear highly dependent on relative velocity. In our case, clear flow stagnation and spearation behaviour dominates and thus the effects are largely independent of relative velocity and lateral separation.

*The University of Manchester, School of MACE, Manchester M60 1QD (corresponding author). E-mail: a.filippone@manchester.ac.uk

†The University of Manchester, School of MACE, Manchester M60 1QD.

[1]Gillieron. J. Soc. Auto. Eng. (2004)

[2]Noger and Széchényi. Flow Induced Vibration. Ecole Polytechnique, Paris (2004)

[3]Szechenyi. In *Progress in Vehicle Aerodynamics III*, Wiedeman & Hucho eds. (2004)

[4]Okumura and Kuriyama. J. Soc. Auto. Eng. (1997)

Some remarks on cooling flows

Lennart Löfdahl[1] and Lasse Christoffersen[1]

Of primary importance for the drag coefficient of a road vehicle is its exterior form, i.e. the styling of the body, air intakes, under body and wheel houses. During the last decade much work has been devoted to the shape of the upper body, and currently the drag coefficient for a passenger car is typically in the range of 0.30-0.32. However, further reduction is possible through detailed consideration of the flow along the under body and in the wheel houses where a complex, drag generating and three-dimensional flow field is formed.

A key issue in this context is to optimize the so-called cooling flow which significantly influences the major part of flow field along the under body. In this paper, a fundamental approach is given on how to design air intakes and outlets for cooling flows. Specific focus is put on cooling air out-lets located inside and in the vicinity of the front wheel houses on passenger cars. The influence from rotating front wheels is discussed briefly together with some methods used for the minimisation of drag generated by the out flowing hot air. This is followed by a discussion of some design trends of cooling air out-lets.

[1] Applied Mechanics, Chalmers University of Technology, 412 96 Göteborg, Sweden

Numerical Study of a Thermal Radiation Performance in Air-Cooling Eddy-Current-Brake

Masami IKEDA[a], Tetsuo SUZUKI[a], Takao TODA[b]

An eddy current brake (ECB retarder) is one of alternative brake system using the eddy-current which is powered by magnetic induction and Lorenz-force in the bullet train as like Shinkansen or Eurostar and so on. ECB based on non-contact action and it is capable of reducing the load on the main brake and other alternative brake system. Therefore, also in the large-truck and tour-bus field, the demand has rapidly increased in recent years.

Air-cooling ECB has simple structure compare to hydraulic-retarder though, however, the interval time tends to be shorter by the temperature rise and the improving of thermal radiation performance is commercially important.

This paper describes the parametric studies of thermal radiation characteristic features about an air-cooling eddy current brake via CFD which was coupled a thermal conduction and a heat radiation phenomenon. It has been made it clear about the contribution of number of cooling fin and fin's helix angle etc.

It is also mentioned about the possibility of quantitative prediction of local temperature distributions in some prototype drums, which have been redesigned in terms of thermal radiation characteristics.

[a] FUSO Engineering Corporation, 50, Nishikase, Nakahara, Kawasaki, Kanagawa, Japan.

[b] TBK Co., Ltd. 4-21-1, Minaminaruse, Machida, Tokyo, Japan.

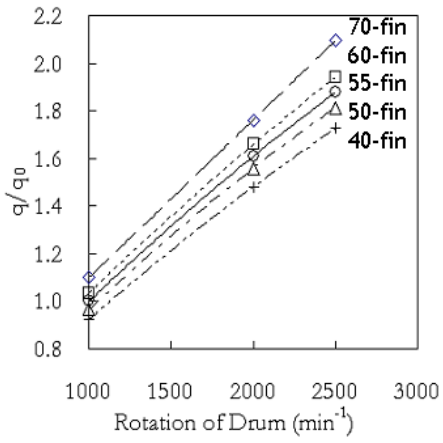

Figure1: Thermal radiation characteristic

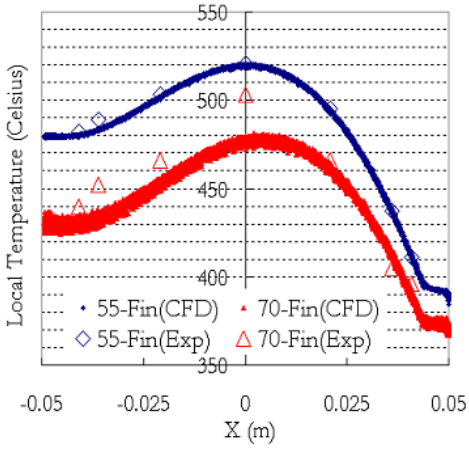

Figure2: Predicting temperature CFD vs. Experiment

Introduction to the design methodology of Ducati high performance motorcycles coolant systems

A. Tarroni[a], S. Di Piazza[a], R. Rossi[b] and D. Nanni[b]

Ducati Motor Holding S.p.A., working in strict collaboration with Laboratorio di Termofluidodinamica Computazionale of the University of Bologna (second faculty of Forlì), has developed an innovative design methodology of coolant systems for high performance motorcycles.

The proposed approach involves both numerical simulations and experimental tests. In details, the analysis of heat exchange processes developing within water and oil coolers is conducted using a numerical technique called "multi-scale"; it combines a very complex formulation finite volume analysis with a technically easier distributed parameters method. Coupling these two approaches allows for a minimization of computing resources and calculation time, preserving a very good accuracy in the description of physical phenomena.

The finite volume-based analysis, performed by means of the commercial package Fluent®, provides a detailed description of the flow field around the vehicle and in particular on both water and oil heat exchangers. The data obtained by means of this method, are then used as a boundary condition into the distributed parameters model, which performs heat exchangers thermal analysis. Air-side efficiency of both oil and water coolers has been investigated for several vehicle velocities, with and without the effect of rolling wheels and in different fairings configurations.

In order to validate the results of the above mentioned analysis, an experimental test campaign was conducted in a full scale wind tunnel. A fully instrumented motorcycle was tested in various configurations, according to the numerical simulations. The results of this activity was the calibration of numerical models and the demonstration that such an approach can be effectively used to estimate heat exchangers performances in an early design stage.

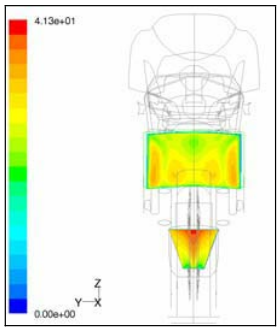

Figure 1: (a) Velocity distribution on heat exchangers. (b) Wind tunnel testing.

[a] Ducati Motor Holding S.p.A., Bologna, Italy.

[b] Laboratorio di Termofluidodinamica Computazionale, Università di Bologna, Forlì, Italy.

Aeroacoustic analysis of car ventilation systems

R. Arina*, F. Barone†, F. Carena† and P. Durello†

In this work we investigate the low speed aerodynamic noise generated in a simplified model of the outlet part of a car ventilation system. One of the major contributions to the aerodynamic sound generation in car ventilation systems is the outlet part, and it constitutes a significant component of interior noise in cars. The outlet part is usually equipped with a butterfly valve placed inside the outlet duct. This device generates high level noise when it is partly closed in order to control the flow rate. In previous experimental and theoretical works on the noise produced in a ventilation duct obstructed by a rigid obstacle, it has been derived that sound power is proportional to the cube of the pressure drop across the obstruction [1].

The aim of the present work is to compare experimental measurements with numerical computations of a simplified model: a test duct of length 1 m, with rectangular section of height H=50 mm and aspect ratio of 4. The butterfly valve is idealized by a flat plate, of length H and placed at 16H from the inlet. The angle of incidence with respect to the flow can be varied from 0° to 30°.

In figure 1(left) the experimental rig is shown. Air is supplied by a blower, located in a separate room, connected via a flexible pipe to the test duct. Piezoelectric pressure transducers are wall flush-mounted inside the duct and microphones are placed far enough to the exit to minimize any near-field effect. The numerical prediction method is a combination of large-eddy simulation (LES) technique and Lighthill theory. LES is well suited for computing the energy-containing eddies, known to be significant contributors to noise generation. The instantaneous turbulent flow field inside the duct and near the outlet is obtained by means of LES (figure 1-right). The radiated noise is then computed from an integral form of the Lighthill equation.

A comparison between the experimental and numerical results (such as sound directivity) will be presented for different mass flow rates for a butterfly valve incidence of 30°.

*DIASP-Politecnico di Torino, Torino, Italy.
†DENSO Thermal Systems, Poirino(Torino), Italy.

[1] Nelson and Morfey, *J. Sound Vibr.* **79(2)**, 263 (1981).

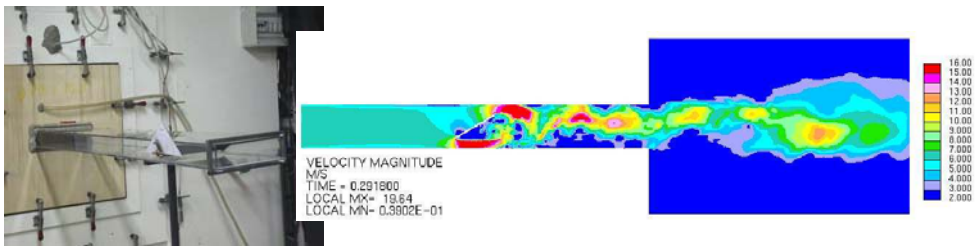

Figure 1: Experimental rig (left), LES computations: instantaneous velocity magnitude (right)

New Aerodynamics Solution in the Ferrari FXX

G. Lombardi[1], M. Maganzi[a], L. Caldirola[2] and F. Cannizzo[b]

The FXX is a development of the ENZO, that represent the state of the art in Ferrari's technology transfer from F1 to road cars: Ferrari offers to valuable clients a very limited series of laboratory-car, in order to test new high innovative contents. These contents are an anticipation of the solutions that will be used on the next generations of Ferrari GT. From the aerodynamic point of view the objective is to test the application of new ideas to be later used on GT cars. The project was developed in three phases: Conceptual, CFD, Wind Tunnel tests. A further key point is to verify the results between WT/CFD/Road, by means of the car instrumentation and the intensive use of high level telemetry and further data analysis. The main aerodynamics developments are the following:

Front Blowing: the ENZO uses flaps placed before the front wheels, moving down to reduce the load and maintain balanced the car. To increase the effect, a blow, spilling air from the radiator duct at high car speed, replaces the flaps. The resulting effect is higher than using the flap, coupled with a higher drag reduction.

Base Bleed: it is a well-known tool for the drag reduction, but, usually, the energy required to activate the base bleed is higher than the drag reduction effect. The idea is that on these cars the drag reduction is necessary only at high speed, in order to increase the maximum speed and/or the acceleration. It is than possible to use the cooling ducts, by using a by-pass at a given speed. The application of this concept leads to a C_x reduction of 0.045.

Front "winglet": the idea is to "clean" the flow in the high curvature front zone, introducing vertical wings to have a better flow direction. As a result, the vertical load increases, without balance modification and a very small increase in the drag.

The new ideas had a positive verification on the FXX car, as can be appreciated by analysing Fig. 1, where the important increase in the vertical load, without drag increase, appear evident. The new ideas are now available to be applied on the future Ferrari GT production.

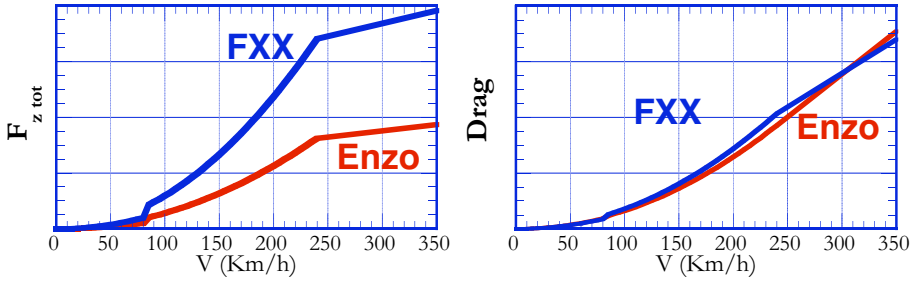

Fig. 1 – Aerodynamics forces on the Ferrari FXX

[1] Department of Aerospace Engineering of Pisa, Italy

[2] Ferrari S.p.A., Maranello (Mo), Italy.

Zero emission high-speed vehicle, Aerotrain

Y. Kohama[a], S. Kikuchi[b], T. Kato[a], F. Ohta[a], S. Yoshioka[a]

The future of the human race has become of serious concern year by year owing to our self produced waste. Our most serious environmental problems are the so called greenhouse effect (production of carbon dioxide) and the production of teratogenic constituents which cause human genetic damage. The Aero-Train project was proposed to answer the question of how to solve serious environmental problem. The concept of the new high speed ground transportation "Aero-Train" was created to establish a zero-emission vehicle. Figure 1 shows a conceptual sketch of the system. First, the vehicle's energy efficiency is minimized as much as possible by introducing the wing in ground effect. Second, low density and unsteady natural energy is cultivated at the place where the vehicle runs. It is necessary to collect several different natural energy resources, and store them in the state of Hydrogen. In such a way, one can store and use natural energy steadily. As shown in the conceptual sketch, this system has solar panels over the guideway and wind mills at the side of the guideway where wind energy is available. Figure 2 shows the energy flow of the system. The Aero-Train runs at 500km/h where the aerodynamic lifting force (wing in ground effect) becomes very large and the drag force becomes smaller compared to the lifting force. The levitated run experiment, see Figure 3, will be explained at the conference.

[a] Institute of Fluid Science, Tohoku University, Sendai, Japan
[b] School of Engineering, Gifu University, Gifu, Japan

Figure 1: Illustration of Aerotrain

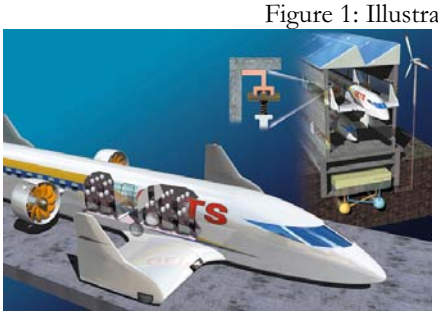

Figure 2: Energy system of Aerotrain

Figure 3: Levitated run experiment

Aerodynamics of high-speed trains at high Reynolds numbers

M. Schober*, S. Loose†, A. Orellano*

With increasing train speed aerodynamic issues are gaining importance. The most prominent topics that are investigated nowadays are aerodynamic drag, tunnel aerodynamics, aerodynamic noise and cross-wind stability. The importance of the last topic was highlighted in 2002 when a train overturned during a heavy storm in Austria.

The Reynolds number of a modern high speed train based on train width and a cruising speed of 350 km/h is approximately $\mathrm{Re} = 2 \times 10^7$ and exceeds the capabilities of most conventional wind tunnels. The uncertainty of extrapolating low Reynolds number aerodynamic data to the full scale values is therefore associated with a high risk, especially for the safety relevant issue of cross-wind stability.

The present investigation utilises the pressurised wind tunnel of the German Aerospace Center (DLR) in Göttingen to perform a detailed Reynolds number study with 1:87 scale models. During the experiments the windtunnel was pressurised up to 10^6 Pa at a temperatur of approximately 300 K. Balance measurements of the aerodynamic forces of the german ICE-2 driving trailer have been performed within the Reynolds-number range of $3 \times 10^5 \leq \mathrm{Re} \leq 6 \times 10^6$. The results are compared with data from conventional testing facilities. Figure 1 shows a photo of the wind tunnel setup with an ICE-2 driving trailer model mounted on an internal balance in the 0.6m × 0.6m test section.

From the extensive data obtained, figure 2 shows the distribution of the roll-moment coefficient $c_{mx} = M_x[0.5Al\rho v_a^2]^{-1}$, which is the most important aerodynamic parameter with respect to cross-wind stability. It can be seen, that there is a slight but distinct decrease of the roll moment at high yaw angles with increasing Reynolds number.

An additional flow-visualistaion study shown in figure 3 reveals, that the roll moment is mainly caused by a lee-ward vortex which is generating substantial under-pressure.

Figure 1: Experimental setup.

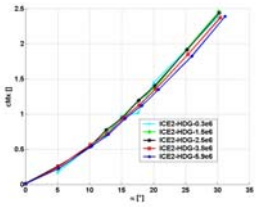

Figure 2: Roll-moment coefficient

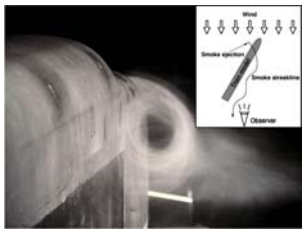

Figure 3: Smoke visualisation of lee-ward vortex

*Centre of Competence Aerodynamics & Thermodynamics, Bombardier Transportation, Am Rathenaupark, 16761 Hennigsdorf, Germany
†German Aerospace Center Bunsenstr. 10, 37073 Göttingen, Germany

Mini-symposium

Swirling flows

Laboratory experiments on Tornado-like vortices

D. Etling*

Tornados are the most violent and most impressive columnar vortices in the atmosphere. As strong tangential and axial wind velocities can be found in these vortices, they are also prominent examples of geophysical swirling flows. The physical origin of Tornados includes a complex process of interaction between large clouds and environmental shear, which is still not fully understood[1] . The properties of the Tornado-vortex itself can however be studied by means of laboratory experiments[1] using air or water as working fluid as has been demonstrated in various publications.

We have constructed a vortex tank suitable for creation of columnar vortices, which have some similarities with the funnel-like form of Tornados. The central, nearly axis-symmetric vortex is produced by a rapidly rotating centrifugal pump at the bottom of a cylindrical tank filled with water as working fluid.

In the case of a free surface, a hollow vortex core filled with air can be observed indicating very strong radial pressure gradients. Strong downdraft forces in the central core of the vortex are demonstrated by large floating bodies with positive buoyancy which are drained towards the bottom within the core. Measurements of tangential velocity profiles have also been obtained. The properties of the laboratory columnar vortices will be composed to observations for atmospheric Tornados.

*Institute of Meteorology and Climatology, University Hannover, 30419 Hannover, Germany

[1]Church et al., The Tornado,*Geophys. Monogr.*, **79**, AGU, pp637 (1990).

Theory of helical vortices

V. L. Okulov[a]

Recent progress in the theory of helical vortices is addressed. New ideas for studying the classical helical vortex problem were due to Hardin[1] who introduced the Biot-Savart law to describe a helical filament of infinitesimal thickness in the form of Kapteyn series from twisted products of modified cylindrical functions. Ricca[2] later employed numerical simulations of the Kapteyn series to determine the influence of the helix torsion on the self-induced motion of the helical vortices. Boersma & Wood[3] derived an integral representation of the Kapteyn series and from that made an asymptotic as well as numerical analyses of the velocity. In addition to this, Wood & Boersma[4] used the same technique to decribe the motion of a system of N helical vortices.

The representation via Kapteyn's series for a helical filament bounded on a circular cylinder has been considered by Okulov[5] who developed an efficient technique for the evolution of the principal parts of the series (see also Kuibin & Okulov[6]). Using the singularity-separation technique, the algebraic approximations for the velocity of self-induced motion of a single helical vortex and the total velocity field of an array consisting of N helical vortices was obtained[7,8] for the first time. Furher, a linear stability analysis of a regular N-gon of point vortices from equilibrium was generalized to be valid for an array of N helical vortices placed in free space[7] as well as for an array embedded in an axisymmetric helical vortex field[8]. The influence of finite-core thickness on the velocity field around a helical vortex tube was investigated by Fukumoto & Okulov[9].

The purpose of the present work is partly to review and summarize the last achievements in the theory of helical vortices and partly to report on some new important mathematical aspects. Exact solutions of the motion of multiple helical vortices are compared to the approximate formulas of Boersma & Wood[5] and Okulov[7] to estimate the domaine of applicability of both approximations. The influence of different types of assigned flows and the question of right or left-handed helical symmetry of the vortices on the stability properties are also discussed.

---

[a] Department of Mechanical Engineering, DTU, DK-2800 Lyngby, Denmark.

[1] Hardin, *Phys. Fluids* **25**, 1949 (1982).
[2] Ricca, *J. Fluid Mech.* **273**, 241 (1994).
[3] Boersma & Wood, *J. Fluid Mech.* **384**, 263 (1999).
[4] Wood & Boersma, *J. Fluid Mech.* **447**, 149 (2001).
[5] Okulov, *Russian J. Engineering Thermophys* **5**, 63 (1995).
[6] Kuibin & Okulov, *Phys. Fluids* **10**, 607 (1998)
[7] Okulov, *J. Fluid Mech.* **521**, 319 (2004).
[8] Okulov & Sørensen, *Stability of helical tip vortices in rotor far wake. Submitted to JFM*
[9] Fukumoto & Okulov, *Phys. Fluids* **17**, 107101 (2005).

Modelling of the flow structure in a hydroturbine draft tube through integral characteristics

P. A. Kuibin[a], V. L. Okulov[a,b] and I. M. Pylev[c]

Among the key problems arising at design and exploitation of hydroturbines one should remark the problems of flow instability and unsteadiness. For regimes of partial or over loading the flow is shown to be essentially three-dimensional and as a rule unsteady. The most often unsteadiness occurs due to precessing vortex rope. The questions of modelling such a vortex and determination of its parameters through integral characteristics are considered in the work.

One of the first approach to solve the problem on determination of the frequency of a precessing vortex rope through given flow rate Q and fluxes of vorticity F_ω, momentum F_m and moment of momentum F_{mm} was made by Fanelli[1]. Nevertheless His attempt failed because using wrong model of a vortex rope supposed by Hashimoto[2]. This work develops Fanelli's idea on the base of Theory of Helical Vortices[3].

Consider a model of vortex with a core in form of helical rope of circular cross-section[3] with radius ε. Let the helix radius is a, pitch $h = 2\pi l$, intensity of vortex is Γ, the helix is placed coaxially in a tube of radius R, and velocity at the tube axis is u_0. Suppose that the axial vorticity component is uniform inside the core and outside it the flow is potential. The problem now is to find ε, a, l, Γ and, consequently, the flow structure and pulsation characteristics through given flux parameters.

The vorticity flux equals intensity of vortex Γ. In supposition that the flow obeys helical symmetry there exists a relationship between axial and circumferential velocities[3]: $u_z + r u_\varphi / l = u_0$, which allows to determine l at given Q, F_m, F_{mm} and u_0: $l = F_{mm}/(u_0 Q - F_m)$. To determine a and ε make transition to dimensionless variables with scales of length R and velocity $\Gamma/(2\pi R)$ and keep the same symbols. Then with help of transformations $Q_0 = Q - \pi u_0$, $F_{m0} = F_m + \pi u_0^2 - 2 u_0 Q$ the problem is reduced to the solution of nonlinear system of two equation, i.e. search for a, ε at given Q_0, F_{m0}. Full analysis for domains of the solution existence is done at various parameters values. The system roots are found with the Method of Quickest Descent.

Thus, at known integral fluxes one can estimate parameters of vortex including frequency of its precession (on the base of formulae derived by Kuibin and Okulov[4]). The results obtained serve as a base for development of methods for prediction of efficiency of vortex devices and their control.

---

[a] Institute of Thermophysics SB RAS, 1 Lavrentyev ave., 630090, Novosibirsk, Russia.
[b] DTU, MEK, 403, Nils Koppels Allé, 2800, Lyngby, Denmark.
[c] Branch of Power Machines – JSC LMZ, 18 Sverdlovskaya nab., 195009, St.Petersburg, Russia.

[1] Fanelli, *J. Hydraulic Research* **27**, 769, (1989).
[2] Hashimoto, *Rep. Inst. High Speed Mech.* **23**(228), 61 (1971).
[3] Alekseenko et al., *J. Fluid Mech.* **382**, 195 (1999).
[4] Kuibin and Okulov, *Phys. Fluids* **10**(3), 607 (1998).

Effects of Swirl Number Magnitudes on the Accuracy of the Linear and Quadratic Reynolds Stress Transport Models

J. Ko*and S. Zahrai†

Swirling flows are present in many industrial applications and much effort had been devoted to the studying of these flows using turbulence models. It is well-known that k-ϵ and RNG k-ϵ models are only accurate for modelling swirling flow at low swirl numbers. Jakirlić *et al.*[1] showed that the Reynolds stress transport (RST) models are superior than the eddy-viscosity models in eight different geometries containing swirling flow. However, the performance of the RST model can also vary depending on the swirl magnitude of the flow examined.

It was reported that the deviatoric terms in the rapid pressure-strain term of the linear RST model disappears under background rotation[2], which would make this model unsuitable for modelling swirling flows. This observation is in agreement with the study by Montavon *et al.*[3] where the linear RST model failed to accurately predict the velocity profiles of the swirling flow in a hydrocyclone. However, these findings contradict the accurate tangential velocity profilescalculated with LRR RST model by Hoekstra *et al.*[4].

Discrepancies in reported data are likely to be related to the swirl number examined in each case. While the linear RST model is accurately in predicting the tangential velocity profiles at low swirl numbers, the quadratic RST model might be necessary when the swirl number exceeds a threshold range. Based on reported results in literature no conclusive judgement can be made regarding the strengths of the different RST models. The present work aims to shed light on this issue.

This study quantifies and discusses the swirl number-dependent accuracy of the different RST models. In particular, confined swirling flows, such as pipe swirling flows created by tangential inlets and hydrocyclone flows, will be studied in detail. The experimental studies by Chang & Dhir[5] and Bergström[6] will be used. These two studies contain experimental data with swirl numbers 2.67, 7.84 and 21, and will provide a rigourous examination of the strength of the linear and the quadratic RST models.

*Laboratoire de Modélisation en Mécanique, Paris VI, France
†FaxénLaboratoriet, KTH, Sweden

[1] Jakirlić *et al.*, AIAA Journal. **40**(10): 2002.
[2] Cambon *et. al*, Phys. Fluids A. **4**(4), 812-824: 1992.
[3] Montavon *et al.*, 5th Int. Conf. on Cyclone Technologies: Vortex Separation. 175-186: 2000.
[4] Hoekstra *et al.*, Chem. Eng. Sci. 54, 2055-2065:1999.
[5] Chang & Dhir, Int. J. of Heat and Fluid Flow. **15**(5), 346-356: 1994.
[6] Bergström, Licentiate Thesis, KTH: 2004.

On Three Dimensional Shear Layers

L. Taubert[a], P. Varghese[a], D. Knyazev[a] and I. Wygnanski[a]

The mixing layer generated two parallel streams separated by a splitter plate whose trailing edge was swept back at 60^0 to the flow, and a wake behind an infinitely yawed cylinder at the same angle of sweep were investigated experimentally using hot wire anemometry and Particle Image Velocimetry (PIV). A variety of perturbations were applied to the flow, some perturbations were periodic and spanned the entire test section some were local and momentary and some lasted until the flow regime changed (i.e. partial reattachment was observed). In the case of the cylinder there were two rows of slots from which the excitation emanated. They are located symmetrically at 110^0 from the leading edge of the cylinder that did not coincide with the front stagnation location whenever partial or asymmetrical actuation was used. The cylinder was 3" in diameter, it held 22 internal actuators and was mounted in a closed loop wind tunnel having a 2' x 3' cross sectional test area. A fence surrounded the cylinder at its upstream end, in order to avoid asymmetries resulting from the necklace vortex created by the interaction of the cylinder with the upstream boundary layers generated on the tunnel walls. Periodic peeling of vortices along the span of the cylinder was observed[1] inspite of the periodic excitation that was applied to the entire span of the cylinder. Surfaces of equal u'v' show it best as demonstrated in Figure 1.

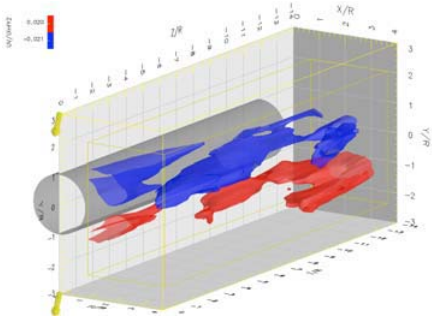

Figure 1: surfaces of constant u'v', measured during asymmetric excitation

The splitter plate separating two parallel streams of different velocities

The mixing layer generated by the merging of two steams having disparate velocities represents a somewhat simpler though similar flow problem. The trailing edge of the splitter plate causes an initial rollup of vortices that are inclined to both streams and therefore possess a component of velocity along the axis of their core. At first blush the mixing layer appears to develop as a planar mixing layer provided the distances are measured from the local spanwise location of the trailing edge however, there are marked differences resulting from the interaction associated with the rolled up vortices that originated on different sides of the notch in the splitter plate. In this case the notch avoids spurious wall effects. The results of these measurements will be discussed

[a] AME Department, The University of Arizona

[1] Thomson, K. D., and Morrison, D. F., *J Fluid Mech*. **50**: 751-783, (1971).

2D and 3D Flow past a rotating cylinder at moderate Reynolds numbers

R. Elakoury[a], M. Braza[a], G. Harran[a] and R. Perrin[a]

The study depends on Reynolds number (Re=UD/ν) and rotation rate (α) which is the ratio between rotation velocity (ω) and free stream velocity (dω/2U), where d is the cylinder diameter. The flow is studied by two and three dimensional direct numerical simulations, at low and moderate Reynolds numbers (up to 500) and for rotation rates up to 6. For low Reynolds numbers (less than 48, the flow remains steady for all rotation rates. For higher Reynolds numbers, for $\alpha < 2$, the flow is unsteady, similar to a vortex shedding, but assymmetric due to the rotation. For Re=200 for example, suppression of vortex shedding occurs for $2 < \alpha < 4.35$. At higher rotation rates, $4.35 < \alpha < 4.9$, a second kind of instability appears where only counter clockwise vortices are detached; the streamlines start to have an oval-like form and the fluid flow forces this structure to be more elongated until detachement. For higher rotation rates, the flow is steady again because the rotation effects keep the vortex structure near the wall and inhibit detachement. Detachement frequency is clearly lower in the second instability. 2D and 3D computations prove that the rotation has a stabilizing effect. The analysis of the organised modes under the rotation effect has been performed by the Proper Orthogonal Decomposition.

Figure 1 shows flow past a fixed cylinder at a Reynolds number Re=200, while flow around a rotating cylindre at Re=300 and α=0.5 is shown in figure 2.

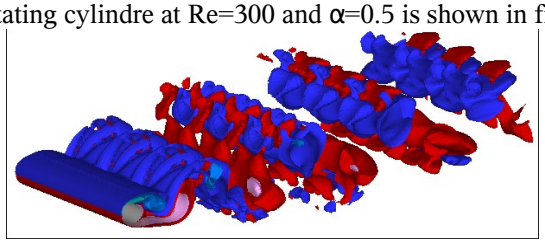

Figure 1: Re=200, α=0

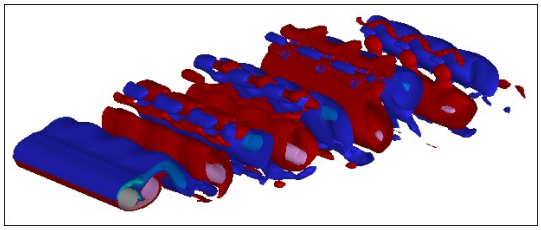

Figure 2: Re=300, α=0.5

[a]Institut de Mécanique des Fluides de Toulouse, allée Camille Soula, 31400, Toulouse, France.

Cellular vortex shedding in the wake of a tapered cylinder

V. D. Narasimhamurthy*, H. I. Andersson* and B. Pettersen†

Three-dimensional vortex shedding may occur in the wake of a circular cylinder for three fundamentally different reasons: i) the vortex dynamics in the wake may be intrinsically three-dimensional, ii) the oncoming flow may be non-uniform, and iii) the cylinder may itself be non-uniform. In the present paper we focus on the latter category, i.e. on the three-dimensionalisation induced by a spanwise variation of the cylinder diameter, as studied experimentally[1]. Vortex shedding in the wake behind a linearly tapered circular cylinder was considered and a pattern of discrete oblique shedding cells, which included both vortex dislocation and vortex splitting was observed. These non-linear vortex phenomena have been qualitatively reproduced in some recent computational studies[2,3] and will be further addressed herein.

In the present investigation we consider flow behind a *linearly* tapered cylinder with taper ratio $l/(d_2 - d_1) = 75{:}1$, where l is the length of the circular cylinder and d_2 and d_1 denote the diameter of its wide and narrow ends, respectively. The Reynolds number Re_2 based on d_2 and the uniform free-stream velocity U is 131, i.e. well below 190 at which the intrinsic 'mode A' instability is known to occur in otherwise two-dimensional configurations. This particular case corresponds to *Run22*[1] and *CaseB*[2]. However, the predicted variation of local Strouhal number versus local Reynolds number did not match the curve fit $St = 0.195 - 5.0/Re$ deduced from the laboratory experiments[1]. The objective of this *computational* study is to clarify the significant deviations between the simulations[2] and the experiments[1] and to provide an in-depth exploration of the topology of the near-wake. Preliminary results with $1.2\text{x}10^6$ grid points are shown in Figure 1, which clearly shows the vortex splitting along the span. Note that the pressure time trace on each side of the boundary of a shedding cell is 180^o out of phase, as a vortex splits.

*NTNU Energy and Process Engineering, 7491 Trondheim, Norway.
†NTNU Marine Technology, 7491 Trondheim, Norway.

[1]Piccirillo and Van Atta, *J. Fluid Mech.* **246**, 163 (1993).
[2]Vallès et al., *J. Fluids Struct.* **16**, 453 (2002).
[3]Parnaudeau et al., *Proc. TSFP4* 111 (2005).

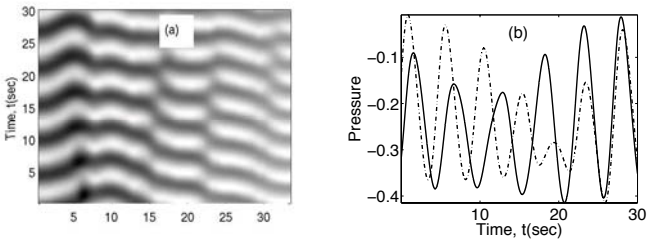

Figure 1: (a) Time evolution of the pressure along the span. (b) Pressure time trace on each side of the boundary of a shedding cell, as a vortex split occurs.

Effect of background rotation on the structure of sphere wake flow

A. Rudert & Ch. Brücker

An experimental study is performed to investigate the flow induced by a sphere moving along the axis of a rotating cylindrical container. Three-dimensional Scanning PIV is used to determine the temporal vorticity distribution in the wake of the sphere for different Reynolds- and Rossby numbers, see the experimental set-up shown in Fig. 1. Several solid bodies such as a sphere or a spherical cap were towed in vertical direction within a rotating cylinder from the bottom to the top. SPIV-measurements were taken in parallel cross-sections downstream of the body and processed to reconstruct the streamwise vorticity distribution in the wake. The objective of this study is to examine the effect of background rotation on the transition to unsteady vortex shedding in the sphere wake at at moderate Reynolds-numbers. Flow structures at Re=200 and 500 were obviously different. In the case of Re=500, periodic vortex shedding was observed. Due to the effect of background rotation, shedding is not preserved in a planar pattern as for Ω =0 but the wake evolves into a bispiral vortex structure showing a double helix-like structure. When the Rossby number is of order unity, the experimental observations showed, clearly, the existence of waves that were stationary relative to the body. To depict the swirling vortex shedding structures in the wake of the sphere, the corresponding patterns of three-dimensional vorticity iso-surface are shown in Fig. 2. Comparison were done with recent results of numerical simulation of sphere wake flow by Wang et al 2004 (Int. J. Numer. Meth. Fluids 2004; 44:905–925) which demonstrate a good qualitative agreement.

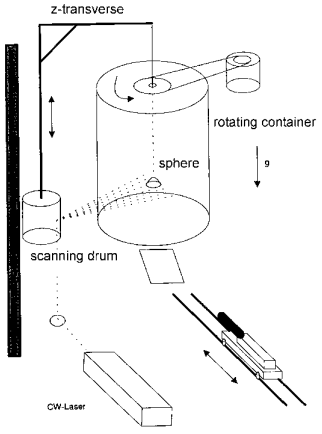

Fig. 1: Experimental set-up

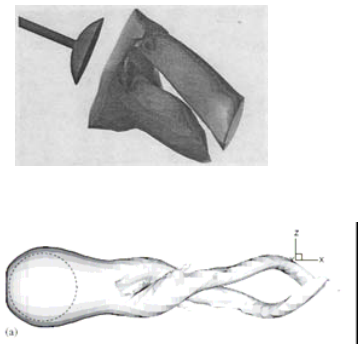

Fig. 2: Double-helical structure

[1] Chair of Fluidmechanics and Fluidmachinery, TU Freiberg, 09599 Freiberg, Germany.

DNS and Wavelet Analysis of a Turbulent Channel Flow with Streamwise Rotation

T. Weller*, K. Schneider†, M. Oberlack* and M. Farge‡

Modeling of rotating turbulent flows plays a major role in engineering applications. Intensive research has been dedicated to rotating channel flows in spanwise direction[1,2]. Investigations of Oberlack et al.[3] using symmetry theory showed that there is a new turbulent scaling law related to the turbulent channel flow rotating about the streamwise direction. The induction of a mean velocity in spanwise direction is the most obvious difference compared to the classical case.

A series of direct numerical simulations (DNS) has been conducted both for different rotation rates and different Reynolds numbers to examine these effects. The present work is divided into two parts.

In the first part the results of the DNS are discussed. The velocity profile in streamwise direction decreases invariably with increasing rotation numbers. The theoretically expected cross flow could be verified. In general the spanwise velocity profiles are skew-symmetric about the centerline. For small rotation rates up to Ro=5 the spanwise mean velocity profiles increase. At rotation number Ro=7 this effect appears to reverse[4]. Statistical evaluations have shown that all six components of the Reynolds stress tensor are non-zero. All of these mentioned effects could be observed for different Reynolds numbers.

The second part concerns coherent vortex extraction (CVE)[5] using orthogonal wavelet decomposition of the vorticity field. Figure 1 shows the isosufaces of a) the coherent part and b) the incoherent part of a 3D vorticity field at rotation rate Ro=10 and Reynolds number Re=180. We found out that few strong wavelet coefficients (3.6%) represent the coherent vortices of the flow (Fig. 1a)) while the remaining weak coefficients correspond to the incoherent background flow (Fig. 1b)).

*Technische Universität Darmstadt, D-64287 Darmstadt, Germany.
†MSNM-CNRS & CMI Universite de Provence, F-13453 Marseille, France.
‡Ecole Normale Supérieure, F-75231 Paris, France.

[1]Johnston et al., *J. Fluid Mech.* **56**, (1972).
[2]Lamballais and Métais, *Intern. J. of Heat and Fluid Flow* **27**, 3 (1996).
[3]Oberlack et al., *Center for Turbulence Research, Stanford University/NASA Ames*, (1998).
[4]Weller and Oberlack, *accepted for publication in Proc. of DLES6*, (2005).
[5]Farge et al., *Phys. Fluids* **15**, 10 (2003).

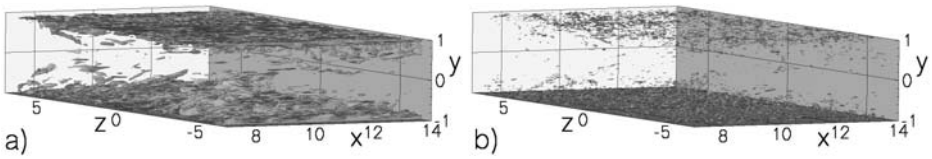

Figure 1: Isosurface of modulus of vorticity: a) 3.6% of the wavelet coefficients represent the coherent component and b) 96.4% the incoherent component.

Eddies induced between two rotating, coaxial cones

Chris Hills*, Oskar Hall†

The flow between rotating, coaxial cylinders is familiar to all students of fluid mechanics as is the rich variety of flow phenomena that can arise within this simple geometry. The accessibility of the Taylor-Couette problem to accurate experimental, numerical and theoretical investigation, has meant that studies of extensions of the classical geometry abound. The truncated two cone geometry has been previously studied experimentally (see for example[1,2]). However, the flow between two coaxial cones has largely been overlooked theoretically despite the numerous interesting phenomena introduced by this variation in geometry.

We study the flow between two coaxial, differentially rotating cones with coincident apices shown in figure 1. The rotation of the cones induces a meridional circulation making the basic flow for this geometry three-dimensional in contrast to Couette flow. This fact has considerable practical importance and the two cone geometry can be found in pumps used in the medical sciences. We are primarily concerned with low Reynolds number, slow flows induced by the rotation of one or both of the conical surfaces about their axes and the formation of viscous eddies.

The appearance of viscous eddies within slow flows is dependent not only upon the geometry but also upon their relative dominance over any background flow. Moffatt first discussed their importance in relation to the flow within a two-dimensional corner and more recently Shankar[3] extended their application to a single cone geometry. However, eddies can also occur in the cavity between two coaxial cones[4] when the internal angle does not exceed a critical value, α_c. Previously, Hewitt studied the slow flow between finite cones driven by the rotation of a spherical cap or lid, showing that toroidal eddies can occur and that the inclusion of an inner cone has a dramatic effect upon the critical angle α_c. Our study discusses the presence of eddies when the basic flow is driven by the rotation of the cones and contrasts our findings with those for the rotating lid. We find that eddies can occur and that interesting new features are introduced by the rotation of the cones. Numerical methods are used to visualise the asymptotic flows and analyse eigenvalue behaviour.

*School of Mathematical Sciences, DIT, Kevin Street, Dublin 8, Ireland.
†School of Engineering, Computer Science & Mathematics, University of Exeter, UK.

[1]Wimmer, *J. Fluid Mech.* **292**, 205 (1995).
[2]Noui-Mehidi et al., *Exp. Fluids* **30**, 84 (2001).
[3]Shankar, *J. Fluid Mech.* **539**, 113 (2005).
[4]Malhotra et al., *J. Fluid Mech.* **522**, 117 (2005).

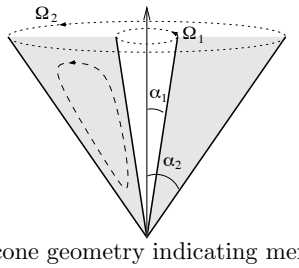

Figure 1: Coaxial cone geometry indicating meridional circulation.

Polygons on a Rotating Fluid Surface

Tomas Bohr[*], Pascal Hersen[*],
Thomas R. N. Jansson [†], Martin P. Haspang[†] and Kåre H. Jensen[†]

We report a novel and spectacular instability of a fluid surface in a rotating system. In a flow driven by rotating the bottom plate of a partially filled, stationary cylindrical container, the shape of the free surface can spontaneously break the axial symmetry and assume the form of a polygon rotating rigidly with a speed different from that of the plate. With water we have observed polygons with up to 6 corners (see (Fig. 1). It has been known for many years that such flows are prone to symmetry breaking, but apparently the polygonal surface shapes have never been observed. The creation of rotating internal waves in a similar setup was observed for much lower rotation rates, where the free surface remains essentially flat [1]. We speculate that the instability is caused by the strong azimuthal shear due to the stationary walls and that it is triggered by minute wobbling of the rotating plate. The slight asymmetry induces a tendency for mode-locking between the plate and the polygon, where the polygon rotates by one corner for each complete rotation of the plate.

[*]Physics Department, The Technical University of Denmark, 2800 Kgs. Lyngby
[†]The Niels Bohr Institute, Blegdamsvej 17, 2100 Copenhagen Ø
[1]J. M. Lopez et al. *J.* Fluid Mech., **502**, 99 (2004)

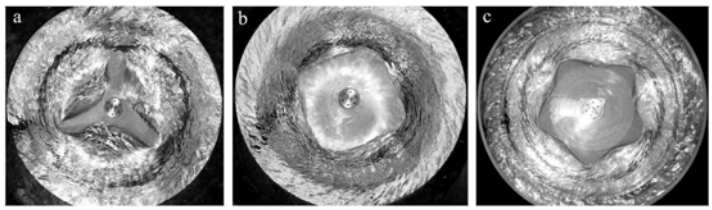

Figure 1: Typical examples of polygons in water, as seen from above: "Triangle" (a), "Square" (b), "Pentagon" (c). For more pictures and a video of the transition go to www.physics.dtu.dk/∼tbohr/RotatingPolygons.

Magnetic dipole induction by the spin-over mode of the elliptical instability in a rotating liquid metal sphere.

W. Herreman*, L. Lacaze*, M. Le Bars*, S. Le Dizès*, P. Le Gal*

The elliptical instability of rotating fluid flows is generated by the resonant interaction of inertial waves. In a slightly elliptically deformed sphere that rotates at a rate Ω, the most unstable linear mode is the spin-over mode, which is a solid body rotation of angular velocity Ω_{SO}, around an axis aligned with the maximum strain direction[1]. In geophysics, the elliptical instability may appear in the molten liquid cores of rotating planets, which are slightly deformed by tidal gravitational effects of close bodies. It may then participate to the general outer core dynamics and possibly to the geodynamo process. In this context, Kerswell and Malkus[2] showed that the puzzling magnetic field of the Jovian satellite Io may be induced by the elliptically unstable motions of its liquid core that deflect Jupiter magnetic field. Our magnetohydrodynamics experiment is a toy-experiment of this geophysical situation and demonstrates the possibility of the induction of a magnetic field by the flow motions created by the elliptical instability. The full analytical calculation of the magnetic dipole induced by the spin-over has been performed and is shown in figure 1. Finally, the exponential growth of the induced magnetic field in a rotating sphere filled with Galinstan liquid metal is measured for different rotating rates. Growth rates compare well with theoretical predictions in the limit of a vanishing Lorentz force.

*IRPHE, 49 rue F. Joliot-Curie, 13384, Marseille, France.

[1]Lacaze, Le Gal and Le Dizès, *J. Fluid Mech.*, **505**, 1-22 (2004).

[2]Kerswell and Malkus, *Geophys. Res. Lett.* **25**, 603-606 (1998).

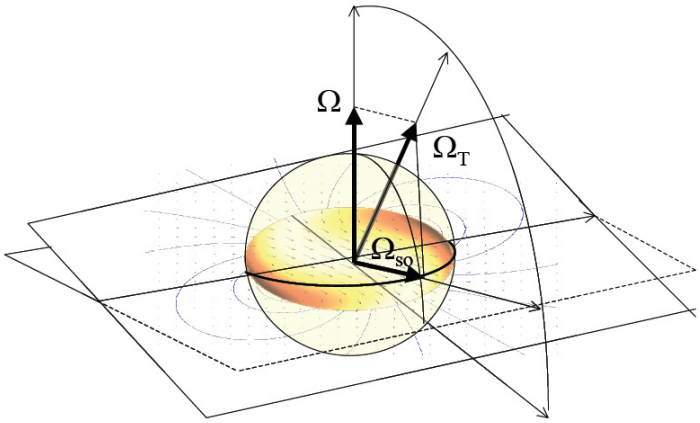

Figure 1: Calculation of the magnetic dipole induction by the elliptical instability in a rotating deformed sphere filled with liquid metal and imbedded in an axial (along Ω) external field. Joule dissipation inside the flow is also represented.

Influence of strong swirl on the stability of an annular flow

N. Bleier*, V. Vasanta Ram*

Subject of our paper falls under the heading of transition of the swirling flow in an annulus. We restrict our attention in the present study when swirl is generated by rotation of the inner cylinder alone. There are two competing transition mechanisms in this flow, viz. the Taylor mechanism and the Tollmien-Schlichting mechanism. Which one of these is effective depends upon a swirl parameter S, which is the ratio of the two characteristic velocities $U_{\mathrm{ref}\,\varphi} = \Omega_i R_i$ and $U_{\mathrm{ref}\,x} = \frac{(R_a - R_i)^2}{8\mu} \left|\frac{\mathrm{d}P_G}{\mathrm{d}x}\right|$ derivable from the angular velocity of the rotating cylinder Ω_i and the axial pressure gradient $\frac{\mathrm{d}P_G}{\mathrm{d}x}$ respectively. Strong swirl corresponds to $S \to \infty$.

Our aim is to gain insight into the nature of the flow in question subsequent to transition through studying the bifurcating solutions of the full (nonlinear) equations of motion for the disturbance to the basic flow which is the fully developed swirling flow in the annulus. The starting point for our study is the propagation characteristics of small-amplitude waves obeying the linearized equations for the disturbance.[1]

The dispersion relationship for this linearized problem may formally be written as

$$\mathcal{F}(\epsilon_R, Re, S, \lambda_x, n_\varphi, \omega) = 0$$

where $\epsilon_R = \frac{R_a - R_i}{R_a + R_i}$, $Re = \frac{U_{\mathrm{ref}\,x}\ (R_a - R_i)}{2\ \nu}$, $S = \frac{U_{\mathrm{ref}\,\varphi}}{U_{\mathrm{ref}\,x}}$ and λ_x is the disturbance wave number in the axial direction, n_φ the corresponding quantity in azimual direction which has to be an integer and ω the frequency.

We present a few sample results of our computations of the linear stability theory which were solved by MATLAB using the spectral collocation method. Figure 1 (a) shows the stability diagramm for $S = 10^5$. The critical Reynolds number for $\epsilon_R = 0.1$ is approx. 75 which corresponds to a Taylor number $Ta = Re^2 \epsilon_R = 563$ and the corresponding wave number λ_x is around 1.5. Figure 1 (b) shows the speed of neutrally stable wave at the critial Reynolds number for different parameter S.

At the time of submission of this abstract the nonlinear bifurcation solution of the problem is in progress. We plan to present results of this investigation at EFMC 6.[2]

*Ruhr-Universität Bochum, Lehrstuhl für Strömungsmechanik IB 6/43, Universitätsstraße 150, D-44780 Bochum, Germany

[1] Drazin, Reid, *Hydrodynamic stability*, Cambridge Univ. Pr., 1982

[2] Schmid, Henningson, *Stability and transition in shear flows*, Springer, 2001

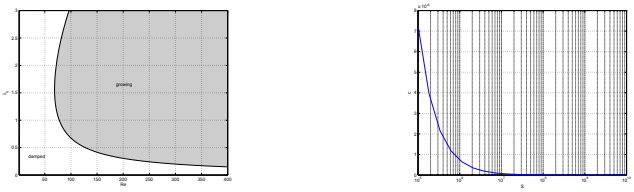

Figure 1: (a) Stability diagramm for $S = 10^5$ and $\epsilon_R = 0.1$
(b) Propagation speed of neutrally stable wave at critical Reynolds number

The structure of the critical layer of a swirling annular flow in transition

J. Hussong*, N. Bleier*, V. Vasanta Ram*

Subject of our paper falls under the heading of transition of the swirling flow in an annulus. Two transition mechanisms with some fundamental differences, which we call the Taylor and the Tollmien-Schlichting mechanisms, compete with each other in this flow. The salient difference referred to is the presence of a *critical layer* in the Tollmien-Schlichting mechanism in which viscous effects gain importance due to the disturbance wave propagating at the same local velocity as of the basic flow. In contrast, such a critical layer is absent in the Taylor mechanism. The focus of attention in our work is the modification swirl causes to the structure of this critical layer in annular flow.

Our basic flow is the fully developed flow with swirl in the annular gap between concentric cylinders, of which the outer cylinder may be rotated at an angular velocity Ω_a and the inner cylinder pulled axially at a translational velocity V_{wi}. The geometrical and flow parameters in our problem are, in a self-explanatory notation: the transverse curvature parameter $\epsilon_R = \frac{R_a - R_i}{R_a + R_i}$, the Reynolds number $Re = \frac{U_{\mathrm{ref}\,x}\ (R_a - R_i)}{2\ \nu}$ with $U_{\mathrm{ref}\,x} = \frac{(R_a - R_i)^2}{8\mu}\ \left|\frac{\mathrm{d}P_G}{\mathrm{d}x}\right|$, the swirl parameter $S_a = \frac{U_{\mathrm{ref}\,\varphi}}{U_{\mathrm{ref}\,x}}$ with $U_{\mathrm{ref}\,\varphi} = \Omega_a R_a$ and the translational wall velocity parameter $T_{wi} = \frac{V_{wi}}{U_{\mathrm{ref}\,x}}$.

We have approached the transition problem in this flow configuration by conducting a modal analysis of the dynamics of the propagation of disturbances in the basic flow in question, starting from small amplitude disturbances for which the governing equations may be linearised. The dispersion relationship for this linearized problem may formally be written as $\mathcal{F}(\epsilon_R, Re, S_a, T_{wi}, \lambda_x, n_\varphi, \omega) = 0$ where ω is the frequency, λ_x the disturbance wave number in the axial direction and n_φ the corresponding quantity in azimuthal direction which has to be an integer. $n_\varphi = 0$ is an axisymmetric disturbance whereas $n_\varphi \neq 0$ represents helical disturbances.

Our analysis of the critical layer, which proceeds along the same lines as for the corresponding case in planar flow (see eg.[1]), brings out the following points as the outstanding features of the critical layer under the influence of swirl:

- Swirl exerts no influence on the scale of thickness of the critical layer through its axisymmetric disturbance mode, $n_\varphi = 0$
- For the nonaxisymmetric modes, $n_\varphi \neq 0$, the thickness of the critical layer retains the same scale as in the case of classical planar flow , viz. $O(\lambda_x Re)^{-\frac{1}{3}}$, as long as the product of the transverse curvature and swirl parameters, $\epsilon_R S_a$, remains small to within $O(Re^{-\frac{1}{3}})$

The linearised equations for the disturbance have been solved numerically by the spectral collocation method using MATLAB over a range of parameters ϵ_R and S_a, and these results are set against the analysis of the critical layer outlined above.

*Ruhr-Universität Bochum, Lehrstuhl für Strömungsmechanik IB 6/43, Universitätsstraße 150, D-44780 Bochum, Germany.

[1] Drazin, Reid, *Hydrodynamic stability*, Cambridge Univ. Pr., 1982

Coherent structures in annular and co-annular swirling jets

M. García-Villalba, J. Fröhlich[†] and W. Rodi

Swirling annular and co-annular jets are widely used in combustion devices, such as gas turbine combustors, to stabilize the flame by means of a swirl-induced recirculation zone. Previous experimental and numerical studies have demonstrated, however, that such flows are prone to instabilities generating large-scale coherent vortical structures[1]. They have a substantial impact on the mixing of scalar quantities such as fuel and oxidizer or hot and cold gas.

We report on large eddy simulations of incompressible flow in unconfined annular and co-annular swirling jets at high Reynolds number ($Re \sim 80000$) and high Swirl number ($S \sim 0.9$) matching realistic conditions. The simulations are validated by comparison with corresponding experiments. Very good agreement has been obtained for mean flow and turbulent fluctuations. Also, the low frequency range of the power spectral density of velocity fluctuations has been found to be in good agreement with the experiments.

Under the flow conditions considered, flow intabilities leading to large-scale coherent structures develop for some of the cases. Two complex shear layers are formed in the flow. An inner one on the boundary of the jet with the recirculation zone and an outer one on the boundary with the surrounding co-flow. Two families of structures appear, an inner structure oriented quasi-streamwise and located in the inner shear layer and an outer structure oriented at a larger angle with respect to the $x-$axis and situated in the outer shear layer. The Kelvin-Helmholtz instability has been identified as the major source for the generation of the coherent vortices. Also a connection between the velocity power spectra and the coherent structures has been established. In the talk, these issues will be discussed together with the impact of the large-scale coherent structures on the mixing of a passive scalar. Furthermore, a conditional-average technique will be described which allows to study the main characteristics of the structures. This is, roughly, done by defining a coordinate system which rotates with the structures and performing the averaging procedure in this rotating system.

Institute of Hydromechanics, University of Karlsruhe, Germany.
[†]Institute for Technical Chemistry and Polymer Chemistry, University of Karlsruhe, Germany.
[1]Coats, *Prog. Energy Comb. Sci.* **22**, 427 (1996).

Mixing characteristics in the near-field of a swirling jet

R. Örlü*

Experiments on swirling jets use different swirl generating methods (e.g. vanes, rotating honeycomb, azimuthal injection of secondary flow) which leave traces in the flow and make it impossible – especially if the near-field is under examination – for accurate comparisons or general conclusions. The purpose of the present work is to analyse the effect of rotation on the near-field of a turbulent swirling jet with and without a passive scalar (in this case the temperature). Experiments have been conducted in a heated swirling jet emanating from a fully developed axially rotating and thermally insulated pipe flow as seen in figure 1(a). The pipe is 6 m long and has a diameter of 60 mm. The Reynolds number (based on pipe diameter and bulk velocity) is Re=24000 and a swirl number S (defined as pipe wall azimuthal velocity divided by the bulk velocity) of 0 and 0.5. The set-up gives well defined streamwise and azimuthal velocity distributions as well as temperature profiles. We have developed a special designed and built combined X-wire and cold-wire which makes it possible to simultaneously acquire the instantaneous axial and azimuthal velocity as well as the temperature.

In the experiment we investigated the effect of rotation on the spreading and the axial decay of a passive scalar, but also investigated the turbulent statistics, such as spectral analysis of the velocity (figure 1(b)), and the temperature, respectively. There are, to the author's knowledge, no previous works on heated turbulent swirling jets issuing from a fully developed rotating pipe flow, but results for the velocity field confirm preliminary studies in an isothermal swirling jet[1]. The temperature field characteristics for the non-swirling jet match results from heated round jets. The implemented measurement technique provides reliable data and confirms the assumption that the temperature acts as a passive scalar as is evident from figure 1(b). Besides the turbulent statistics, access to the axial and azimuthal heat fluxes contribute to the understanding of passive scalar transport as well as heat transfer processes.

*KTH Mechanics, SE-100 44 Stockholm, Sweden.

[1]Facciolo, *TeknL thesis, KTH Mechanics*, (2003).

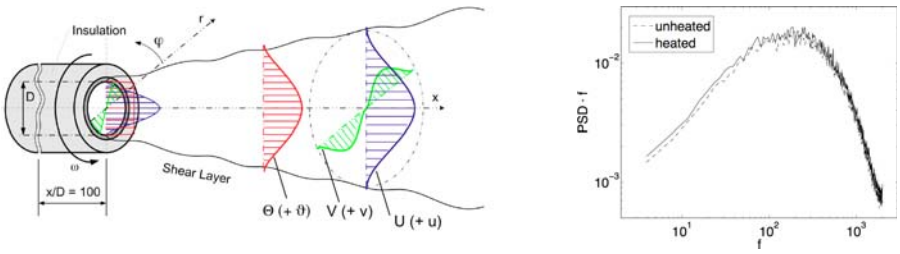

Figure 1: (a) Definition of physical quantities (b) Axial velocity spectrum for the unheated and heated jet at Re=24000 and S=0.5.

Nonlinear wave structures in swirling columnar flows

A.Ni[a]

A weakly nonlinear theory for transcritical transitions in incompressible viscous axisymmetric swirling flows developed. It takes into account viscous effects additional to those covered by the models[1,2] . The introduced into the governing equations viscous terms are responsible for rapid transitions in the swirled flow from one state to the other in the direction of the flow motion. The subsequent analysis of the equations confirmed a strong influence of the introduced viscous terms to the nonlinear wave structure. A complete mathematical similarity between nonlinear transcritical transitions in vortical flows and transonic phenomena in compressible gas dynamics established. It is shown that the evolution of the base supercritical columnar swirling flow to another subcritical swirling columnar flow is governed by the equation completely identical to that of governing the shock waves formation in supersonic compressible flows[3]. It is shown that at least for "weakly" supercritical flows the transition to subcritical states follows the scenario suggested in[4].

On the basis of the developed theory the vortex breakdown phenomena are interpreted as nonlinear wave transitions within swirling flows. The unsteady wave analysis provides guidelines to a consistent explanation of the mechanism leading to axisymmetric the vortex breakdown in high Reynolds swirling flows in pipes. The theory describes at least qualitatively the vortex breakdown transitions and confirms the high sensitivity of the transitions from the approach flow profile and the flow Reynolds number observed in the experiments. The model reproduces different experimental vortex breakdown flow patterns. As an example, nonlinear flow transitions with one and two recirculation bubbles are presented in Fig.1.

---

[a] ALSTOM (Schweiz) AG, TTC-TT Technology Centre, Zentralstrasse 40, 5242 Birr, Switzerland

[1] Leibovich, Randall, Phys. Fluids, 14(12),2559(1973)

[2] Wang, Rusak, J. Fluid Mech. 340,177 (1997)

[3] Ni, Adv. Fluid Mech.V, WitPress, 159(2004)

[4] Benjamin, J.Fluid Mech.14, 593(1962)

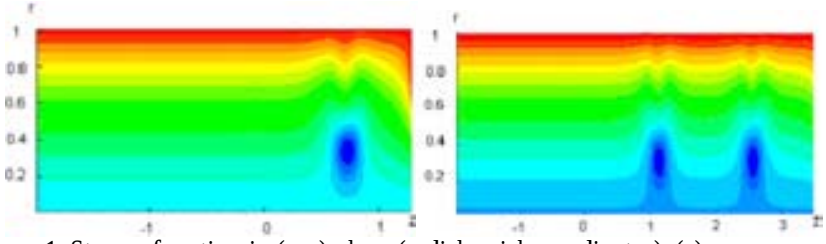

Figure 1: Stream function in (r, z) plane (radial, axial coordinates). (a) one recirculation bubble; (b) two recirculation bubbles.

Mini-symposium

Two phase flows

Leonardo's paradox: Wake instability of a rising bubble

A. Prosperetti*, B. Yang†

"Leonardo's paradox" refers to the fact that a gas bubble with a diameter greater than about 1.8 mm in still water rises in a zigzag or spiral path. A linear analysis of this process is presented assuming that the bubble has a prescribed Reynolds number and a fixed ellipsoidal shape of with different aspect ratio. The results exhibit a strong similarity to the stability features of the flow past a solid sphere. By focusing on the $m = 1$ azimuthal mode, it is found that a double-threaded wake responsible for the deviation from the vertical path develops when the aspect ratio is sufficiently large. The stability analysis of "frozen" states before steady conditions are achieved shows that the amount of vorticity accumulated at the rear of the bubble plays an essential role for the instability. An analysis of the results indicates that the appearance of the first instability is related to the development of a local maximum in the vorticity of the axisymmetric wake of a rectilinearly rising bubble (see figure). When the aspect ratio of the bubble is increased further, a second eigenvalue becomes unstable and two local maxima appear in the vorticity distribution. The results suggest that the development of local maxima in the wake vorticity might be a generic mechanism leading to the non-rectilinear rising or sinking of axisymmetric bodies.

*Faculty of Applied Sciences and Burgerscentrum, University of Twente, AE 7500 Enschede, The Netherlands and Department of Mechanical Engineering, Johns Hopkins University, Baltimore MD 21218 USA

†Department of Mechanical Engineering, Johns Hopkins University, Baltimore MD 21218 USA

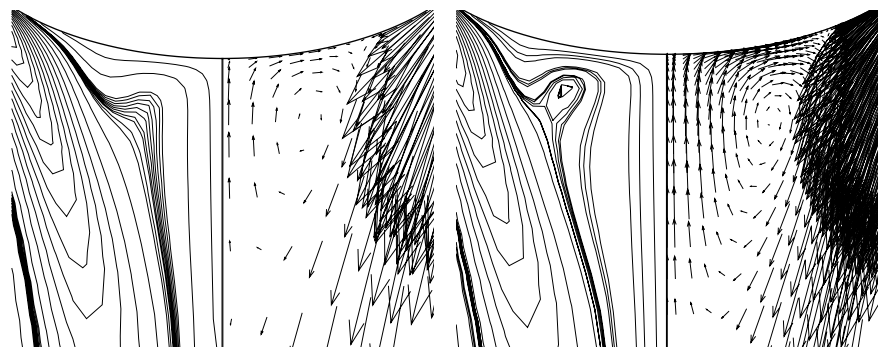

Figure 1: Vorticity iso-lines and velocity vectors near the rear stagnation point of an ellipsoidal bubble with $Re = 660$ and an aspect ratio of $\chi = 2.0$ (left) and $\chi = 2.1$. The vorticity distribution in the second case, for which the rectilinear motion is unstable, exhibits a local maximum. The $\chi = 2.0$ case is stable.

Particle rotation in shear, strain, and rotational flow

J. J. Bluemink[*], L. van Wijngaarden[*], A. Prosperetti[†*], and D. Lohse[*]

We investigate the effect of stream-and crosswise shear components on a sphere in an otherwise uniform flow with help of the DNS code Physalis[1]. A sphere with diameter d is fixed at $(X, Y) = (\frac{x}{d}, \frac{y}{d}) = (-20, 0)$, but it is free to rotate. The flow velocity is given by:

$$\mathbf{U} = -\alpha\omega y\mathbf{e}_x + \omega x\mathbf{e}_y. \tag{1}$$

The parameter α is varied between -1 and 1. The vorticity is $\nabla\times\mathbf{U} = \omega(1+\alpha)$. When $\alpha = -1$, a pure strain is added to the uniform component, for $\alpha = 0$ a linear shear flow is added, and for $\alpha = 1$ a solid body rotation. The angular velocity of the particle Ω_p is determined for steady flow. It is found to depend linearly on α. When $\alpha = -1$ (figure 1(a)) the particle rotates clockwise with $\Omega_p = -0.6\omega$, although the undisturbed flow is non-rotational. The flowfield is locally composed of a uniform flow and a pure strain, flow types that separately do not induce rotation. For $\alpha = 0$ (figure 1(b)): $\Omega_p = 0.3\,\nabla\times\mathbf{U} = 0.3\omega$. For $\alpha = 1$ (figure 1(c)): $\Omega_p = 0.6\,\nabla\times\mathbf{U} = 1.2\omega$, meaning that a particle in a solid body rotation will rotate faster than the surrounding flow (which rotates with $\omega = 0.5\,\nabla\times\mathbf{U}$). The results indicate that the crosswise shear component is extremely important when a uniform flow is added to the flowfield. As can be seen in figure 1, the crosswise components give rise to very large wake deflections.

Other surprising results are found for the drag and lift forces. The drag increases when $|\alpha|$ increases: $F_D \sim \alpha^2$. Going from the linear shear flow case ($\alpha = 0$) to the solid body rotation case ($\alpha = 1$), the drag increases, although the shear decreases to zero. The lift force increases linearly with α.

[*]Faculty of Applied Sciences, Physics of Fluids, University of Twente, The Netherlands
[†]Department of Mechanical Engineering, Johns Hopkins University, Baltimore, Maryland 21218
[1]Z. Zhang and A. Prosperetti., *J. Comput. Phys.* **210**, 292 (2005).

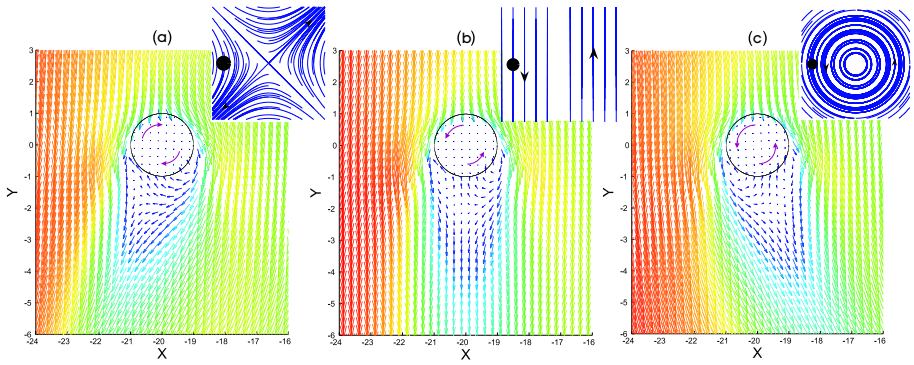

Figure 1: Cross-section of the flowfield around the sphere. (a) Strain, $\alpha = -1$. (b) Linear shear, $\alpha = 0$. (c) Solid body rotation, $\alpha = 1$. In the upper right corner the streamline profile is shown.

Wake of a spherical bubble or a solid sphere in a turbulent flow

A. Merle[a], D. Legendre[a], and J. Magnaudet[a]

Under laminar flow conditions, the centreline velocity defect in the far wake behind a body is known to decrease as x^{-1}, x being the downstream distance to the body[1]. In contrast, this quantity decreases as $x^{-2/3}$ in a turbulent wake developing in a quiescent environment[2]. Wu and Faeth[3] carried out experiments with a rigid sphere surrounded by a turbulent flow, the sphere Reynolds number based on the diameter and relative velocity being in the range [*100*, *300*]. They found the centreline velocity defect to decay as x^{-1} within the first *20* diameters downstream of the sphere, whereas further downstream they observed the wake to decay faster than any other axisymmetric wake region observed thus far.

The wake of a clean spherical bubble and that of a solid sphere set fixed on the axis of a turbulent pipe flow are studied using Large-Eddy Simulation. The wake characteristics are analyzed for particle Reynolds number $Re_p=500$ and $Re_p=200$ (based on the particle diameter and centreline velocity in the pipe) and bulk Reynolds number $Re=6000$ and $Re=20000$ (based on the pipe diameter and bulk velocity). They are also compared to recent numerical results on the wake of a solid sphere in an isotropic turbulent flow obtained by Bagchi and Balachandar[4].

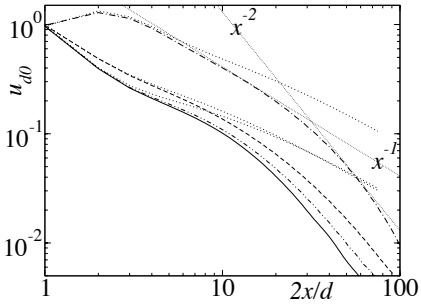

Figure 1: Centreline velocity defect.
Bubbles: —— 500/6000
- - - - 200/6000 - · · · 500/20000
Solid sphere: - · - · - 200/6000
Corresponding laminar wake: ·····

A theoretical analysis and the numerical data obtained indicate that the velocity and shear stress defects obey self-similar evolution laws in which the characteristic r.m.s. turbulent velocity is explicitly involved. Present results also provide a clear evidence of the crucial influence of an outer turbulence on the characteristics of the axisymmetric wake developing behind a spherical particle, for particle Reynolds numbers of some hundreds. In particular, it shows that the radial expansion of such a wake - with a half-width of the wake evolving as αx where α is an increasing function of the external turbulence intensity - is more rapid than those of both a laminar and a turbulent wake developing in a quiescent environment. Similarly, the centreline velocity defect is found to decrease as x^{-2} (cf. figure 1) which is much faster than in the classical situations[1,2], in line with experimental findings previously reported[3].

---

[a] IMFT, UMR CNRS/INPT/UPS 5502, 2 Allée du Prof. Camille Soula, 31400 Toulouse, France

[1] Batchelor, *An Introduction to Fluid Dynamics* (Cambridge University Press, Cambridge, 1967).
[2] Tennekes and Lumley, *A first course in turbulence* (The MIT Press, Cambridge, 1972).
[3] Wu and Faeth, *AIAA Journal* **33**, 353 (1994).
[4] Bagchi and Balachandar, *J. Fluid Mech.* **518**, 95 (2004).

The transition from spherical cap bubbles to toroidal bubbles

Thomas Bonometti[a] and Jacques Magnaudet[a]

Large gas bubbles rising in a slightly viscous liquid frequently adopt either a spherical cap shape or undergo a topological transition beyond which they become toroidal. Here we report on the main results of a numerical investigation of the evolution of such large bubbles starting from rest. The numerical approach is based on a Volume of Fluid method that does not reconstruct interfaces.

We first determine the localization of the transition from spherical cap to toroidal bubbles in the parameter space built on the Bond ($Bo=\rho g D^2/\sigma$) and Archimedes ($Ar=\rho g^{1/2} D^{3/2}/\mu$) numbers comparing the magnitude of inertial effects to that of surface tension and viscosity, respectively (the density and viscosity ratios are kept fixed to 10^3 and 10^2, respectively). Two different transition scenarios, corresponding to the limit of large Ar and large Bo, respectively, are identified. In the capillary limit where viscous effects are negligibly small, we find in agreement with available studies, that the hydrostatic pressure difference between the two poles of the bubble induces an upward liquid jet from the rear. If surface tension is unable to limit the upward velocity, this jet eventually pierces the bubble front (this transition is found to take place in the range $32<Bo<35$). The transition mechanism turns out to be different in the viscous limit where capillary effects are negligibly small. In this case we observe that a similar, however broader, jet forms but does not succeed to pierce the front. However, owing to the lack of the restoring surface tension effect, the front of the bubble cannot sustain the local pressure maximum and becomes concave, forming a downward jet which pierces the rear of the bubble (this second transition takes place in the range $79<Ar<84$).

We also discuss a puzzling feature of large buoyancy-driven bubbles which is that, given an initial gas volume, the final bubble topology strongly depends on the initial conditions. To analyze this sensitivity, we consider the evolution of three bubbles of identical volume and increasing initial oblateness, for a given Bond number. For instance, while the initially spherical bubble becomes doubly-connected beyond $Ar=185$ for $Bo=100$, bubbles with initial aspect ratios of 2 and 3 remain simply-connected even for $Ar=400$. This remarkable influence of the initial shape is shown to be due to the reduction of both the hydrostatic pressure difference between the two poles and the bubble acceleration, as the oblateness increases. Both effects contribute to reduce the upward velocity in the liquid jet, increasing spectacularly the domain of existence of spherical cap bubbles.

[a]*IMFT, UMR CNRS-INPT-UPS 5502, Allée Camille Soula 31400 Toulouse France*

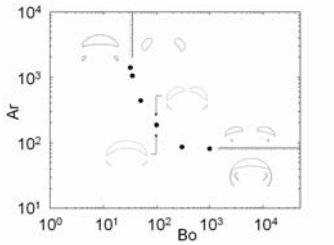

Figure 1. Transition curve in the (Bo, Ar) plane.

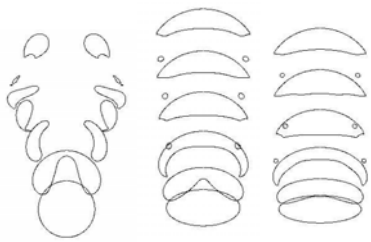

Figure 2. Evolution of bubbles of increasing oblateness for $Bo=100$, $Ar=400$.

Interaction between path, wake and shape dynamics of a rising bubble

C.H.J. Veldhuis*, A. Biesheuvel†, P.D.J. van Oostrum* and L. van Wijngaarden*

This paper concerns an experimental study of bubbles with diameters (D_{eq}) in the range from 1 to 6 millimeter, rising in purified water. A stereoscopic Schlieren setup provides two perpendicular 2D views of the bubble and its wake, recorded at 500 to 1000 frames a second. Analysis of the digital data provides a description of the three-dimensional path and shape of the bubble. The experiments give new information on the onset of bubble shape oscillations and the different wake structures that occur as the bubble diameter increases. The well-known double-threaded wakes are recovered for the smaller bubbles ($D_{eq} \sim 2$ mm). Shape oscillations are not observed in this regime and the path of the bubble eventually becomes a pure spiral. For somewhat larger bubbles ($D_{eq} \sim 3$ mm) characteristic vortex shedding frequencies and bubble shape oscillations are observed. The data shows that there are two basic shape oscillation modes in this regime. The axisymmetric shape oscillations are reflected in variations of the bubble velocity (see figure 1) and the non-axisymmetric shape oscillations are coupled to distortions of the wake behind the bubble. The path of the bubble now finally becomes a pure zigzag. Larger bubbles ($D_{eq} \sim 4$ mm) have a turbulent wake and the bubble velocity fluctuates 'randomly'. Analysis of the forces acting in the tangential, normal and bi-normal directions reveals new information on the time dependent character of lift and drag.

*Physics of Fluids Group, Langezijds, University of Twente, 7500 AE Enschede, The Netherlands.
†Engineering Fluid Dynamics Group, Horst, University of Twente, 7500 AE Enschede, The Netherlands.

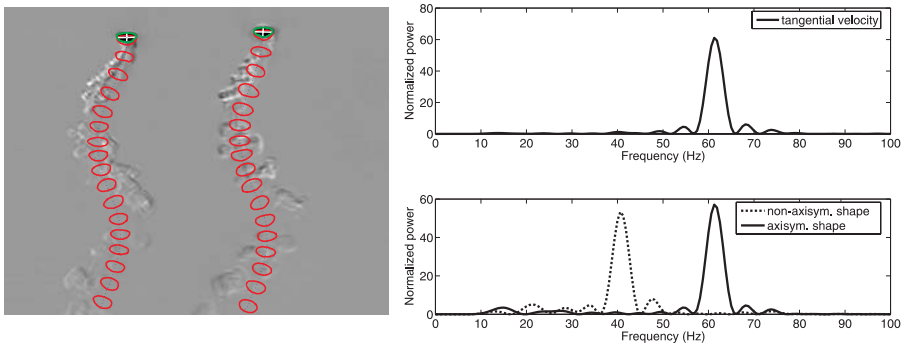

Figure 1: Left: Stereoscopic view of a rising bubble and its wake structure. The left part of each frame shows the yz-plane and the right part the xz-plane. Right: The frequency spectra of the tangential velocity and the axiymmetric and non-axisymmetric shape oscillations.

Fully coupled simulations of monodisperse and bidisperse suspensions in a linear shear flow

M. Abbas[a], E. Climent[a] and O. Simonin[b]

The dynamics of macroscopically homogenous sheared suspensions of neutrally buoyant, non-Brownian spheres is investigated in the limit of very small Reynolds and Stokes numbers using the Force Coupling Model (Lomholt & Maxey[1]). In this numerical approach, the velocity disturbance is obtained by a low order multipole expansion (particle forcing on the flow is represented by monopole and dipole terms spread on a finite volume envelop related to particle radius). Multi-body interactions are achieved by direct solution of Stokes flow equations coupled with the lagrangian tracking of particles in a fully periodic domain (typical size of the computational domain is 48 particle radius; 9% particulate concentration corresponds to 2400 particles). Short-range interactions between particles are modelled by a repulsion force that prevents non-physical overlapping of fluid volume occupied by particles.

The numerical model has been first validated on the analytic expressions of hydrodynamic interactions between two particles (Batchelor & Green[2]). The accuracy is very good when the distance between the two particle surfaces is larger than 25% of the particle radius. It means that our numerical simulations are limited to moderately concentrated suspensions typically less than 20% volumetric concentration.

Then, statistical quantities (translation and rotation velocity fluctuation tensors, particle self-diffusion tensor) were compared to the reference work of Drazer *et. al*[3]. Velocity fluctuation tensors (translation and rotation) grow linearly with the particle concentration and are highly anisotropic. Only one non diagonal term is found to be non zero. This is clearly related to trajectory symmetry breaking induced by the non-hydrodynamic repulsion force. Particle self-diffusion coefficients were both calculated from the long time behaviour of the particle displacement variance, and from lagrangian velocity autocorrelation functions. The self-diffusion tensor was found to be anisotropic. Determination of the self-diffusion coefficient in the flow direction is complicated by a combination of advection in the mean flow and diffusion in the direction of shear. The evolution of this coefficient has been rarely investigated in the literature. Probability density functions of velocity fluctuations showed a transition from exponential to Gaussian behaviour as particle concentration varies.

Similar analysis is carried out on bidisperse suspensions for various concentrations of both species. We also included inertia effect in the particulate phase that leads gradually (as Stokes number increases) to collision dominated regimes. These statistical data can be embedded in macroscopic modelling of solid-liquid suspensions based on kinetic theory of granular media.

---

[a] Laboratoire de Génie Chimique, 5 rue Paulin Talabot, 31106 - Toulouse, France
[b] Institut de Mécanique des Fluides, Allée du Pr. Camille Soula 31400 - Toulouse France

[1] Lomholt & Maxey *J. Comp. Phys.* **184** , 381 (2003)
[2] Batchelor & Green, *J. Fluid Mech.* **56**, 375 (1972)
[3] Drazer et al. , *J. Fluid Mech.* **511**, 237 (2004)

Axisymmetric oscillations and collapse of an encapsulated microbubble subject to acoustic disturbances

K. Tsiglifis[a], N. A. Pelekasis[a]

The large-amplitude axisymmetric oscillations and collapse of a gas mibrobubble encapsulated by an elastic membrane and surrounded by an ideal inompressible liquid are examined theoretically and numerically. In the theoretical analysis, infinitesimal deformations of the microbubble shape are examined in order to determine the stability of a radially pulsating microbubble. The numerical model implements a hybrid boundary-finite element method in order to solve for the nonlinear evolution of the velocity potential and shape deformation of an axisymmetric microbubble subject to acoustic disturbances. The stresses developing on the membrane due to its elasticity, surface tension and bending resistance, are accounted for. Inertia forces prevail therefore viscous dissipation is neglected. Two different constitutive laws that relate stresses with membrane deformations are employed, namely the Mooney-Rivlin and the Skalak laws that describe strain softening and strain hardening materials, respectively. Linear stability analysis and numerical simulations reveal that the membrane buckles when the stresses that develop on the membrane due to its deformation take a critical negative value. This negative value depends on the membrane bending resistance and surface tension, which both play a stabilizing role. The buckling modes depend on the above parameters as well as the membrane constitutive law. Post-buckling shapes reproduce a number of aspects of experimental observations of collapsing contrast agents[1], provided reasonable estimates of the membrane viscoelastic properties are available. Linear stability analysis also shows that a parametric instability, similar to that of an oscillating free bubble, is possible for an encapsulated microbubble as well albeit under restrictive conditions.

[a] Department of Mechanical and Industrial Engineering, University of Thessaly, Volos 38334, Greece

[1] J. E. Chomas, P. A. Dayton, Donovan May & J. Allen., *Appl. Phys. Lett.,* **77**(7), 2000

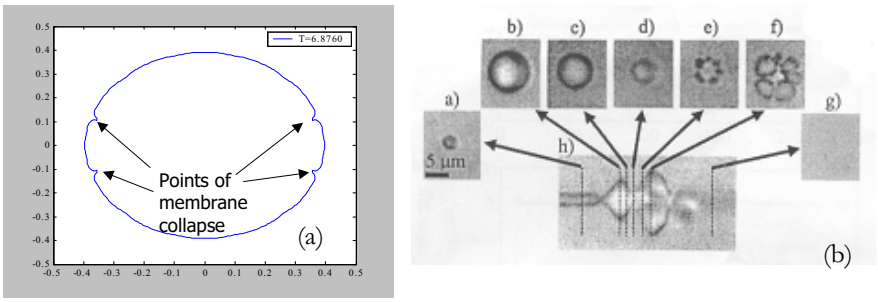

Figure 1: Microbubble shape during collapse. Comparison between (a) simulations and (b) experiments[1] and; $P_{\infty} = P_{St}\left[1+\varepsilon\sin\left(2\pi\nu_f t\right)\right]$, ε=12, ν_f=2.4 MHz, P_{St}=1 bar.

Detachment of bubbles from an oscillating needle

J. Vejrazka[a], M. Fujasova[a], P. Stanovsky[a]

For experimental studies of bubbly flows, it is sometimes needed to produce bubbles of desired volume and detaching at a given frequency. A method for control of both these parameters by means of needle oscillations is proposed. A device, which uses the needle oscillations to get bubbles in a controlled manner, was built and tested.

The model of Oguz & Prosperetti[1] was adapted to describe the bubble formation and detachment in this device. The model was used to determine the range of parameters (gas flow rate, needle diameter and length, chamber volume, movement frequency and acceleration), for which the device succeeds to produce desired bubbles.

The bubble formation on both fixed and oscillating needle was studied experimentally using a high-speed camera. In the case of fixed needle, the bubble volume agrees reasonably well with the prediction of the model, indicating model's suitability for the device description.

Finally, the device tests demonstrate that the needle oscillations are suitable to control the bubble volume and detachment frequency (c.f. Figure 1).

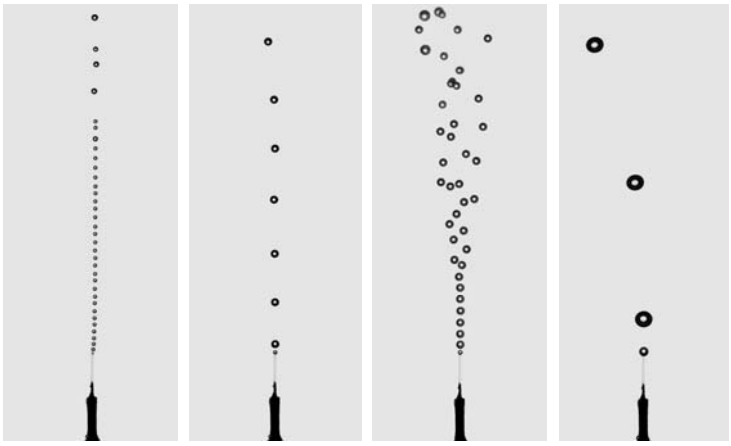

Figure 1: Examples of bubbles formed in pure water at an oscillating needle of inner diameter 20 μm. Bubble sizes are 0.22, 0.43, 0.47 and 0.95 mm, formation frequencies are 160, 40, 250 and 30 Hz (from left).

Acknowledgement: This research was supported by Grant Agency of the Czech Republic (project no. 101/05/P229 and 104/05/2566).

[a] Institute of Chemical Process Fundamentals, Rozvojova 135, 16502 Prague, Czech Republic.

[1] Oguz and Prosperetti, *J. Fluid Mech.* **257**, 111 (1993).

Phase inversion in an oil-water flow through a pipeloop

K. Piela*, R. Delfos*, G. Ooms*, J. Westerweel*, R.V.A. Oliemans†, R.F. Mudde†

We investigated phase inversion in an oil-water flow through a horizontal pipeloop. To that purpose we carried out wash-out type experiments by starting with the flow of a single liquid through the pipeloop and then gradually adding the second liquid using different types of injectors and applying different injection flow rates. We performed experiments starting with water and then adding oil (water-to-oil experiments) and the other way around (oil-to-water experiments). Phase inversion was determined by step changes in the pressure drop and in the electrical conductivity. Much attention was given to the possibility of postponing phase inversion to higher values of the dispersed phase volume fraction, the possibility of multiple droplet formation, the pressure drop at the point of inversion and the phase inversion mechanism. Some results are shown in Fig. 1. It was found that the point of inversion could be postponed to high values of the dispersed phase volume fraction (> 0.8). Samples were taken from the flowing mixture and inspected with the aid of a microscope. For water-to-oil experiments multiple drops (water droplets in oil drops) are not formed before inversion; the volume fraction of the (pure) oil drops increases until their concentration becomes so high that phase inversion occurs. For oil-to-water experiments multiple drops (oil droplets in water drops) are formed before inversion; these (multiple) drops grow continuously in size by entrainment of oil until their volume fraction is so large that inversion takes place.

*Delft University of Technology, Laboratory for Aero and Hydrodynamics, Leeghwaterstraat 21, 2628 CB Delft, The Netherlands

†Delft University of Technology, Kramers Laboratorium, Prins Bernhardlaan 6, 2628 BW Delft, The Netherlands

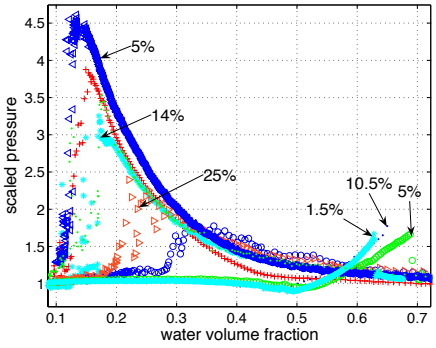

Figure 1: Scaled pressure drop as a function of water volume fraction for water-to-oil experiments (injection rates 5%, 14% and 25% of the mixture flow rate in the pipeloop) and for oil-to-water experiments (injection rates 1.5%, 5% and 10.5%).

Damping of pressure waves in a porous medium saturated with an oil-water mixture

X. Tu[a], G. Ooms[a] and F. van der Bas[b]

An experimental investigation has been made of the damping of a high-frequency acoustic wave in a porous medium saturated with a water-oil mixture. It was found, that the damping coefficient for this case is considerably larger than the damping coefficient for the case of a porous medium saturated with water only. The damping mechanism introduced by the disperse oil droplet was discussed.

In figure 1 our experimental results are shown for the damping coefficient (of the fast wave) for the case of a core saturated with a water-oil mixture and for the case of a core saturated with water only, as function of temperature and for six values of the acoustic power input. It is clear that the damping coefficient for the case of a water-oil mixture is significantly larger than for the water case. Moreover the influence of the temperature on the damping coefficient is almost negligible for the mixture case, but for the water case the coefficient decreases strongly with increasing temperature. The influence of the difference in acoustic power input is negligible for both cases.

---

[a] J.M.Burgerscentrum, TU Delft. Leeghwaterstraat 21, 2628 CB Delft, the Netherlands

[b]Shel international EP, P.O. Box 60, 2280 AB, Rijswijk, the Netherlands

1. P. Poesio, G. Ooms, A.P. Schraven and F.v.d. Bas Phys. Rev. E 66 (2002) art.no: 016309.
2. D.M.J. Smeulders and M.E.H. van Dongen, J. Fluid Mech. 343 (1997) 351-373.

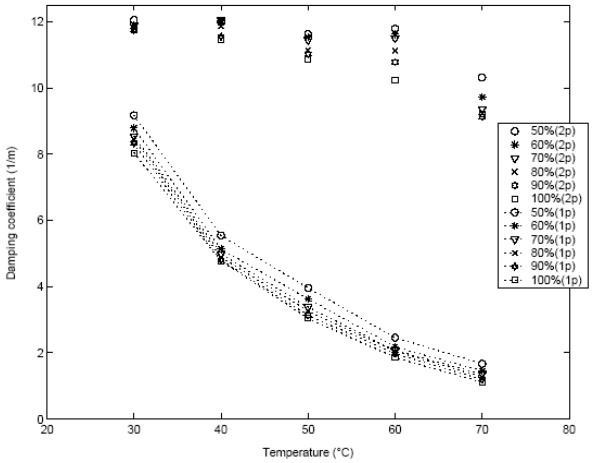

Figure 1: Damping coefficient as function of temperature for the case of a core saturated with a water-oil mixture (2p) and for the case of a core saturated with water only (1p), as function oftemperature and for six values of the acoustic power input.

Non-universal features of moving contact lines

J.H. Snoeijer*, G. Delon, M. Fermigier, B. Andreotti

The problem of moving contact lines extends beyond classical hydrodynamics and still constitutes a great challenge. The various contact line models that have been proposed often lead to similar macroscopic predictions and are difficult to discriminate experimentally. In this talk we study the relaxation of perturbed receding contact lines, which was proposed to be very sensitive to the microscopic physics. Experimentally, we perturb the contact line by wetting defects on a plate withdrawn from a liquid bath, while theoretically we compute the relaxation within lubrication theory using a slip-model (Fig. 1). In both cases, we find that the relaxation is "quasi-steady" and can be understood in terms of an apparent contact angle that depends on the contact line velocity. However, we show that a description using an apparent contact angle is rather limited: it does not correctly predict the threshold velocity for liquid deposition, and it is not universal for different geometries. In particular we find that the threshold dewetting velocity for sliding drops is very different from the critical velocity of the Landau-Levich problem.

*PMMH, ESPCI, 10 rue Vauquelin, 75005 Paris, France.

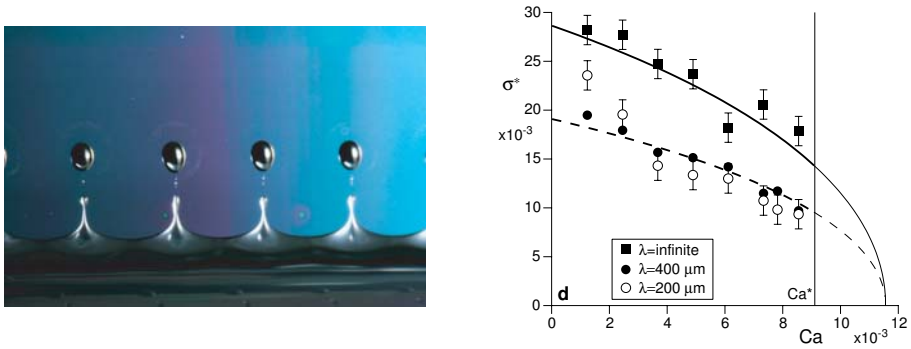

Figure 1: (a) A dewetting contact line is perturbed by periodic wetting defects on a solid plate, at wavelenght λ, passing through the meniscus. (b) Rescaled relaxation rates σ^* as a function of dimensionless plate velocity Ca.

Drops sliding down an incline: flow structure and interface geometry.

N. Le Grand-Piteira[a-b], E. Rio[a], J. Snoeijer[a,b], B. Andreotti[a], A. Daerr[a-b] and L. Limat[a,b]

When a drop slides down an incline, its shape undergoes successive bifurcations with appearance of a point singularity at the drop rear. At low velocity, the drop is rounded. Increasing the velocity, a "corner" develops in which two inclined contact lines are meeting at a singular point. At higher velocities, the corner evolves towards a "cusp" which itself undergoes a "pearling" transition, with deposition of smaller droplets equally spaced behind the main drop. We have investigated both the structure of the interface and that of the flow, especially very near the singularity. Far from the singularity, the problem reduces to a 2D wetting or dewetting situation in a plane normal to the contact line "1". In the corner regime, at the singularity itself, the flow and the interface structure (conical singularity) are autosimilar, both being well described by a simple lubrication model "2,3". At small scale, the singularity is regularized by formation of a locally highly curved contact line. Additional capillary forces mobilized by the curvature are able to delay liquid deposition that should be expected at the corner tip "3". Above a critical capillary number, this equilibrium can not be hold and pearling should occur. A model of this transition is under construction with J. Eggers and H. A. Stone.

---

[a] Laboratoire PMMH, UMR 7636 of CNRS, ESPCI, 10 rue Vauquelin, 75005 Paris, France
[b] Laboratoire MSC, UMR 7057 of CNRS, Paris 7 University, Paris, France.

[1] Rio, Andreotti, Daerr, Limat, *Phys. Rev. Lett.* **94**, 024503 (2005)
[2] Le Grand, Daerr, Limat, *J. Fl. Mech.* **541**, 293 (2005).
[3] Snoeijer, Le Grand, Rio, Limat, *Physics of Fluids* , **17**, 072101 (2005).

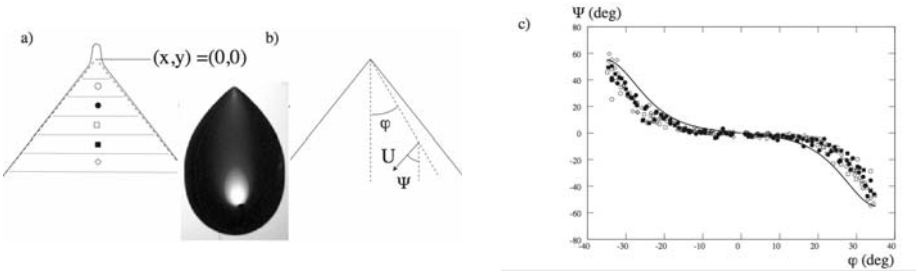

Figure: (a-b) Silicon oil drop sliding down fluoropolymers, and in which accurate velocity measurements have been perfomed near the tip. (c) Autosimilarity of the fluid velocity U visualized with the velocity inclination. Black line is a lubrication model.
.

Influence of fibres on length scales in decaying turbulence

F. Lundell*& L. D. Söderberg†

The effect of stiff fibres on the length scales in decaying turbulence has been studied by flow visualization. The turbulence is generated at the inlet of a square duct with 50m̃m sides. Iriodin platelets, which orient themselves according to the local shear, are used to visualize the turbulent motions in the flow as the turbulence decays in the downstream direction (x). The effect of fibre length (l) and fibre concentration ($N = nl^3$ where $n$is the number density of the fibres) has been studied. Figure 1(a) shows two examples of the visualization images after some treatment which enhances the variations produced by the flow. Flow is from left to right and the top shows pure water while the bottom shows the case with a considerable concentration of 2 mm long fibres. In the case of pure water (top), there are small scales to the left and as the turbulence decay downstream, the dominant scales become larger and larger. With fibres, as shown in the bottom image, the small-scale variations remain further downstream. This observation is quantified in figure 1(b) where the dominant turbulent scale, obtained via image analysis, is shown for two fibre lengths, 0.5 mm and 2 mm in the left and right plot, respectively. The arrows show the trend of increasing fibre concentration. Without fibres, the dominant scale is increasing in the downstream direction but with fibres, the downstream development changes, especially for the case with 2 mm long fibres. With fibres added, the scales in the downstream end of the test section decreases and at the highest concentration of 2 mm long fibres, the dominant scale is even decreasing as the turbulence develops.

*KTH Mechanics, SE-100 44 Stockholm, Sweden.
†STFI-Packforsk AB, Box 5604, SE-114 86 Stockholm, Sweden.

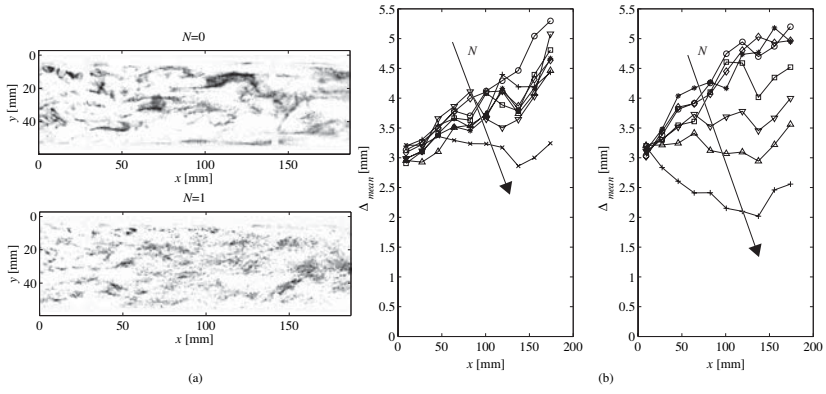

Figure 1: (a) Example images without (top) and with (bottom) 2 mm long fibres. (b) Development of the dominant length scales in the image as a function of streamwise position. Left: 0.5 mm long fibres; right: 2 mm long fibres. The arrows indicate the trend with increasing fibre concentration.

Fibre orientation in the presence of solid boundaries

A. Carlsson*, F. Lundell * and L.D. Söderberg†

An experimental study concerning the orientation of individual fibres in a fibre suspension has been performed. The flow under study is a shear layer, formed by letting the gravitational force drive a fibre suspension down an inclined plate. The main focus of the study is to analyse how the wall influences the fibre orientation. Furthermore it is of interest to investigate the possibility of manipulating the fibre orientation by modifying the surface structure of the wall.

To visualise the flow a CCD camera is mounted at the side of the flow as well as below the flow, in order to capture the velocity profile and orientation of the fibres, respectively, see figure 1(a). A feature detection algorithm finds the orientation and position of the fibres in the captured images. The velocity is found from the position of the fibres in three subsequent images. The velocity profile of the fibres agrees with the theoretical velocity profile for steady Newtonian flow down an inclined plane. This makes it possible to determine the distance from the wall, of individual fibres, through the velocity.

Figure 1(b) shows the probability density function for two different surface structures. The first is a smooth surface and the second is a surface with ridges. The ridges are oriented at -30 degrees to the flow direction and have a depth and width of 0.5 mm, which is also the length of the fibres. It is seen in the figure that close to the smooth surface a considerable amount of the fibres orient themselves at $\theta = 90^o$, i.e. perpendicular to the flow direction. This effect is however more or less eliminated for the surface with ridges, where most of the fibres are oriented close to the flow direction ($\theta = 0^o$).

*KTH Mechanics TR 8, SE-100 44 Stockholm, Sweden.
†STFI-Packforsk AB, Box 5604, SE-114 86 Stockholm, Sweden

(a) (b)

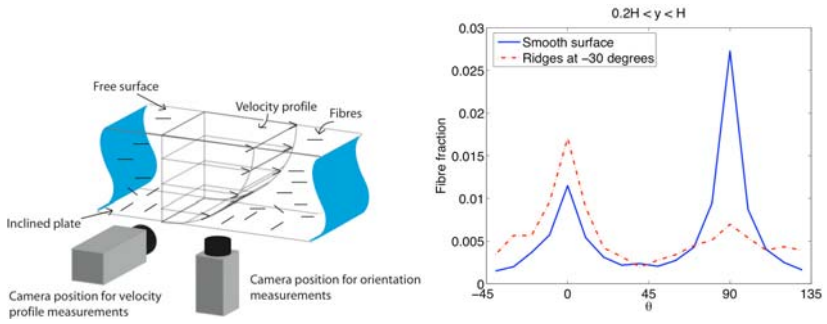

Figure 1: (a) Sketch of the experimental setup. (b) Probability density functions for the fibre orientation θ, where $\theta = 0$ represents the flow direction. The distance from the wall is the region $0.2H < y < H$, where $H = 0.5$ mm.

List of authors

Ordinary lectures and mini-symposia

LIST OF AUTHORS

LIST OF AUTHORS

LIST OF AUTHORS

LIST OF AUTHORS

LIST OF AUTHORS